UNIVERSIDAD POLITÉCNICA DE MADRID
Escuela Técnica Superior de Ingenieros Industriales

Encoded surfaces that are read by three-dimensional radar imaging systems

DOCTORAL THESIS

Submitted for the degree of Doctor by:

Alejandro Badolato Martín
Ingeniero de Telecomunicación

Madrid, 2024

UNIVERSIDAD POLITÉCNICA DE MADRID
Escuela Técnica Superior de Ingenieros Industriales

Doctoral Degree in Mechanical Engineering

Encoded surfaces that are read by three-dimensional radar imaging systems

DOCTORAL THESIS

Submitted for the degree of Doctor by:

Alejandro Badolato Martín
Ingeniero de Telecomunicación

Under the supervision of:
Dr. Juan de Dios Sanz Bobis

Madrid, 2024

Title: Encoded surfaces that are read by three-dimensional radar imaging systems

Author: Alejandro Badolato Martín

Doctoral Programme: Mechanical Engineering

Thesis Supervision:

Dr. Juan de Dios Sanz Bobis, Profesor Contratado Doctor, Universidad Politécnica de Madrid

External Reviewers:

Thesis Defense Committee:

Thesis Defense Date:

Dedicado a la memoria de mi Padre

Acknowledgements

A la Universidad Politécnica de Madrid, por formarme como Ingeniero y por seleccionar, como proyecto ganador del concurso ActúaUPM en su certamen del año 2016, a la empresa Auto Drive Solutions S.L. Al Grupo de Microondas y Radar de la Escuela Técnica Superior de Ingenieros de Comunicación de la UPM por mi formación como investigador en tecnología radar. Al CDTI por su apoyo financiero para la realización de los prototipos desarrollados en esta tesis a través de sus programas NEOTEC y CIEN. A Avalmadrid por facilitar ayuda financiera para la realización de los proyectos de investigación de esta tesis. A ENISA por el impulso que supuso en este proyecto su préstamo participativo. Al Ministerio de Ciencia, Innovación y Universidades por su beca Torres Quevedo. Al Instituto Fraunhofer por ofrecerse a colaborar en el proyecto EUREKA. A Carlos A. Fernandes del Instituto de Telecomunicações de Lisboa por el diseño de la lente de enfoque empleada en los prototipos ferroviarios de esta tesis. A Julián Arribas de la empresa Keysight Technologies por su apoyo y por facilitar equipos de instrumentación y medida para realizar ensayos. A Wolfgang Winkler de la empresa Silicon Radar Gmbh por facilitar prototipos radar para la realización de los prototipos.

A Metro de Madrid, por facilitar sus trenes e instalaciones para realizar ensayos. A la Dirección General de Infraestructuras de Transporte Colectivo de la Consejería de Transportes, Movilidad e Infraestructuras de la Comunidad de Madrid por su autorización de acceso a las vías de la linea Pinto-San Martin de la Vega para la realización de ensayos. A Frederic, Polis y Joan de la empresa Masats S.A. por su interés y colaboración para implementar el sistema de parada precisa que se propone en esta tesis en su sistema de puertas de andén. A los Ferrocarrils de la Generalitat de Catalunya por facilitar la realización de ensayos de parada precisa con sus trenes en sus instalaciones.

A Javier Herrero, responsable del área de vías y obras del Ayuntamiento de León, por su apoyo al proyecto y por facilitar el despliegue de una pista de pruebas para dar soporte al transporte público mediante la solución de guiado que se propone en esta tesis.

A todos aquellos que han contribuido, de alguna manera, a que haya podido realizar esta tesis. A todos vosotros, muchas gracias.

A Juan de Dios por aceptarme como alumno para la elaboración de esta tesis, por todo el conocimiento que me ha transmitido, por toda la ayuda que me ha prestado incondicionalmente y por su amistad.

A mi compañero de trabajo y amigo Javier. Por su apuesta personal por este proyecto, por sus ideas y por su sentido del humor.

A mi íntimo amigo, socio y compañero de estudios de Doctorado Jesús Antonio del Castillo. Jesús estuvo apoyándome este proyecto de tesis desde sus inicios. Gracias a sus conocimientos como Ingeniero de Caminos Canales y Puertos, descubrimos juntos la forma óptima de adaptar la carretera mediante marcas de pintura en relieve. Su colaboración también ha sido esencial a la hora de fundar y gestionar la empresa Auto Drive Solutions S.L. que ambos dirigimos y cuyo objetivo no es otro que el de tratar de desarrollar y comercializar las soluciones tecnológicas que se proponen en esta tesis.

A mis amigos por estar siempre ahí cuando se les necesita y por los divertidos momentos que compartimos.

A mi numerosa familia. A todos ellos, por sus ánimos y por su interés en mi proyecto. A mi Padre Alfonso, a mi Madre María del Carmen y a mis hermanos Cristina, Alfonso y Andrés por su apoyo. También quiero agradecer a Andrés la paciencia y dedicación que ha demostrado trabajando estrechamente conmigo en este proyecto.

A mis suegros, Fernando y María Luísa, por toda la ayuda y cariño que he recibido de ellos.

A mis hijos y sobrinos Noa, Pablo, Lucas y Marcos, por aguantarme cada día y por el tiempo que les he podido robar durante mis estudios. Especialmente, en sus años de infancia.

A mi compañera de viaje en la vida y mi mujer María Luísa. Sin duda, es la persona a la quiero agradecer su incondicional apoyo con más énfasis y a la que debo reconocer el mérito y el esfuerzo que ha permitido que pueda dedicarme al estudio durante tantos años. Gracias a ella hoy finalizo esta tesis.

Abstract

Millimeter wave radars, due to their high performance, have typically been used for space exploration and security applications. Currently, they are used massively in the automotive sector so that vehicles can perceive objects in their environment.

This Thesis proposes a new use of these devices that consists of using radars as a reading system on board a vehicle so that it can read encoded information over the infrastructure that is deployed along its trajectory. By reading this information, the vehicle can know its position safely and reliably with centimeter precision. This approach is of special interest in rail transport and road transport.

The operating principle of the reader system consists of determining the distance between the onboard radar and the surface of each of the elements that encode the information. These coding elements are low-cost, low-maintenance passive devices that facilitate their deployment. Depending on the scope of application, a set of metal sheets arranged at different heights on the tracks or a certain combination of embossed 6 mm high two-component cold-plastic paint marks on the asphalt is used.

As it is a radar reading system, its reliability is independent of the ambient lighting conditions, it is not necessary for the surfaces to be clean or have good retro-reflectivity and they can support traffic speeds greater than 360 km/h.

Precise train stopping at stations for platform screen doors deployment or impact protection against buffer stops are some of its applications in the railway industry. In road transport, this system provides an additional guidance mechanism to the LDWS/ALKS systems that has greater reliability than optical systems and better resilience on roads that are in poor condition. On the other hand, the precise positioning and orientation of vehicles offered by this solution enables the sharing of target-detection vectors between vehicles. This allows vehicles to have a network of sensors deployed at different points to better perceive the environment.

Another application that is of interest is to serve as a reference for ISA systems for the adoption of a progressive speed limitation system in urban environments or to serve as a reference for unmanned truck convoys.

In this Thesis, a valid encoding system is proposed and implemented for massive deployment in the road network around the world using road markings that are commonly used on numerous roads to improve the visibility of road markings in rainy environments. A coding system that uses PVC pipes with metal sheets inside to facilitate a precise stopping system for trains is also manufactured and tested in real environments.

Two prototypes are presented for each of the two areas of application and the results obtained. The ability of a vehicle to follow a track of raised paint markings is demonstrated and the ability of a train to know its stopping point with an accuracy of better than 2.5 cm is demonstrated.

The thesis concludes that vehicles equipped with an appropriate millimetre-wave radar sensor can read information encoded in the infrastructure and, thanks to this, can determine their position with centimeter precision. It also demonstrates that it is possible to make a simple adaptation of the road network to achieve digitalization through rapid, low-cost deployment that requires zero maintenance during the useful life of the asphalt.

Resumen

Los radares de ondas milimétricas, por sus elevadas prestaciones, han sido utilizados típicamente para la exploración espacial y en aplicaciones de seguridad. En la actualidad, son utilizados de forma masiva en el sector de la automoción para que los vehículos puedan percibir objetos en su entorno.

Esta tesis contempla un nuevo uso de estos dispositivos que consiste en utilizar los radares como un sistema de lectura embarcado en un vehículo para que este pueda leer información codificada sobre la infraestructura que está desplegada a lo largo de su trayectoria. Gracias a la lectura de esta información, el vehículo puede conocer su posición de manera segura y fiable con precisión centimétrica. Esta aproximación resulta de especial interés en el transporte ferroviario y en el transporte por carretera.

El principio de funcionamiento del sistema lector consiste en determinar la distancia existente entre el radar embarcado y la superficie de cada uno de los elementos que codifica la información. Estos elementos de codificación son dispositivos pasivos de bajo coste y bajo mantenimiento que facilitan su despliegue. Dependiendo del ámbito de aplicación, se emplea un conjunto láminas metálicas dispuestas a diferentes alturas sobre las vías o una determinada combinación de marcas de pintura de plástico frío de doble componente en relieve de 6 mm de altura sobre el asfalto.

Al tratarse de un sistema de lectura radar, su fiabilidad es independiente de las condiciones lumínicas ambientales, no es necesario que las superficies estén limpias o presenten una buena retro-reflectividad y soportan velocidades de circulación superiores a 360 km/h.

La parada precisa del tren en estaciones para facilitar el despliegue de puertas de andén o la protección de impacto contra toperas son algunas de sus aplicaciones en la industria ferroviaria. En el transporte por carretera, este sistema facilita un mecanismo adicional de guiado a los sistemas LDWS/ALKS que presenta una fiabilidad mayor que los sistemas ópticos y una mejor resiliencia en aquellas vías que tienen un mal estado de conservación. Por otro lado, el posicionamiento y la orientación precisa de los vehículos que ofrece esta solución habilitan la compartición entre vehículos de los vectores de detección de objetos. Se permite así que los vehículos puedan disponer de una red de sensores desplegados en diferentes puntos para percibir mejor el entorno.

Otra aplicación que resulta de interés es servir de referencia a los sistemas ISA para la adopción de un sistema de limitación de velocidad progresivo en entornos urbanos o servir de referencia a los convoyes no tripulados de camiones.

En esta tesis se propone y se realiza un sistema de codificación válido para su despliegue de forma masiva en la red de carreteras de todo el mundo mediante marcas viales que se utilizan habitualmente en numerosas carreteras para mejorar la visibilidad de las marcas viales en entornos lluviosos. También se fabrica y prueba en entornos reales un sistema de codificación que emplea tuberías de PVC con láminas metálicas en su interior para facilitar un sistema de parada preciso a los trenes.

Se presentan dos prototipos para cada uno de los dos ámbitos de aplicación los resultados obtenidos. Se demuestra la capacidad de un vehículo para seguir una pista de marcas de pintura en relieve y se demuestra la capacidad de un tren para conocer su punto de parada con una precisión mejor que 2,5 cm.

La tesis concluye que los vehículos equipados con radares de ondas milimétricas adecuados pueden leer información codificada en la infraestructura y que, gracias a ello, pueden determinar su posición con precisión centimétrica. También demuestra que es posible realizar una sencilla adaptación de la red de carreteras para lograr su digitalización mediante un rápido despliegue de bajo coste que requiere de un mantenimiento nulo durante la vida útil del asfalto.

Table of Contents

List of Figures

List of Tables

Abbreviations and Acronyms

ACC	Adaptive Cruise Control
ADAS	Advanced Driving Assistance Systems
ADC	Analog to Digital Converter
ALKS	Automatic Lane Keeping System
APM	Automated People Movers
BTM	Balise Transmission Module
BW	Band Width
CBTC	Communications Based Train Control
DEEC	Departamento de Ingeniería Eléctrica e Informática
ERTMS	European Rail Traffic Management System
ETSII	Escuela Tecnica Superior de Ingenieros Industriales
ETSIT	Escuela Tecnica Superior de Ingenieros de Telecomunicación
FFT	Fast Fourier Transform
FGC	Ferrocarrils de la Generalitat de Catalunya
FoV	Field of View
FPGA	Field Programmable Gate Array
GB	Giga Byte
GMR	Grupo de Microondas y radar
GNSS	Global Navigation Satellite System
HDPE	High Density Polyethylene
HMI	Human Machine Interface
IMU	Inertial Motion Unit
IA	Inteligencia Artificial
ISA	Intelligent Speed Adaptation
ISAR	Inverse Synthetic Aperture Radar

JPL	Jet Propulsion Laboratory
LDWS	Lane Departure Warning System
LFMCW	Linear Frequency Modulation Continuous Wave
LIDAR	Light Detection and Ranging
LZB	Linienzugbeeinflussung
MIT	Massachusetts Institute of Technology
NASA	National Aeronautics and Space Administration
PCB	Printed Circuit Board
PSD	Platform Screen Doors
PLL	Phase Locked Loop
PoE	Power over Ethernet
PSF	Point Spread Function
QFN	Quad Flat No-lead package
QoS	Quality of Service
RADAR	Radar Detection And Ranging
RFID	Radio-frequency identification
SAE	Society of Automobile Engineers
SAR	Synthetic Aperture Radar
SIL	Safety Integrity Level
ToF	Time of Flight
UPM	Universidad Politécnica de Madrid
UWB	Ultra Wide Band
VCO	Voltage Cristal Oscillator

1. Introduction

1.1. Motivation and objectives of the Thesis

After finishing my degree in Telecommunications Engineering, I started my PhD studies at the Microwave and Radar Group of the Polytechnic University of Madrid. During my 4 years as a researcher in this group, I worked on developing a novel millimeter wave radar (300-330 GHz) [1], [2], [3], [4], [5], [6], [7], [8], [9], [10], [11] for remote detection of coanceled weapons and explosives under clothing described in 4.1. This radar is capable of scanning a person's torso at 8 meters distance and obtaining a three-dimensional image of it. Since clothing is a material permeable to millimeter waves, it is possible to detect potentially dangerous hidden objects concealed under it.

In this research project, I had the opportunity to learn about the capabilities of this type of radars such as:

- Ability to measure distances with millimeter precisión
- Ability to detect any material
- Ability to measure in times of tens of microseconds
- Ability to focus radiated energy on a centimeter area
- Ability to detect two targets separated by less than 1 cm from each other
- Ability to pass through plastics

Given these properties, I wondered whether these devices could be used to help guide and position wheeled vehicles. I considered two approaches to the problem. The first approach involves installing radar devices in the infrastructure that are capable of detecting the position of the vehicles. However, this solution was quickly discarded due to the high installation and maintenance costs involved in deploying it across the entire network. The second approach involves installing sensors in the vehicles that detect certain patterns in the infrastructure that allow the position and orientation of the vehicle to be determined accurately. For this second approach to be valid, the infrastructure must have a sufficiently precise unique radar signature that remains stable over time.

Taking advantage of the measurement capabilities of millimetre wave radars and taking into account the characteristics of the infrastructure, I conclude, in a first approximation, that it is necessary to modify the latter in order to provide it with

a valid signature. This signature must consist of a certain type of information that is encoded along the path followed by the vehicles. Given the enormous length of the network, such modification must be low cost, easy to deploy and require very low maintenance.

Reading information encoded using millimetre wave radars poses numerous challenges. One option for encoding information that can be read by these radars may be to modify the surface of the infrastructure to vary its reflectivity. In this way, a logical level of 0 or 1 can be associated depending on the power level received. However, this approach is not the most appropriate. The signal received from a millimetre wave radar does not allow a metallic reflector to be easily distinguished from a reflector with absorbent material. This is because the shape of the surface on which the waves hit and, above all, the angle at which the waves hit said surface, can cause variations in the power of the received signal in the order of tens of decibels. Another possibility for encoding logical levels is to generate dielectric change boundaries at different radial distances from the radar. In this way, a reflection will occur at said dielectric change boundaries and the radar will be able to accurately measure the distance to it. By associating different distances with different logical levels, information can be encoded.

It is also possible to encode information by associating logical levels with different thicknesses of a wave-permeable material such as plastic. In addition to proposing these solutions, I conducted a search in scientific publications and in the patent database. Not finding any similar solution, I decided to file a patent application to solve the problem of precise and reliable positioning. This patent has been published, among other countries, in the United States, Australia and Israel and is pending publication in Europe.

This solution for positioning vehicles is also applicable to railways. However, I did not initially consider this solution to be of interest as I thought that there would be simpler solutions to solve the problem. By design, this means of transport is guided by the tracks laid out along the route. Therefore, a simple odometer should solve the problem. Later, I discovered the difficulties that train detection systems have in determining the position accurately and I applied the same operating principle to railway vehicles.

This thesis aims to present the solution for vehicle positioning using radar devices that I have designed from a theoretical and technical point of view, to analyse its possible advantages and disadvantages with respect to other existing

technologies and to carry out a feasibility study for a possible mass deployment. The ultimate motivation of this thesis is to try to improve transport safety and efficiency.

1.2. Organization of the Thesis

The Thesis is structured in 6 chapters. Chapter 1 is introductory and sets out the motivation and objectives of this Thesis, provides a brief introduction to millimetre wave radar systems and describes the state of the art of guidance and positioning systems for railway vehicles and road vehicles.

Chapter 2 describes the methodology implemented to achieve the objectives of the Thesis. It describes the different designs, prototypes and tests carried out that have allowed the proposed ideas to be validated.

Chapter 3 explains in greater detail the operating principle of radars, with special emphasis on continuous wave and frequency modulated radars.

Chapter 0 presents, as an introduction to millimetre wave radar systems, a radar system for the detection of objects hidden under clothing, which I have collaborated in developing during my experience as a researcher. This introduction also proposes a positioning solution for railway vehicles and a guidance and positioning system for road vehicles that uses this type of radar and which are the result of my invention.

In subsequent sections, the proposed solutions are described in greater detail and the adaptation of the respective infrastructures is proposed so that the on-board radar sensors can read the information encoded in them, and the different deployments of these adaptations are described.

This chapter also describes the mechanism by which the sensor reads the encoded information and allows the position of the vehicle to be determined in each of the two cases. It also presents 2 prototypes manufactured for each of the two environments and the results obtained in the different tests.

Chapter 5 presents the different applications of the positioning systems developed in both environments and refers to the results obtained in the tests of each of the 4 prototypes manufactured, the collaboration in research projects, the presentations, the publications and the patents that are the result of this Thesis.

Finally, Chapter 6 presents the conclusions and proposes future lines of action.

En este capítulo, también se describe el mecanismo mediante el cual el sensor lee la información codificada y permite determinar la posición del vehículo en cada uno de los dos casos. También se presentar 2 prototipos fabricados para cada uno de los dos entornos y los resultados obtenidos en los diferentes ensayos.

1.3. Millimeter wave radar systems

The word radar comes from the acronym Radio Detection And Ranging. These are devices that, through the propagation of radio waves, are capable of detecting the presence of an object and measuring the radial distance to it. Radars were developed during the Second World War to detect the presence of enemy aircraft. Since then, the main field of research and development of this technology has remained in the military field. The first radars worked in frequency bands of hundreds of megahertz and, later, as components such as oscillators, frequency multipliers or higher frequency circulators have been developed, radars have gradually increased their frequency. The main advantages of increasing frequency are greater compactness of the radiating system and greater resolution. The resolution of a radar is the ability to detect 2 targets that are very close to each other and not confuse them with a single target.

Two-dimensional scanning radars (distance and azimuth) are those used to detect aircraft in a given volume. These radars have two types of resolution: longitudinal resolution and transverse resolution. Longitudinal resolution allows the detection of two nearby targets that are at two different distances from the radar in the same radial direction. This type of resolution is directly proportional to the bandwidth transmitted by the radar and its theoretical value is governed by equation (1) where c is the speed of light in the medium and BW is the transmitted bandwidth.

$$\Delta R = \frac{c}{2\,BW} \qquad (1)$$

The bandwidth transmitted by a radar is usually limited by approximately 20% of the radar's central frequency. Thus, the higher the operating frequency, the greater the bandwidth available and the radar's range resolution can be improved. On the other hand, the transverse resolution is the ability of a radar to detect two targets close to each other that are at the same range from the radar but are observed at a different azimuth angle. Transverse resolution depends on

the directivity of the radiating system. The narrower the radiation beam, the better the transverse resolution obtained. Directivity, in turn, is related to the electrical size of the antenna. The electrical size of an antenna is defined as the ratio between the physical dimensions of the antenna with respect to the transmitted wavelength. The higher the frequency, the shorter the wavelength and the larger the electrical size of the antenna for given dimensions.

Radars are typically built with components coupled in waveguides whose dimensions are reduced with frequency to ensure monomodal propagation along the frequency. These waveguides must be coated on the inside with a conductive material. The higher the working frequency, the smaller the cross-section of the waveguide and the lower the machining tolerances.

At the end of the 20th century, the state of the art did not reflect the existence of components in the millimetre wave spectrum area, which comprises the frequency range [30-300] GHz. Subsequently, improvements in machining precision have been achieved and components in waveguides of hundreds of gigahertz have been developed. However, these components are usually quite expensive and are mainly used in defence and space exploration applications.

Over the last two decades, thanks to projects such as DOTSEVEN (FP7), advances in semiconductor cut-off frequencies have enabled the development of silicon components capable of operating at up to 800 GHz [12]. Other projects such as ELIRAD (H2020) have collaborated in the development of millimetre wave radars. These new radars do not require waveguides and are integrated into a single chip which also includes the antennas. Thanks to their high compactness and the drastic reduction in manufacturing costs, these radars enable a new spectrum of applications in the industrial field [9], [10], [11], [13], [14], [15], [16], [17]. Among these new applications, driving assistance radar systems stand out.

1.4. State of the art of vehicle guidance and positioning systems

1.4.1. Positioning of railway vehicles

The main objective of train positioning is to regulate traffic safely. The main railway traffic regulation systems are based on movement authorizations [18], [19][20], [21], [22] that are sent from the control center that manages the infrastructure to the trains as they circulate. If a train exceeds its movement authorization without receiving a new authorization from the control center, it stops. In order to properly manage movement authorizations, the control center has deployed a series of equipment for train detection. These equipments include axle counters [23], [24], [25], [26], [27], [28], [29], [30], track circuits [31], [32], [33], [34], [35], [36], [37], [38] and radio frequency beacons [39], [40], [41], [42], [43], [44], [45], [46]. Axle counters are devices installed at at least two points along the route that detect when a bogie axle passes over the sensor. The operating principle of this sensor is based on the variation of the magnetic field produced by the presence of a metal wheel in its vicinity. In this way, these sensors generate a signal for each wheel axle that passes over the sensor. The objective of these sensors is to detect the occupation of a segment of the track called a block. The block will remain occupied until the output axle counter detects the same number of axles as the input sensor detected. Otherwise, it is possible that one of the wagons has become uncoupled from the rest of the composition, compromising traffic safety. This solution does not position the train but rather aims to detect whether a track segment is free or not so that another train can circulate through it. It is a fairly simple mechanism to determine whether the block is occupied, however, it requires an initialization process during start-up to ensure that no wagon is stopped inside the block.

The main objective of train positioning is to regulate traffic safely. The main railway traffic regulation systems are based on movement authorizations [18], [19] that are sent from the control center that manages the infrastructure to the trains as they circulate. If a train exceeds its movement authorization without receiving a new authorization from the control center, it stops. In order to properly manage movement authorizations, the control center has deployed a series of equipment for train detection. These equipments include axle counters [23], [24], [25], [26], [27], [28], [29], [30] , track circuits [31], [32], [33], [34], [35],

[36], [37], [38] and radio frequency beacons [39], [40], [41], [42], [43], [44], [45], [46]. Axle counters are devices installed at at least two points along the route that detect when a bogie axle passes over the sensor. The operating principle of this sensor is based on the variation of the magnetic field produced by the presence of a metal wheel in its vicinity. In this way, these sensors generate a signal for each wheel axle that passes over the sensor. The objective of these sensors is to detect the occupation of a segment of the track called a block. The block will remain occupied until the output axle counter detects the same number of axles as the input sensor detected. Otherwise, it is possible that one of the wagons has become uncoupled from the rest of the composition, compromising traffic safety. This solution does not position the train but rather aims to detect whether a track segment is free or not so that another train can circulate through it. It is a fairly simple mechanism to determine whether the block is occupied, however, it requires an initialization process during start-up to ensure that no wagon is stopped inside the block.

Another similar device for managing the occupation of blocks is the so-called track circuits. The operating principle of track circuits consists of electrically isolating each of the two rails that make up a section of the track and transmitting a signal of a known frequency through one of them. This signal does not propagate to the other rail thanks to the insulation between the two rails. When a train or wagon is located inside the track circuit, it short-circuits the two rails with its metal axis, allowing the signal to propagate to the other rail. This device has the advantage, compared to axle counters, that it does not require an initialisation process during its start-up. On the contrary, it requires that the rails are suitably insulated and limits the maximum length of the circuit to several kilometres. Track circuits, like axle counters, do not determine the position of a specific train.

Another device that does allow a train to be positioned is radio frequency beacons. These beacons are classified into two types: active or passive depending on whether they incorporate a power source that energizes them.

In the case of passive beacons, a sensor located on the underbody of the train and called the Balise Transmission Module (BTM) [47], [48], [49] transmits a frequency typically at 4.2 MHz. The radiated energy, when in the vicinity of the beacon, resonates in the receiving antenna of the same and serves to energize a transmitter that it incorporates and that transmits a pre-coded signal at the frequency of 29 MHz that uniquely identifies the installed beacon. The receiving

antenna of the BTM decodes the received telegram and the train signaling systems associate this telegram with a specific position according to the database that it has pre-configured in its memory. This information can be shared by means of a radio link with the control center. The margin of error in the positioning of the train is usually about 2 meters. In order to determine the direction of travel of the train, it is necessary to deploy 2 different beacons close to each other and take into account the reading order of each of them.

Another similar device for managing the occupation of blocks is the so-called track circuits. The operating principle of track circuits consists of electrically isolating each of the two rails that make up a section of the track and transmitting a signal of a known frequency through one of them. This signal does not propagate to the other rail thanks to the insulation between the two rails. When a train or wagon is located inside the track circuit, it short-circuits the two rails with its metal axis, allowing the signal to propagate to the other rail. This device has the advantage, compared to axle counters, that it does not require an initialisation process during its start-up. On the contrary, it requires that the rails are suitably insulated and limits the maximum length of the circuit to several kilometres. Track circuits, like axle counters, do not determine the position of a specific train.

Another device that does allow a train to be positioned is radio frequency beacons. These beacons are classified into two types: active or passive depending on whether they incorporate a power source that energizes them.

In the case of passive beacons, a sensor located on the underbody of the train and called the Balise Transmission Module (BTM) [47], [48], [49] transmits a frequency typically at 4.2 MHz. The radiated energy, when in the vicinity of the beacon, resonates in the receiving antenna of the same and serves to energize a transmitter that it incorporates and that transmits a pre-coded signal at the frequency of 29 MHz that uniquely identifies the installed beacon. The receiving antenna of the BTM decodes the received telegram and the train signaling systems associate this telegram with a specific position according to the database that it has pre-configured in its memory. This information can be shared by means of a radio link with the control center. The margin of error in the positioning of the train is usually about 2 meters. In order to determine the direction of travel of the train, it is necessary to deploy 2 different beacons close to each other and take into account the reading order of each of them.

On the other hand, active beacons exchange information with the BTM when the train is moving over it. The information received by the beacon can be transmitted to the control centre if the beacon has an appropriate communication channel.

Another solution that serves to determine the position of the train is the German system called Linienzugbeeinflussung (LZB) [50], [51]. This system involves the deployment of an inductive loop along about 40 km of track where the outbound wire is close to one rail and the return wire to the other. Both wires cross every 25 or 100 metres. The inductive loop serves as a means of communication between the control centre and the antennas equipped on the train to exchange information. Each time the train passes a crossing, a phase change occurs in the received signal. In this way, the detection of the train's progress is increased by counting the phase changes produced. This system is still operational in many countries. However, the new European ERTMS signalling standard, which guarantees interoperability throughout the Union, does not contemplate the use of this system.

Signaling systems for mass transit use the technique called moving block, which allows increasing the amount of traffic that a given network can support compared to fixed block systems. This technique consists of assigning a moving block to each train that moves in solidarity with it. To implement this technique, it is necessary to have, at all times, communication between the train and the control center that allows determining the position of the train. Thus, these systems are called Communications Based Train Control (CBTC) [52], [53], [54]. Typically, a radiating wire deployed along the route is used to serve as a means of communication between the train and the control center [55]. This radiating wire consists of a coaxial cable that has certain slots in its shielding every certain length through which the signals are propagated. The antenna on board the train points towards the radiating wire with a radiation pattern narrow enough to illuminate 2 or 3 slots in the cable. The radio equipment connected to the radiating wire analyses the signal transmitted by the train at each end of the radiating wire and, taking into account the propagation times at each of the two ends, determines the point where the train is located. Its use is typically restricted to high-traffic lines such as metro lines due to their high installation and maintenance costs. Currently, Madrid Metro operates two of its train lines with this CBTC system.

In addition to the signaling equipment deployed on the tracks to facilitate the positioning of trains, there is a series of equipment that can be loaded onto trains to estimate the position of the train or its progress [56], [57], [58], [59], [60], [61], [62], [63]. Among this equipment, the tachometer, the Doppler radar, the Inertial Motion Unit (IMU) sensor and the GNSS receiver stand out. The first two are used to determine the odometry of the train while the last one allows the estimation of the positioning. The tachometer is an inductive sensor that detects each revolution of one of the train's axles. For the measurement to be accurate, it is necessary to continuously calibrate the wheel radius to avoid drifts due to wheel wear. Despite this calibration, the tachometer has inaccuracies caused by the conicity of the train wheels that cause a variable radius depending on the lateral displacement of the train with respect to the track and the slippage and blockages that occur between the rail and the wheel.

A more accurate method for calculating train odometry is achieved by combining the information from the tachometer with the speed information provided by a Doppler radar. The radar is installed on the underside of the train with a given angle of attack that maximizes the reflection of the transmitted signal in the dihedral that occurs between the ground plane and one of the vertical faces that make up the sleepers or the train supports or the reflections that occur in the ballast. The radar transmits a given frequency (typically 24 GHz) and the reflected signal is received with a frequency variation caused by the Doppler effect. This variation is proportional to the speed of the train. The Doppler radar usually has typical accuracies close to ±3%. These inaccuracies are caused because the angle formed by the reflecting surface with the plane on which the rails are supported is not fixed. The inaccuracy of the tachometer and the Doppler radar cause a cumulative error in determining the position of the train as it advances. An accuracy of ±3% in determining speed means a position ambiguity of 600 metres after the train has travelled 10 km. To eliminate the accumulated error, an RFID beacon is usually installed at certain distances.

The on-board GNSS receiver allows train positioning and is considered as a possible candidate to determine the train position in the future ERTMS 3 version [64], [65], [66]. However, GNSS systems have not yet demonstrated sufficient availability, especially in environments with complex orography or in tunnels, and do not meet the required Safety Integrity Level requirements. Finally, IMU devices are able to determine the acceleration to which the sensor is subjected in

each of the 3 axes and allow to resolve, to a certain extent, this lack of availability.

Other solutions to determine the progress of the train based on temporal correlation between sensors have been explored but have not been commercially successful due to their lack of reliability. The temporal correlation technique consists of deploying at least two sensors arranged on a longitudinal axis. Each of the sensors monitors the infrastructure and obtains a characteristic signal of the infrastructure as the train advances. The temporal correlation of both signals in a given period in which the speed of the train is considered to be constant allows the delay between both signals to be determined. From the calculated delay, the speed of the train can be estimated if the separation between both sensors is known. This technique has been used in [67], [68], [69], [70] using as sensors: 2 optical cameras that point to the ground, 2 Doppler radars and 2 magnetic sensors that monitor one of the rails.

The state of the art described above meets the current needs of the railway industry. However, this thesis proposes the use of radar devices to read information from the infrastructure, which resolves some limitations of current systems. For example, precise train stopping or protection against buffer impacts, which are detailed in sections 5.1.2 and 5.1.3 respectively.

1.4.2. Positioning and guidance of road vehicles

In the automotive industry, advanced driver assistance systems (ADAS) increase traffic safety. There are numerous ADAS systems that serve to warn the driver of potential risks or to activate safety systems in certain circumstances. An example of these systems are those that, using radar sensors [71], [72], [73], [74], [75], [76], [77], [78], [79], [80], [81], [82], [83], [84], [85], [86], detect that another vehicle is approaching the vehicle in the left lane and warn the driver when the latter begins the maneuver to change lanes. Another example of an ADAS system is one that activates emergency braking when a vehicle approaches another vehicle traveling at a slower speed at high speed or when the vehicle approaches a pedestrian at an inappropriate speed [87], [88], [89], [90], [91], [92], [93], [94], [95], [96], [97], [98], [99], [100], [101]. There are also ADAS systems to warn the driver about an inappropriate trajectory or to keep the vehicle in its lane. The main ADAS systems of this type are: the Lane Departure Warning System

(LDWS) [102], [103], [104], [105], [106], [107], [108], [109], [110], [111], [112], [113], [114], [115], [116], [117], [118], [119], [120], [121], [122], [123], [124], [125], [126], [127], [128], [129] and the Automatic Lane Keeping Assist System (ALKS) [130], [131], [132], [133], [134], [135], [136], [137], [138], [139], [140], [141], [142], [143], [144], [145], [146], [147], [148], [149]. Both have been massively deployed in the market for a decade.

The LDWS system sends a warning signal to the driver when the vehicle leaves its lane without using the appropriate indicator. It can also slightly correct the steering wheel for a limited period of time to slightly modify the trajectory and warn the driver. Unlike the LDWS system, the ALKS system acts on the steering wheel for the entire time that the system is operating, allowing the vehicle to remain in its lane without the driver having to act on the steering wheel.

LDWS and ALKS systems use video cameras to detect the road markings that delimit the lane. From the images obtained, they calculate the vanishing point of the projection of the same. To achieve sufficient precision, it is necessary that, in addition to detecting the markings that are a few meters from the vehicle, it is also necessary to detect the markings that are dozens of meters ahead. In many cases, these markings cannot be detected adequately because they are covered by other vehicles traveling in front, due to a lack of image contrast or due to changes in elevation. Under these conditions, the system may lose reference to the vanishing point and stop working abruptly. In the LDWS system, this sudden loss of operation means the disabling of a safety system that is not considered critical. When the system is re-armed, it will again warn the driver of possible inappropriate lane departures. However, in the ALKS system, the lack of availability requires rapid intervention by the driver. This transition in which the driver has to regain control of the vehicle's direction is critical and is called handover. The ALKS system requires the driver to keep his or her hands on the steering wheel and to monitor the correct operation of the system at all times. Its use is only recommended on dual carriageways or motorways with driving speeds below 60 km/h.

As automation systems are implemented in vehicles, drivers tend to overestimate the effectiveness of these systems, especially if failures or unavailability of these systems occur only rarely. This results in drivers becoming more relaxed in assessing potential risks associated with driving and in less awareness of their surroundings.

The response time for a driver to properly perform a handover maneuver when not paying attention to the road ranges from 6 to 45 seconds [150], [151]. Unfortunately, with such high reaction times and the current state of the art, problems associated with handover when driving at high speeds cannot be adequately resolved. This problem is one of the biggest impediments to developing reliable ADAS systems and limits the deployment of Level 3, 4, and 5 autonomous driving solutions in environments that do not have geographical restrictions.

As automation systems are implemented in vehicles, drivers tend to overestimate the effectiveness of these systems, especially if failures or unavailability of these systems occur only rarely. This results in drivers becoming more relaxed in assessing potential risks associated with driving and in less awareness of their surroundings.

The response time for a driver to properly perform a handover maneuver when not paying attention to the road ranges from 6 to 45 seconds [150], [151]. Unfortunately, with such high reaction times and the current state of the art, problems associated with handover when driving at high speeds cannot be adequately resolved. This problem is one of the biggest impediments to developing reliable ADAS systems and limits the deployment of Level 3, 4, and 5 autonomous driving solutions at non-geofenced environments.

In addition to guidance systems based on digital processing of video images to guide the vehicle along its lane, there are so-called Simultaneous Localization and Mapping (SLAM) solutions that allow positioning vehicles by generating maps of the environment [152], [153], [154], [155]. One way to achieve this is to use LIDAR cameras to recognize the environment and compare it with a known map that is stored in the memory of the positioning system. LIDAR cameras emit laser beams in multiple directions that are reflected on surfaces and objects and some bounce back to the camera. These beams are analyzed using ToF (Time of Flight) techniques and with the information obtained a point cloud is obtained with which a three-dimensional reconstruction of the environment through which the vehicle is traveling is made. Subsequently, the reconstruction is compared with a previous model that is stored in the memory of the positioning system and that contains known references such as the cornices of certain buildings. In this way, the position of the vehicle is obtained with centimeter precision. This

technology is used by some of the companies that are offering level 4 driving services. However, it poses numerous difficulties that prevent a mass deployment. The main one is that it requires a continuous update of the maps since the environment changes over time. For this reason, these companies offer their services only in certain cities.

In addition to guidance systems based on digital processing of video images to guide the vehicle along its lane, there are so-called Simultaneous Localization and Mapping (SLAM) solutions that allow positioning vehicles by generating maps of the environment [152], [153], [154], [155]. One way to achieve this is to use LIDAR cameras to recognize the environment and compare it with a known map that is stored in the memory of the positioning system. LIDAR cameras emit laser beams in multiple directions that are reflected on surfaces and objects and some bounce back to the camera. These beams are analyzed using ToF (Time of Flight) techniques and with the information obtained a point cloud is obtained with which a three-dimensional reconstruction of the environment through which the vehicle is traveling is made. Subsequently, the reconstruction is compared with a previous model that is stored in the memory of the positioning system and that contains known references such as the cornices of certain buildings. In this way, the position of the vehicle is obtained with centimeter precision. This technology is used by some of the companies that are offering level 4 driving services. However, it poses numerous difficulties that prevent a mass deployment. The main one is that it requires a continuous update of the maps since the environment changes over time. For this reason, these companies offer their services only in certain cities.

A similar approach has been developed by a team at MIT, in which the subsoil is monitored with a ground-penetrating radar and compared with a known model [156]. This system allows the vehicle to be positioned with centimetre precision and has the advantage of being able to operate even on snowy surfaces [157]. As with positioning systems based on LIDAR cameras, the main drawback of this solution is that the radar maps of the subsoil vary over time depending on the degree of humidity of the different substrates.

There are other types of solutions for guiding and positioning a vehicle that require adaptation of the infrastructure. An example of this is the solution presented by VOLVO in 2017, in which 3,000 neodymium magnets are embedded in each kilometre of lane and the vehicle is equipped with magnetic sensors that can detect them and thus determine the lateral displacement of the vehicle with

respect to the centre of the lane with an error of better than 10 centimetres and the longitudinal advance with an error of one metre [158]. There are also solutions in which metal sheets are deployed over road markings and inductive sensors or Ultra Wide Band radars are installed in the vehicle to detect them [159].

A similar approach has been developed by a team at MIT, in which the subsoil is monitored with a ground-penetrating radar and compared with a known model [156]. This system allows the vehicle to be positioned with centimetre precision and has the advantage of being able to operate even on snowy surfaces [157]. As with positioning systems based on LIDAR cameras, the main drawback of this solution is that the radar maps of the subsoil vary over time depending on the degree of humidity of the different substrates.

There are other types of solutions for guiding and positioning a vehicle that require adaptation of the infrastructure. An example of this is the solution presented by VOLVO in 2017, in which 3,000 neodymium magnets are embedded in each kilometre of lane and the vehicle is equipped with magnetic sensors that can detect them and thus determine the lateral displacement of the vehicle with respect to the centre of the lane with an error of better than 10 centimetres and the longitudinal advance with an error of one metre [158]. There are also solutions in which metal sheets are deployed over road markings and inductive sensors or Ultra Wide Band radars are installed in the vehicle to detect them [159].

The current state of the art in vehicle positioning and guidance does not offer ADAS systems the reliability and availability required to relieve the driver of liability while driving. Despite the advances made in AI, ADAS systems and autonomous driving systems still need to be supervised by a remote driver or operator. This thesis proposes an improvement of the infrastructure through digitalisation of the infrastructure and an improvement of vehicle positioning and guidance systems using on-board radar devices that can help to solve the current limitations as described in 1.4.2.

2. Methodology

This thesis is the result of research conducted within the framework of a PhD in the Industrial Doctorate modality, where the study and thesis development were embedded within an R&D project carried out in collaboration between a company and the University. The research leverages a deductive methodology, grounded in the established measurement capabilities of millimetre-wave radars, and applies this technology under specific working conditions to validate the hypothesis. The core hypothesis posits that these radars can equip cars and trains with a reading system capable of extracting information from the infrastructure over which they travel, allowing the vehicles to accurately determine their position based on the radar data.

Thus, the focus of this thesis is not to develop new lines of research in radar technology itself, but rather to explore and develop new applications for radar technology and advance the industrialisation process of innovative products using such systems. Achieving this goal required exploring the current limits of commercial millimetre-wave radars, particularly regarding their ability to perform rapid measurements and to detect objects located within short distances of a few centimetres.

The concept of using on-board radars for vehicles is not novel. Previous applications primarily involved the detection of reflectors installed along the infrastructure, which altered the power level of the reflected signal. However, this approach presented significant challenges. Firstly, installing and maintaining numerous reflectors across large infrastructures, especially asphalt surfaces, proved to be logistically and financially demanding. Secondly, the received signal strength often varied unpredictably due to external factors such as the angle of incidence or the presence of liquids on the surface.

To circumvent these issues, a novel method was proposed, based on measuring the distance between the radar and the reflecting surface, thus enabling the encoding of different logical levels of information. The initial approach involved the use of a 6-centimetre thick plastic strip with internal air cavities at various depths, which was laid along the vehicle's path. The radar emitted waves that were partially reflected by the surface of the strip, with the remaining waves penetrating the material and being reflected by the internal cavities. This

approach, while promising, revealed several implementation challenges. Integrating a plastic track into continuous asphalt surfaces proved difficult, and potential water leaks at the joints threatened to obstruct the radar's performance. Additionally, ensuring that the surface remained free from water films thick enough to block radio wave penetration became a concern.

In response, a new approach was developed, replacing the plastic track with raised paint markings to encode the necessary information. The initial concept proposed varying the thickness of the paint marks to represent different logical levels; however, practical implementation difficulties led to the adoption of an alternative solution. Instead of varying the thickness, the paint marks were arranged along both longitudinal and transverse axes of the road, enabling the encoding of information through different combinations of marks. This configuration required the on-board radar sensor to scan a wider area, effectively capturing the information encoded across the road surface.

Based on this concept, prototypes were designed, manufactured, and validated in relevant environments. The advantages and potential applications of the proposed positioning system were then analysed.

For railway transport, however, the road-based solution proved unsuitable. The infrastructure of railway systems, characterised by ballast stones, sleepers, and other track equipment, presented an irregular surface that required a different approach. As a result, a system using PVC pipes embedded with metal reflectors at varying heights was developed. Like the road vehicle solution, two sensor prototypes were designed and manufactured, with 100 metres of coded pipe installed for testing in real-world railway environments. The feasibility of this system and its potential applications within the railway sector were thoroughly examined.

The dissemination of the results from this thesis has primarily occurred through presentations at conferences and publications in specialised journals. As the focus is on the industrialisation of new products and applications, rather than extending the frontiers of scientific knowledge, the emphasis has been on practical, real-world applications of radar technology.

From this framework, the methodology employed in this research is rooted in a deductive framework through experimental plan, building upon established principles of millimetre-wave radar technology. The overarching goal was to

determine whether these radars could be effectively utilised to equip vehicles with a system capable of extracting positional information from their surrounding infrastructure. This chapter outlines the steps taken to validate this hypothesis, from theoretical design to practical implementation and testing.

2.1. Experimental Plan and Hypothesis Validation

The research followed an experimental approach, starting with a clear hypothesis based on the known capabilities of millimetre-wave radar systems. Specifically, the hypothesis posited that millimetre-wave radars, traditionally used in military and aerospace applications, could be repurposed to guide and position vehicles on road and railway networks. To validate this, it was necessary to adapt the infrastructure such that it provided a consistent radar signature. On-board radar devices would then read this signature to determine the vehicle's exact position with high precision. The methodology focused on modifying existing commercial radar technologies to meet the specific demands of vehicle guidance systems.

2.2. Prototype Development

The research progressed through several iterative phases of design, prototyping, and testing. Each phase addressed specific technical challenges identified in the previous iterations.

- First Prototype – Road Vehicles: The initial approach involved deploying a plastic strip with embedded air cavities along the vehicle's path. While theoretically sound, practical issues with water accumulation and integration into asphalt led to the exploration of alternative solutions.
- Second Prototype – Raised Paint Markings: A more robust and scalable solution involved using **raised paint markings** to encode positional data. These markings were arranged on transverse and longitudinal axes, with radar sensors on the vehicle scanning these patterns to determine position.
- Railway Vehicle Positioning: In the railway context, the infrastructure's complexity required a different solution. The final prototype for railways involved a PVC pipe with embedded metal reflectors, which allowed radar sensors to read encoded information at key points along the track.

2.3. Testing and Validation

Rigorous testing was a crucial aspect of the methodology, ensuring that the systems developed could function effectively in real-world conditions. Tests were conducted both in controlled environments and on actual roads and railways.

- Controlled Testing: Laboratory simulations were used to fine-tune the prototypes, ensuring that they could accurately read encoded information under varying conditions
- Field Testing – Road: Tests on road vehicles equipped with radar sensors confirmed the system's accuracy at high speeds (up to 120 km/h) and under different environmental conditions.
- Field Testing – Railways: In railway tests, the radar systems were able to detect position with high precision, even at speeds of 100 km/h. The system's ability to provide centimetre-level accuracy in vehicle stopping positions was particularly noteworthy.

2.4. Technical Challenges

Several technical hurdles were encountered, including signal interference, precision at high speeds, and cost constraints. These were addressed through iterative design improvements and the selection of commercially available radar components

2.5. Conclusion

Through a systematic and iterative process, the methodology demonstrated the feasibility of using millimetre-wave radars for precise vehicle positioning. The solutions developed in this research have the potential to significantly enhance the safety and efficiency of vehicle navigation systems, both in road and railway context.

3. Introduction to radar systems

This Thesis proposes using on-board radars as reading devices. A brief introduction to radar systems is provided below, emphasizing the type of radars considered most suitable for this application.

3.1. Operating principle and types of radars

Radar systems are devices that are capable of determining the distance to an object called a target. They are classified according to their operating principle as primary radars and secondary radars. Primary radars are mainly used in defense applications and do not require the cooperation of the target in the measurement process. In secondary radars, the target has a device called a transponder that emits a response signal when it is interrogated by the radar station. Its main advantage over primary radars is a greater detection range. This type of radar is typically used in civil aviation applications. Primary radars emit an electromagnetic signal and detect the time it takes for this signal to propagate to the target and return to the radar after part of the energy is reflected by the target.

Radars are also classified as continuous or pulsed depending on the type of signal they transmit. Pulsed radars transmit an electromagnetic pulse and then activate their receiver to detect the echo of said pulse. Continuous wave radars transmit energy throughout the measurement process. One of the aspects that determine the range of a radar is the amount of energy transmitted. This range is greater the greater the amount of energy transmitted. Thus, a continuous wave radar that transmits the same power as a pulsed radar with similar characteristics will have a greater range. On the other hand, a pulsed radar has greater difficulty in detecting nearby targets compared to a continuous wave radar since, during the time in which the radar transmits the pulse, the receiver must be deactivated. Thus, in pulsed radars the appropriate balance must be established between the maximum range and the minimum detection distance depending on the application to be implemented.

Another advantage of continuous wave radars is that their hardware architecture is simpler, which mainly affects their price and the size of the device. In contrast, continuous wave radars are easier to detect in electronic warfare applications and can use a single radiating system to transmit and receive, as opposed to

continuous wave radars which require the use of a transmitting and receiving antenna.

3.2. Linear Frequency-Modulation Continuous-Wave radar

Continuous-Wave radars transmit a signal in which the amplitude, phase or frequency is modulated in a sustained manner over time throughout the measurement process. The most commonly used continuous-wave radars are frequency modulated, where the frequency varies linearly with time. They are identified by the acronym LFMCW (Linear Frequency-Modulation Continuous-Wave) and the signal they transmit is called a chirp. Figure 1 shows the operating principle of a LFMCW radar where, at a distance R, a surface is located that reflects part of the energy transmitted by the transmitting antenna. Part of this signal is captured by the receiving antenna. A mixer combines this signal with a copy of the signal being transmitted and, at its output, a signal called a beat signal is obtained. The graph on the right of the same figure shows, in black, the instantaneous frequency that is transmitted and, in red, the instantaneous frequency of the signal that is received.

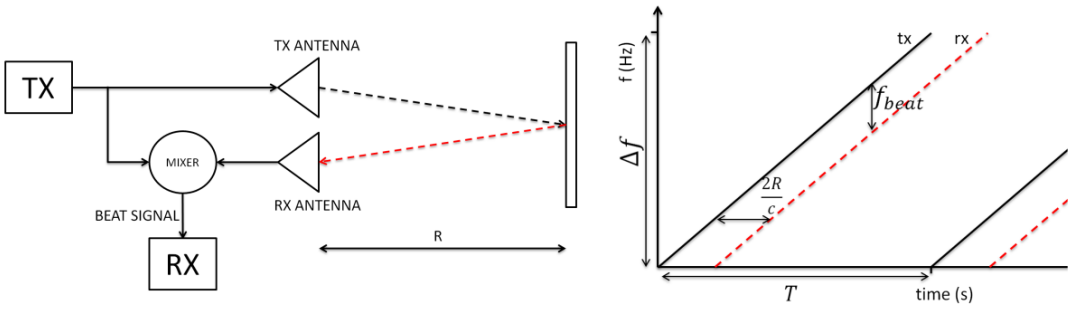

Figure 1: Operating principle of a LFMCW radar

The instantaneous frequency of a chirp signal from a LFMCW radar is determined by equation (2) where Δf corresponds to the bandwidth being transmitted, T is the period of the chirp signal and f_0 corresponds to the

frequency of the signal at the beginning of each period. The waveform of a chirp signal in the time domain is shown in Figure 2

$$f_i(t) = f_0 + \frac{\Delta f}{T} t = f_0 + \alpha t \quad (2)$$

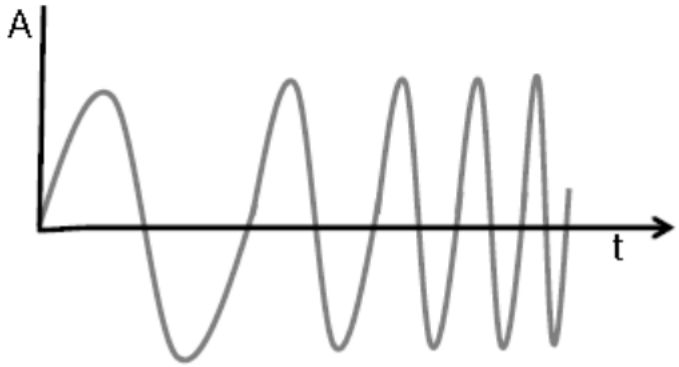

Figure 2: Chirp signal transmitted by a LFMCW radar

Equation (3) shows the phase of the signal obtained by integrating the instantaneous frequency:

$$\varphi(t) = \int f_i(t)dt = \int (f_0 + \alpha t)\, dt = f_0 t + \frac{\alpha t^2}{2} \quad (3)$$

Equation (4) corresponds to the phasor expression of the signal with amplitude A transmitted by the radar:

$$f_i(t) = Ae^{-j2\pi\left(f_0 t + \frac{\alpha t^2}{2}\right)} \quad (4)$$

The time taken by the transmitted signal to reach the target and return to the receiving antenna is called the flying time and is determined by equation (5) where R is the distance to the target and c is the speed of electromagnetic waves in the medium.

$$t_0 = \frac{2R}{c} \quad (5)$$

For simplicity, a perfect reflector is considered whose reflection coefficient is ρ=1. Thus, equation (6) expresses the signal received by the reflecting antenna, which is an identical copy of the transmitted signal delayed t_0 and multiplied by a

factor K that takes into account the losses caused by attenuation and by the reflected power that is not captured by the receiving antenna.

$$r_i(t) = KAe^{-j2\pi[f_0(t-t_0)+\frac{\alpha(t-t_0)^2}{2}]} \qquad (6)$$

The beating signal present at the output of an ideal mixer that does not present conversion losses is obtained by the simple multiplication of both signals and is determined by equation (7).

$$m_i(t) = KAe^{-j2\pi f_0 t_0 - \frac{\alpha({t_0}^2-2tt_0)^2}{2})} \qquad (7)$$

The frequency of this beat signal is determined by equation (8) where φ(t) is the phase of the signal $m_i(t)$:

$$f_{beat}(t) = \frac{\partial\varphi(t)}{\partial t} = \alpha t_0 = \alpha\frac{2R}{c} \qquad (8)$$

In this expression, it can be seen that the frequency of the beat signal, when the radar is aimed at a single target, is constant and its value αt_0 is proportional to the distance to the target.

The beat signal of a radar that is aimed at several targets is the sum of sinusoids corresponding to the distances to each target. In this case, in order to identify each of the targets, it is necessary to observe the signal in the frequency domain. One way to achieve this is by means of a FFT (Fast Fourier Transform) of the signal. Thus, radar receivers typically have an analogue-to-digital converter to digitise the beat signal and a digital signal processing system to extract the information of the targets detected in the frequency domain. On the left side of Figure 3, the excitation signal of the local oscillator that generates the chirp signal of the equipment described in 4.2.3 is shown. On the right side of the figure, the FFT of the beat signal is shown when the radar is pointed at a target located 28 cm away. In this same graph, a target can also be identified at a distance of 16 cm, which is associated with the reflection produced in the lens of the equipment used to focus the radiated energy.

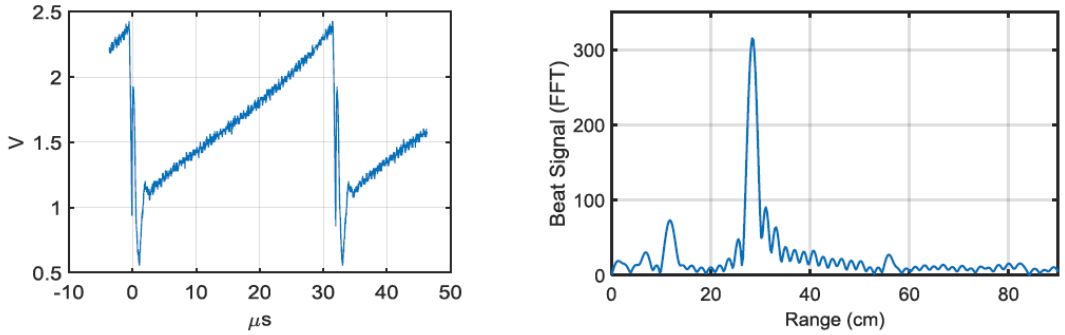

Figure 3: Excitation signal of a VCO to generate a chirp signal and a beat signal of a target located 28 cm away

3.2.1. Radar resolution

Radar resolution is defined as the ability of a radar to detect two targets close to each other. The radar must be able to identify that they are two independent targets whenever the separation between them is greater than the radar resolution. There are two types of resolution: range or longitudinal resolution and transverse or azimuth resolution. Transverse resolution is related to the directivity of the radar's radiating system. The greater the directivity of the antenna, that is, the smaller the width of the radiation beam, the better the transverse resolution of the radar. This greater directivity is typically achieved with larger electrical antennas [160], [161], [162], [163]. An example of radar with good azimuth resolution is the surface radars that are typically installed in airport control towers. The longitudinal or distance resolution is determined by equation (1) where c is the speed of light in the medium and ΔB is the bandwidth of the signal transmitted by the radar[164], [165], [166], [167].

Radar resolution is defined as the ability of a radar to detect two targets close to each other. The radar must be able to identify that they are two independent targets whenever the separation between them is greater than the radar resolution. There are two types of resolution: range or longitudinal resolution and transverse or azimuth resolution. Transverse resolution is related to the directivity of the radar's radiating system. The greater the directivity of the antenna, that is, the smaller the width of the radiation beam, the better the transverse resolution of the radar. This greater directivity is typically achieved with larger electrical antennas [160], [161], [162], [163]. An example of radar with good azimuth resolution is the surface radars that are typically installed in

airport control towers. The longitudinal or distance resolution is determined by equation (1) where c is the speed of light in the medium and ΔB is the bandwidth of the signal transmitted by the radar [164], [165], [166], [167].

The longitudinal resolution of a radar will be better the greater the transmitted bandwidth. In turn, this bandwidth is usually limited by the central frequency at which the radar transmits. The design of electronic filters and antennas usually have a typical bandwidth of approximately 20% of the central frequency. Thus, the higher the radar's working frequency, the greater its bandwidth and the better its distance resolution.

4. Applications of millimeter-wave radars

In the frequency band between 30 and 300 GHz the wavelength in vacuum is 1 mm ≤ λ ≤ 1 cm. Until recently, no applications had been developed in this area of the spectrum due to the limited variety of circuits capable of working at such frequencies. Currently, commercial technology is beginning to exist that allows new applications to be designed in this frequency range as shown in Table 1.

At these frequencies, radiating systems are small in size and a high bandwidth can be transmitted. Taking advantage of these properties, new radar applications are being developed such as driving assistance or ACC (Adaptive Cruise Control) [168], aircraft landing assistance [169] or obtaining high-resolution SAR/ISAR (Inverse Synthetic Aperture Radar) images [170], [171]. In addition, in this frequency range the waves have a great capacity to penetrate tissues and a wide variety of materials.

Therefore, other applications at these frequencies are imaging radar systems such as those shown in Table 1 that allow non-intrusive inspections of objects. Currently, there are systems on the market capable of scanning a person's torso in order to detect whether they are carrying weapons or explosives hidden under their clothing [172], [173], [174]. As an alternative to these systems, there are also devices based on X-ray backscattering [175], [176].

Table 1 Millimeter-Wave Imaging Radar Systems

	f_c(GHz)	Forma de onda	B(MHz)	ΔR(m)	Aplicación
Huggard *et al* [23]	94.0275	Diente de sierra	-	16-30	Perfilado de nubes
Guldogan *et al* [24]	77	Diente de sierra	150	1	registros Micro-Doppler
Brooker *et al* [25]	94	Diente de sierra	250	1.2	Industria y minería
Rangwala *et al* [26]	94.75	Diente de sierra	500	0.3	Aterrizaje asistido para helicópteros
Johannes *et al* [27]	94	Diente de sierra	1000	0.15	Imágenes SAR
Van Caekenbergue *et al* [28]	77	OFDM	2000	0.075	Sistema automático de aterrizaje
Essen *et al* [29]	94	Diente de sierra/SF	4000/800	0.035/19	Imágenes ISAR
Hantscher *et al* [30]	97.5	-	3000	0.05	Controles de seguridad
Kapilevich *et al* [31]	94	Diente de sierra	6000	0.025	Detección Standoff

Tabla 1.1: Sistemas radar en banda W.

	f_c(GHz)	Tipo	B (GHz)	ΔR (mm)	Resolución transversal(mm)	Distancia (m)	t_{adq} (s)	Campo de visión (m^2)
Gu *et al* [32]	205	Transceptor basado en VNA	10	15	7(H), 4(V)	4.5	<3	2x0.6
Song *et al* [33]	200	Radar CW	-	15	0.85	0.135		0.4x0.2
Goyette *et al* [34]	1560	Sistema optoelectrónico	-	-	15	2.54	0.5	0.51x0.51
Cooper *et al* [35]	676.5	Radar CW-LFM	29	5.2	10	25	<1	0.4x0.4
Sheen *et al* [36]	350	Radar CW-LFM	9.6	15.6	10	5	10	1.5x2.5
Weg *et al* [37]	300	Radar CW-LFM	90	16.7	8	0.5-1.5	9	0.2x0.3
Weg *et al* [37]	645	Radar CW-LFM	10	15	4	0.75-1.5	9	0.2x0.3

Tabla 1.2: Sistemas de imagen en ondas milimétricas y submilimétricas.

4.1.300 GHz radar to detect coanceled objects

Before starting my PhD studies in the Department of Mechanical Engineering at ETSII, I spent 3 years studying PhD in the Microwave and Radar Group belonging to the Department of Signals, Systems and Radiocommunications at ETSIT. During my research, I collaborated in the design, manufacture, start-up and characterization of a millimeter wave body scanner in the 300 GHz band.

The scanner performs a similar function to the equipment shown in Figure 1, which is deployed at security checkpoints in numerous airports.

Figure 4 Millimeter-wave portal for coanceled object detection

When the person enters the cabin, a set of radars deployed in a vertical array rotate around the person for a few seconds. Each radar measures the distance to the body in each of the rotation positions. By combining the detections of all the radars in the array in the different rotation positions, a three-dimensional image of the body is obtained. Part of the signal emitted by each radar is reflected by the person's clothing and part penetrates through the fabric and is reflected on the skin. In this way, 2 detections are obtained for each measurement and, ignoring the first detection, it is possible to observe whether the person is carrying any suspicious objects between the clothing or the skin. Figure 5 shows an image obtained with this type of scanner.

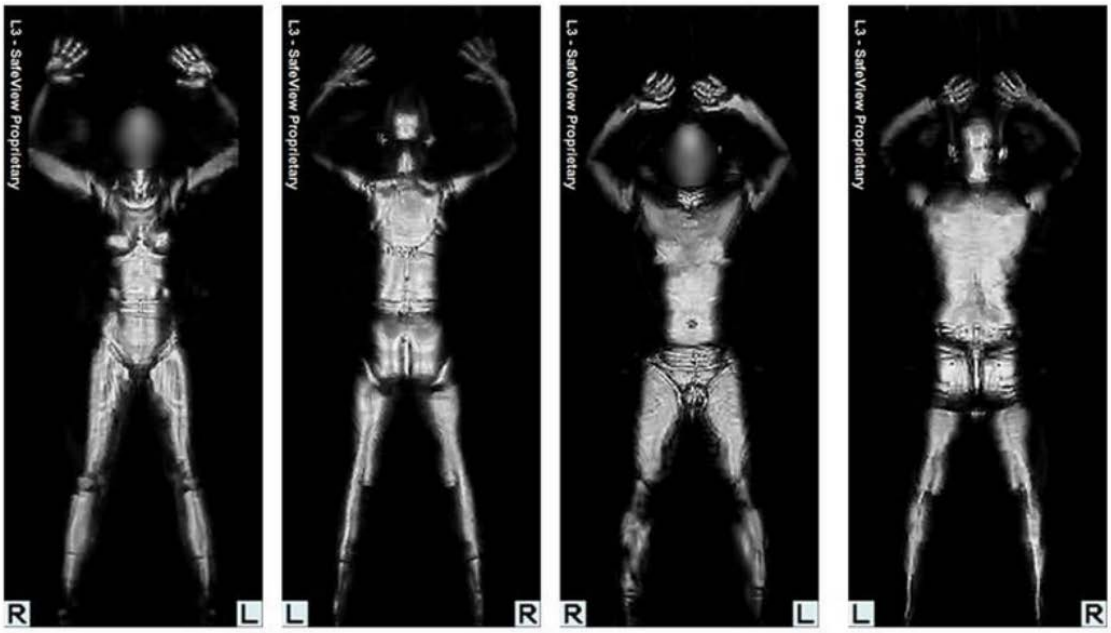

Figure 5: Radar images obtained at a coanceled object inspection portal

Unlike this type of cabin equipment, the GMR scanner obtains a body image using a single radiating system located 8 meters from the object to be scanned. The system obtains three-dimensional images of the torso in times close to a second. The scanner scans an area 50 cm wide by 1 meter high located 65 cm from the ground. This area covers approximately the area between the knee and the neck of the torso of an adult person. The three-dimensional image obtained has a resolution of less than 1.5 cm in each of its three orthogonal axes. Figure 6 shows the upper part of the structure that incorporates all the components of the scanner except for the HMI (Human Machine Interface) which consists of a mouse, keyboard and screen.

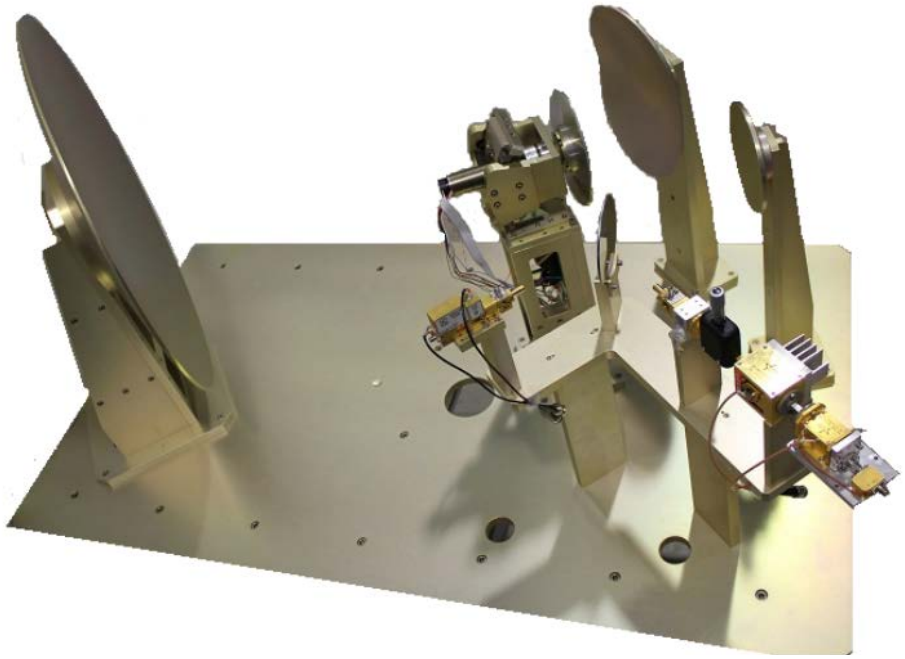

Figure 6. Stand-off radar for the detection of coanceled objects

In the lower part of the structure, part of the radio frequency systems, the power supply system, the synchronization box, the signal generation box, the rotation and elevation motor controllers, the computer that houses the ADC (Analog to Digital Converter) and runs the software necessary to obtain the image are hidden.

A device with similar features is the one developed by the JPL (Jet Propulsion Laboratory), belonging to the NASA (National Aeronautics and Space Administration) [177], [178]. Table 2 shows a comparison between both systems.

Table 2. Comparison of radar systems

	JPL	GMR	
Frequency	675	300	(GHz)
Bandwidth	28.8	27	(GHz)
T chirp	0.1	0.0001 - 1744	(ms)
Tx power	-1.5	0	(dBm)
Acquisition time	1	0.5 - 1	(s)
Standoff range	25	8/10	(m)
Spot diameter	1.3	1.3	(cm)
Main antenna aperture	1	0.65	(m)
Field of View	0.4x0.4	0.9x0.5	(m^2)

In References [1], [2], [3], [4], [5], [6], [7], [8], the design and operation of the radar are detailed, as well as the results obtained.

As a result of this research work, I considered using millimeter wave radars on board vehicles so that they could monitor the infrastructure as they moved through it. After carrying out an analysis of the state of the art and verifying that there was no scientific documentation or published patents in this regard, I decided to reorient my Thesis in this new direction and register the set of patents described in Annex B.

In section 4.2 a positioning system for railway vehicles is proposed and in section 4.3 a guidance and positioning system for road vehicles is proposed.

4.2. Radar positioning system for railway vehicles

4.2.1. Radar signature of the infrastructure

Railway infrastructure is typically made up of a surface of ballast stones and a set of sleepers arranged approximately every 60 cm. The upper surface of these sleepers, being flat, contrasts with the characteristic surface patterns of the ballast. In addition, as this surface is usually slightly raised with respect to the average level of the ballast, it is relatively easy to detect them by observing a cross section of the infrastructure. This profile may seem, at first, to be a repetitive pattern, considering that all the sleepers are at the same height and

that there is a constant separation between sleepers. However, in the report of the tests carried out on the Madrid Metro test track in Annex B, it can be seen that the infrastructure presents a characteristic signature. This signature can be used to identify the position of the train on the track. In addition to the signature generated by the arrangement of each sleeper, the track equipment or switch points also generate characteristic profiles that enrich the signature of the infrastructure.

4.2.2. Adaptation of the infrastructure to improve the radar signature

It is possible to increase the signature of the infrastructure by deploying structures on it that generate known patterns when scanned by millimetre wave radar. In this way, it is possible to encode information at points that may be of special interest, such as stations, or at points where the radar signature is too monotonous, as may occur in slab track areas. An example of this type of structure is used in the test described in Annex C, where 125 mm diameter PVC pipes are installed between the rails containing a set of reflectors installed every 5 centimetres at different heights. The height of each reflector encodes a different logical level.

5 heights are defined that encode 5 logical levels: S (start), E (end), 0, 1 and W (word). The data sequence is fixed and repetitive with the following pattern S, X, E where X can be a bit 0, 1 or W. In this way, each coded PVC pipe has at each end a sequence S, W, E and, between both ends, there are as many sequences S, Y, E as data bits to be encoded where Y can take the value 0 or 1. This coding system that includes logical levels S and E allows to easily identify the reading direction of the different bits so that the receiver is able to adequately reorder the bits to read the encoded data. The pipe segment obtained can be installed discreetly at those points that are considered of interest and represent a low-cost alternative to deployed RFID beacons.

When the train is moving over one of these pipe segments, the radar receiver reads the beacon code whose value can be associated with a position or a specific information or limitation, identifies the reading direction and measures the speed at which the train is moving through it thanks to the logic level transitions that are detected every 5 cm.

The beacons can also be deployed continuously as shown in the figure by concatenating 3-metre-long pipe segments to facilitate permanent feedback from the train.

Figure 7. Continuous beacon

Once the infrastructure has been adapted, the data sequence deployed is geo-referenced and stored in the receiver's memory in a geo-referenced manner. When a train equipped with a radar sensor suitable for reading the beacon circulates over it and travels a first code completely, the sensor determines the position of the train with centimetre precision. From this moment on, each time the train advances 5 centimetres and the sensor detects a logic level transition, it updates the position and speed of the train. This continuous positioning can be used as a precise station stop system, as described in 5.1.2, or as a buffer protection system, as described in 5.1.3. Thanks to the chosen coding system, the radar equipment is able to identify the direction of advance of a train stopped on a beacon that starts moving in less than 6 centimetres.

4.2.3. Design and results of the first prototype

In order to properly monitor the infrastructure, it is necessary to have a sufficiently directional radiating system capable of concentrating the transmitted energy on the area of the infrastructure to be explored [179], [180].]. If this area, which is typically circular and called a spot, is too large, the energy of the beat

signal in the frequency domain will be concentrated in the frequency range that corresponds to the average distance of the reflections obtained. In addition, certain frequency peaks will also appear on those reflective surfaces scanned by the radar that present a significant radar section and that are at least the minimum resolution away from the average surface level. In the case of a railway infrastructure, the appropriate spot size for monitoring is considered to be 1 cm in diameter.

As with the radiant system shown in 4.1, it is necessary that the spot remains well defined in a range of distances without increasing its size. That is, the aiming must not have a single focus given that the distance between the on-board sensor and the surface of the infrastructure can vary. Thus, it has been established as a design requirement for the radiant system that the spot remains well defined in the range of distances between 200 and 700 mm.

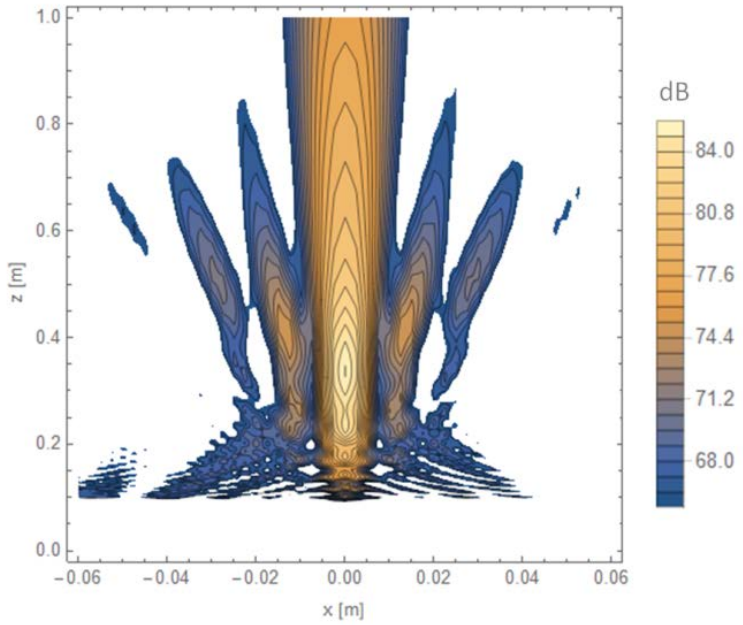

Figure 8. Radiation diagram of the 120 GHz lens

As in 4.1, the design of the radiating system can be done using reflectors. However, in this case, a design using dielectric lenses has been chosen to facilitate greater compactness of the sensor. In order for the antenna integrated into the designed radar chip to properly illuminate the lens, the separation between both must be 120 mm.

Figure 9 shows the HDPE (High Density Polyethylene) lens designed by the Department of Electrical and Computer Engineering (DEEC) of the Instituto Superior Técnico (IST), Faculty of Engineering of the University of Lisbon together with a 3D printed frame that allows the radar to be positioned in the correct position.

Figure 9. 120 GHz lens prototype

This lens is illuminated by a Silicon Radar model TRX_120_001 radar integrated into the 8 x 8 mm QFN56 chip shown in Figure 10. The frequency multipliers, the VCO (Voltage Controlled Oscillator), the transmitting and receiving antennas, and the frequency mixer are integrated inside the chip. The radar hardware architecture is shown in Figure 11.

This lens is illuminated by a Silicon Radar model TRX_120_001 radar integrated into the 8 x 8 mm QFN56 chip shown in Figure 10. The frequency multipliers, the VCO (Voltage Controlled Oscillator), the transmitting and receiving antennas, and the frequency mixer are integrated inside the chip. The radar hardware architecture is shown in Figure 11.

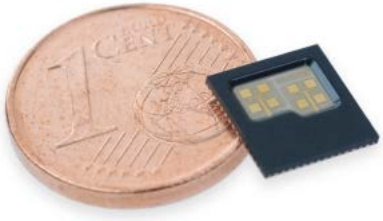

Figure 10. Radar model TRX_120_001 from Silicon Radar

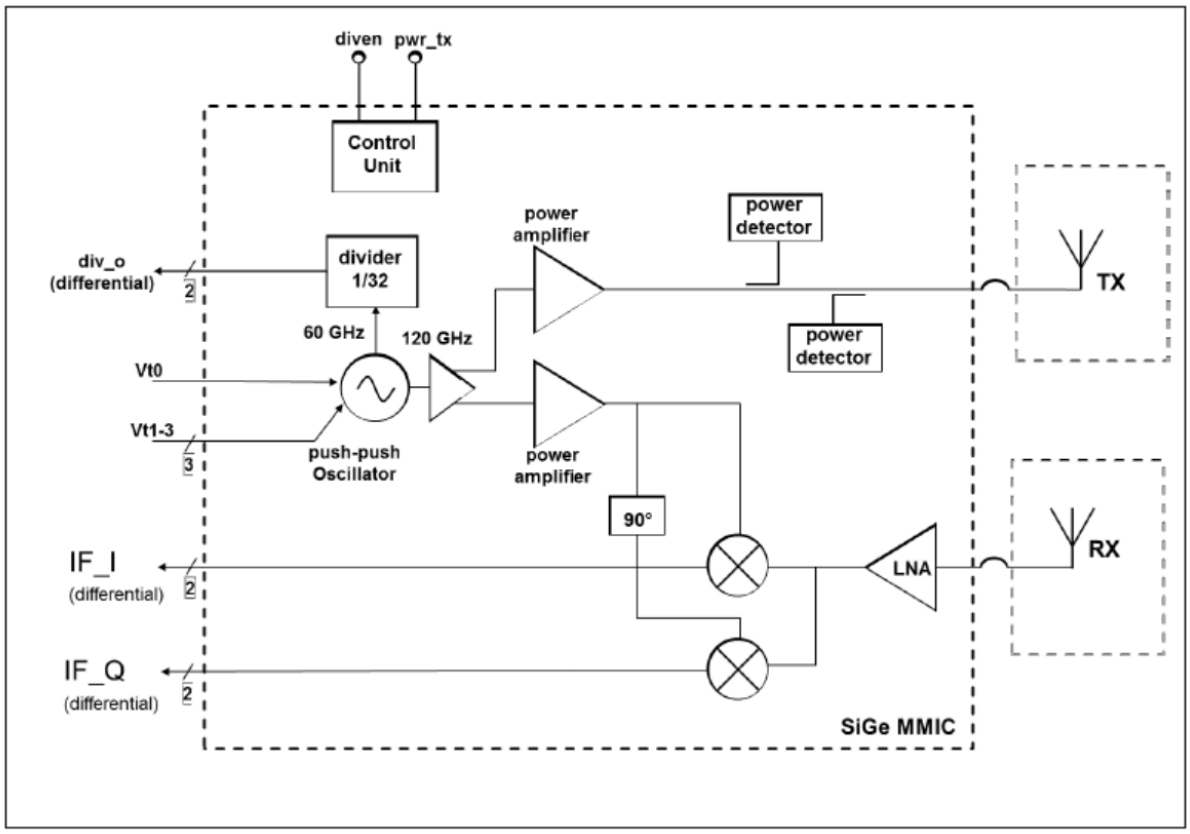

Figure 11 Radar system architecture

The radar has a bandwidth of 7 GHz and transmits in the frequency range [120,-127] GHz. The VCO of this radar is excited by an external PLL (Phase Locked Loop) model ADF4159 from the manufacturer Analog Devices, which in turn receives the signal generated by the VCO as a reference. The PLL is programmed so that the RADAR transmits its bandwidth in 30 μs. In this way, a radar on board a train travelling at 360 km/h samples the infrastructure every 3 millimetres.

The beat signal obtained from the mixer phase channel is conveniently filtered and amplified by an external amplifier and then digitized by an AD9446 ADC that samples the signal at a rate of 80 Megasamples per second. The digitized samples are introduced into a Zynq 7010 FPGA from the manufacturer Xilinx that processes the signal in real time. This processing consists of performing a

16k point FFT and detecting the maximum power spectral density in the bin range that corresponds to the distances between 20 and 70 cm.

The same architecture described is duplicated within the same sensor except for the FPGA which is shared by both radars. This new radar is integrated within the same equipment casing at a distance of 60 cm. The equipment is installed on the underside of the locomotive frame so that both radars are arranged on the same longitudinal axis defined by the rails that make up the track. Figure 8 shows the prototype built.

The same architecture described is duplicated within the same sensor except for the FPGA which is shared by both radars. This new radar is integrated within the same equipment casing at a distance of 60 cm. The equipment is installed on the underside of the locomotive frame so that both radars are arranged on the same longitudinal axis defined by the rails that make up the track. Figure 12 shows the prototype built.

Figure 12. First radar prototype for railway applications

The objective of integrating a second radar is to be able to determine the speed of the train by means of the temporal correlation of the radar profiles as described in 5.1.1.

Figure 13 shows the profile obtained by one of the radars when it is moved along a railway-like infrastructure.

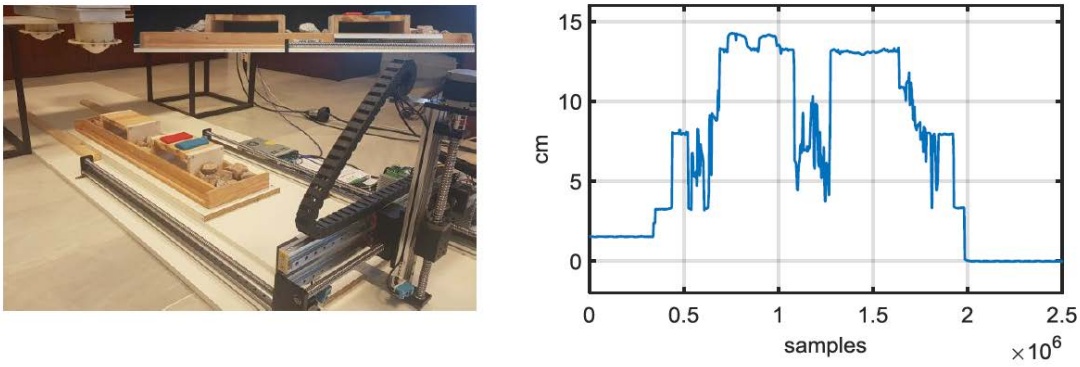

Figure 13. Laboratory tests of the prototype

The prototype has been mounted on a bimodal-road rail vehicle and tested in real environments. Figure 14 shows the profile obtained by the 2 radars when it passes over a defined structure. This structure consists of a set of wood with bumps at different heights. The structure encodes information by placing each bump at a different height. It can be seen that the structure has 4 initial bumps that encode the start and stop sequence 4 times and then starts a repetitive sequence in which a start bit is encoded, higher than the rest, a data bit, whose height defines logical levels W, 1 or 0 in a similar way to the encoding system described in 4.2.2 and a stop bit whose height is the lowest of all.

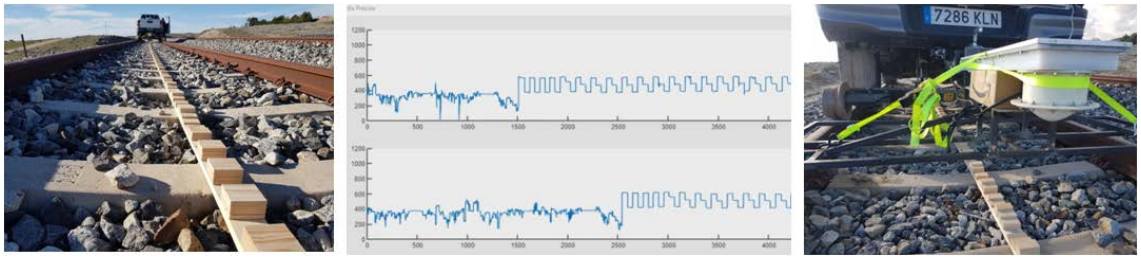

Figure 14. Testing the prototype in real environments

The results obtained are shown in Annex C.

4.2.4. Design and results of the second prototype

A second prototype design has been carried out, shown in Figure 15Figure 15, in which both radars have been made completely independent by adding another FPGA to process the second radar channel. The devices are galvanically isolated

from each other and share a 1 Gbps optical fibre link to exchange information between them. Each of them has a PoE (Power Over Ethernet) port through which it receives power and communicates at 100 Mbps with the device that records the radar profiles obtained.

Figure 15. Second radar prototype for railway applications

This second prototype is aimed at metro applications where traffic speeds are usually less than 100 km/h. For this reason and to achieve greater compactness of the equipment, the distance between radars has been reduced to 17.5 cm. In this way, when a radar points to the centre of one of the bits, the other radar points to the transition between 2 bits, thus reducing the uncertainty of the stopping point to 2.5 cm and the detection of the direction of advance of a train that begins its movement to less than 3 cm.

The results of the precise stopping tests obtained with this equipment on board a Ferrocarrils de la Generalitat de Catalunya train are available in Annex C.

Figure 16. Precise stopping tests carried out with the second prototype

4.3. Radar positioning system for road vehicles

4.3.1. Adaptation of infrastructure

The objective of adapting the infrastructure is to encode information in it so that, when it is read by a suitable sensor on board the vehicle, the vehicle can know its position accurately.

Adapting the road network is an enormous challenge due to its enormous extension. Therefore, this adaptation must not only meet the technical requirements established in the design of the solution, but must also be simple, easy to deploy, low cost and, above all, very low maintenance. In addition, it must not interfere with road signs or road users.

The adaptation proposed for this purpose consists of deploying 6 mm high raised road markings in structured paint. This type of paint is commonly used on roads to improve the retro-reflectivity of road markings in rainy environments. Figure 17 shows an example of this type of marking. These markings have glass spheres attached to their surface that act as reflectors and diffusers of light. Due to the curved surface of the sphere, part of the light emitted by vehicle headlights is reflected back towards the driver, thus improving the visibility of road markings.

Figure 17. Structured paint

Two types of materials are commonly used to deploy this type of marking: thermoplastic paint and two-component cold plastic paint. Thermoplastic paint is applied after heating the material and the recommended ambient temperature for its application must be above 15 degrees. It is a relatively soft material so its durability is not very high and the glass spheres easily come off its surface. For this reason, the spheres are mixed with the material before application. As the plastic is worn away by the passage of wheels over it, new spheres from the interior emerge to the surface.

Unlike thermoplastic paint, cold plastic paint is applied by mixing 90% of a plastic material and 10% of a catalyst. It can be applied at ambient temperatures close to 0 degrees and is therefore much more widely used in northern European countries. It is also used to deploy speed-reducing rumble strips that are deployed in a checkerboard pattern at the approach to some roundabouts as shown in Figure 18.

Figure 18. Rumble strips for speed reduction

This is an extremely hard and abrasion-resistant material. Due to its extreme hardness, the spheres adhere strongly to the surface, so it is not necessary to mix the paint with the spheres and these are applied in the form of a spray once the paint has been deposited on the asphalt. At room temperature, the catalyst acts in less than 5 minutes and the material acquires its final hardness.

Both types of road markings are printed with the help of trucks, such as the one shown in Figure 19, which travel at typical speeds of around 8 km/h and their approximate cost is about €1,000/km per lane [181]. This cost is similar to the cost of deploying 3 vertical traffic signs per kilometer.

This is an extremely hard and abrasion-resistant material. Due to its extreme hardness, the spheres adhere strongly to the surface, so it is not necessary to mix the paint with the spheres and these are applied in the form of a spray once the paint has been deposited on the asphalt. At room temperature, the catalyst acts in less than 5 minutes and the material acquires its final hardness.

Both types of road markings are printed with the help of trucks, such as the one shown in Figure 19, which travel at typical speeds of around 8 km/h and their approximate cost is about €1,000/km per lane [181]. This cost is similar to the cost of deploying 3 vertical traffic signs per kilometer.

Figure 19 Paint truck for 2-component cold-plastic structured paint

Due to the above-mentioned characteristics, the material selected as optimal for the adaptation of the proposed road network is cold double-component plastic. It

is proposed to continuously deploy this type of markings in the centre of the lane in black so as not to interfere with the rest of the road markings.

The coding system of the track must be simple and make it easy for the sensor in charge of reading it to be resilient to possible errors in the track. It must also allow the entire road network to be coded in a unique way.

The proposed track consists of a sequence of rows deployed on transverse axes of the lane separated every 90 mm. In each row, one of the 4 defined logical levels is coded: Start, 0, 1 and End by means of a combination of 4 drops of paint. This combination, in turn, is deployed on 4 longitudinal axes located in the centre of the lane that are 90 mm apart from each other. Figure 20 shows the different combinations of paint drops that define each of the logical levels.

Due to the above-mentioned characteristics, the material selected as optimal for the adaptation of the proposed road network is cold double-component plastic. It is proposed to continuously deploy this type of markings in the centre of the lane in black so as not to interfere with the rest of the road markings.

The coding system of the track must be simple and make it easy for the sensor in charge of reading it to be resilient to possible errors in the track. It must also allow the entire road network to be coded in a unique way.

The proposed track consists of a sequence of rows deployed on transverse axes of the lane separated every 90 mm. In each row, one of the 4 defined logical levels is coded: Start, 0, 1 and End by means of a combination of 4 drops of paint. This combination, in turn, is deployed on 4 longitudinal axes located in the centre of the lane that are 90 mm apart from each other. Figure 20 shows the different combinations of paint drops that define each of the logical levels.

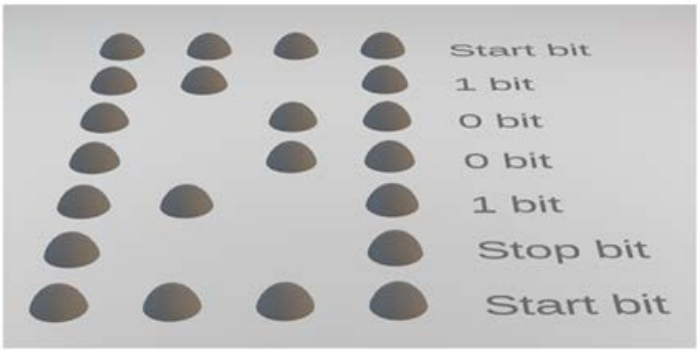

Figure 20. Coding system

The outer columns of the track serve as a clock signal to the receiver to facilitate the identification of each bit. They also serve to accurately determine the speed of the vehicle and to calibrate the effective radius of the wheels. Once the effective radius of the wheel is known and with the information supplied by the wheel encoder, the receiver is also able to identify the loss of several consecutive rows in those tracks that present errors, thus allowing the synchronization of the successive bits not to be lost.

The track encodes a set of words that are defined by a first Start bit, a succession of data bits 0 and 1 and a last End bit. The set of data bits must be of a sufficient size to allow the road network to be encoded uniquely worldwide.

The earth's surface has a surface area of 510.1 million km2[182]According to equation (9), each square centimeter of the earth's surface can be encoded uniquely by a combination of 63 bits.

The outer columns of the track serve as a clock signal to the receiver to facilitate the identification of each bit. They also serve to accurately determine the speed of the vehicle and to calibrate the effective radius of the wheels. Once the effective radius of the wheel is known and with the information supplied by the wheel encoder, the receiver is also able to identify the loss of several consecutive rows in those tracks that present errors, thus allowing the synchronization of the successive bits not to be lost.

The track encodes a set of words that are defined by a first Start bit, a succession of data bits 0 and 1 and a last End bit. The set of data bits must be of a sufficient size to allow the road network to be encoded uniquely worldwide.

The earth's surface has a surface area of 510.1 million km²[182]. According to equation (9), each square centimeter of the earth's surface can be encoded uniquely by a combination of 63 bits.

$$Log_2(510{,}1\ km^2) = Log_2(510 \cdot 10^{18}\ cm^2) = 62{,}1 \qquad (9)$$

The area covered by the road network is a very small percentage of the total surface of the planet, which also includes the area occupied by the oceans, the poles and the mountain ranges where there are no roads. In addition, it must be taken into account that a 64-bit code corresponds to 5.94 metres of lane, the area of which includes more than 20,000 square centimetres that do not need to be coded.

Thus, it is considered that a 64-bit coding dimension will allow the entire existing network to be coded. It will also be sufficient to contemplate future expansions of the network or modifications to the infrastructure due to possible resurfacing tasks. In these works, the existing codes will be replaced by new codes to avoid problems of inconsistency with previous versions of road maps that have not been conveniently updated.

To facilitate easy deployment of the track, it is proposed to use a unique pseudo-random sequence. To do this, each of the painting trucks must have a set of unique codes that, once printed, cannot be repeated. This track will be printed in the vicinity of the central axis without the need for the geometry of the track to match the geometry of the central axis of the lane to facilitate painting tasks.

Once the painting is finished, a vehicle equipped with precision odometry, cameras for detecting the markings that delimit the lane and a GNSS receiver travels along the track storing the sequence of codes together with its GNSS position and the deviations recorded with respect to the real geometry of the lane. This information will then be stored in the memory of vehicles that have a track reader. Since this is information of a few hundred bytes per kilometer of lane, it is estimated that a 32 GB flash memory will be sufficient to store the entire road network deployed in the world.

The coded track is only passed over by the wheels of vehicles when they change lanes. Taking into account that the material used to code the track is extremely resistant to abrasion and that the reading systems are resilient to occasional

track failures, it is estimated that the track's useful life will be longer than the asphalt's useful life, so that track maintenance will not be necessary and a new track will only be deployed each time new asphalt is laid.

4.3.2. Testing a first deployment

A road painting truck has been adapted to deploy a coding system similar to that proposed 4.3.1 to deploy 1,200 meters of track in the City of León. The adaptation of the truck has consisted of inserting a relay in each of the cables that activate the 4 extruders that print the markings. These relays are governed by a micro-controller that determines which extruders are activated and which are not in each row. The paint marks deployed are made of thermoplastic material and are white in color and their choice responds to a criterion of machinery availability. Their approximate dimensions are 45x45x6 mm3. A subsequent painting in green has been carried out on the track to demarcate a safe area in the lane for low-mobility vehicles such as scooters and bicycles. The word size has been reduced to 17 bits instead of 64 to facilitate the identification of complete position codes to optical devices. The purpose of deploying this track is to serve as a demonstrator for assisting public transport buses. Figure 21 shows several sections of the track.

Figure 21 Coded track deployed in Leon city to support public transport

A device has been installed on one of the municipal buses, which has a camera that takes images of the asphalt every 4 seconds. The images obtained have demonstrated the capacity of this type of sensor to read the track under all types of lighting conditions thanks to the shadows generated at the edges of each mark. A radar sensor has not been installed on the underside of the vehicle due to the space and technical difficulties involved in its installation.

The track has been in place for a year. Although thermoplastic paint is a softer material than dual-component cold plastic paint, no damage or signs of wear on the track have been observed during this time. No incidents have been reported with pedestrians, scooters, bicycles or motorcycles.

4.3.3. Reading the coded track

The coded track can be read by optical cameras such as those fitted in rear-view mirrors or on the back of some vehicles. Although the markings are black, similar to that of asphalt, the shadows generated at the edges of each drop when illuminated by the sun or by the vehicle's headlights facilitate their identification, and computer vision systems allow the track to be decoded. However, this reading method is considered more appropriate when the vehicle is stopped or travelling at low speed.

Reading the track using a radar sensor has multiple advantages over reading using optical cameras or other types of sensors. In this case, the sensor does not measure the retro-reflectivity of the surface but the distance between the sensor and the surface where the waves are reflected. In this way, the reading is not affected by dirt that may affect the sensor, by low retro-reflectivity of the surface, by low lighting of the environment or by adverse weather conditions. In addition to these advantages, the radar can perform measurements with sampling frequencies greater than 30 kHz. This sampling frequency corresponds to a sample every 1.1 millimetres of advance on the infrastructure when a vehicle travels at 120 km/h. Table 33 shows a comparison of the different sensors capable of reading a coded track.

	Precisión de la medida	Tiempo de la medida	Fiabilidad en condiciones lumínicas adversas	Fiabilidad en entornos sucios	Bajo coste
Cámara óptica	-	*	*	*	***
Lidar	**	**	**	**	*
Infrarrojos	**	**	**	**	**
Radar de ondas milimétricas	***	***	***	***	***

Table 3 Comparison of sensors for reading the coded track

The sensor is installed on the underside of the vehicle and consists of a linear array of 24 radars arranged every 20 millimetres perpendicular to the longitudinal axis of the vehicle. Each radar scans an area of the asphalt with a diameter of 1 cm called a spot and measures the distance to the surface with an error of better than one millimetre.

The sensor can detect each bit in real time as it passes over it. Taking into account that the diameter of the drops is 45 mm, that the width of the radiation spot of each radar is 10 mm and that there is a sufficient sampling frequency to determine the exact moment of passing over the highest point of the drop, the positioning error when a radar points to the centre of a drop is close to one centimetre.

When a sensor starts reading the track, it begins to detect the sequence of bits that it passes over. Once the vehicle has advanced at least 6 metres, the sensor has read a complete 64-bit code. In this way, the location of this code can be consulted in the memory map, the direction of travel of the vehicle can be determined and other parameters associated with the position can be consulted, such as the maximum speed and the recommended speed of the track segment in question. In addition, the following codes in the sequence and their geometry can be consulted in said memory. From this moment on, each time the sensor passes a new row, it is checked that the bit read matches the expected one in the sequence. In this case, the position of the vehicle is updated by increasing the previous position by 90 millimetres.

The information supplied during the reading of the track by the wheel and steering wheel encoders is used to calibrate the steering system and calculate the effective radius of the wheels. In addition, this information must match the geometry of the track stored in the vehicle memory. Otherwise, a possible malfunction of the system or manipulation of the track will be detected and the last valid position and the data from the encoders will be taken as a reference to estimate the position of the vehicle using the dead-reckoning technique.

This same position estimation technique allows, in the event of a sudden failure of the track reading system, the vehicle to continue travelling in its lane for 200 metres using only the wheel and steering wheel encoders as sources of information provided that the initial starting point, the orientation of the vehicle with respect to the centre axis of the lane and the effective radius of the wheels are accurate [183].

4.3.4. Design and results of the first prototype

A first prototype sensor has been designed, built and tested. The aim of this first prototype is to demonstrate the ability of radars to read tracks encoded by means of raised paint marks. The sensor consists of two printed circuits. A first circuit integrates an array of 4 radars arranged linearly. The radars have a dielectric lens coupled to concentrate the radiation pattern as shown in Figure 22. This card is coupled to another printed circuit equipped with an FPGA where the signal from the 4 radars is processed.

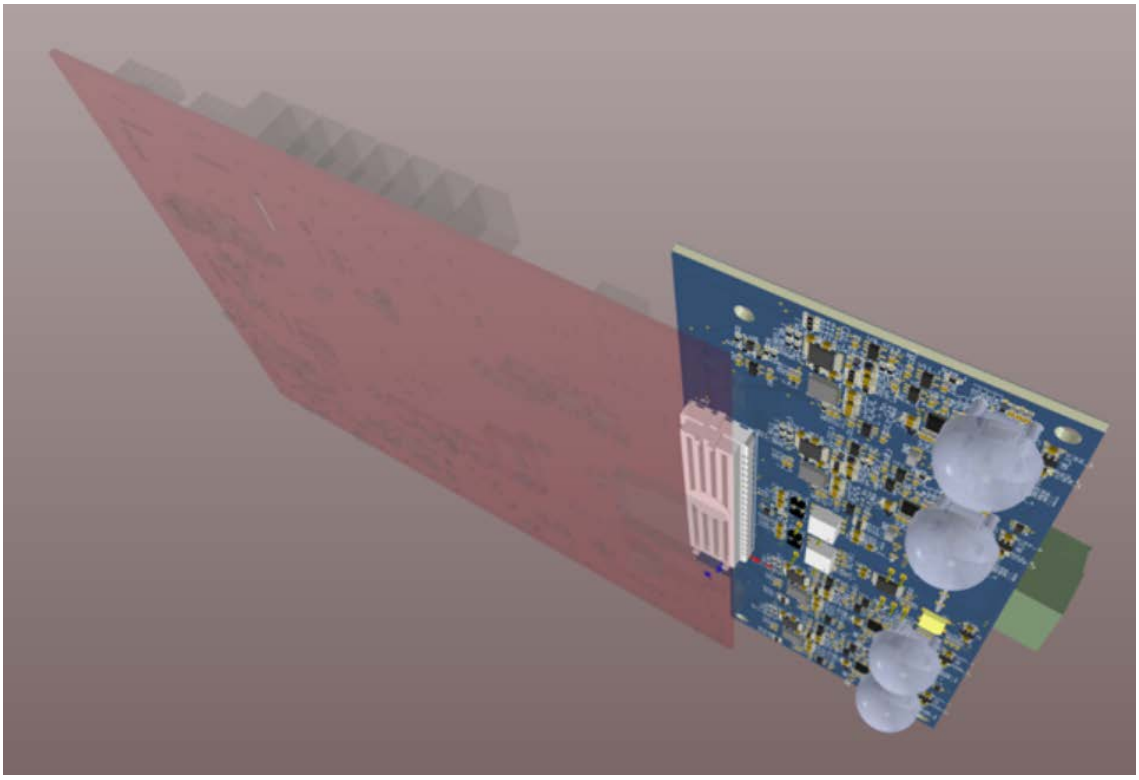

Figure 22. Design of the second prototype

Each lens generates a circular spot of 1 cm in diameter at a distance of 12 cm, which corresponds to the typical distance between the underside of a conventional vehicle and the road surface. The sensor has been installed on the underside of an electric vehicle for children that is driving on a test track.

The separation between the two inner radars is 60 millimetres. The outer radars are 30 millimetres from the inner radars. Each radar integrates a 5 mm by 5 mm QFN32 chip similar to that used 4.3.4. However, the chip model used is TRA_120_031 which, unlike the previous model, transmits a bandwidth of 18 GHz. The reason why a different model with a higher bandwidth has been selected is to be able to detect targets that are very close in frequency.

Continuous wave and FM radars have difficulty detecting very close targets that are not received with high power. This is due to the coupling that exists between the transmitting and receiving antennas due to their close proximity to each other. This coupling causes the beat signal to have a strong component close to 0 hertz, which corresponds to a signal with a flight time (the time it takes for the signal to propagate from the transmitting to the receiving antenna) of almost zero.

In an ideal case, the beat signal generated when the radar scans a single static target at a specific distance is a sinusoidal signal whose frequency depends on the distance. The Fourier transform of this signal observed during the period of the chirp signal corresponds to a sinc signal centered on the beat frequency. Figure 22 shows the Fourier transform of an observation window of size T0.

Continuous wave and FM radars have difficulty detecting very close targets that are not received with high power. This is due to the coupling that exists between the transmitting and receiving antennas due to their close proximity to each other. This coupling causes the beat signal to have a strong component close to 0 hertz, which corresponds to a signal with a flight time (the time it takes for the signal to propagate from the transmitting to the receiving antenna) of almost zero.

In an ideal case, the beat signal generated when the radar scans a single static target at a specific distance is a sinusoidal signal whose frequency depends on the distance. The Fourier transform of this signal observed during the period of the chirp signal corresponds to a sinc signal centered on the beat frequency. Figure 23 shows the Fourier transform of an observation window of size T_0.

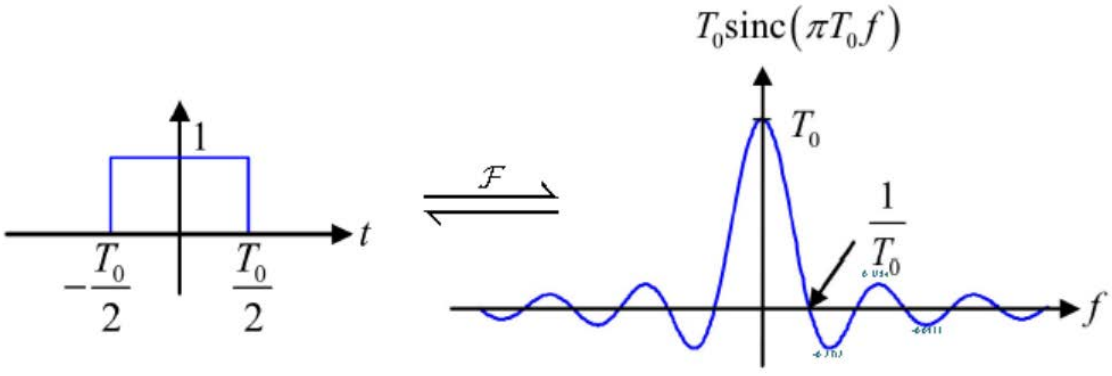

Figure 23. Fourier transform of a rectangular observation window

This ideal sync signal is distorted in real radars for various reasons such as the oscillator phase noise, the non-linearities of the signal generation system and the frequency multipliers used to reach the working frequency, the amplitude modulations caused by a frequency response of the different components and

antennas of the system that varies throughout the transmitted bandwidth, etc. Thus, the signal of a single target in the frequency domain has a specific form for each type of radar and working configuration, which is called PSF (Point Spread Function). The PSF that appears centered at 0 hertz extends towards higher frequencies and can hide the signal of a nearby target that is less powerful than the coupling between antennas. One way of trying to solve the problem could be to increase the target beat frequency by decreasing the period T of equation (2). However, with this, the PSF also widens proportionally, so the problem of overlapping between signals continues to occur, although the same phenomenon occurs at a higher frequency. One way to avoid this problem is to increase the radar bandwidth until the target's beat frequency does not fall within the PSF of the antenna coupling. Thanks to this new chip model that transmits at 18 GHz, it is possible to correctly identify targets at a distance of 12 centimeters.

The designed sensor consists of 4 radars that are integrated into a single PCB as shown in Figure 23 where each beat signal is also amplified and digitized.

The designed sensor consists of 4 radars that are integrated into a single PCB as shown in Figure 24 where each beat signal is also amplified and digitized.

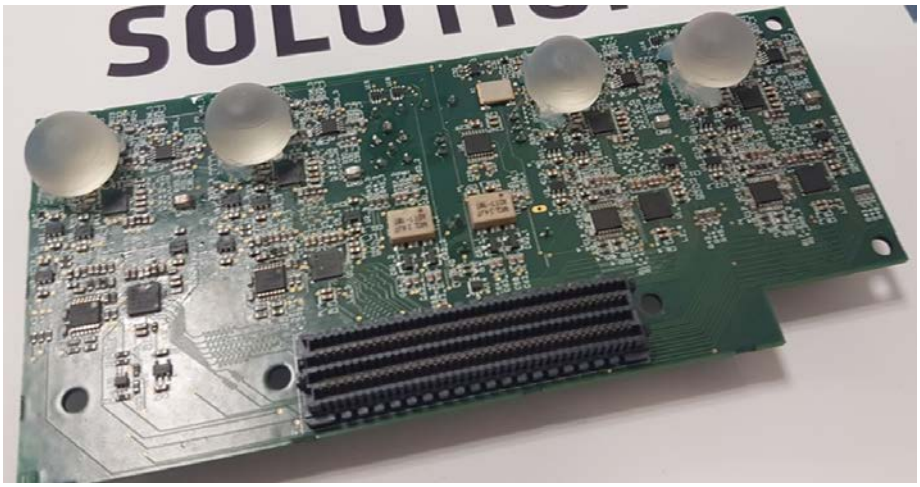

Figure 24. 4-channel radar prototype for low-speed vehicle guidance

A second card that is coupled to this one is responsible for processing the signals in real time as shown in Figure 25. . This card is the Picozed model from AVNET that integrates a Zynq-7010 model FPGA from the manufacturer Xilinx.

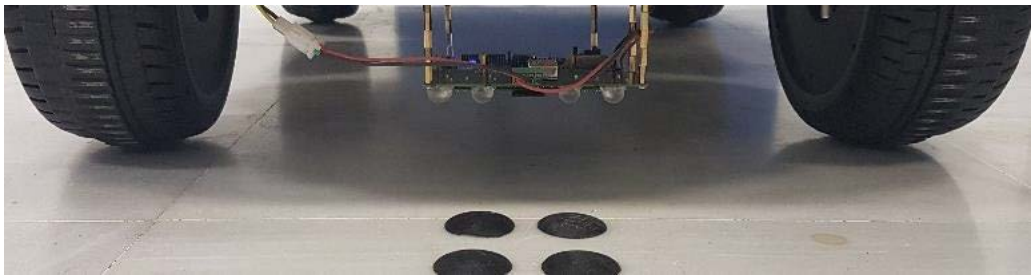

Figure 25. Detail of the experiment setup

Given the sensor's limitation in terms of the number of available radar channels, the test track consists of a series of rows of 2 drops of paint that do not encode information. This prototype could serve as a line-following sensor with progress control by detecting each row of a vehicle traveling at low speed.

The track consists of drops of cold, dual-component plastic paint, 45 millimeters in diameter and 6 millimeters high, arranged on two longitudinal axes that are 90 millimeters apart. Figure 25 shows the test track setup and the vehicle equipped with the radar sensor.

Given the sensor's limitation in terms of the number of available radar channels, the test track consists of a series of rows of 2 drops of paint that do not encode information. This prototype could serve as a line-following sensor with progress control by detecting each row of a vehicle traveling at low speed.

The track consists of drops of cold, dual-component plastic paint, 45 millimeters in diameter and 6 millimeters high, arranged on two longitudinal axes that are 90 millimeters apart. Figure 26 shows the test track setup and the vehicle equipped with the radar sensor.

Figure 26. Low speed vehicle guidance track setup

In this figure, two drops of paint can be seen that are slightly displaced from their axes. Figure 26 shows the Boolean decisions of each of the signal processing systems of each radar to determine the presence or absence of a drop on the radar along the track. In this figure, it can be observed how, due to the effect of the acceleration of the vehicle, the pulse corresponding to each row of drops is compressed as the vehicle advances and increases its speed.

In this figure, two drops of paint can be seen that are slightly displaced from their axes. Figure 27 shows the Boolean decisions of each of the signal processing systems of each radar to determine the presence or absence of a drop on the radar along the track. In this figure, it can be observed how, due to the effect of the acceleration of the vehicle, the pulse corresponding to each row of drops is compressed as the vehicle advances and increases its speed.

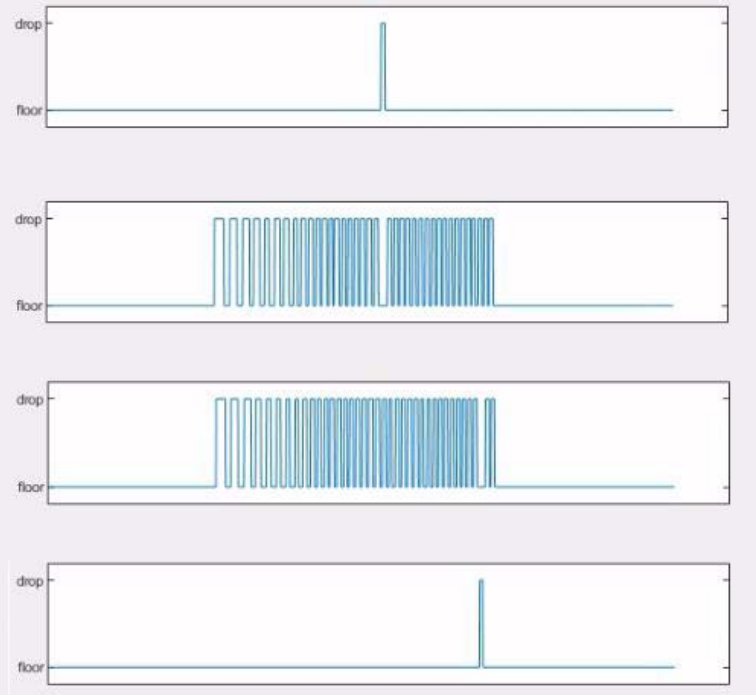

Figure 27. Drop detections from each of the 4 radar channels

It can also be observed how the drops that are slightly displaced are not detected by the corresponding central channel and, however, are detected by the adjacent outer channel.

4.3.5. Design and results of the second prototype

The track deployed in 3.3.3 does not have a sufficient number of columns to encode the information described in 3.3.1. Furthermore, the dynamic conditions of a vehicle travelling at speeds of up to 120 km/h are very different from those of the vehicle used in 3.3.3, so there will be a lateral displacement of the vehicle which will cause it to not travel exactly on the track. For this reason, it is necessary to increase the number of radar elements in the array to an appropriate size. Taking into account that each row of the track has a width of 315 mm, it is proposed to develop a sensor equipped with 24 radar channels equally spaced every 2 centimetres. In this way, a FoV of 480 mm is achieved, which is considered sufficient for a sensor on board a vehicle travelling at 120 km/h to be able to read the track. In the event of a misalignment greater than that allowed by the sensor, the number of columns of the track read by the radar sensor will be progressively reduced.

The track deployed in 4.3.4 does not have a sufficient number of columns to encode the information described in 4.3.1 Furthermore, the dynamic conditions of a vehicle travelling at speeds of up to 120 km/h are very different from those of the vehicle used in 4.3.4 so there will be a lateral displacement of the vehicle which will cause it to not travel exactly on the track. For this reason, it is necessary to increase the number of radar elements in the array to an appropriate size. Taking into account that each row of the track has a width of 315 mm, it is proposed to develop a sensor equipped with 24 radar channels equally spaced every 2 centimetres. In this way, a FoV of 480 mm is achieved, which is considered sufficient for a sensor on board a vehicle travelling at 120 km/h to be able to read the track. In the event of a misalignment greater than that allowed by the sensor, the number of columns of the track read by the radar sensor will be progressively reduced.

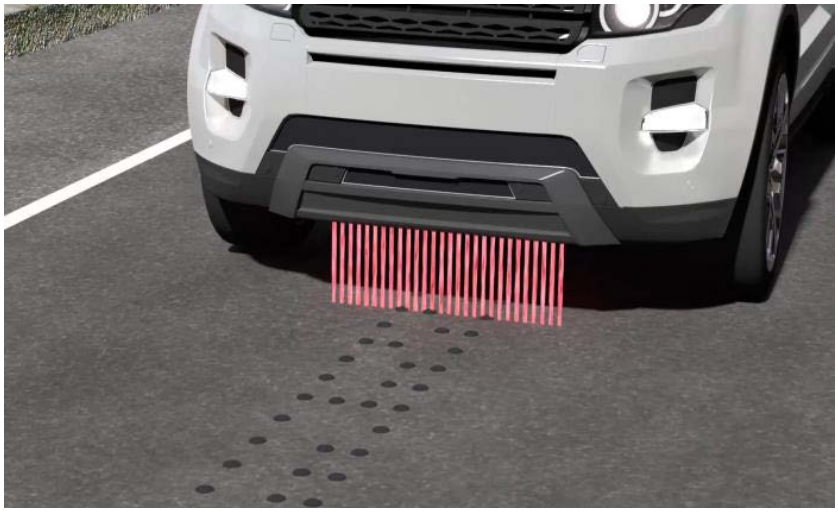

Figure 28. 24-channel radar array

Scaling the design described in 4.3.5 requires a high investment due to the cost associated with each channel. Table 4 details the approximate costs of the main elements of this architecture.

Radar frontend 120 GHz	300 €
PLL	10 €
ADC	60 €
FPGA	150 €

Table 4 Approximate costs of a radar sensor

To reduce the final cost of the sensor, a new design has been made that uses radars typically used in the automotive industry for obstacle detection. The model chosen is the TI6843AOP from the manufacturer Texas Instruments. Like the radar used in 4.2.3 the chip includes the VCO, the frequency multipliers, the mixer and the antennas. In addition, this model incorporates the PLL that controls the VCO, the beat signal amplifier, the ADC and the signal processing required to determine the distance to the target. Its approximate cost is €16. However, its bandwidth is limited to 4 GHz. Due to the limitations described in 4.3.4, this bandwidth is insufficient to resolve targets at 12 centimeters.

One way to avoid this limitation is to increase the distance to the target by inserting an elliptical reflector in between as shown in Figure 29.

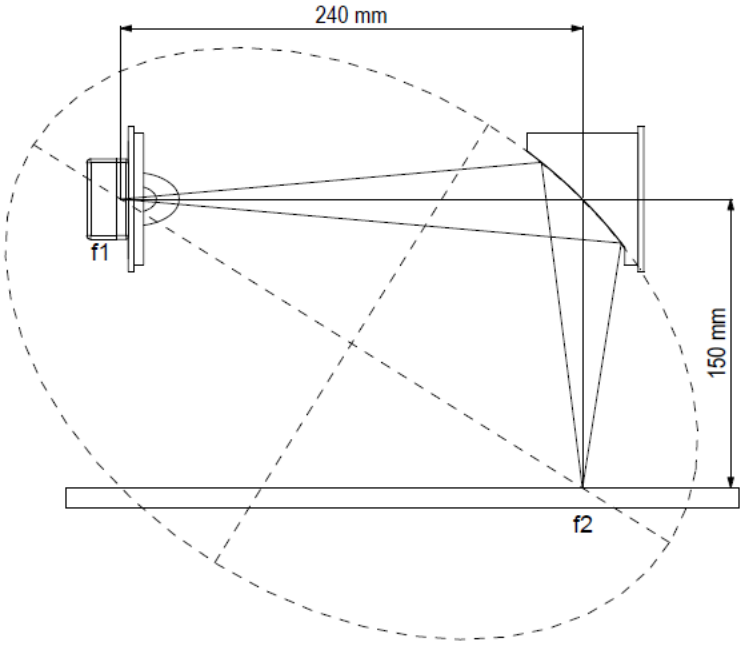

Figure 29. Elliptical reflector design

In order for the reflector to focus correctly, the radar antenna must be positioned at the focus of the ellipse and the radar must concentrate its energy on the surface of the reflector. This is achieved by means of a lens that is attached to the surface of the chip.

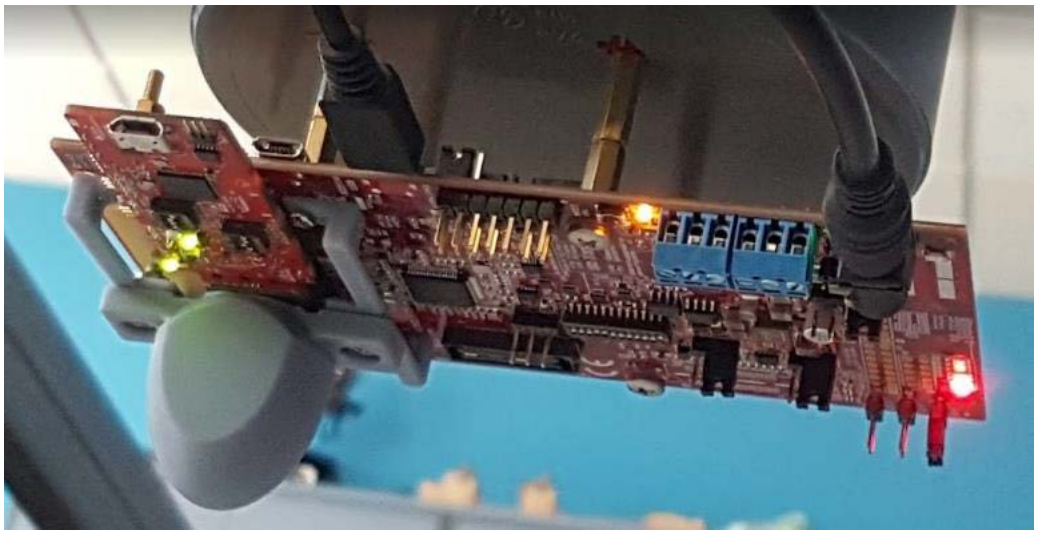

Figure 30. IWR4803AOP RAAR Evaluation Board with Lens Attached

The correct positioning of the prototype is achieved with the help of a PVC pipe and a pair of custom-made parts made with a 3D printer. The first of these is attached to the inside of the tube and has a surface with the required elliptical curve that acts as a reflector. A metallic paper has been glued to this surface to improve the reflection of the radar signal. The second piece is also attached to the inside of the tube at the other end and has the appropriate supports to correctly anchor the evaluation board supplied by the radar manufacturer.

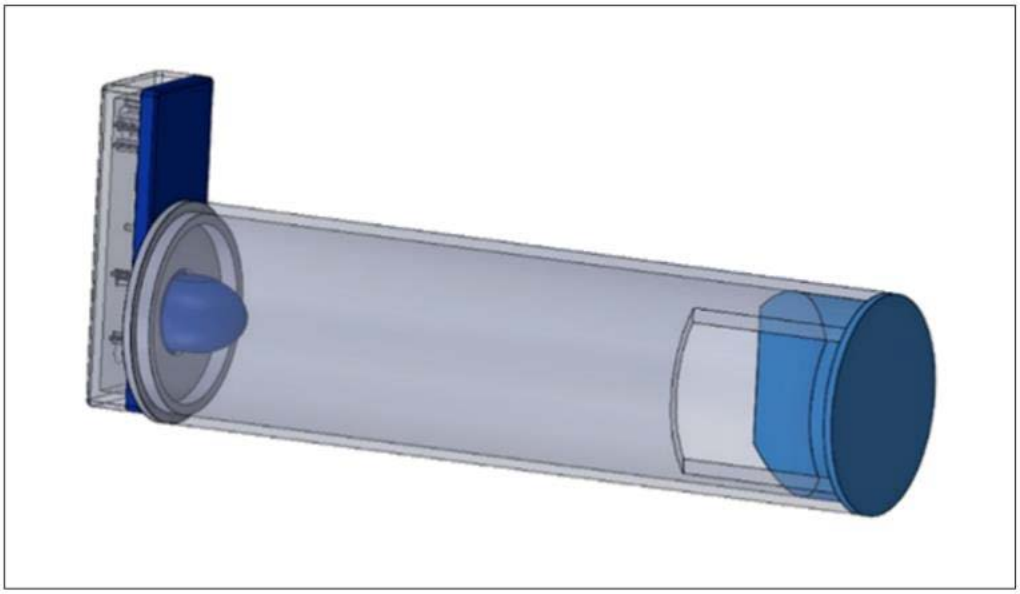

Figure 31. Radar sensor and elliptical reflector positioning system

Measurements have been taken to check that the radiant system concentrates the energy on an area of approximately one centimetre in diameter above the ground with the help of a metal rod. One of the drops of paint used in 4.3.4 has also been moved over the spot to check that the sensor detects it correctly.

Figure 32 shows the sensor temporarily attached to the body of a vehicle and a set of paint drops deployed in a suitable manner so that they are passed over by the sensor when the vehicle starts moving. It has been verified that the sensor detects the drops correctly. A short 1 km route has also been made to explore the asphalt and check that its surface is measured correctly throughout the journey.

Figure 32. Onboard radar setup

Once the capabilities of this prototype to detect and measure asphalt and raised droplets have been demonstrated, it is proposed to make a third prototype that incorporates 24 identical radar sensors and a processing system that allows the track to be decoded from the radar profiles supplied by each chip. The objective of this prototype is to demonstrate the ability to read a coded track at high speed in a real environment and the vehicle's guidance capacity.

Due to time constraints, this prototype is outside the scope of this Thesis and is proposed as a future line of action in 6.

5. Applications of radar positioning

5.1. Railway applications

5.1.1. Correlation of radar profiles for speed determination

In 1.4.1, the main techniques for determining train speed using on-board sensors and the main drawbacks of each are described. The importance of determining the speed of the train with high precision to determine the position of the train using odometry is also described.

Other techniques based on the temporal correlation of signals have been explored to determine train speed. In these, a first sensor records a measurement that remains invariant over time for a given static position but that varies with the progress of the train. In this way, this measurement behaves as if it were a signature present in the infrastructure. A second identical sensor, installed at a known distance, records the same information. Subsequently, a signal processing system performs a correlation of both records to detect the delay that exists between both signals.

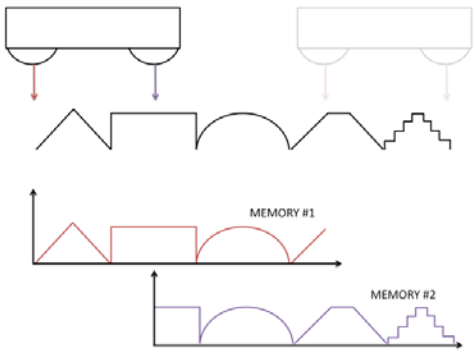

Figure 33. Working principle of the time correlation system

The main advantage of this type of technique is that it allows the measurement error to be limited by increasing the distance between sensors. Figure 33 shows the relative error in determining the speed by correlating samples taken every 30 µs by two sensors 60 cm apart.

The main advantage of this type of technique is that it allows the measurement error to be limited by increasing the distance between sensors. Figure 34 shows the relative error in determining the speed by correlating samples taken every 30 µs by two sensors 60 cm apart.

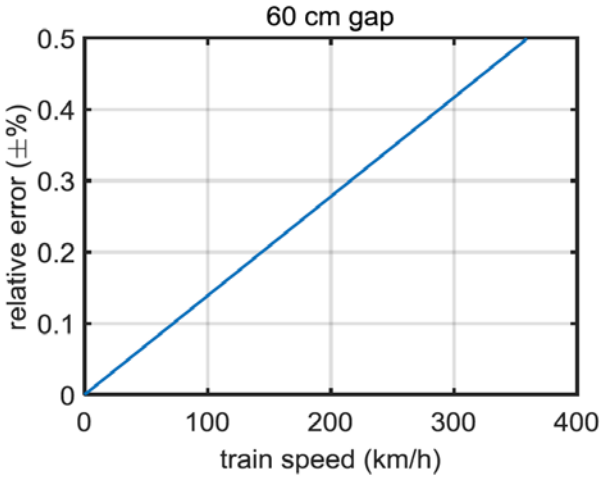

Figure 34. Relative speed error obtained by correlating 30 µs samples and 60 cm gap

In [69], [184], [185] this technique is applied using optical cameras that point at the floor of the infrastructure. For a correct operation of this solution, it is necessary that both sensors are free of dirt. In addition, the system must be able to function in extreme or changing lighting conditions.

In [68], [186], [187] two magnetic sensors are used to detect the disturbances caused by the rail and by the presence of the rail fixing screws and clamps. In [67]], two Doppler radars are used. Due to the lack of repeatability, reliability and precision, none of these solutions are currently commercially exploited.

Another correlation method proposed in this Thesis is to use as a correlation signal the profile obtained by a millimetre wave radar which obtains a detailed profile of the infrastructure as the vehicle advances. Appendix D describes the operating principle and shows the results obtained from a prototype.

5.1.2. Precise stop

Precise train stopping is a necessary requirement at stations equipped with platform doors. To facilitate passenger boarding, the doors of the train cars must match the platform doors at the stopping point. These platform doors are

typically deployed at subway stations and mass transit systems such as Automated People Movers.

Figure 35. Platform doors

Platform doors prevent people from falling onto the track, which causes numerous human losses and huge service interruptions, increase passenger capacity at stations, reduce passenger boarding and disembarking times, allow for more efficient station air conditioning and facilitate a higher level of automation in train operations.

The most commonly used technique consists of deploying a beacon a few metres from the stopping point and applying, as it passes, a calibrated braking force[188], [189], [190], [191], [192], [193], [194], [195], [196], [197], [198], [199]. This calibration is obtained for each station through a series of previous tests in which a specific train approaches at different speeds. There are also systems that self-calibrate the braking curve at all times taking as a reference the errors made at the last stops. The precision of this technique is usually about ±25 cm since there are numerous parameters that influence the result that are considered constant in the calculation but that can be variable over time such as the number of passengers on board or the coefficient of friction between wheel and rail at each point of the route. This last parameter can vary abruptly in the event of an oil or liquid spill on the track.

The most commonly used technique consists of deploying a beacon a few metres from the stopping point and applying, as it passes, a calibrated braking force [188], [189], [190], [191], [192], [193], [194], [195], [196], [197], [198], [199]. This calibration is obtained for each station through a series of previous tests in which

a specific train approaches at different speeds. There are also systems that self-calibrate the braking curve at all times taking as a reference the errors made at the last stops. The precision of this technique is usually about ±25 cm since there are numerous parameters that influence the result that are considered constant in the calculation but that can be variable over time such as the number of passengers on board or the coefficient of friction between wheel and rail at each point of the route. This last parameter can vary abruptly in the event of an oil or liquid spill on the track.

The beacon described in 4.2.2 is an alternative to this technique that provides feedback of the train's position and speed to the braking system in real time and accurately throughout the stopping process. In this way, the braking system can dynamically calculate the braking intensity at each instant. In addition, it allows the safety systems to verify that the train is stopped in the correct position once the braking process has finished. In Annex D, you can consult the results obtained on a Ferrocarrils de la Generalitat de Catalunya train with the prototype described in 4.2.4.

5.1.3. Protection against impact to buffer stops

The rail ends of railway yards or the ends of the line usually have a buffer stop to prevent the train from advancing [200]. Although both the train and the buffers usually have shock absorbers to absorb part of the energy in the event of an impact, their effectiveness is very limited due to the enormous amount of movement that the train can accumulate when travelling at speed. Figure 35 shows examples of impacts against buffers that have occurred in Spain in recent years.

The rail ends of railway yards or the ends of the line usually have a buffer stop to prevent the train from advancing [200]. Although both the train and the buffers usually have shock absorbers to absorb part of the energy in the event of an impact, their effectiveness is very limited due to the enormous amount of movement that the train can accumulate when travelling at speed. Figure 36 shows examples of impacts against buffers that have occurred in Spain in recent years.

Figure 36: Trains crashing into buffer stops in Spain

For this reason, many buffer zones have an additional safety mechanism consisting of one or more RFID beacons deployed at a certain safety distance. Each of them can trigger an emergency braking of the train if the speed exceeds a certain threshold. They can also trigger an emergency braking regardless of the speed if the beacon exceeded delimits a no-traffic zone.

This protection system has two problems. The first is that, if the emergency braking system is triggered at the beacon closest to the buffer zone and the driver, once the train has stopped, starts moving again, the protection system is disabled. The second problem with this system is related to the safety distance between the closest beacon and the buffer zone. An end-of-line station usually has a beacon deployed at the entrance to it that limits the approach speed of the train. To ensure smooth traffic, this speed threshold is usually set at 20 km/h. Thus, it may be the case that a train passes the last safety beacon at 20 km/h. In such a case, a sufficiently large distance to the buffer must be available to allow the speed to be reduced to a safe level where the impact is adequately absorbed. This condition may entail a high investment, especially if the end of the line is located underground.

Similarly, the precise stopping system described in 4.1.2 can be used as a safety system to prevent an approach to an end of line or buffer. This solution solves the two problems raised above. On the one hand, a continuous beacon makes it possible to define an approach speed limit every 5 cm. In this way, the speed limit can be progressively reduced even at very low running speeds as the position approaches the buffer. On the other hand, a continuous beacon system makes it possible to reset the safety trigger as many times as necessary. Once the train enters the prohibited zone, each time the train moves in the wrong direction, the alarm will be triggered.

Similarly, the precise stopping system described in 5.1.2 can be used as a safety system to prevent an approach to an end of line or buffer. This solution solves the two problems raised above. On the one hand, a continuous beacon makes it possible to define an approach speed limit every 5 cm. In this way, the speed limit can be progressively reduced even at very low running speeds as the position approaches the buffer. On the other hand, a continuous beacon system makes it possible to reset the safety trigger as many times as necessary. Once the train enters the prohibited zone, each time the train moves in the wrong direction, the alarm will be triggered.

5.1.4. Other applications

The precise positioning of a train described in 4.2.1, which uses the infrastructure signature itself as a source of information, can be useful for implementing moving-block type systems, eliminating or reducing to a minimum the necessary track equipment. It can also be used as a system to assist in the digitalisation of the infrastructure [227] or to apply efficient driving algorithms in which the train's traction is modulated based on the specific point of the route and the result of the simulations obtained that consider the train dynamics and the characteristics of the route.

5.2. Road transport applications

5.2.1. LDWS/ALKS

The operating principle of current LDWS/ALKS systems and their limitations are described in 1.4. These driving assistance systems reduce accidents [202]. However, these systems still lack sufficient availability and reliability. Therefore, other solutions should be explored to complement the decision-making of these systems to improve their availability and reliability. The adaptation proposed in 4.3.1 can help in this regard. This adaptation provides suitably equipped vehicles with a new lane-keeping mechanism that does not have the difficulties presented by systems based on optical cameras and the retro-reflectivity of road markings.

In addition to increasing the reliability and availability of current LDW/ALKS systems, this solution provides a safe handover mechanism to SAE Level 3 autonomous driving systems that addresses the high-speed driving issue described in 1.4.2 by providing safe guidance using the dead-reckoning technique

for 200 meters. This safety distance can be used to progressively reduce the vehicle speed, thus providing sufficient response time to the driver or, in the worst case, to stop the vehicle if necessary.

5.2.2. Intelligent Speed Assistance

European Union regulations require that the ISA (Intelligent Speed Assistance) system be incorporated into all vehicles manufactured in Europe from 2022 onwards. This system uses the information captured by the video cameras equipped on board to identify those signs that limit the speed and thus know the maximum speed allowed on the section of road on which the vehicle is travelling [203], [204], [205]. This regulation also contemplates being able to estimate the speed limit of the road on which the vehicle is travelling using the information supplied by a GNSS receiver and the information from a road map stored in the vehicle's memory. The objective of the ISA system is to alert the driver that he or she is travelling at an inappropriate speed. The European Union contemplates that, once the ISA system detects that the vehicle is travelling at a speed higher than that established, this system notifies the driver of the excess speed through three possible mechanisms. The first mechanism consists of a hardening of the accelerator pedal that forces the driver to exert greater force on the pedal to maintain the same level of acceleration. The second mechanism consists of an electronic restriction of the vehicle's thrust system that limits the engine power. The third mechanism consists of an acoustic and light signal that warns the driver of the excess. The driver has the option of temporarily deactivating this warning system. However, the system will automatically re-arm itself the next time the vehicle is started.

European Union regulations require that the ISA (Intelligent Speed Assistance) system be incorporated into all vehicles manufactured in Europe from 2022 onwards. This system uses the information captured by the video cameras equipped on board to identify those signs that limit the speed and thus know the maximum speed allowed on the section of road on which the vehicle is travelling [203], [204], [205]. This regulation also contemplates being able to estimate the speed limit of the road on which the vehicle is travelling using the information supplied by a GNSS receiver and the information from a road map stored in the vehicle's memory. The objective of the ISA system is to alert the driver that he or she is travelling at an inappropriate speed. The European Union contemplates that, once the ISA system detects that the vehicle is travelling at a speed higher

than that established, this system notifies the driver of the excess speed through three possible mechanisms. The first mechanism consists of a hardening of the accelerator pedal that forces the driver to exert greater force on the pedal to maintain the same level of acceleration. The second mechanism consists of an electronic restriction of the vehicle's thrust system that limits the engine power. The third mechanism consists of an acoustic and light signal that warns the driver of the excess. The driver has the option of temporarily deactivating this warning system. However, the system will automatically re-arm itself the next time the vehicle is started.

Current ISA systems are limited in their reliability in estimating the speed limit of the road on which a vehicle is travelling. Sometimes video cameras are obscured by extreme ambient lighting conditions, or image processing systems fail to adequately detect road signs due to poor weather conditions. There are also occasions when other large vehicles driving or stopped in front of the vehicle prevent the cameras from seeing the signs. Speed estimation based on GNSS positioning also suffers from unreliability. Sometimes the position accuracy is not good enough to identify the exact road on which a vehicle is travelling, or it is simply not available. Speed maps stored in the vehicle's memory may also not be up-to-date.

The adaptation of the infrastructure proposed in 3.3.1 allows to increase the reliability and availability of current ISA systems. In addition, the reading of the coded track allows to define speed limits every 90 mm. This property is of particular interest in urban environments as it allows to define a progressive maximum speed curve as a vehicle approaches, for example, a pedestrian crossing. In this case, when the vehicle approaches the pedestrian crossing, the speed limit can be progressively reduced to 5 km/h. At this speed, a pedestrian can escape from a threatening vehicle and the damage suffered in the event of an impact is mitigated.

The adaptation of the infrastructure proposed in 4.3.1 allows to increase the reliability and availability of current ISA systems. In addition, the reading of the coded track allows to define speed limits every 90 mm. This property is of particular interest in urban environments as it allows to define a progressive maximum speed curve as a vehicle approaches, for example, a pedestrian crossing. In this case, when the vehicle approaches the pedestrian crossing, the speed limit can be progressively reduced to 5 km/h. At this speed, a pedestrian

can escape from a threatening vehicle and the damage suffered in the event of an impact is mitigated.

5.2.3. Data sharing between vehicles

Current vehicles can identify an object in a vectorized manner by estimating its distance and angle to the object and are even able to classify it as a pedestrian or a vehicle. However, even though many advances have been made [206], [207], [208], [209], [210], [211], they are still not able to perceive the environment with adequate precision. These limitations are typically related to an insufficient dynamic range and an insufficient instantaneous dynamic range of the sensors. Dynamic range is the relationship between the highest intensity level that the sensor can record without distorting the signal and the minimum detectable level or sensitivity. The instantaneous dynamic range is the dynamic range that a sensor has at a given instant in which it can simultaneously detect both limit excitations.

Another limitation characteristic of the sensors used to perceive the environment properly is their limited detection range and the difficulties in detecting objects behind other objects, beyond changes in elevation or before going around corners. These limitations are directly related to the lack of spatial dispersion of the sensors. All the sensors are on board the vehicle and all perspectives start from the same point.

These limitations could be reduced if the vehicles could share the detection vectors of their sensors via radio with the rest of the connected vehicles. However, in order to be able to transpose a vector, it is necessary to have the exact coordinates of the position and orientation of the two vehicles that exchange information with respect to an absolute reference system.

The adaptation of the infrastructure described in 4.3.1 facilitates an absolute reference system that enables the transposition of detection vectors. This capability exponentially increases vehicle perception since, in addition to being able to use its sensor network, it can use the sensor network of vehicles circulating in the vicinity.

5.2.4. Unmanned Platooning

The technique known as platooning involves a group of trucks travelling in a convoy in a synchronised manner by means of a virtual coupling between vehicles

with the aim of reducing energy consumption and polluting emissions [212], [213]. These improvements are achieved by reducing the aerodynamic resistance of the group thanks to a minimum separation between vehicles. The first vehicle in the convoy is called the leader and the rest of the vehicles are called followers. Drivers of follower vehicles have a driving assistance system that automatically manages the acceleration and braking of the vehicle to maintain a fixed distance from the preceding vehicle. This distance between vehicles, for safety reasons, is usually about 6 metres.

There is a variant of platooning called unmanned platooning which is also being tested, in which drivers are eliminated from follower vehicles thanks to a higher level of automation of the vehicles [214], [215], [216], [217], [218], [219], [220], [221], [222], [223], [224], [225]. In this way, a platoon or convoy is led by a single driver. The main advantage of this variant is the reduction of road transport costs associated with the driver, which typically account for 40% of the final costs.

The follower vehicles of unmanned platooning systems have a set of cameras that identify the position of the vehicle in front of them and radar sensors to measure the distance to it. With this information, the vehicle guidance system can follow the vehicle at a given distance. However, this type of virtual coupling between vehicles suffers from a cumulative error in the position of the follower vehicles, which causes the last vehicles in long convoys to invade another lane.

The adaptation of the infrastructure described in 4.3.1 resolves these limitations. The leader vehicle records the precise trajectory it follows, taking the coded track as a reference. This information is shared with the other vehicles in the convoy and replicated by them. In this way, it is possible to implement long convoys that act as a train on the asphalt in which all vehicles describe the same trajectory. This solution is claimed in one of the patents in Annex A.

This patent also provides for a secure communications network between vehicles. This communications network is achieved through a wired system between vehicles similar to the helical cables that interconnect the tractor units of trucks with their trailers to transmit brake force and lights. Thanks to this wired network, communication with quality of service or QoS (Quality of Service) can be provided, which, unlike radio networks, guarantees that the information transmitted by the leader is propagated to the rest of the vehicles within a certain time. In the event of a failure in the interconnection, the vehicles detect

the communication failure and the convoy switches to a safe mode in which the speed of the vehicle is progressively reduced.

Current Ethernet communication networks allow transmission speeds of 10 Gbps and propagation delays of less than 1.3 µs between nodes [226]. This makes it possible to reduce the safety distance between vehicles to 1 meter. This increases the aerodynamic efficiency of the convoy and simplifies the physical interconnection of vehicles using helical cables. In the event of a failure or disconnection, a follower vehicle traveling at 100 km/h that identifies the communication failure in less than 50 µs will travel 1.4 mm to react appropriately. Assuming that the speed of the predecessor vehicle is like that of the vehicle that loses communication at the time of the failure, the safety distance will remain unchanged when the vehicles in the convoy switch to safe driving mode.

The physical interconnection between vehicles using helical cables, in addition to providing a QoS communication channel, enables the exchange of energy between vehicles. This exchange of energy allows the vehicles in the convoy to have a small electric battery to operate autonomously for a limited time during exceptional situations, but normally receive a flow of energy from another unit in the convoy. Thus, for example, one or more of the vehicles in the convoy can have a hydrogen-powered generator that supplies energy to the rest of the vehicles. This solution makes it possible to reduce the weight of the batteries in electric vehicles and to reduce the costs of equipping each vehicle in the convoy with a hydrogen generator.

5.2.5. Path recording

It is becoming more and more common to find vehicles on the road with driver assistance systems and even vehicles equipped with autonomous driving systems. The introduction of this type of vehicle poses a challenge for insurance companies or the police to determine responsibility in the event of an accident. Detecting possible malfunctions in the software systems that make decisions about driving can be a tedious task due to the enormous amount of code used. Having a device that records, like a black box, the trajectory, speed and position of the vehicle accurately can be of great help in clarifying what happened and simplifying the determination of responsibility.

5.2.6. Synchronized traffic flows

One of the challenges of mobility in urban environments is to provide safe transport to users and pedestrians, which is free of polluting emissions and is agile and efficient. Current traffic light systems for regulating traffic do not optimise mobility to the maximum. The capacity of these systems to work in a coordinated manner is limited and their decision algorithms do not take into account the individual routes planned for each vehicle.

The adaptation of the infrastructure described in 3.3.1 allows vehicles to share their position and speed with a traffic regulating element that can make decisions based on the type of vehicle, its current position and its destination. These decisions can affect, for example, something as simple as the authorisation of a vehicle or group of vehicles to access a crossing, but they can also affect the authorisations for movement of each vehicle individually, in a similar way to how rail traffic is regulated. For example, it is possible for vehicles connected to the regulating element to cross a junction in a coordinated manner with the other connected vehicles circulating at the junction without the risk of collision between them. This solution prevents the regulating element from having to prioritise the movement of the vehicles, allowing for greater energy efficiency and greater mobility capacity.

One of the challenges of mobility in urban environments is to provide safe transport to users and pedestrians, which is free of polluting emissions and is agile and efficient. Current traffic light systems for regulating traffic do not optimise mobility to the maximum. The capacity of these systems to work in a coordinated manner is limited and their decision algorithms do not take into account the individual routes planned for each vehicle.

The adaptation of the infrastructure described in 4.3.1 allows vehicles to share their position and speed with a traffic regulating element that can make decisions based on the type of vehicle, its current position and its destination. These decisions can affect, for example, something as simple as the authorisation of a vehicle or group of vehicles to access a crossing, but they can also affect the authorisations for movement of each vehicle individually, in a similar way to how rail traffic is regulated. For example, it is possible for vehicles connected to the regulating element to cross a junction in a coordinated manner with the other connected vehicles circulating at the junction without the risk of collision between them. This solution prevents the regulating element from having to

prioritise the movement of the vehicles, allowing for greater energy efficiency and greater mobility capacity.

6. Conclusions and future work

This Thesis proposes a solution for vehicle positioning and guidance in which on-board radar sensors read information encoded in the infrastructure.

The prototypes described in 4.2.3, 4.2.4, 4.3.4 and 4.3.5 show that it is possible to read information encoded in the infrastructure using on-board radar devices in a vehicle following a track. These radar devices detect different logical levels of information depending on the distance they measure to the exact location on the structure on which they are travelling where the waves are reflected. This type of reading has numerous advantages over others, including its speed and high reliability in adverse lighting or weather conditions or in dirty environments.

Vehicles that read information encoded in the infrastructure can know their position with centimetre precision as described in 4.3.3. To achieve this, a map previously stored in the vehicle's memory associates each information code with a specific position. When the sensor reads a complete code, the vehicle knows its position. From this point on, the vehicle can update its position at bit level as it reads the track without having to read another complete code. That is, it can update its position every 9 centimetres of progress.

In railway environments, this solution is implemented in 4.2.2 using PVC pipes that have a set of metal sheets inside at different heights. In 4.2.4 it is demonstrated that the developed system can stop a train at an exact point with a precision better than 2.5 cm. This solution is of particular interest to achieve the precise stopping of the train in stations that have platform doors. It can also be applied to avoid train collisions with line ends or buffers.

In 5.1.1, an on-board method is described for determining the speed of a train by temporal correlation of two radar profiles of the infrastructure, which is an order of magnitude more accurate than the sensors used by current signalling systems.

A future line of work remains to be defined, which train control device will receive the information supplied by the equipment described in 4.2.4 and the format in which both devices will share the information so that this equipment becomes a commercial product.

In road transport, the adaptation of the infrastructure described in 4.3.1 allows the entire road network to be digitalised without interfering with road users in a

simple, low-cost way that does not require any maintenance throughout the life of the asphalt. A 1,200-metre-long track has been deployed in the city of León using the coding system proposed in this thesis. During the year that the test has lasted, the track has not generated interference problems with the different types of users, including buses, vans, cars, motorcycles, bicycles, electric scooters, pedestrians and people with reduced mobility.

This adaptation allows to substantially improve the current reliability of the LDWS and ALKS systems and solves the problems associated with the driver's reaction time in the high-speed handover of SAE Level 3 autonomous driving systems.

It also allows ISA systems to define progressive speed limits in urban environments that substantially improve pedestrian safety.

Vehicle driving assistance systems have a better perception of the environment if, instead of using only their own sensors, they also use the sensors of other vehicles circulating in the vicinity. These other sensors have a different perspective of the scene and allow the detection distance to be increased. The absolute reference system provided by the coded track allows the transposition of the detection vectors between vehicles as described in 5.2.3.

Nowadays, the European Union is promoting the transport technique called Platooning with the aim of reducing polluting emissions and improving road transport capacity. The proposed system solves the current length limitations of unmanned convoys by eliminating the cumulative positioning error between vehicles. It also allows reducing the safety distance between vehicles to facilitate a physical interconnection between vehicles that allows the exchange of energy while driving.

Patents US 10,853,606 B2, US 10,824,152 B2, US 11,814,089 B2, US 11,565,733 B2 and US 2021/0232156 A1 described in Annex B recognize the innovative nature of the different solutions developed in this Thesis.

In 4.3.5, the future work proposes the design of a sensor equipped with 24 radar devices that allows testing the high-speed vehicle guidance system in real environments.

Regardless of the advances that other technologies may offer to improve vehicle positioning, having a digitalized infrastructure that allows vehicles to read

information from it to position themselves will always provide a higher level of safety.

In the era of digitalization, it is foreseeable that, sooner or later, the road network will also end up being digitalized to improve the efficiency, capacity and safety of the transport of goods and people. Given the enormous extension of the road network, this digitalization must involve an adaptation that is easy to deploy and low cost. This Thesis proposes a solution that meets both requirements.

6.1. Achievements and technical constraints

This Thesis proposes a solution that meets both requirements, demonstrating the feasibility of using millimetre-wave radar systems to guide and position vehicles on both road and rail infrastructure. Through the design, prototyping, and testing of multiple systems, this research has shown that radar devices can effectively read information encoded within the infrastructure to determine the precise position of vehicles, offering a reliable solution under various environmental conditions. These conclusions reflect the achievements of the project using this set of key concepts:

1. The research confirmed the viability of using on-board radar sensors to extract encoded data from infrastructure elements. The use of radar technology presents significant advantages compared to traditional methods, such as its resilience to adverse weather conditions, including poor lighting, heavy rainfall, or fog. Additionally, radar systems are unaffected by debris, dirt, or contaminants that could compromise optical or camera-based systems.

- The primary challenge addressed was how to adapt road and railway infrastructure to be compatible with radar technology without significant modifications to the existing network. By deploying paint markings for roads and PVC pipes with embedded metal reflectors for railway tracks, this research provided a low-cost, easily scalable solution for integrating radar-readable signatures into existing infrastructures.
- The research produced several working prototypes, which were tested in controlled and real-world environments. In road vehicle applications, paint

markings were successfully deployed along a 1200-metre section of road in León, Spain. Testing showed that radar-equipped vehicles could detect these markings at speeds of up to 120 km/h with centimetre-level accuracy. For railways, PVC pipes with embedded reflectors allowed a train to be stopped within a precision of 2.5 cm, an essential feature for metro systems and stations with platform doors.

- Technological Innovation in Radar Systems is one of the key contributions of this thesis, contributing of how commercially available radar technology can be adapted for vehicle guidance. By employing radar components commonly used in automotive industries, such as Texas Instruments' radar chips, the project achieved significant cost savings while maintaining high performance. This technological innovation lays the groundwork for future industrialisation of the system.

2. The successful deployment of radar-based vehicle positioning systems offers several notable advantages over existing technologies.
    - Millimetre-wave radars provide highly accurate distance measurements, allowing vehicles to determine their exact position with minimal error. This capability is particularly valuable for applications requiring high precision, such as autonomous vehicle guidance or collision avoidance systems in both road and rail environments. The radar systems tested in this research demonstrated centimetre-level precision, a critical feature for tasks like precise vehicle stopping in metro stations or determining a vehicle's lane position on motorways.
    - Resilience to Environmental Factors as key aspects of radar uses. Unlike optical systems or LIDAR, millimetre-wave radars are unaffected by poor lighting, fog, rain, or snow. This robustness ensures that the systems can function effectively in diverse conditions without requiring additional sensors or supplementary technologies. For example, during the year-long road tests in León, the system showed no interference from varying weather conditions or road users, maintaining consistent performance.
    - The proposed radar-guidance systems offer significant advantages in terms of low maintenance and scalability. The infrastructure modifications, such as raised paint markings or embedded reflectors in PVC pipes, are designed to be long-lasting and resistant to environmental wear. These

modifications also do not interfere with regular traffic, meaning that they can be implemented without major disruption to current road or railway networks. The simplicity and durability of the system make it an attractive option for large-scale deployment.

3. Despite the success of the prototypes, several challenges and technical limitations remain that must be addressed in future research.

- One of the main technical challenges encountered was radar signal interference from environmental factors, such as water. While raised paint markings were designed to mitigate this, radar signals could still be affected by large pools of water accumulating on the road surface. Similarly, railway tracks faced challenges from uneven surfaces or obstacles like debris on the tracks, which could impact the radar's ability to accurately read reflectors.
- Another limitation identified was the difficulty of ensuring precise radar detection at high speeds. While the road vehicle system functioned well at speeds up to 120 km/h, there were instances where vehicle misalignment or uneven track surfaces caused signal loss. Further refinements to radar antenna design and processing algorithms are necessary to ensure reliable performance at higher speeds and with greater misalignment tolerances.
- Although the project successfully reduced costs by using commercially available radar components, further cost optimisations are needed to make the system viable for widespread industrial use. Additionally, integrating the radar data with existing vehicle control systems, such as autonomous driving platforms or signalling systems, presents another challenge. Future work must focus on standardising the data formats and ensuring seamless communication between the radar sensors and vehicle control systems.

6.2. Future Directions and Recommendations

The conclusions of this thesis point to several promising directions for future research and development. Key recommendations include:

- Further Prototyping and Testing.

  While the prototypes developed for both road and railway systems showed great promise, further testing is needed to refine these systems for commercial deployment. Larger-scale tests, with longer road and railway sections, will provide more data on the system's performance under varying conditions, including different weather patterns, vehicle types, and speeds .

- Integration with Autonomous Systems.

  The radar-based positioning system has the potential to play a significant role in future autonomous driving technologies. Integrating this system with autonomous vehicle platforms, including platooning and smart city infrastructures, is a crucial next step. The ability to provide precise positioning data will greatly enhance the safety and reliability of autonomous vehicles .

- Exploring Other Applications.

  Beyond vehicle positioning, millimetre-wave radar technology can be explored for other applications, including industrial automation, robotics, and even aviation. Its capacity to detect objects in complex environments makes it a valuable tool for a wide range of sectors where precise, real-time data is required.

- Addressing Legal and Regulatory Considerations.

  As the deployment of radar-based systems increases, addressing legal and regulatory frameworks will be essential. Collaboration with government agencies and transport authorities will ensure that the system complies with existing safety regulations while promoting innovation in transport technologies. The development of standardised protocols for radar communication and data-sharing will also be important for international adoption.

6.3. Final considerations

This thesis has contributed significantly to the development of millimetre-wave radar technology for vehicle positioning and guidance. Through innovative design, prototyping, and real-world testing, the research has shown that radar

systems can offer a precise, reliable, and scalable solution for both road and railway vehicles. The advantages of radar technology—its resilience to environmental conditions, high precision, and low maintenance—make it an ideal candidate for future transport systems, especially in the context of increasing automation and smart city infrastructure.

However, challenges such as signal interference, high-speed detection, and integration with existing systems must be addressed to ensure the system's commercial viability. The future of transport will likely rely heavily on such advancements, and the foundations laid by this research provide a strong platform for continued innovation in this field. By refining the technology, addressing the remaining challenges, and exploring new applications, millimetre-wave radar systems have the potential to revolutionise the way vehicles interact with their environments, ultimately contributing to safer, more efficient transport networks.

References

[1] A. Garcia-Pino *et al.*, "Bifocal Reflector Antenna for a Standoff Radar Imaging System With Enhanced Field of View," *IEEE Trans Antennas Propag*, vol. 62, no. 10, pp. 4997–5006, 2014, doi: 10.1109/TAP.2014.2346214.

[2] B. Mencia-Oliva, J. Grajal, O. A. Yeste-Ojeda, G. Rubio-Cidre, and A. Badolato, "Low-Cost CW-LFM Radar Sensor at 100 GHz," *IEEE Trans Microw Theory Tech*, vol. 61, no. 2, pp. 986–998, 2013, doi: 10.1109/TMTT.2012.2235457.

[3] J. Grajal *et al.*, "3-D High-Resolution Imaging Radar at 300 GHz With Enhanced FoV," *IEEE Trans Microw Theory Tech*, vol. 63, no. 3, pp. 1097–1107, 2015, doi: 10.1109/TMTT.2015.2391105.

[4] G. Rubio-Cidre *et al.*, "Characterization of a 300 GHz imaging radar for standoff detection," in *2014 International Radar Conference*, 2014, pp. 1–6. doi: 10.1109/RADAR.2014.7060389.

[5] F. García-Rial *et al.*, "Optimization of a compact THz imaging radar for real-time operation," in *2016 Global Symposium on Millimeter Waves (GSMM) & ESA Workshop on Millimetre-Wave Technology and Applications*, 2016, pp. 1–4. doi: 10.1109/GSMM.2016.7500299.

[6] A. Badolato *et al.*, "A 300 GHz imaging radar for standoff anomaly detection," in *2015 9th European Conference on Antennas and Propagation (EuCAP)*, 2015, pp. 1–5.

[7] J. Grajal *et al.*, "Compact Radar Front-End for an Imaging Radar at 300 GHz," *IEEE Trans Terahertz Sci Technol*, vol. 7, no. 3, pp. 268–273, 2017, doi: 10.1109/TTHZ.2017.2673544.

[8] B. Mencia-Oliva, J. Grajal, A. Badolato, A. García-Pino, J. L. Besada Sanmartín, and O. A. Yeste-Ojeda, "Experimental radar imager with sub-cm range resolution at 300 GHz," in *2013 IEEE Radar Conference (RadarCon13)*, 2013, pp. 1–6. doi: 10.1109/RADAR.2013.6586084.

[9] R. J. Dengler *et al.*, "600 GHz Imaging Radar with 2 cm Range Resolution," in *2007 IEEE/MTT-S International Microwave Symposium*, 2007, pp. 1371–1374. doi: 10.1109/MWSYM.2007.380468.

[10] A. Maestrini *et al.*, "A 540-640-GHz high-efficiency four-anode frequency tripler," *IEEE Trans Microw Theory Tech*, vol. 53, no. 9, pp. 2835–2843, 2005, doi: 10.1109/TMTT.2005.854174.

[11] R. J. Dengler, F. Maiwald, and P. H. Siegel, "A Compact 600 GHz Electronically Tunable Vector Measurement System for Submillimeter Wave Imaging," in *2006 IEEE MTT-S International Microwave Symposium Digest*, 2006, pp. 1923–1926. doi: 10.1109/MWSYM.2006.249792.

[12] P. S. Chakraborty *et al.*, "A 0.8 THz f_ MAX SiGe HBT Operating at 4.3 K," *IEEE Electron Device Letters*, vol. 35, no. 2, pp. 151–153, 2014, doi: 10.1109/LED.2013.2295214.

[13] K. Schmalz, R. Wang, J. Borngräber, W. Debski, W. Winkler, and C. Meliani, "245 GHz SiGe transmitter with integrated antenna and external PLL," in *2013 IEEE MTT-S International Microwave Symposium Digest (MTT)*, 2013, pp. 1–3. doi: 10.1109/MWSYM.2013.6697430.

[14] E. Öztürk *et al.*, "A 120 GHz SiGe BiCMOS Monostatic Transceiver for Radar Applications," in *2018 13th European Microwave Integrated Circuits Conference (EuMIC)*, 2018, pp. 41–44. doi: 10.23919/EuMIC.2018.8539874.

[15] O. Momeni and E. Afshari, "A 220-to-275GHz traveling-wave frequency doubler with −6.6dBm Power at 244GHz in 65nm CMOS," in *2011 IEEE International Solid-State Circuits Conference*, 2011, pp. 286–288. doi: 10.1109/ISSCC.2011.5746321.

[16] E. Öjefors, B. Heinemann, and U. R. Pfeiffer, "Active 220- and 325-GHz Frequency Multiplier Chains in an SiGe HBT Technology," *IEEE Trans Microw Theory Tech*, vol. 59, no. 5, pp. 1311–1318, 2011, doi: 10.1109/TMTT.2011.2114364.

[17] K. Sengupta and A. Hajimiri, "Distributed active radiation for THz signal generation," in *2011 IEEE International Solid-State Circuits Conference*, 2011, pp. 288–289. doi: 10.1109/ISSCC.2011.5746322.

[18] H. Song, H. Liu, and E. Schnieder, "A Train-Centric Communication-Based New Movement Authority Proposal for ETCS-2," *IEEE Transactions on*

Intelligent Transportation Systems, vol. 20, no. 6, pp. 2328–2338, 2019, doi: 10.1109/TITS.2018.2868179.

[19] E. Ates and I. Ustoglu, "An Approach for Moving Block Signalling System and Safe Distance Calculation," in *2018 6th International Conference on Control Engineering & Information Technology (CEIT)*, 2018, pp. 1–4. doi: 10.1109/CEIT.2018.8751745.

[20] D. Zamouche, S. Aissani, M. Omar, and N. Saad, "Safety-Oriented Train Control Systems Monitoring in Smart Railway Transportation: A Review," in *2022 4th International Conference on Pattern Analysis and Intelligent Systems (PAIS)*, 2022, pp. 1–8. doi: 10.1109/PAIS56586.2022.9946872.

[21] H. Song, S. Gao, Y. Li, L. Liu, and H. Dong, "Train-Centric Communication Based Autonomous Train Control System," *IEEE Transactions on Intelligent Vehicles*, vol. 8, no. 1, pp. 721–731, 2023, doi: 10.1109/TIV.2022.3192476.

[22] A. Kochan and E. Koper-Olecka, "Mathematical Model of the Movement Authority in the ERTMS/ETCS System," 2020, pp. 215–224. doi: 10.1007/978-3-030-27687-4_22.

[23] M. V Nikolić, B. D. Kosić, M. D. Milanović, N. M. Antonić, Ž. M. Stojković, and I. Z. Kokić, "Railway axle counter prototype," in *2014 22nd Telecommunications Forum Telfor (TELFOR)*, 2014, pp. 694–697. doi: 10.1109/TELFOR.2014.7034503.

[24] Y. Liu, W. Tong, X. Jin, and Z. Li, "Magnetic Circuit Modeling and Analysis of Unilateral Axle-Counting Sensor," *IEEE Access*, vol. 6, pp. 51834–51842, 2018, doi: 10.1109/ACCESS.2018.2868293.

[25] C. Wei *et al.*, "A Fiber Bragg Grating Sensor System for Train Axle Counting," *IEEE Sens J*, vol. 10, no. 12, pp. 1905–1912, 2010, doi: 10.1109/JSEN.2010.2049199.

[26] G. Stroud, "Managing a culture change - introduction of axle counters," in *The IEE Seminar on Safety Assurance, 2005. (Ref. No. 2005/11081)*, 2005, pp. 11 pp.–9/9. doi: 10.1049/ic:20050412.

[27] N. T. Hai and D. Q. Thach, "Design and Manufacturing of Axle Counting Equipment," in *2023 12th International Conference on Control, Automation and Information Sciences (ICCAIS)*, 2023, pp. 51–55. doi: 10.1109/ICCAIS59597.2023.10382316.

[28] P. R. Goundan and A. Jhunjhunwala, “Axle counter based block signalling for safe and efficient train operations,” in *Gateway to 21st Century Communications Village. VTC 1999-Fall. IEEE VTS 50th Vehicular Technology Conference (Cat. No.99CH36324)*, 1999, pp. 824–828 vol.2. doi: 10.1109/VETECF.1999.798444.

[29] I. Z. Kokić, M. V Nikolić, B. D. Kosić, M. D. Milanović, N. M. Antonić, and Ž. M. Stoiković, “Railway axle counter remote supervision system,” in *2014 22nd Telecommunications Forum Telfor (TELFOR)*, 2014, pp. 698–701. doi: 10.1109/TELFOR.2014.7034504.

[30] M. V Nikolić, B. D. Kosić, M. D. Milanović, N. M. Antonić, Ž. M. Stojković, and I. Z. Kokić, “Railway axle counter prototype,” in *2014 22nd Telecommunications Forum Telfor (TELFOR)*, 2014, pp. 694–697. doi: 10.1109/TELFOR.2014.7034503.

[31] L. Zhao, B. Cai, J. Xu, and Y. Ran, “Study of the Track–Train Continuous Information Transmission Process in a High-Speed Railway,” *IEEE Transactions on Intelligent Transportation Systems*, vol. 15, no. 1, pp. 112–121, 2014, doi: 10.1109/TITS.2013.2274617.

[32] T. Serdiuk, M. Feliziani, and K. Serdiuk, “About Electromagnetic Compatibility of Track Circuits with the Traction Supply System of Railway,” in *2018 International Symposium on Electromagnetic Compatibility (EMC EUROPE)*, 2018, pp. 242–247. doi: 10.1109/EMCEurope.2018.8485034.

[33] S. Tetiana, K. Vitaliy, S. Kseniia, N. Anatoliy, K. Yevheniia, and K. Alisa, “Improvement of Technical Service of Track Circuits,” in *2019 IEEE 6th International Conference on Energy Smart Systems (ESS)*, 2019, pp. 28–32. doi: 10.1109/ESS.2019.8764191.

[34] J. Fan and W. Yang, “Impedance Analysis of Track Circuit with Power Eye Graph,” in *2020 IEEE 23rd International Conference on Intelligent Transportation Systems (ITSC)*, 2020, pp. 1–5. doi: 10.1109/ITSC45102.2020.9294713.

[35] L. Zhao, B. Cai, J. Xu, and Y. Ran, “Study of the Track–Train Continuous Information Transmission Process in a High-Speed Railway,” *IEEE Transactions on Intelligent Transportation Systems*, vol. 15, no. 1, pp. 112–121, 2014, doi: 10.1109/TITS.2013.2274617.

[36] B. Xu, Y. Tong, K. Li, L. Zhu, K. Zheng, and S. Ma, "Key Technology Research on Jointless Track Circuit in High-speed Railway," in *2018 International Conference on Information Systems and Computer Aided Education (ICISCAE)*, 2018, pp. 443–445. doi: 10.1109/ICISCAE.2018.8666892.

[37] X. Du, J. Zou, and Z. Wang, "Calculation of the Impedance of a Rail Track With Earth Return for the High-Speed Railway Signal Circuit Using Finite-Element Method," *IEEE Trans Magn*, vol. 51, no. 3, pp. 1–4, 2015, doi: 10.1109/TMAG.2014.2360884.

[38] X. Du, J. Zou, and Z. Wang, "Calculation of the Impedance of a Rail Track With Earth Return for the High-Speed Railway Signal Circuit Using Finite-Element Method," *IEEE Trans Magn*, vol. 51, no. 3, pp. 1–4, 2015, doi: 10.1109/TMAG.2014.2360884.

[39] S. Dhahbi, A. Abbas-Turki, S. Hayat, and A. El Moudni, "Study of the high-speed trains positioning system: European signaling system ERTMS / ETCS," in *2011 4th International Conference on Logistics*, 2011, pp. 468–473. doi: 10.1109/LOGISTIQUA.2011.5939444.

[40] T. Kurz, R. Hornstein, H. Schweinzer, M. Balik, and M. Mayer, "Time Synchronization in the Eurobalise Subsystem," in *2007 IEEE International Symposium on Precision Clock Synchronization for Measurement, Control and Communication*, 2007, pp. 70–77. doi: 10.1109/ISPCS.2007.4383776.

[41] H. Guo, J. Z. Wei Sim, B. Veeravalli, and J. Lu, "Protecting Train Balise Telegram Data Integrity," in *2018 21st International Conference on Intelligent Transportation Systems (ITSC)*, 2018, pp. 806–811. doi: 10.1109/ITSC.2018.8569616.

[42] D. Franco, M. Aguado, C. Pinedo, I. Lopez, I. Adin, and J. Mendizabal, "A Contribution to Safe Railway Operation: Evaluating the Effect of Electromagnetic Disturbances on Balise-to-BTM Communication in Railway Control Signaling Systems," *IEEE Vehicular Technology Magazine*, vol. 16, no. 2, pp. 104–112, 2021, doi: 10.1109/MVT.2021.3051567.

[43] T. Wang and L. Zhao, "Modeling and optimization for balise coupling process in high speed railway," in *2017 7th IEEE International Symposium*

on Microwave, Antenna, Propagation, and EMC Technologies (MAPE), 2017, pp. 176–179. doi: 10.1109/MAPE.2017.8250829.

[44] D. Liang, H. Zhao, and H. Quan, "Research on dynamic pattern of balise up-link signal based on the electromagnetic field theory," in *2013 IEEE International Conference on Intelligent Rail Transportation Proceedings*, 2013, pp. 154–158. doi: 10.1109/ICIRT.2013.6696285.

[45] S. Ping, L. Xueming, S. Gang, F. Caixin, T. Wanxiu, and Y. Zhongkang, "Research on Electromagnetic Interference Coupling Law of BTM Antenna on EMU," in *2022 5th Asia Conference on Energy and Electrical Engineering (ACEEE)*, 2022, pp. 140–146. doi: 10.1109/ACEEE56193.2022.9851865.

[46] Y. Wen, Q. Geng, J. Xiao, Y. Zhu, and D. Zhang, "Study on the Electromagnetic Susceptibility of Balise Transmission Module System," in *2018 International Conference on Electromagnetics in Advanced Applications (ICEAA)*, 2018, pp. 667–670. doi: 10.1109/ICEAA.2018.8520469.

[47] Y. Wen, Q. Geng, J. Xiao, Y. Zhu, and D. Zhang, "Study on the Electromagnetic Susceptibility of Balise Transmission Module System," in *2018 International Conference on Electromagnetics in Advanced Applications (ICEAA)*, 2018, pp. 667–670. doi: 10.1109/ICEAA.2018.8520469.

[48] Y. Wen, Q. Geng, J. Xiao, Y. Zhu, and D. Zhang, "Study on the Electromagnetic Susceptibility of Balise Transmission Module System," in *2018 International Conference on Electromagnetics in Advanced Applications (ICEAA)*, 2018, pp. 667–670. doi: 10.1109/ICEAA.2018.8520469.

[49] T. Wang and L. Zhao, "Modeling and optimization for balise coupling process in high speed railway," in *2017 7th IEEE International Symposium on Microwave, Antenna, Propagation, and EMC Technologies (MAPE)*, 2017, pp. 176–179. doi: 10.1109/MAPE.2017.8250829.

[50] H. Sporleder, "Continuous automatic train control and cab signalling with the LZB 80," in *International Conference on Main Line Railway Electrification 1989*, 1989, pp. 40–46.

[51] H. Sporleder, "Continuous automatic train control and cab signalling with the LZB 80," in *International Conference on Main Line Railway Electrification 1989*, 1989, pp. 40–46.

[52] T. Chen, H. Wang, B. Ning, Y. Zhang, T. Tang, and K. Li, "Architecture Design of a Novel Train-centric CBTC System," in *2018 International Conference on Intelligent Rail Transportation (ICIRT)*, 2018, pp. 1–5. doi: 10.1109/ICIRT.2018.8641603.

[53] X. Wang, T. Tang, and S. Liu, "Study on modeling and verification of CBTC interlocking system," in *5th IET International Conference on Wireless, Mobile and Multimedia Networks (ICWMMN 2013)*, 2013, pp. 350–354. doi: 10.1049/cp.2013.2439.

[54] "IEEE Standard for Communications-Based Train Control (CBTC) Performance and Functional Requirements," *IEEE Std 1474.1-2004 (Revision of IEEE Std 1474.1-1999)*, pp. 0_1-45, 2004, doi: 10.1109/IEEESTD.2004.95746.

[55] W. Sun, H. Wang, and B. Bu, "Feasibility research on train-ground information transmission based on leaky coaxial cable in CBTC," in *Proceedings of 2011 IEEE International Conference on Service Operations, Logistics and Informatics*, 2011, pp. 574–578. doi: 10.1109/SOLI.2011.5986626.

[56] C. Stallo *et al.*, "Geo-Distributed Simulation and Verification Infrastructure for safe train Galileo-based positioning," in *2020 European Navigation Conference (ENC)*, 2020, pp. 1–10. doi: 10.23919/ENC48637.2020.9317431.

[57] A. Basili, L. Ghisu, F. Rispoli, B. Buttarazzi, A. Neri, and F. Senesi, "A roadmap for the adoption of space assets for train control systems: The Test Site in Sardinia," in *2012 IEEE First AESS European Conference on Satellite Telecommunications (ESTEL)*, 2012, pp. 1–6. doi: 10.1109/ESTEL.2012.6400066.

[58] J. Otegui, A. Bahillo, I. Lopetegi, and L. E. Díez, "A Survey of Train Positioning Solutions," *IEEE Sens J*, vol. 17, no. 20, pp. 6788–6797, 2017, doi: 10.1109/JSEN.2017.2747137.

[59] A. P. Gonzalo *et al.*, "Observations on track evolution from onboard inertial measurements," in *2022 UKACC 13th International Conference on Control (CONTROL)*, 2022, pp. 18–23. doi: 10.1109/Control55989.2022.9781456.

[60] T. Qin, G. Zheng, D. Jin, and J. Wang, "A novel Doppler Effect testing approach for highspeed railway wireless communication systems," in *2011 International Conference on Electronics, Communications and Control (ICECC)*, 2011, pp. 657–660. doi: 10.1109/ICECC.2011.6066666.

[61] T. Thi Huong and N. Duc Anh, "Doppler frequency compensation basing the velocity of train and high-speed railway scenario," in *2019 International Conference on Advanced Technologies for Communications (ATC)*, 2019, pp. 155–159. doi: 10.1109/ATC.2019.8924519.

[62] Y. Niu, J. Ding, D. Fei, Z. Zhong, and Y. Liu, "Doppler Effect on High-Speed Railway at 465 MHz," in *2019 IEEE International Symposium on Antennas and Propagation and USNC-URSI Radio Science Meeting*, 2019, pp. 2117–2118. doi: 10.1109/APUSNCURSINRSM.2019.8888372.

[63] T. Liu, X. Ma, R. Zhao, H. Dong, and L. Jia, "Doppler Shift Estimation for High-Speed Railway Scenario," in *2016 IEEE 83rd Vehicular Technology Conference (VTC Spring)*, 2016, pp. 1–5. doi: 10.1109/VTCSpring.2016.7504198.

[64] A. Neri, F. Rispoli, and P. Salvatori, "A GNSS based solution for supporting virtual block operations in train control systems," in *2015 International Association of Institutes of Navigation World Congress (IAIN)*, 2015, pp. 1–6. doi: 10.1109/IAIN.2015.7352253.

[65] O. Himrane, J. Beugin, and M. Ghazel, "Implementation of a Model-Oriented Approach for Supporting Safe Integration of GNSS-Based Virtual Balises in ERTMS/ETCS Level 3," *IEEE Open Journal of Intelligent Transportation Systems*, vol. 4, pp. 294–310, 2023, doi: 10.1109/OJITS.2023.3267142.

[66] R. Liu, "Simulation model of speed control for the moving-block systems under ERTMS Level 3," in *2016 IEEE International Conference on Intelligent Rail Transportation (ICIRT)*, 2016, pp. 322–327. doi: 10.1109/ICIRT.2016.7588750.

[67] D. H. Murillas and L. Poncet, "Safe odometry for high-speed trains," in *2016 IEEE International Conference on Intelligent Rail Transportation (ICIRT)*, 2016, pp. 244–248. doi: 10.1109/ICIRT.2016.7588739.

[68] M. Spindler, D. Stein, and M. Lauer, "Low power and low cost sensor for train velocity estimation," in *2016 IEEE International Conference on*

Intelligent Rail Transportation (ICIRT), 2016, pp. 259–264. doi: 10.1109/ICIRT.2016.7588742.

[69] E. Mortlock and G. Hubbs, "Implementing Optical Speed Measurement (OSMES) for Communications Based Train Control," Jun. 2004, pp. 205–211. doi: 10.1109/RRCON.2004.1300921.

[70] S. Wrobel, M. Ahmadian, M. Craft, and J. Munoz, "Multifunction LIDAR Sensors for Non-Contact Speed Measurement in Rail Vehicles: Part 2 — Data Collection and Analysis," Jun. 2013. doi: 10.1115/JRC2013-2500.

[71] C. Waldschmidt, J. Hasch, and W. Menzel, "Automotive Radar — From First Efforts to Future Systems," *IEEE Journal of Microwaves*, vol. 1, no. 1, pp. 135–148, 2021, doi: 10.1109/JMW.2020.3033616.

[72] Venkatesha. K, A. Vengadarajan, and U. Singh, "Detection and Simple Tracking Method for ADAS using a mmWave Radar," in *2023 IEEE 4th Annual Flagship India Council International Subsections Conference (INDISCON)*, 2023, pp. 1–5. doi: 10.1109/INDISCON58499.2023.10270092.

[73] Z. E. Ekolle *et al.*, "A Reliable 79GHz Band Ultra-Short Range Radar for ADAS/AD Vehicles Using FMCW Technology," in *2023 IEEE International Automated Vehicle Validation Conference (IAVVC)*, 2023, pp. 1–6. doi: 10.1109/IAVVC57316.2023.10328083.

[74] D. Wachtel, T. Rothmeier, T. von dem Bussche, W. Huber, and M. Vossiek, "Radar in the Rain: Understanding and Simulating Environmental Effects on ADAS Radar Sensors," in *2024 IEEE Radar Conference (RadarConf24)*, 2024, pp. 1–6. doi: 10.1109/RadarConf2458775.2024.10548570.

[75] V. Winkler, "Range Doppler detection for automotive FMCW radars," in *2007 European Microwave Conference*, 2007, pp. 1445–1448. doi: 10.1109/EUMC.2007.4405477.

[76] W. Menzel and A. Moebius, "Antenna Concepts for Millimeter-Wave Automotive Radar Sensors," *Proceedings of the IEEE*, vol. 100, no. 7, pp. 2372–2379, 2012, doi: 10.1109/JPROC.2012.2184729.

[77] P. Swerling, "Probability of detection for fluctuating targets," *IRE Transactions on Information Theory*, vol. 6, no. 2, pp. 269–308, 1960, doi: 10.1109/TIT.1960.1057561.

[78] A. Al Teneiji, M. S. Khan, N. Ali, and A. Al Tunaiji, "Improving the Detection Accuracy of Frequency Modulated Continuous Wave Radar," in *2018 International Conference on Signal Processing and Information Security (ICSPIS)*, 2018, pp. 1–4. doi: 10.1109/CSPIS.2018.8642764.

[79] J. Yongqi, H. Guoyu, X. Yongbin, and F. Hui, "A FTDC technique to improve the range resolution of short range FMCW radar," in *2002 3rd International Conference on Microwave and Millimeter Wave Technology, 2002. Proceedings. ICMMT 2002.*, 2002, pp. 480–483. doi: 10.1109/ICMMT.2002.1187741.

[80] H.-H. Ko, K.-W. Cheng, and H.-J. Su, "Range resolution improvement for FMCW radars," in *2008 European Radar Conference*, 2008, pp. 352–355.

[81] W. Jiang, S. R. Pennock, and P. R. Shepherd, "FMCW Radar Range Performance Improvement With Modified Adaptive Sampling Method," *IEEE Geoscience and Remote Sensing Letters*, vol. 9, no. 4, pp. 668–671, 2012, doi: 10.1109/LGRS.2011.2177958.

[82] J. Hasch, E. Topak, R. Schnabel, T. Zwick, R. Weigel, and C. Waldschmidt, "Millimeter-Wave Technology for Automotive Radar Sensors in the 77 GHz Frequency Band," *IEEE Trans Microw Theory Tech*, vol. 60, no. 3, pp. 845–860, 2012, doi: 10.1109/TMTT.2011.2178427.

[83] W. Wiesbeck, L. Sit, M. Younis, T. Rommel, G. Krieger, and A. Moreira, "Radar 2020: The future of radar systems," in *2015 IEEE International Geoscience and Remote Sensing Symposium (IGARSS)*, 2015, pp. 188–191. doi: 10.1109/IGARSS.2015.7325731.

[84] K. Bimbraw, "Autonomous cars: Past, present and future a review of the developments in the last century, the present scenario and the expected future of autonomous vehicle technology," in *2015 12th International Conference on Informatics in Control, Automation and Robotics (ICINCO)*, 2015, pp. 191–198.

[85] K. Sengupta and A. Hajimiri, "A 0.28THz 4×4 power-generation and beam-steering array," in *2012 IEEE International Solid-State Circuits Conference*, 2012, pp. 256–258. doi: 10.1109/ISSCC.2012.6176999.

[86] J.-D. Park, S. Kang, S. V Thyagarajan, E. Alon, and A. M. Niknejad, "A 260 GHz fully integrated CMOS transceiver for wireless chip-to-chip

communication," in *2012 Symposium on VLSI Circuits (VLSIC)*, 2012, pp. 48–49. doi: 10.1109/VLSIC.2012.6243783.

[87] J. Ma, "Modeling and Simulation of Automatic Emergency Braking Control System for Unmanned All-Terrain Vehicle," in *2021 6th International Conference on Mechanical Engineering and Robotics Research (ICMERR)*, 2021, pp. 106–109. doi: 10.1109/ICMERR54363.2021.9680851.

[88] O. Garcia-Bedoya, S. Hirota, and J. V Ferreira, "Control system design for an Automatic Emergency Braking system in a sedan vehicle," in *2019 2nd Latin American Conference on Intelligent Transportation Systems (ITS LATAM)*, 2019, pp. 1–6. doi: 10.1109/ITSLATAM.2019.8721353.

[89] Y. Zhu, R. Xu, H. An, A. Zhang, and K. Lu, "Research on automatic emergency braking system development and test platform," in *2022 Fifth International Conference on Connected and Autonomous Driving (MetroCAD)*, 2022, pp. 1–6. doi: 10.1109/MetroCAD56305.2022.00006.

[90] B. S P, H. V M, K. L. Reddy, L. M, and H. V. Kumar, "Effective Method for Vehicle-Automatic Emergency Braking System and Blind Spot Detection Using Radar and IoT," in *2023 International Conference on Smart Systems for applications in Electrical Sciences (ICSSES)*, 2023, pp. 1–5. doi: 10.1109/ICSSES58299.2023.10200594.

[91] Z. Yu, J. Bai, S. Chen, L. Huang, and X. Bi, "Camera-radar data fusion for target detection via Kalman filter and Bayesian estimation," 2018.

[92] Z. Song, L. Cao, and C. C. Chou, "Development of test equipment for pedestrian-automatic emergency braking based on C-NCAP (2018)," *Sensors*, vol. 20, no. 21, p. 6206, 2020.

[93] K. Guo, Y. Yan, J. Shi, R. Guo, and Y. Liu, "An investigation into c-ncap aeb system assessment protocol," 2017.

[94] M. Z. C. Mustafar and S. A. A. Bakar, "Optimal design of an Autonomous Emergency Braking (AEB) system for a passenger vehicle," in *IOP Conference Series: Materials Science and Engineering*, 2020, p. 12088.

[95] D. Zeng *et al.*, "Improved AEB algorithm combined with estimating the adhesion coefficient of road ahead and considering the performance of EHB," *Proceedings of the Institution of Mechanical Engineers, Part D: Journal of Automobile Engineering*, vol. 237, no. 10–11, pp. 2415–2430, 2023.

[96] J. C. M. W. O. Z. Mervyn Edwards Andrew Nathanson and N. Lubbe, "Assessment of Integrated Pedestrian Protection Systems with Autonomous Emergency Braking (AEB) and Passive Safety Components," *Traffic Inj Prev*, vol. 16, no. sup1, pp. S2–S11, 2015, doi: 10.1080/15389588.2014.1003154.

[97] H. Tan, F. Zhao, H. Hao, Z. Liu, A. A. Amer, and H. Babiker, "Automatic Emergency Braking (AEB) System Impact on Fatality and Injury Reduction in China," *Int J Environ Res Public Health*, vol. 17, no. 3, 2020, doi: 10.3390/ijerph17030917.

[98] B. Fildes *et al.*, "Effectiveness of low speed autonomous emergency braking in real-world rear-end crashes," *Accid Anal Prev*, vol. 81, pp. 24–29, 2015, doi: https://doi.org/10.1016/j.aap.2015.03.029.

[99] Y. Gao, Z. Xu, X. Zhao, G. Wang, and Q. Yuan, "Hardware-in-the-Loop Simulation Platform for Autonomous Vehicle AEB Prototyping and Validation," in *2020 IEEE 23rd International Conference on Intelligent Transportation Systems (ITSC)*, 2020, pp. 1–6. doi: 10.1109/ITSC45102.2020.9294704.

[100] C.-H. Yu, Y.-Z. Chen, and I.-C. Kuo, "The benefit of Simulation Test Application on the Development of Autonomous Driving System," in *2020 International Automatic Control Conference (CACS)*, 2020, pp. 1–5. doi: 10.1109/CACS50047.2020.9289717.

[101] C. Berger *et al.*, "Large-Scale Evaluation of an Active Safety Algorithm with EuroNCAP and US NCAP Scenarios in a Virtual Test Environment – An Industrial Case Study," in *2015 IEEE 18th International Conference on Intelligent Transportation Systems*, 2015, pp. 2280–2286. doi: 10.1109/ITSC.2015.368.

[102] A. Kamble and S. Potadar, "Lane Departure Warning System for Advanced Drivers Assistance," in *2018 Second International Conference on Intelligent Computing and Control Systems (ICICCS)*, 2018, pp. 1775–1778. doi: 10.1109/ICCONS.2018.8663242.

[103] Y. A. Ahmed, A. T. Mohamed, and A. M. B. Aly, "Robust Lane Departure Warning System for ADAS on Highways," in *2022 4th Novel Intelligent and Leading Emerging Sciences Conference (NILES)*, 2022, pp. 321–324. doi: 10.1109/NILES56402.2022.9942370.

[104] S. Dragaš, R. Grbić, M. Brisinello, and K. Lazić, "Development and Implementation of Lane Departure Warning System on ADAS Alpha Board," in *2021 International Symposium ELMAR*, 2021, pp. 53–58. doi: 10.1109/ELMAR52657.2021.9550915.

[105] I. Gamal *et al.*, "A Robust, Real-Time and Calibration-Free Lane Departure Warning System," in *2019 IEEE International Symposium on Circuits and Systems (ISCAS)*, 2019, pp. 1–4. doi: 10.1109/ISCAS.2019.8702360.

[106] S. Luo, X. Zhang, J. Hu, and J. Xu, "Multiple Lane Detection via Combining Complementary Structural Constraints," *IEEE Transactions on Intelligent Transportation Systems*, vol. 22, no. 12, pp. 7597–7606, 2021, doi: 10.1109/TITS.2020.3005396.

[107] D. C. Andrade *et al.*, "A Novel Strategy for Road Lane Detection and Tracking Based on a Vehicle's Forward Monocular Camera," *IEEE Transactions on Intelligent Transportation Systems*, vol. 20, no. 4, pp. 1497–1507, 2019, doi: 10.1109/TITS.2018.2856361.

[108] N. J. Zakaria, M. I. Shapiai, R. A. Ghani, M. N. M. Yassin, M. Z. Ibrahim, and N. Wahid, "Lane Detection in Autonomous Vehicles: A Systematic Review," *IEEE Access*, vol. 11, pp. 3729–3765, 2023, doi: 10.1109/ACCESS.2023.3234442.

[109] J. H. Yoo, S.-W. Lee, S.-K. Park, and D. H. Kim, "A Robust Lane Detection Method Based on Vanishing Point Estimation Using the Relevance of Line Segments," *IEEE Transactions on Intelligent Transportation Systems*, vol. 18, no. 12, pp. 3254–3266, 2017, doi: 10.1109/TITS.2017.2679222.

[110] M. Marzougui, A. Alasiry, Y. Kortli, and J. Baili, "A Lane Tracking Method Based on Progressive Probabilistic Hough Transform," *IEEE Access*, vol. 8, pp. 84893–84905, 2020, doi: 10.1109/ACCESS.2020.2991930.

[111] Y. Saito, M. Itoh, and T. Inagaki, "Bringing a Vehicle to a Controlled Stop: Effectiveness of a Dual-Control Scheme for Identifying Driver Drowsiness and Preventing Lane Departures Under Partial Driving Automation Requiring Hands-on-Wheel," *IEEE Trans Hum Mach Syst*, vol. 52, no. 1, pp. 74–86, 2022, doi: 10.1109/THMS.2021.3123171.

[112] S. Sivaraman and M. M. Trivedi, "Integrated Lane and Vehicle Detection, Localization, and Tracking: A Synergistic Approach," *IEEE Transactions on*

Intelligent Transportation Systems, vol. 14, no. 2, pp. 906–917, 2013, doi: 10.1109/TITS.2013.2246835.

[113] H. Wang, W. Hao, J. So, Z. Chen, and J. Hu, "A Faster Cooperative Lane Change Controller Enabled by Formulating in Spatial Domain," *IEEE Transactions on Intelligent Vehicles*, vol. 8, no. 12, pp. 4685–4695, 2023, doi: 10.1109/TIV.2023.3317957.

[114] R. Utriainen, M. Pöllänen, and H. Liimatainen, "The Safety Potential of Lane Keeping Assistance and Possible Actions to Improve the Potential," *IEEE Transactions on Intelligent Vehicles*, vol. 5, no. 4, pp. 556–564, 2020, doi: 10.1109/TIV.2020.2991962.

[115] Y. Bian, J. Ding, M. Hu, Q. Xu, J. Wang, and K. Li, "An Advanced Lane-Keeping Assistance System With Switchable Assistance Modes," *IEEE Transactions on Intelligent Transportation Systems*, vol. 21, no. 1, pp. 385–396, 2020, doi: 10.1109/TITS.2019.2892533.

[116] P. Das, N. A. Asif, Md. M. Hasan, S. H. Abhi, M. Jahin Tatha, and S. D. Bristi, "Intelligent Door Controller Using Deep Learning-Based Network Pruned Face Recognition," in *2022 25th International Conference on Computer and Information Technology (ICCIT)*, 2022, pp. 120–124. doi: 10.1109/ICCIT57492.2022.10056094.

[117] C.-B. Wu, L.-H. Wang, and K.-C. Wang, "Ultra-Low Complexity Block-Based Lane Detection and Departure Warning System," *IEEE Transactions on Circuits and Systems for Video Technology*, vol. 29, no. 2, pp. 582–593, 2019, doi: 10.1109/TCSVT.2018.2805704.

[118] W. Wang, D. Zhao, W. Han, and J. Xi, "A Learning-Based Approach for Lane Departure Warning Systems With a Personalized Driver Model," *IEEE Trans Veh Technol*, vol. 67, no. 10, pp. 9145–9157, 2018, doi: 10.1109/TVT.2018.2854406.

[119] P. Angkititrakul, R. Terashima, and T. Wakita, "On the Use of Stochastic Driver Behavior Model in Lane Departure Warning," *IEEE Transactions on Intelligent Transportation Systems*, vol. 12, no. 1, pp. 174–183, 2011, doi: 10.1109/TITS.2010.2072502.

[120] A. Biswas *et al.*, "State-of-the-Art Review on Recent Advancements on Lateral Control of Autonomous Vehicles," *IEEE Access*, vol. 10, pp. 114759–114786, 2022, doi: 10.1109/ACCESS.2022.3217213.

[121] S. Mammar, S. Glaser, and M. Netto, "Time to line crossing for lane departure avoidance: a theoretical study and an experimental setting," *IEEE Transactions on Intelligent Transportation Systems*, vol. 7, no. 2, pp. 226–241, 2006, doi: 10.1109/TITS.2006.874707.

[122] Md. A. B. Siddiki Abir, M. Z. Chowdhury, and Y. M. Jang, "Software-Defined UAV Networks for 6G Systems: Requirements, Opportunities, Emerging Techniques, Challenges, and Research Directions," *IEEE Open Journal of the Communications Society*, vol. 4, pp. 2487–2547, 2023, doi: 10.1109/OJCOMS.2023.3323200.

[123] Y. Gao and Z. Liu, "Disturbance Compensation-Based Optimal Tracking Control for Perturbed Nonlinear Systems," *IEEE Access*, vol. 11, pp. 50619–50630, 2023, doi: 10.1109/ACCESS.2023.3278211.

[124] V. Gaikwad and S. Lokhande, "Lane Departure Identification for Advanced Driver Assistance," *IEEE Transactions on Intelligent Transportation Systems*, vol. 16, no. 2, pp. 910–918, 2015, doi: 10.1109/TITS.2014.2347400.

[125] W. Wang and D. Zhao, "Evaluation of Lane Departure Correction Systems Using a Regenerative Stochastic Driver Model," *IEEE Transactions on Intelligent Vehicles*, vol. 2, no. 3, pp. 221–232, 2017, doi: 10.1109/TIV.2017.2756342.

[126] Y. Gao and T. Gordon, "Optimal Control of Vehicle Dynamics for the Prevention of Road Departure on Curved Roads," *IEEE Trans Veh Technol*, vol. 68, no. 10, pp. 9370–9384, 2019, doi: 10.1109/TVT.2019.2927333.

[127] Y. Zhang, Z. Lu, X. Zhang, J.-H. Xue, and Q. Liao, "Deep Learning in Lane Marking Detection: A Survey," *IEEE Transactions on Intelligent Transportation Systems*, vol. 23, no. 7, pp. 5976–5992, 2022, doi: 10.1109/TITS.2021.3070111.

[128] K. Herman Muraro Gularte *et al.*, "Safeguarding the V2X Pathways: Exploring the Cybersecurity Landscape Through Systematic Review," *IEEE Access*, vol. 12, pp. 72871–72895, 2024, doi: 10.1109/ACCESS.2024.3402946.

[129] M. Li, H. Xu, Y. Wei, and A. Deng, "Deep Neural Network-Based Linear Quadratic Programming for Vehicle Path Tracking," in *2023 5th International Conference on Robotics, Intelligent Control and Artificial*

Intelligence (RICAI), 2023, pp. 446–451. doi: 10.1109/RICAI60863.2023.10489492.

[130] J. Zhang and D. Ren, "Lateral Control of Vehicle for Lane Keeping in Intelligent Transportation Systems," in *2009 International Conference on Intelligent Human-Machine Systems and Cybernetics*, 2009, pp. 446–450. doi: 10.1109/IHMSC.2009.119.

[131] V. Cerone, M. Milanese, and D. Regruto, "Experimental results on combined automatic lane keeping and driver's steering," in *2007 American Control Conference*, 2007, pp. 3126–3131. doi: 10.1109/ACC.2007.4282727.

[132] T.-K. Jhang and C. Lin, "Scenario-based simulation environmental and Integration of a Lane Keeping System with Vehicle Dynamics Control," in *2022 International Automatic Control Conference (CACS)*, 2022, pp. 1–6. doi: 10.1109/CACS55319.2022.9969850.

[133] F. Li *et al.*, "Lane-Keeping Control of Automatic Steering Systems via Adaptive Fuzzy Sliding-Mode Approach," *IEEE Trans Syst Man Cybern Syst*, vol. 54, no. 3, pp. 1683–1693, 2024, doi: 10.1109/TSMC.2023.3302618.

[134] C. Hatipoglu, U. Ozguner, and K. A. Unyelioglu, "On optimal design of a lane change controller," in *Proceedings of the Intelligent Vehicles '95. Symposium*, 1995, pp. 436–441. doi: 10.1109/IVS.1995.528321.

[135] C. Hatipoglu, U. Ozguner, and K. A. Redmill, "Automated lane change controller design," *IEEE Transactions on Intelligent Transportation Systems*, vol. 4, no. 1, pp. 13–22, 2003, doi: 10.1109/TITS.2003.811644.

[136] S. Tsugawa, "Vision-based vehicles in Japan: machine vision systems and driving control systems," *IEEE Transactions on Industrial Electronics*, vol. 41, no. 4, pp. 398–405, 1994, doi: 10.1109/41.303790.

[137] V. Cerone and D. Regruto, "Robust performance controller design for vehicle lane keeping," in *2003 European Control Conference (ECC)*, 2003, pp. 348–353. doi: 10.23919/ECC.2003.7084979.

[138] V. Cerone and D. Regruto, "Vehicle lateral controller design exploiting properties of SITO systems," in *Proceedings of the 2003 American Control Conference, 2003.*, 2003, pp. 4365–4370 vol.5. doi: 10.1109/ACC.2003.1240525.

[139] V. Cerone, A. Chinu, and D. Regruto, "Experimental results in vision-based lane keeping for highway vehicles," in *Proceedings of the 2002 American Control Conference (IEEE Cat. No.CH37301)*, 2002, pp. 869–874 vol.2. doi: 10.1109/ACC.2002.1023125.

[140] C. Hatipolglu, K. Redmill, and U. Ozguner, "Steering and lane change: a working system," in *Proceedings of Conference on Intelligent Transportation Systems*, 1997, pp. 272–277. doi: 10.1109/ITSC.1997.660487.

[141] R. H. Byrne, C. T. Abdallah, and P. Dorato, "Experimental results in robust lateral control of highway vehicles," *IEEE Control Systems Magazine*, vol. 18, no. 2, pp. 70–76, 1998, doi: 10.1109/37.664657.

[142] J. Guldner, W. Sienel, H.-S. Tan, J. Ackermann, S. Patwardhan, and T. Bunte, "Robust automatic steering control for look-down reference systems with front and rear sensors," *IEEE Transactions on Control Systems Technology*, vol. 7, no. 1, pp. 2–11, 1999, doi: 10.1109/87.736743.

[143] J. Ackermann, J. Guldner, W. Sienel, R. Steinhauser, and V. I. Utkin, "Linear and nonlinear controller design for robust automatic steering," *IEEE Transactions on Control Systems Technology*, vol. 3, no. 1, pp. 132–143, 1995, doi: 10.1109/87.370719.

[144] M. Tomizuka, M. Tai, J.-Y. Wang, and P. Hingwe, "Automated lane guidance of commercial vehicles," in *Proceedings of the 1999 IEEE International Conference on Control Applications (Cat. No.99CH36328)*, 1999, pp. 1359–1364 vol. 2. doi: 10.1109/CCA.1999.801170.

[145] P. Hingwe and M. Tomizuka, "A variable look-ahead controller for lateral guidance of four wheeled vehicles," in *Proceedings of the 1998 American Control Conference. ACC (IEEE Cat. No.98CH36207)*, 1998, pp. 31–35 vol.1. doi: 10.1109/ACC.1998.694619.

[146] S. Patwardhan, H.-S. Tan, and J. Guldner, "A general framework for automatic steering control: system analysis," in *Proceedings of the 1997 American Control Conference (Cat. No.97CH36041)*, 1997, pp. 1598–1602 vol.3. doi: 10.1109/ACC.1997.610853.

[147] S. E. Shladover *et al.*, "Automated vehicle control developments in the PATH program," *IEEE Trans Veh Technol*, vol. 40, no. 1, pp. 114–130, 1991, doi: 10.1109/25.69979.

[148] J. Tanaka, S. Ishida, H. Kawagoe, and S. Kondo, "Workload of using a driver assistance system," in *ITSC2000. 2000 IEEE Intelligent Transportation Systems. Proceedings (Cat. No.00TH8493)*, 2000, pp. 382–386. doi: 10.1109/ITSC.2000.881093.

[149] R. E. Fenton and R. J. Mayhan, "Automated highway studies at the Ohio State University-an overview," *IEEE Trans Veh Technol*, vol. 40, no. 1, pp. 100–113, 1991, doi: 10.1109/25.69978.

[150] C. Gold, D. Damböck, L. Lorenz, and K. Bengler, ""Take over!' How long does it take to get the driver back into the loop?," *Proceedings of the Human Factors and Ergonomics Society Annual Meeting*, vol. 57, no. 1, pp. 1938–1942, Sep. 2013, doi: 10.1177/1541931213571433.

[151] M. Johns, G. Strack, and W. Ju, "Driver Assistance after Handover of Control from Automation," in *2018 21st International Conference on Intelligent Transportation Systems (ITSC)*, 2018, pp. 2104–2110. doi: 10.1109/ITSC.2018.8569499.

[152] Y. Zhang, J. Liu, Y. Zhao, L. Hou, and Y. Zhang, "Analysis on Simultaneous Localization and Mapping of Mobile Robot Based on Two Multi-sensor Fusion Algorithm," in *2023 IEEE 11th Joint International Information Technology and Artificial Intelligence Conference (ITAIC)*, 2023, pp. 1843–1847. doi: 10.1109/ITAIC58329.2023.10408763.

[153] J. K. Makhubela, T. Zuva, and O. Y. Agunbiade, "A Review on Vision Simultaneous Localization and Mapping (VSLAM)," in *2018 International Conference on Intelligent and Innovative Computing Applications (ICONIC)*, 2018, pp. 1–5. doi: 10.1109/ICONIC.2018.8601227.

[154] J. Jiang and L. Tuan-jie, "A Method for Distributed Multi-Robot Simultaneous Localization and Mapping," in *2012 International Conference on Industrial Control and Electronics Engineering*, 2012, pp. 358–362. doi: 10.1109/ICICEE.2012.101.

[155] Y. Toda, N. Kubota, and N. Baba, "Intelligent planning based on multi-resolution map for simultaneous localization and mapping," in *2011 IEEE Workshop on Robotic Intelligence In Informationally Structured Space*, 2011, pp. 144–150. doi: 10.1109/RIISS.2011.5945794.

[156] M. Cornick, J. Koechling, B. Stanley, and B. Zhang, "Localizing Ground Penetrating RADAR: A Step Toward Robust Autonomous Ground Vehicle Localization," *J Field Robot*, vol. 33, Jun. 2015, doi: 10.1002/rob.21605.

[157] M. Cornick, J. Koechling, B. Stanley, and B. Zhang, "Localizing Ground Penetrating RADAR: A Step Toward Robust Autonomous Ground Vehicle Localization," *J Field Robot*, vol. 33, Jun. 2015, doi: 10.1002/rob.21605.

[158] M. K. Dawane, V. G. Asutkar, and M. W. Trikande, "Modeling and control of steering using road way magnets," in *2008 IEEE International Conference on Systems, Man and Cybernetics*, 2008, pp. 2122–2126. doi: 10.1109/ICSMC.2008.4811605.

[159] D.-H. Kim, "Lane Detection Method with Impulse Radio Ultra-Wideband Radar and Metal Lane Reflectors," *Sensors*, vol. 20, no. 1, 2020, doi: 10.3390/s20010324.

[160] M. T. Ghasr, S. Kharkovsky, R. Bohnert, B. Hirst, and R. Zoughi, "30 GHz Linear High-Resolution and Rapid Millimeter Wave Imaging System for NDE," *IEEE Trans Antennas Propag*, vol. 61, no. 9, pp. 4733–4740, 2013, doi: 10.1109/TAP.2013.2270174.

[161] J. Wan, Y. Zhao, W. Weng, S. Xu, and W. Zou, "Super-Resolution Method for Microwave Front-Looking Imaging Using Broadband Signals and Spatial Spectrum Shifting," *IEEE Trans Microw Theory Tech*, vol. 72, no. 7, pp. 4309–4316, 2024, doi: 10.1109/TMTT.2023.3341896.

[162] Y. Wu, H. Ma, Y. Zhang, Q. Zhang, Z. Wu, and J. Huangfu, "Microwave Imaging Method Based on Reconfigurable Spatial Dispersion Radiation," *IEEE Trans Microw Theory Tech*, vol. 72, no. 5, pp. 3235–3246, 2024, doi: 10.1109/TMTT.2023.3319027.

[163] J. A. Paredes, M. Hansard, K. Z. Rajab, and F. J. Álvarez, "Spatial Calibration of Millimeter-Wave Radar for Close-Range Object Location," *IEEE Sens J*, vol. 24, no. 12, pp. 19407–19416, 2024, doi: 10.1109/JSEN.2024.3393030.

[164] F. Rosu and I. Rosu, "SiGe Push–Push VCO for Low-Power C-Band FMCW High-Resolution Radar Applications," *IEEE Microwave and Wireless Components Letters*, vol. 31, no. 10, pp. 1150–1153, 2021, doi: 10.1109/LMWC.2021.3108816.

[165] T. Jaeschke, C. Bredendiek, S. Küppers, and N. Pohl, "High-Precision D-Band FMCW-Radar Sensor Based on a Wideband SiGe-Transceiver MMIC," *IEEE Trans Microw Theory Tech*, vol. 62, no. 12, pp. 3582–3597, 2014, doi: 10.1109/TMTT.2014.2365460.

[166] A. Dürr *et al.*, "High-Resolution 160-GHz Imaging MIMO Radar Using MMICs With On-Chip Frequency Synthesizers," *IEEE Trans Microw Theory Tech*, vol. 67, no. 9, pp. 3897–3907, 2019, doi: 10.1109/TMTT.2019.2906176.

[167] S. Kueppers, T. Jaeschke, N. Pohl, and J. Barowski, "Versatile 126–182 GHz UWB D-Band FMCW Radar for Industrial and Scientific Applications," *IEEE Sens Lett*, vol. 6, no. 1, pp. 1–4, 2022, doi: 10.1109/LSENS.2021.3130709.

[168] J. Hasch, E. Topak, R. Schnabel, T. Zwick, R. Weigel, and C. Waldschmidt, "Millimeter-Wave Technology for Automotive Radar Sensors in the 77 GHz Frequency Band," *IEEE Trans Microw Theory Tech*, vol. 60, no. 3, pp. 845–860, 2012, doi: 10.1109/TMTT.2011.2178427.

[169] W. Johannes *et al.*, "Miniaturized high resolution Synthetic Aperture Radar at 94 GHz for microlite aircraft or UAV," in *SENSORS, 2011 IEEE*, 2011, pp. 2022–2025. doi: 10.1109/ICSENS.2011.6127301.

[170] W. C. Carrara, etc., R. S. Goodman, R. M. Majewski, and Williams, *Spotlight synthetic aperture radar*. in Remote sensing library. Norwood, MA: Artech House, 1995.

[171] M. Soumekh, *Synthetic aperture radar signal processing with MATLAB algorithms*. Nashville, TN: John Wiley & Sons, 1999.

[172] R. Appleby and H. B. Wallace, "Standoff Detection of Weapons and Contraband in the 100 GHz to 1 THz Region," *IEEE Trans Antennas Propag*, vol. 55, no. 11, pp. 2944–2956, 2007, doi: 10.1109/TAP.2007.908543.

[173] National Research Council, Division on Engineering, P. Sciences, National Materials Advisory Board, and Committee on Assessment of Security Technologies for Transportation, *Assessment of millimeter-wave and terahertz technology for detection and identification of concealed explosives and weapons*. Washington, D.C., DC: National Academies Press, 2007.

[174] K. B. Cooper, R. J. Dengler, N. Llombart, B. Thomas, G. Chattopadhyay, and P. H. Siegel, "THz Imaging Radar for Standoff Personnel Screening,"

IEEE Trans Terahertz Sci Technol, vol. 1, no. 1, pp. 169–182, 2011, doi: 10.1109/TTHZ.2011.2159556.

[175] A. Arodzero, S. Boucher, P. Burstein, S. V Kutsaev, R. C. Lanza, and V. Palermo, "Security X-ray Screening with Modulated-Energy Pulses," in *2019 IEEE International Symposium on Technologies for Homeland Security (HST)*, 2019, pp. 1–6. doi: 10.1109/HST47167.2019.9032928.

[176] A.-S. Lalleman *et al.*, "A dual X-ray backscatter system for detecting explosives: Image and discrimination of a suspicious content," in *2011 IEEE Nuclear Science Symposium Conference Record*, 2011, pp. 299–304. doi: 10.1109/NSSMIC.2011.6154503.

[177] K. B. Cooper *et al.*, "A High-Resolution Imaging Radar at 580 GHz," *IEEE Microwave and Wireless Components Letters*, vol. 18, no. 1, pp. 64–66, 2008, doi: 10.1109/LMWC.2007.912049.

[178] K. B. Cooper, R. J. Dengler, N. Llombart, B. Thomas, G. Chattopadhyay, and P. H. Siegel, "THz Imaging Radar for Standoff Personnel Screening," *IEEE Trans Terahertz Sci Technol*, vol. 1, no. 1, pp. 169–182, 2011, doi: 10.1109/TTHZ.2011.2159556.

[179] A. Bisognin *et al.*, "3D-Printed ABS plastic Peanut-Lens with Integrated Ball Grid Array-Module for High-Data Rate Communications in F-band," *IET Microwaves, Antennas & Propagation*, vol. 11, Jun. 2017, doi: 10.1049/iet-map.2017.0190.

[180] A. Boriskin, R. Sauleau, J. Costa, and C. Fernandes, *Integrated lens antennas*. 2018.

[181] T. Burghardt and A. Pashkevich, "Materials selection for structured horizontal road markings: financial and environmental case studies," *European Transport Research Review*, vol. 12, Jun. 2020, doi: 10.1186/s12544-020-0397-x.

[182] Michael Pidwirny, *M. Surface Area of Our Planet Covered by Oceans and Continents*. University of British Columbia, Kelowna, BC, Canada, 2006.

[183] D. Gruyer, R. Belaroussi, and M. Revilloud, "Map-aided localization with lateral perception," in *2014 IEEE Intelligent Vehicles Symposium Proceedings*, 2014, pp. 674–680. doi: 10.1109/IVS.2014.6856528.

[184] G. D'Amico *et al.*, "TrainSim: A Railway Simulation Framework for LiDAR and Camera Dataset Generation," *IEEE Transactions on Intelligent Transportation Systems*, vol. 24, no. 12, pp. 15006–15017, 2023, doi: 10.1109/TITS.2023.3297728.

[185] Y. Wang *et al.*, "Rail Vehicle Localization and Mapping With LiDAR-Vision-Inertial-GNSS Fusion," *IEEE Robot Autom Lett*, vol. 7, no. 4, pp. 9818–9825, 2022, doi: 10.1109/LRA.2022.3190093.

[186] M. Spindler and M. Lauer, "High Accuracy Estimation of Velocity and Position for Railway Vehicles using Ferromagnetic Inhomogeneities," in *2018 21st International Conference on Intelligent Transportation Systems (ITSC)*, 2018, pp. 1202–1207. doi: 10.1109/ITSC.2018.8569919.

[187] B. Kröper, M. Lauer, and M. Spindler, "Using the Ferromagnetic Fingerprint of Rails for Velocity Estimation and absolute Localization of Railway Vehicles," in *2020 European Navigation Conference (ENC)*, 2020, pp. 1–10. doi: 10.23919/ENC48637.2020.9317512.

[188] C. Y. Zhongsheng Hou Yi Wang and T. Tang, "Terminal iterative learning control based station stop control of a train," *Int J Control*, vol. 84, no. 7, pp. 1263–1274, 2011, doi: 10.1080/00207179.2011.569030.

[189] S. Jin, Z. Hou, and R. Chi, "Optimal Terminal Iterative Learning Control for the Automatic Train Stop System," *Asian J Control*, vol. 17, no. 5, pp. 1992–1999, 2015, doi: https://doi.org/10.1002/asjc.1065.

[190] D. Chen, R. Chen, Y. Li, and T. Tang, "Online Learning Algorithms for Train Automatic Stop Control Using Precise Location Data of Balises," *Intelligent Transportation Systems, IEEE Transactions on*, vol. 14, pp. 1526–1535, Jul. 2013, doi: 10.1109/TITS.2013.2265171.

[191] S. Yasunobu, S. MIYAMOTO, and H. Ihara, "A Fuzzy Control for Train Automatic Stop Control," *Transactions of the Society of Instrument and Control Engineers*, vol. 19, Jul. 1983, doi: 10.9746/sicetr1965.19.873.

[192] D. Chen and C. Gao, "Soft computing methods applied to train station parking in urban rail transit," *Appl. Soft Comput.*, vol. 12, pp. 759–767, Jul. 2012, doi: 10.1016/j.asoc.2011.10.016.

[193] P. Wu and Q. Wang, "Research of the automatic train stop control based on adaptive generalized predictive control," in *Proceedings of the 33rd Chinese*

Control Conference, 2014, pp. 3399–3404. doi: 10.1109/ChiCC.2014.6895502.

[194] Q. Wang, P. Wu, X. Feng, and Y. Zhang, "Precise automatic train stop control algorithm based on adaptive terminal sliding mode control," vol. 38, pp. 56–63, Jul. 2016, doi: 10.3969/j.issn.1001-8360.2016.02.008.

[195] Y. Wang, Z. Hou, and X. Li, "A novel automatic train operation algorithm based on iterative learning control theory," in *2008 IEEE International Conference on Service Operations and Logistics, and Informatics*, 2008, pp. 1766–1770. doi: 10.1109/SOLI.2008.4682815.

[196] S. Sekine, N. Imasaki, and T. Endo, "Application of fuzzy neural network control to automatic train operation and tuning of its control rules," in *Proceedings of 1995 IEEE International Conference on Fuzzy Systems.*, 1995, pp. 1741–1746 vol.4. doi: 10.1109/FUZZY.1995.409917.

[197] L. Huichao, Z. Miao, and F. Xiaoyun, "Research and simulation of a high-performance algorithm for subway train control," in *2008 7th World Congress on Intelligent Control and Automation*, 2008, pp. 4387–4390. doi: 10.1109/WCICA.2008.4593627.

[198] B. Ning, T. Tang, Z. Gao, F. Yan, F.-Y. Wang, and D. Zeng, "Intelligent Railway Systems in China," *IEEE Intell Syst*, vol. 21, no. 5, pp. 80–83, 2006, doi: 10.1109/MIS.2006.99.

[199] H. Dong, B. Ning, B. Cai, and Z. Hou, "Automatic Train Control System Development and Simulation for High-Speed Railways," *IEEE Circuits and Systems Magazine*, vol. 10, no. 2, pp. 6–18, 2010, doi: 10.1109/MCAS.2010.936782.

[200] P. Guziur, "DESIGN PARAMETERS OF BUFFER STOPS," *Acta Polytech CTU Proc*, vol. 5, p. 17, Sep. 2016, doi: 10.14311/app.2016.5.0017.

[201] J. A. del Castillo Igareda, "Posicionamiento mediante radar de vehículos y su representación mediante realidad extendida," 2023. [Online]. Available: https://hdl.handle.net/10902/29401

[202] S. Sternlund, J. Strandroth, M. Rizzi, A. Lie, and C. Tingvall, "The effectiveness of lane departure warning systems—A reduction in real-world passenger car injury crashes," *Traffic Inj Prev*, vol. 18, p. 0, Jun. 2016, doi: 10.1080/15389588.2016.1230672.

[203] P. F. Oliveira, B. F. Wissingh, J. Van De Sluis, E. G. Broenink, M. M. T. J. De Kruijf, and Z. Domagala-Schmidt, "Misbehaviour Detection System for Intelligent Speed Assistance (ISA)," in *2024 IEEE Intelligent Vehicles Symposium (IV)*, 2024, pp. 1792–1799. doi: 10.1109/IV55156.2024.10588773.

[204] A. Ya'u Gital *et al.*, "Review of GPS-GSM Based Intelligent Speed Assistance Systems: Development and Research Opportunities," in *2023 3rd International Conference on Intelligent Communication and Computational Techniques (ICCT)*, 2023, pp. 1–8. doi: 10.1109/ICCT56969.2023.10076115.

[205] K. Brookhuis and D. de Waard, "Limiting speed, towards an intelligent speed adapter (ISA)," *Transp Res Part F Traffic Psychol Behav*, vol. 2, no. 2, pp. 81–90, 1999, doi: https://doi.org/10.1016/S1369-8478(99)00008-X.

[206] E. Arnold, M. Dianati, R. de Temple, and S. Fallah, "Cooperative Perception for 3D Object Detection in Driving Scenarios Using Infrastructure Sensors," *IEEE Transactions on Intelligent Transportation Systems*, vol. 23, no. 3, pp. 1852–1864, 2022, doi: 10.1109/TITS.2020.3028424.

[207] C. Liu, Y. Chen, J. Chen, R. Payton, M. Riley, and S.-H. Yang, "Cooperative Perception With Learning-Based V2V Communications," *IEEE Wireless Communications Letters*, vol. 12, no. 11, pp. 1831–1835, 2023, doi: 10.1109/LWC.2023.3295612.

[208] J. Wang *et al.*, "Dynamic Clustering and Cooperative Scheduling for Vehicle-to-Vehicle Communication in Bidirectional Road Scenarios," *IEEE Transactions on Intelligent Transportation Systems*, vol. 19, no. 6, pp. 1913–1924, 2018, doi: 10.1109/TITS.2017.2743821.

[209] R. Xu, H. Xiang, X. Xia, X. Han, J. Li, and J. Ma, "OPV2V: An Open Benchmark Dataset and Fusion Pipeline for Perception with Vehicle-to-Vehicle Communication," in *2022 International Conference on Robotics and Automation (ICRA)*, 2022, pp. 2583–2589. doi: 10.1109/ICRA46639.2022.9812038.

[210] D. Na and S. Park, "Blockchain-Based Dashcam Video Management Method for Data Sharing and Integrity in V2V Network," *IEEE Access*, vol. 10, pp. 3307–3319, 2022, doi: 10.1109/ACCESS.2022.3140419.

[211] Q. Chen, S. Tang, Q. Yang, and S. Fu, "Cooper: Cooperative Perception for Connected Autonomous Vehicles Based on 3D Point Clouds," in *2019 IEEE 39th International Conference on Distributed Computing Systems (ICDCS)*, 2019, pp. 514–524. doi: 10.1109/ICDCS.2019.00058.

[212] E. Uhlemann, "Platooning: Connected Vehicles for Safety and Efficiency [Connected Vehicles]," *IEEE Vehicular Technology Magazine*, vol. 11, no. 3, pp. 13–18, 2016, doi: 10.1109/MVT.2016.2583140.

[213] S. Tsugawa, S. Jeschke, and S. E. Shladover, "A Review of Truck Platooning Projects for Energy Savings," *IEEE Transactions on Intelligent Vehicles*, vol. 1, no. 1, pp. 68–77, 2016, doi: 10.1109/TIV.2016.2577499.

[214] L. Jingwen, Y. Fang, N. Yaqian, W. Jingzhi, and Y. Yongsheng, "Research on driverless truck PLATOON control based on improved variable time headway policy," in *2022 International Symposium on Sensing and Instrumentation in 5G and IoT Era (ISSI)*, 2022, pp. 24–28. doi: 10.1109/ISSI55442.2022.9963384.

[215] D. Yanakiev and I. Kanellakopoulos, "Nonlinear spacing policies for automated heavy-duty vehicles," *IEEE Trans Veh Technol*, vol. 47, no. 4, pp. 1365–1377, 1998, doi: 10.1109/25.728529.

[216] L. Jingwen, Y. Fang, N. Yaqian, W. Jingzhi, and Y. Yongsheng, "Research on driverless truck PLATOON control based on improved variable time headway policy," in *2022 International Symposium on Sensing and Instrumentation in 5G and IoT Era (ISSI)*, 2022, pp. 24–28. doi: 10.1109/ISSI55442.2022.9963384.

[217] Y. Zheng, S. Eben Li, J. Wang, D. Cao, and K. Li, "Stability and Scalability of Homogeneous Vehicular Platoon: Study on the Influence of Information Flow Topologies," *IEEE Transactions on Intelligent Transportation Systems*, vol. 17, no. 1, pp. 14–26, 2016, doi: 10.1109/TITS.2015.2402153.

[218] Y. Zheng, S. Eben Li, J. Wang, D. Cao, and K. Li, "Stability and Scalability of Homogeneous Vehicular Platoon: Study on the Influence of Information Flow Topologies," *IEEE Transactions on Intelligent Transportation Systems*, vol. 17, no. 1, pp. 14–26, 2016, doi: 10.1109/TITS.2015.2402153.

[219] D. Yanakiev and I. Kanellakopoulos, "Nonlinear spacing policies for automated heavy-duty vehicles," *IEEE Trans Veh Technol*, vol. 47, no. 4, pp. 1365–1377, 1998, doi: 10.1109/25.728529.

[220] J. Xu, Z. Q. Sun, Y. S. Long, and L. Zhan, "Car-following behavior of passenger cars on river crossing bridge based on naturalistic driving data," *China Journal of Highway and Transport*, vol. 35, no. 005, pp. 170–178, 2022.

[221] C. L. Kang and Y. Ai, "Study on the influence of road attachment coefficient on the safety distance of cars," *Highways and Automotive Applications*, no. 3, pp. 45–47, 2018.

[222] D. Yanakiev and I. Kanellakopoulos, "Nonlinear spacing policies for automated heavy-duty vehicles," *IEEE Trans Veh Technol*, vol. 47, no. 4, pp. 1365–1377, 1998.

[223] J. Y. Wang, Z. Z. Li, J. W. Zhang, and H. Z. Xu, "Intelligent Driver Model in Haze Weather onStraight Section of Expressway," *Transport Research*, vol. 1, no. 1, pp. 86–91, 2015.

[224] M. Treiber, A. Hennecke, and D. Helbing, "Congested traffic states in empirical observations and microscopic simulations," *Phys Rev E*, vol. 62, no. 2, p. 1805, 2000.

[225] V. Rajaram and S. C. Subramanian, "Heavy vehicle collision avoidance control in heterogeneous traffic using varying time headway," *Mechatronics*, vol. 50, pp. 328–340, 2018.

[226] Y. Chen and I. Darwazeh, "Quality of service (QoS) analysis of an Internet traffic trace over gigabit Ethernet," in *ICT 2013*, 2013, pp. 1–4. doi: 10.1109/ICTEL.2013.6632116.

[227] V. Gomez-Jauregui *et al.*, "New methods and functionalities for railway maintenance through a draisine prototype based on RADAR sensors," *IET Intelligent Transport Systems*, vol. 17, no. 8, pp. 1608–1628, Aug. 2023, doi: 10.1049/itr2.12353.

Annexes

Annex A: PRESENTATIONS AND COLLABORATIONS IN RESEARCH PROJECTS

This thesis has resulted in a series of presentations, collaborations in research projects and patents.

This thesis is part of the industrial doctorate program. For this reason, the dissemination of the results of this thesis has not focused on scientific journals but on participation in conferences, specialized events of each of the industries and the publication of articles in specialized journals. The most important ones presented are listed below in chronological order.

Presentations

- Autosens – Brussels , September 2017
- Ideas from Europe – Tallin, November 2017
- LA Comotion – Los Angeles, November 2017
- Misión tecnológica CDTI – Sidney, December 2017
- Metro World Congress RailLive – Bilbao, April 2018
- United Nations Economic Council Europa – IoT Forum – Geneva, April 2018
- Automated Driving Conference – Washington DC, June 2018
- EU Strategic Transport Research & Innovation Agenda – Grazz, November 2018
- Automotive Sensors & Electronics Summit – Munich, February 2019
- EU Connected Cooperative Autonomous Mobility – Brussels, June 2019
- International Road Federation R2T Conference – Las Vegas, November 2019
- World Congress Rail Research – Tokyo, October 2019
- Wunder Mobility Summit – Hamburg, November 2019

Collaborations in research projects

- 2016 - 2017 Eureka Project E!11759 RPS Railways in collaboration with the IZM Group (Institute for Reliability and Microintegration IZM) of the

Fraunhofer Institute, the Microperipheral Technology Research Group of the Faculty of Electrical Engineering and Computer Science of the Technische Universität Berlin and the German company ECD.

- 2019 – 2021 CIEN Project for the development of a CBTC in collaboration with CAF Signalling, INTEGRATED TECHNOLOGY SYSTEMS, S.L, TELTRONIC SAU and MASATS S.A.

Annex B: PATENTS

This thesis has generated a set of intellectual property that has been claimed in numerous countries. For simplicity, reference is made to patents registered in the USA.

- US 10,853,606 B2: Encoded surfaces that are read by three-dimensional radar imaging systems
- US 10,824,152 B2: Automated guidance system for vehicles by means of dielectric changes in a prerecorded rail-guide
- US 11,814,089 B2: Encoded information means located on infrastructure to be decoded by sensors located on mobiles
- US 11,565,733 B2: Speed Control and track change detection device suitable for railways
- US 2021/0232156 A1: Semi-automated convoy transport system for vehicles

US010853606B2

(12) **United States Patent**
Martin

(10) **Patent No.: US 10,853,606 B2**
(45) **Date of Patent: Dec. 1, 2020**

(54) **ENCODED SURFACES THAT ARE READ BY THREE-DIMENSIONAL RADAR IMAGING SYSTEMS**

(71) Applicant: **Auto Drive Solutions S.L.**, Madrid (ES)

(72) Inventor: **Alejandro Badolato Martin**, Madrid (ES)

(73) Assignee: **AUTO DRIVE SOLUTIONS S.L.**, Madrid (ES)

(*) Notice: Subject to any disclaimer, the term of this patent is extended or adjusted under 35 U.S.C. 154(b) by 0 days.

(21) Appl. No.: **16/464,266**

(22) PCT Filed: **Nov. 25, 2016**

(86) PCT No.: **PCT/IB2016/057119**
§ 371 (c)(1),
(2) Date: **May 25, 2019**

(87) PCT Pub. No.: **WO2018/096388**
PCT Pub. Date: **May 31, 2018**

(65) **Prior Publication Data**

US 2019/0392185 A1 Dec. 26, 2019

(51) **Int. Cl.**
G06K 7/14 (2006.01)

(52) **U.S. Cl.**
CPC ***G06K 7/1404*** (2013.01)

(58) **Field of Classification Search**
CPC G06K 7/1404; G06K 9/3216; G06K 9/00791; G06K 19/06046; G06K 7/10376; G06K 19/06037; G06K 7/1417; G05D 1/0257; G05D 1/0251
See application file for complete search history.

(56) **References Cited**

U.S. PATENT DOCUMENTS

2,996,137	A	8/1961	Yaohan et al.	
6,529,154	B1	3/2003	Schramm et al.	
9,665,779	B2 *	5/2017	Ooi	G06K 9/00798
2018/0052464	A1 *	2/2018	Badolato Martin	G01S 13/751

FOREIGN PATENT DOCUMENTS

ES	2184602	4/2003
WO	2016180992	11/2016

OTHER PUBLICATIONS

International Search Report dated Sep. 5, 2017.
Written Opinion dated Sep. 5, 2017.

* cited by examiner

Primary Examiner — Seung H Lee
(74) *Attorney, Agent, or Firm* — Aslan Law, P.C.

(57) **ABSTRACT**

The invention relates to encoded surfaces that are read by a three-dimensional radar imaging system. The reader scans different zones in a pre-determined area of the encoded surface, each of said zones comprising projections or indentations, similar to Braille. The image obtained can be used to estimate the position of the camera relative to the known pattern. The relative movement between the reader and the encoded surface allows other areas of the surface to be scanned and, in this way, the sensor can decode a message etched along the path followed by the imaging sensor.

4 Claims, 1 Drawing Sheet

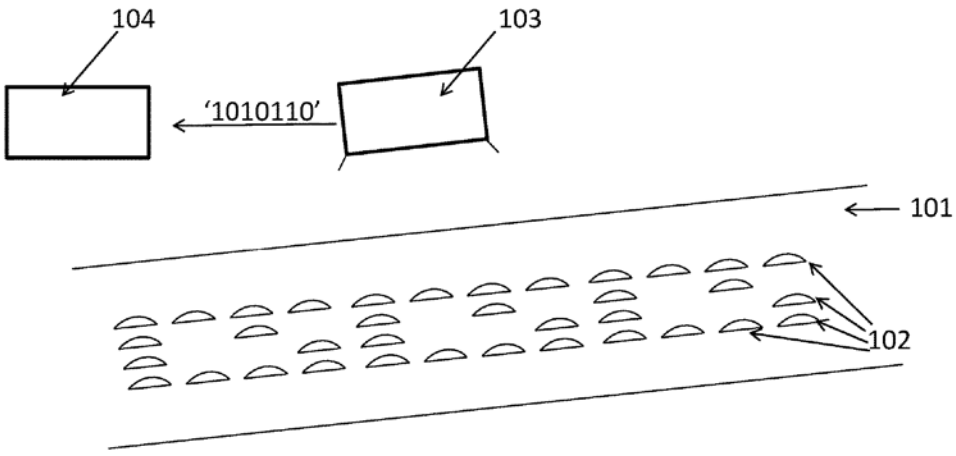

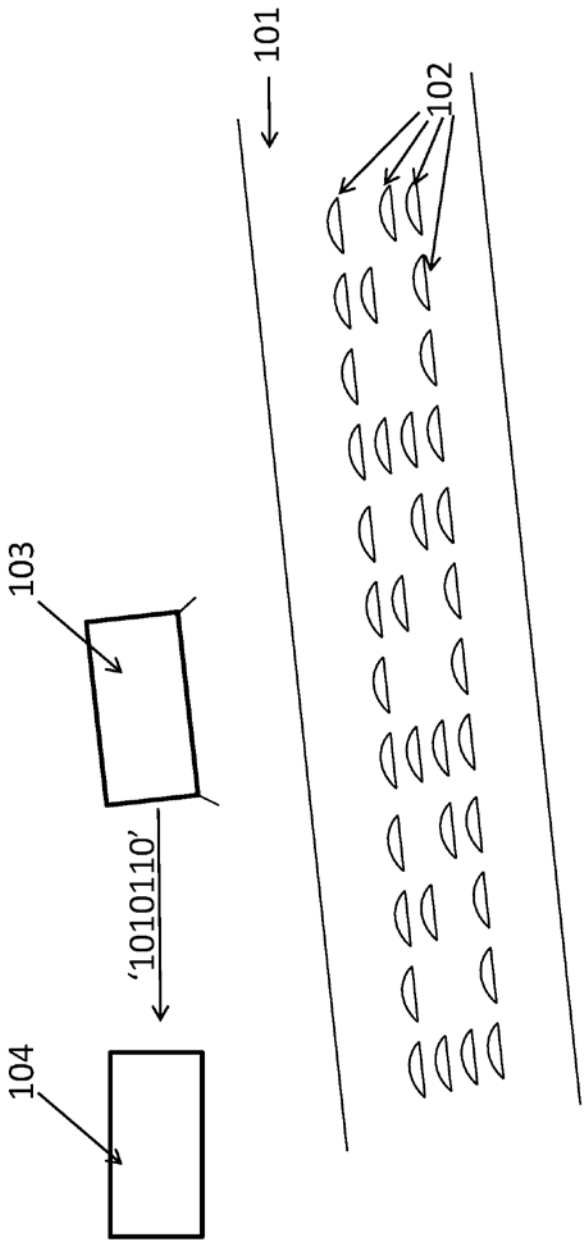
101
102
103
'1010110'
104

ENCODED SURFACES THAT ARE READ BY THREE-DIMENSIONAL RADAR IMAGING SYSTEMS

CROSS-REFERENCE TO RELATED APPLICATION

This application is a 35 U.S.C. § 371 national stage application of PCT Application No. PCT/IB2016/057119, filed on Nov. 25, 2016, which is incorporated herein by reference in their entireties. The above-referenced PCT International Application was published as International Publication No. WO2018/096388 A1 on May 31, 2018.

OBJECT OF THE INVENTION

The proposed invention relates to encoded surfaces that are read by a three-dimensional radar imaging system during the displacement of the reader.

The reader examines different zones of a determined area of the encoded surface where each one of the zones exhibits protrusions or indentations similar to the braille coding system.

The image obtained allows the position of the camera to be estimated with respect to the known pattern.

The relative movement of the reader with respect to the encoded surface allows other areas of the surface to be examined and in this way the sensor is capable of decoding a message recorded along the trajectory followed by the image sensor.

These encoded surfaces can be used, amongst other things, to determine the absolute position of the reader, provided information is encoded about the position with respect to an absolute coordinate system in the surface and the reader is capable of determining its relative position and said information.

It also serves to identify that the reader has scanned a surface encoded with a determined pattern which identifies an object and even for systems of numeric control of objects.

FIELD OF THE INVENTION

The field of the invention is the high-tech industry of positioning and control of mobile phones and objects which can be applied preferably in surface transport devices and in assembly lines or cranes.

BACKGROUND OF THE INVENTION

There is some background for devices which carry out a similar information reading function.

Among which, the inventor is also the inventor of the international patent PCT/ES2015/070378 where as an encoding means a rail guide is described installed at the level of the road surface, although it can optionally be hidden under a layer of asphalt treated with a layer of hydrophobic material with preferred dimensions of 1.5 cm width by 5 cm depth and where hollows are machined in its interior, the preferred form of the hollows being dihedrals since the planes of the dihedrals increase the reflected signal, therefore facilitating its detection.

Similarly, the same inventor has registered the international patent PCT/IB2016/051159 where other information means are detailed with the same purpose. These reading and information encoding systems have more applications wherein it is not necessary for the sensor to be installed on a mobile phone and the encoded information does not have the sole purpose of determining the relative position of the sensor with respect to the encoded medium.

But the case where the reader not only examines in one pointing direction, but rather is capable of exploring an area of the surface, obtaining a three-dimensional image where there are determined protrusions of variable thickness or indentations with different depth has not been thus far resolved and this is what the proposed invention achieves.

There is no prior art known by the inventor incorporating the arrangements presented in the present invention, nor the advantages which said arrangement entails.

BRIEF DESCRIPTION OF THE DRAWINGS

FIG. **1** is a functional block diagram illustrating a three-dimensional radar imaging system according to one or more embodiments described herein.

DESCRIPTION OF THE INVENTION

The proposed invention relates to encoded surfaces **102** that are read by a three-dimensional radar imaging system **103** as illustrated in, for example, FIG. **1**. The reader examines different areas of a determined area of the encoded surface where each one of the areas presents protrusions or indentations similar to the braille encoding system. The image obtained allows the position of the camera to be estimated with respect to the known pattern.

The relative movement of the reader with respect to the encoded surface allows other zones of the surface **101** (e.g., asphalt) to be examined and in this way the sensor is capable of decoding a message recorded along the trajectory followed by the image sensor.

These encoded surfaces can be used, amongst other things, to determine the absolute position of the reader, provided information is encoded about the position with respect to an absolute coordinate system in the surface and the reader is capable of determining its relative position and said information via element **104** (e.g., a data decoder and positioning system). It also serves to identify that the encoded surface has overrun the sensor or vice versa and even for systems of numeric control of objects.

The information is extracted by means of detecting the borders of dielectric change of the medium or by means of detecting the dielectric metal borders where the changes are detected by means of image sensors such as high resolution radar device or other similar detector

These borders are examined by means of a sensor for pressure or electromagnetic waves and, by measuring the time taken by the ways to return to the sensor, it is possible to determine the distances at which that reflections are produced and thereby extract the information. The information is encoded by means of various mechanisms. One of these is to modify the thickness of the protrusions or the depth of the indentations. Another mechanism is to locate the projection or indentation in a determined position with respect to the other projection or indentation. A third mechanism is to combine the two foregoing mechanisms.

It is possible to replace the image radar sensor, which is capable of examining different zones of the explored area by means of electronic pointing, with a set of sensors distributed on the axis transversal to the trajectory and separated from each other by a determined distance such that the senses coincide with the longitudinal axes where the information is encoded. When the sensors at the ends are detecting the projections on each transversal axis, the information

resides in the detection of a projection which is detected by one or another intermediate sensor.

An exemplary application which emerges from this reading and encoding system is the guidance and positioning of vehicles where a surface close to the location where the vehicle is displayed is encoded and where the vehicle incorporates a three-dimensional image system. Another application is the identification of objects which encode in their surface information with a determined pattern and a radar reader which detects add patterns.

PREFERRED EMBODIMENT OF THE INVENTION

The preferred embodiment consists of an infrastructure which has paint speckles on its surface along its trajectory.

The paint speckles have a 1 cm squared surface and a thickness of 0.5 cm. The information is encoded, having two paint speckles with a separation of 10 cm on an axis perpendicular to that of the trajectory of the infrastructure. The locating of a third paint speckle between both determines the logic level of the transversal axes as is described:

1 speckle separated by 2 cm from the left speckle in the direction of travel of the vehicle determines a logic level 1.

1 speckle separated by 4 cm from the left speckle in the direction of travel of the vehicle determines a logic level 0.

1 speckle separated by 6 cm from the left speckle in the direction of travel of the vehicle determines a logic level word start bit.

1 speckle separated by 8 cm from the left speckle in the direction of travel of the vehicle determines the logic level word end bit.

The information is encoded forming words starting with a start bit, then 64-bit of data 1 or 0 are encoded and lastly they have a stop bit. The separation between each one of the transversal axes where 3 speckles are encoded is 2 cm.

This encoded surface is read by means of high resolution radar which, coupled to the underside of the vehicle, has electronic pointing capacity and explores each square centimetre of a visual field of approximately 50×50 cm squared.

In addition, the sensor can be coupled to the vehicle via a motorised mobile transversal axis which allows it to be displaced from one wheel to another to facilitate the reading.

The displacement of the vehicle along the trajectory allows other zones of the medium to be examined and in this way the sensor is capable of decoding a message recorded about the situation and positioning

With the nature of the invention sufficiently described and the manner of putting it into practice, it should be stated that the arrangements previously indicated and represented in the attached drawings can be modified in detail once they do not alter their fundamental principles, established in the previous paragraphs and summarised in the following claims.

What is claimed is:

1. Encoded surfaces that are read by a three-dimensional radar imaging system, the encoded surfaces comprising:

surfaces encoded by shapes which can be readable by sensitive readers located apart for reading the surface encoded by shapes,

wherein sensitive readers emit pressure or electromagnetic waves to examine each one of a plurality of zones of an explored area and obtain information on a distance at which each one of possible reflections is produced due to a change between a boundary between two different media, and

wherein information being encoded in an axis transversal to a trajectory is defined by a presence of two projections, including a first projection and a second projection, separated by x cm from one another and a third projection located between said two of said projections with respect to said first projection in a direction of travel of said trajectory, in the following manner:

a) at a distance of A cm to associate said axis with a logic level 0;

b) at a distance of B cm to associate said axis with a logic level 1;

c) at a distance of C cm to associate said axis with a logic level word start bit; and

d) at a distance of D cm to associate said axis with a logic level word end bit,

wherein A<B<C<D<X, and

wherein A>0.

2. The encoded surfaces according to claim **1** wherein said surface has projections and indentations arranged on axis transversal to a trajectory and a reader is formed by a radar configured to emit energy by pressure or electromagnetic waves to examine each one of said zones of said explored area and detects the presence of said projections and said indentations arranged on said axis by determining a distance at which a reflection is produced due to a change between a boundary between two different media.

3. Encoded surfaces that are read by a three-dimensional radar imaging system, the encoded surfaces comprising:

a plurality of paint speckles disposed on the encoded surface along a trajectory of the encoded surface and wherein said paint speckle have a surface of 1 cm squared and a thickness of 0.5 cm wherein information being encoded is defined by two paint speckles including a left paint speckle and a right paint speckle with a separation of 10 cm on an axis perpendicular to that of said trajectory;

said paint speckles including a third paint speckle wherein locating of said third paint speckle between said two paint speckles determines logic levels of a transversal axis wherein:

said third paint speckle is separated by 2 cm from said left speckle in a direction of travel of a vehicle defining a logic level 1;

said third paint speckle is separated by 4 cm from said left speckle in the direction of travel of the vehicle defining a logic level 0;

said third paint speckle is separated by 6 cm from said left speckle in the direction of travel of the vehicle defining a logic level word start bit;

said third paint speckle separated by 8 cm from said left speckle in the direction of travel of the vehicle defining a logic level word end bit;

wherein separation between each one of said transversal axes where said paint speckles are encoded is 2 cm;

wherein information being encoded forms words starting with a start bit, then 64-bit of data including 1 or 0, and lastly a stop bit;

wherein the encoded surface is read by a high resolution radar coupled to an underside of the vehicle, having an electronic pointing capacity and configured to explore each square centimeter of a visual field of approximately 50×50 cm squared; and

wherein a sensor is coupled to the vehicle via a motorized mobile transversal axis allowing said sensor to be displaced from one wheel to another to facilitate with the reading.

4. The encoded surfaces according to claim 3 wherein information being encoded in said axis transversal to said trajectory is defined by a presence of two of said projections, including a left projection and a right projection, separated by 10 cm from one another and a third projection located between said two of said projections with respect to said left projection in a direction of travel of said trajectory, in the following manner:

a) at a distance of 2 cm to associate said axis with a logic level 0;

b) at a distance of 4 cm to associate said axis with a logic level 1;

c) at a distance of 6 cm to associate said axis with a logic level word start bit; and

d) at a distance of 8 cm to associate said axis with a logic level word end bit.

* * * * *

US010824152B2

(12) **United States Patent**
Badolato Martin

(10) **Patent No.: US 10,824,152 B2**
(45) **Date of Patent: Nov. 3, 2020**

(54) **AUTOMATIC GUIDANCE SYSTEM FOR VEHICLES BY MEANS OF DIELECTRIC CHANGES IN A PRERECORDED RAIL-GUIDE**

(71) Applicant: **AUTO DRIVE SOLUTIONS S.L.**, Madrid (ES)

(72) Inventor: **Alejandro Badolato Martin**, Madrid (ES)

(73) Assignee: **AUTO DRIVE SOLUTIONS S.L.**, Madrird (ES)

(*) Notice: Subject to any disclaimer, the term of this patent is extended or adjusted under 35 U.S.C. 154(b) by 0 days.

(21) Appl. No.: **14/913,384**

(22) PCT Filed: **May 12, 2015**

(86) PCT No.: **PCT/ES2015/070378**
§ 371 (c)(1),
(2) Date: **Feb. 22, 2016**

(87) PCT Pub. No.: **WO2016/180992**
PCT Pub. Date: **Nov. 17, 2016**

(65) **Prior Publication Data**

US 2018/0052464 A1 Feb. 22, 2018

(51) **Int. Cl.**

G05D 1/02	(2020.01)
H01Q 1/32	(2006.01)
H01Q 15/00	(2006.01)
G01S 13/75	(2006.01)

(52) **U.S. Cl.**
CPC ***G05D 1/0212*** (2013.01); ***G01S 13/751*** (2013.01); ***G05D 1/027*** (2013.01); ***G05D 1/0257*** (2013.01); ***G05D 1/0278*** (2013.01); ***H01Q 1/3225*** (2013.01); ***H01Q 15/0006*** (2013.01); *G05D 2201/0213* (2013.01)

(58) **Field of Classification Search**
CPC G05D 1/0212; G05D 1/0257; G05D 1/027; G05D 1/0278; G05D 2201/0213; H01Q 1/3225; H01Q 15/0006; G01S 13/751; G01S 13/88
USPC 701/23
See application file for complete search history.

(56) **References Cited**

U.S. PATENT DOCUMENTS

2,996,137	A *	8/1961	Yaohan	G01S 13/75 180/168
3,550,077	A *	12/1970	Swift	G05D 1/0265 340/905
8,831,800	B2 *	9/2014	Parienti	G05D 1/0234 180/167

* cited by examiner

Primary Examiner — Muhammad Shafi
(74) *Attorney, Agent, or Firm* — Aslan Law, P.C.

(57) **ABSTRACT**

System of automatic guidance of vehicles by means of the detection of changes of the dielectric properties in a pre-recorded rail-guide, wherein the dielectric changes are detected by a high resolution radar device and wherein there is a control system of the vehicle that has the ancillary means required to convert it to an auto guidance system characterized in that the system is composed by a pre-recorded rail-guide (**1**) an information reading device (**11**) and auxiliary means of vehicle control (**12**).

20 Claims, 8 Drawing Sheets

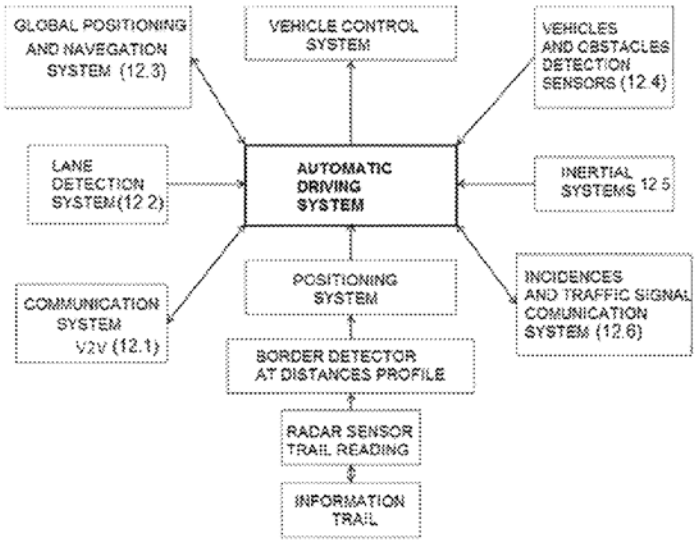

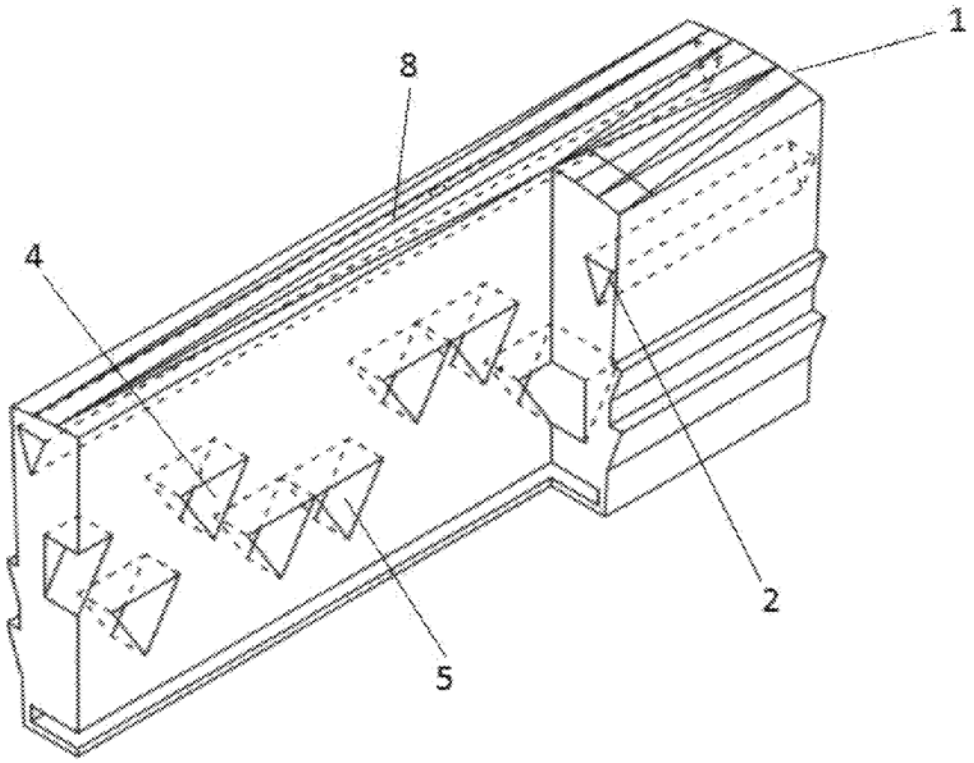

FIG. 1

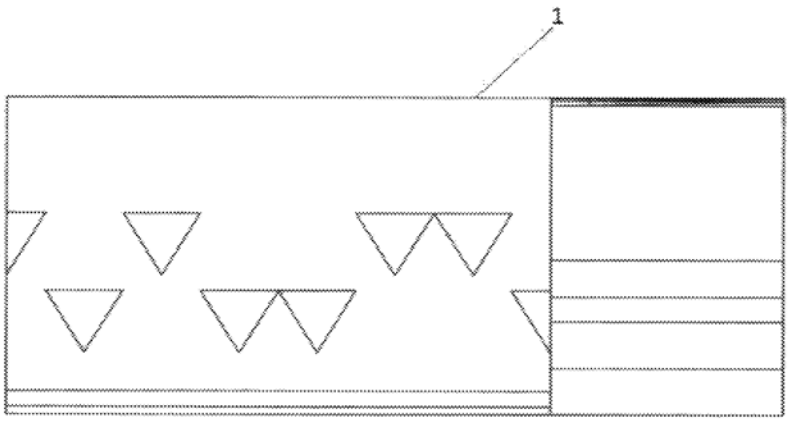

FIG. 2

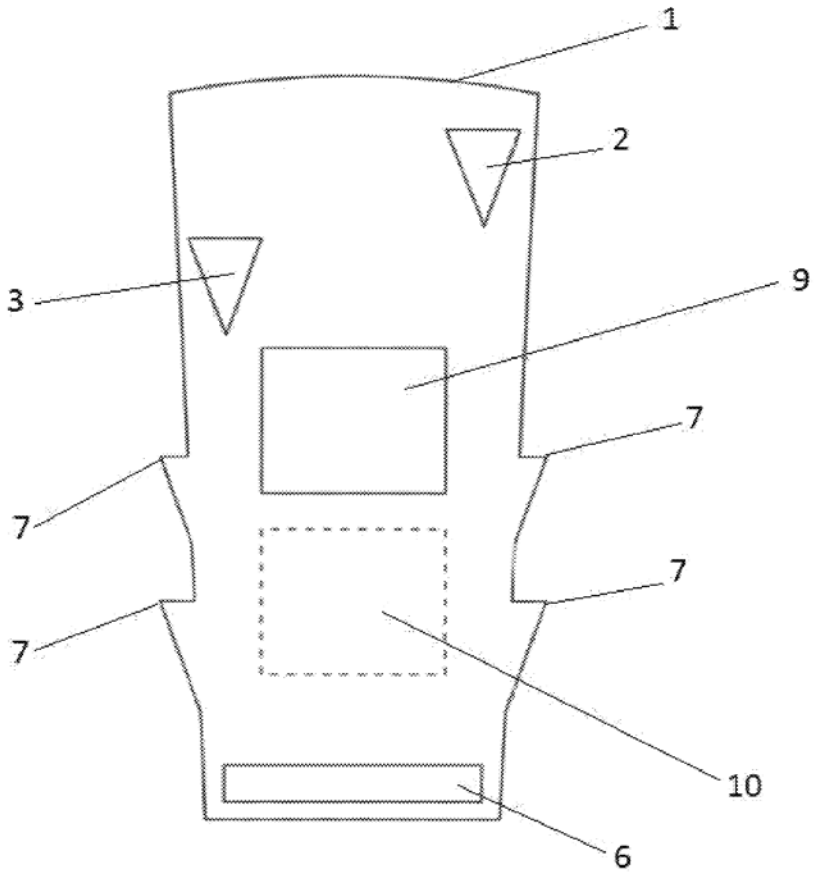

FIG. 3

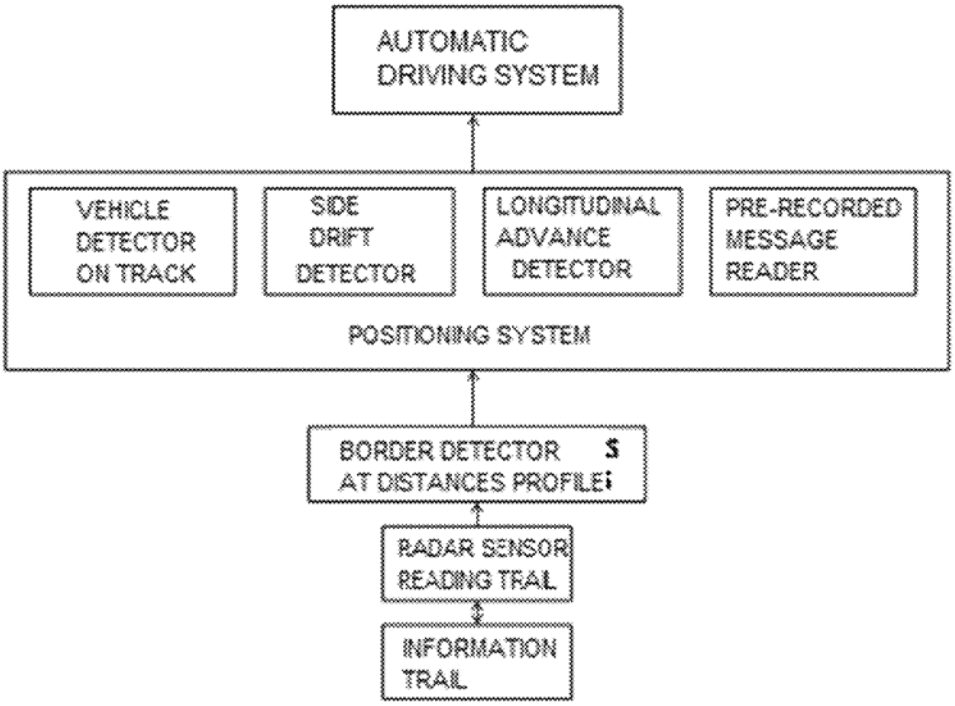
AUTOMATIC DRIVING SYSTEM
VEHICLE DETECTOR ON TRACK
SIDE DRIFT DETECTOR
LONGITUDINAL ADVANCE DETECTOR
PRE-RECORDED MESSAGE READER
POSITIONING SYSTEM
BORDER DETECTOR AT DISTANCES PROFILE Si
RADAR SENSOR READING TRAIL
INFORMATION TRAIL

FIG. 4

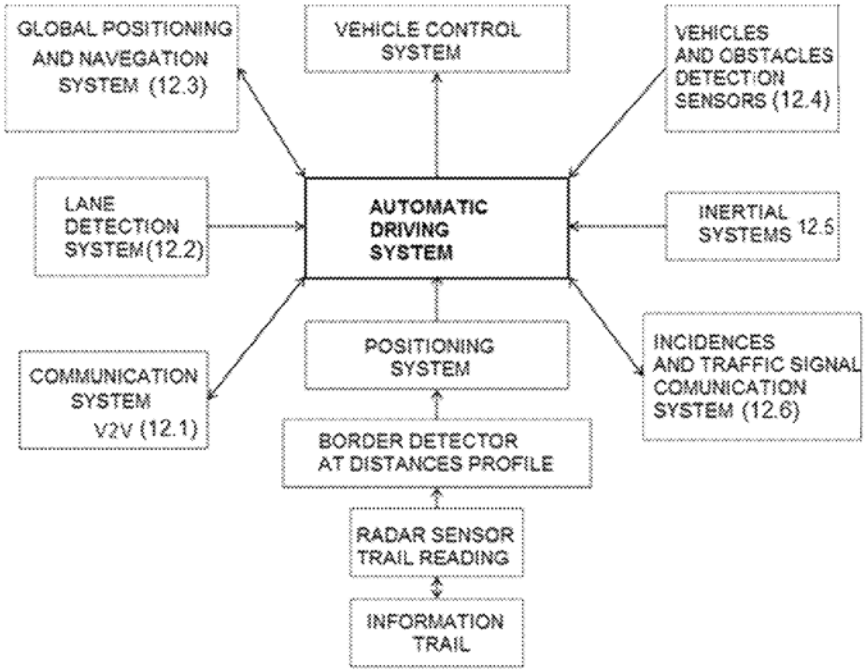
GLOBAL POSITIONING AND NAVEGATION SYSTEM (12.3)
VEHICLE CONTROL SYSTEM
VEHICLES AND OBSTACLES DETECTION SENSORS (12.4)
LANE DETECTION SYSTEM(12.2)
AUTOMATIC DRIVING SYSTEM
INERTIAL SYSTEMS 12.5
COMMUNICATION SYSTEM V2V (12.1)
POSITIONING SYSTEM
INCIDENCES AND TRAFFIC SIGNAL COMUNICATION SYSTEM (12.6)
BORDER DETECTOR AT DISTANCES PROFILE
RADAR SENSOR TRAIL READING
INFORMATION TRAIL

FIG. 5

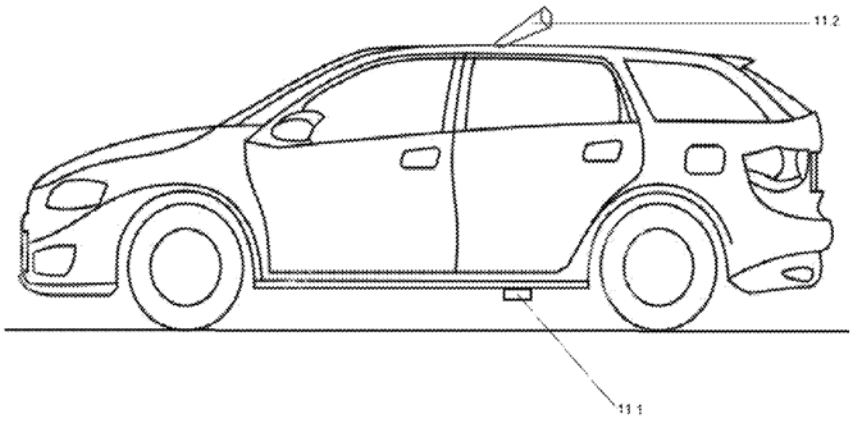

FIG. 6

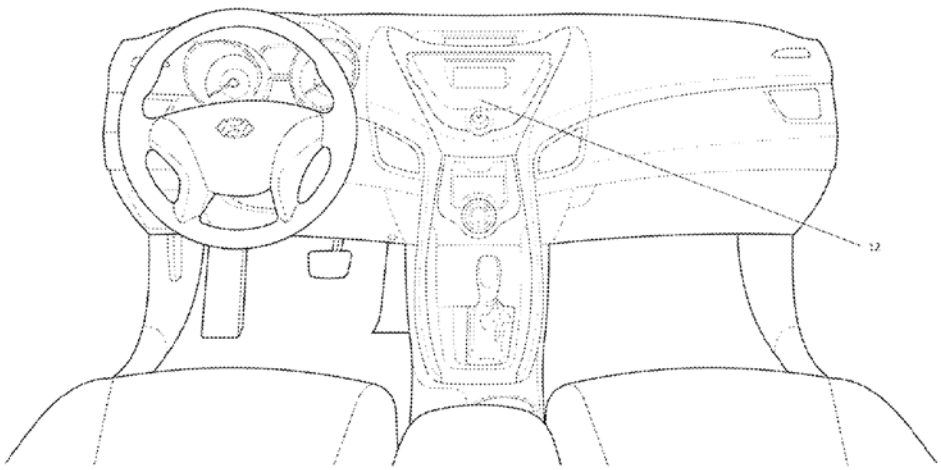

FIG. 7

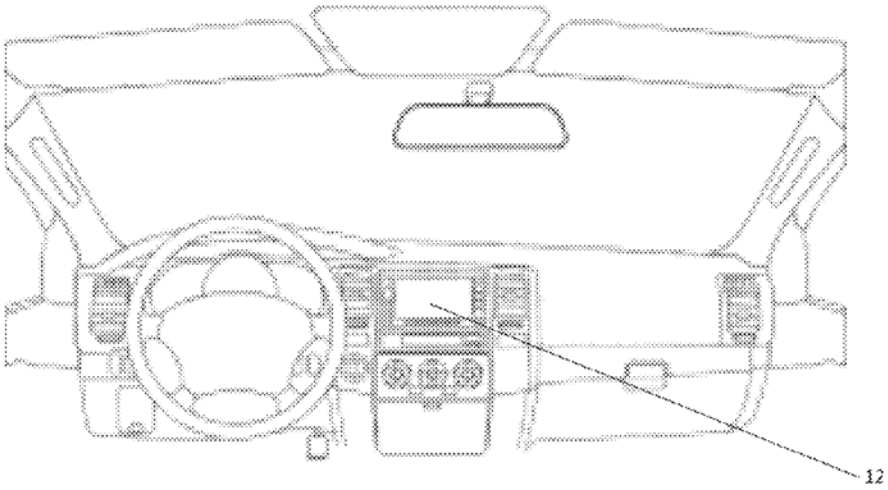

FIG. 8

AUTOMATIC GUIDANCE SYSTEM FOR VEHICLES BY MEANS OF DIELECTRIC CHANGES IN A PRERECORDED RAIL-GUIDE

CROSS-REFERENCE TO RELATED APPLICATIONS

Not Applicable

STATEMENT REGARDING FEDERALLY SPONSORED RESEARCH OR DEVELOPMENT

Not Applicable

THE NAMES OF THE PARTIES TO A JOINT RESEARCH AGREEMENT

Not Applicable

STATEMENT REGARDING PRIOR DISCLOSURES BY THE INVENTOR OR A JOINT INVENTOR

Not Applicable

BACKGROUND OF THE INVENTION

Field of the Invention

The field of the invention is the auxiliary automotive industry as well as the electronics industry.

Description of Related Art

There are a number of precedents on devices that perform the same function of autonomous driving of vehicles.

Among them the inventor knows the following:

U.S. Pat. No. 3,550,077 A. This invention relates to a guidance system for vehicles on the ground.

More particularly this system refers to a guidance system of vehicles using as the guiding element a copper cable.

This system is much more limited than that proposed in the present invention since it does not provide longitudinal or position information.

Moreover, the system installed on the road is not passive. It needs a generator.

U.S. Pat. No. 8,831,800: Refers to an automatic system of transportation that includes at least a vehicle without a driver that moves from one point to another following a rail integrated in the pavement that has optical characteristics and a set of chips arranged at regular intervals.

This system, more evolved than the one previously described, suffers from major problems, since the guidance system is optical and is therefore subjected to great lighting contrasts that hinder the operation of the detectors.

Under fog or rainy conditions the system may be seriously affected.

The transponder system does not allow having an appropriate longitudinal resolution (it is not possible to install a transponder each centimeter).

Furthermore, these transponders also can be affected by working in extreme environmental conditions or by the existence of interferences.

On the other hand, the integrity of the system is compromised as an interfering transmission can simulate the signal from one of the transponders.

The proposed invention in this specification solves all of the above problems with absolute reliability because the proposed system has a centimeter resolution throughout the track and not only in the places where the transponders have been placed.

It is also important to highlight that the media where the data is recorded in the proposed system can be a polymeric material which has a good preservation capacity in adverse environments and also, due to a high transmitting bandwidth, the capacity for interference is negligible since, if the interfering signal is minimally different from the transmitted signal (something that happens in practice with two identical systems), the processing gain will be low (see spread-spectrum techniques) and the received power will not be correctly added.

The inventor is not aware of any prior background incorporating the provisions that are provided by the current invention, nor the advantages inherent in these provisions.

BRIEF SUMMARY OF THE INVENTION

The proposed invention refers to a system of automatic guidance of vehicles by means of the detection of changes of the dielectric properties in a pre-recorded rail-guide, wherein the dielectric changes are detected by a high resolution radar device and wherein the control system of the vehicle has the ancillary means required to convert it to an auto guidance system.

BRIEF DESCRIPTION OF THE SEVERAL VIEWS OF THE DRAWINGS

For a better understanding of the invention attached can be found a sheet of drawings in which the following is appreciated

FIG. **1**. Perspective view and with a side cut in the lane.

FIG. **2**.—Lateral cut view of the lane.

FIG. **3**.—Perpendicular section view of the lane.

FIG. **4**.—Diagram that represents the pre-recorded message that may exist on the road, namely, the radar sensor detects the borders in the distances profile, being configured as a positioning system, detecting the vehicle on the rail-guide, the lateral drift and the longitudinal advance.

FIG. **5**.—Diagram presenting the auxiliary means of the control of the vehicle

FIG. **6**.—Shows the information reading devices (**11**)

FIGS. **7** AND **8**.—Show the auxiliary means of the control of the device (**12**)

And in said figures, identical elements have the same reference, among which it can be distinguished:

(1).—rail-guide,
(2).—dihedral from the right side band
(3).—dihedral from the left side band,
(4).—dihedral in the logic level "1",
(5).—dihedral in the logic level "0",
(6).—border at the end of the trail,
(7).—collocation shoulders,
(8).—upper border non visible,
(9).—logic level "1",
(10).—logic level "0",
(11).—information reading device
(11.1).—radar sensor
(11.2).—antenna
(12).—auxiliary means of the control of the device
(12.1).—communication means by systems V2V,
(12.2).—means to detect the rail-guide,
(12.3).—global positioning an navigation means,

(12.4).—vehicle and obstacle detection means.
(12.5).—inertial systems,
(12.6).—incidences and traffic signals communication means.

DETAILED DESCRIPTION OF THE INVENTION

The proposed invention refers to a system of automatic guidance of vehicles by means of the detection of changes of the dielectric properties in a pre-recorded rail-guide, wherein the dielectric changes are detected by a high resolution radar device and wherein the control system of the vehicle has the ancillary means required to convert it to an auto guidance system.

It is proposed a solution that allows for the information encoded in a non-conducting material to be read through the existence or not of boundaries of change in the dielectric constant in the medium which are perceivable using radar techniques.

The boundaries in the change of dielectric in a non-conducting material cause that part of the energy radiated toward the material is reflected. This reflected energy is detected by the radar system being possible to determine the radial distance where the discontinuity is to be found.

The boundaries of change of dielectric can be set using two materials or substances whose dielectric constants are different or using a single material where the boundary is set between the material and the vacuum or the material or a gas or substance. An example of the latter is the difference that is created in a polymeric material that presents holes or recesses filled with air.

Using in the radar system an electromagnetic energy radiating system (Antenna or horn) which radiation diagram is narrow, it is possible to channel the greater part of the transmitted energy in a small volume.

By applying these principles, it is possible to build a sensor that is capable of determining the existence of a characteristic pattern of reflections that the system is capable of interpreting as binary information or other sort of information.

An example of an application of this technology is a guidance system of vehicles that reads the previously recorded information in a non-conducting material. The reading of this information may help to be able to accurately determine its position, which can be of help for an automatic guidance system of vehicles.

The proposed system is a radar device in the millimeter or sub-millimeter bands and even higher frequency (up to the limit of the visible spectrum) that transmits with a high bandwidth. Thanks to the high working frequency, it is possible to build electrically large radiant systems that allow for highly directive radiation beams with reduced physical dimensions.

A radiant element of these features docked in a car (preferably on the underside of the same) can light up a surface on the track (located preferably at a distance to the radar below one meter) the area of which is less than one square centimeter.

The radar queries the lighted up area at constant intervals of time (which are of the order of microseconds) transmitting at a particular bandwidth (on the order of tens of gigahertz). With the received signal and by processing using techniques of radar processing, a profile of the distances is obtained (level of detection of reflected signal as a function of the radial distance from the radar). At those radial distances where there is a boundary of change of dielectric, an increase at the level of received power will occur.

Whenever the beam of the antenna lights up the track, a reflection is produced at the boundaries identified as **4** and **5**, generating a known pattern determined by the distance between the two surfaces. The pattern shift control will detect such a pattern and will recalculate the distances of the detections taking as a reference of origin the surface **4**.

Based on the information supplied by the pattern shift control, the boundary identifier will decode the information stored in the aiming direction of the antenna denoting the information read from the central band of the track and the possible detection of each one of the lateral bands.

If the combination of the boundaries identified in a particular radar query matches one of the possible combinations that the track can generate at a certain point, the system will increase a counter. Similarly, each time that the combination does not correspond to one of the possible combinations the counter will be decremented.

When the counter value exceeds a certain threshold of accounting of possible combinations the detector of vehicle on track will flag the detection of the track to the positioning system. When the threshold is not reached, the detector will likewise notify.

When the beam of the antenna is perfectly centred in the central band of information (**3**), the dihedrals of detection of lateral offset (**1** and **2**) are not lit up. This way, there will not be any detection associated to the radial distance of none of the dihedrals (**1** and **2**) in the distances profile. When the beam is slightly offset to one side, the corresponding side dihedral is partially lit up, producing a reflection. Identifying the distance at which the reflection occurs, the system is able to determine the side to which the trajectory has to be corrected.

Analyzing the sequence of the distances profiles, an implemented algorithm is able to detect the transition between two consecutive pre-recorded information. When such an event happens, the progress will be notified to the positioning system the information of the position of the vehicle can be updated.

Provided that the detector of vehicle over the track indicate a correct lighting and taking advantage of the detections of the longitudinal advance, this detector will store consecutively each piece of information associated with the central strip. Using a synchronism header known or a similar mechanism, the detector will be able to identify the first information about the message of positioning. Analysing several consecutive information the system is able to read the pre-recorded code on the tape. This code corresponds to a univocal identification between the start of the message position and a system of coordinates of the land surface that is known by the system. This message is recorded continuously over the entire track. In addition, since the system has in its memory recorded the route followed by the track, each time that you detector information of longitudinal advance are received, the positioning system is able to recalculate the new position of the vehicle and report it to the automatic driving system.

The automatic driving system is capable of conducting the vehicle to the destination chosen by the navigation system. To do this, it is mainly supported by the positioning system and by the inertial systems of the vehicle.

Performing at a high working frequency allows the devices to transmit a bandwidth of about tens of Gigahertz that allow clarifications to the extent of the radial distance from the radiant element to the border of dielectric change below one millimeter (this does not depend on the band-

width but on the frequency of work) and resolutions (ability to discern two borders of change of dielectric next) lower than one centimeter. Furthermore, the penetration capacity of waves on materials at these frequencies is high (provided that the media is not the driver or is composed of water).

An example of a non-conducting means wherein it is possible to record the information may be a plastic band dimensions of which are in the range of cm and even lower.

Taking as an example a continuous wave radar and frequency modulated to transmit a bandwidth of 34 GHz (for example, at the frequency of 340 GHz wherein there is a window of atmospheric absorption that implies a low attenuation) it is possible to project the energy radiated in the firm of a road where there is located level with thereof or a few centimeters under the asphalt layer a plastic band with dimensions that can be 1.5 cm wide and 5 cm deep. As shown in the drawing, the plastic guide embedded in the road has a number of gaps that produce reflections that are detected by the radar system and interpreted as information.

A possible ramp time chirp can be 37.5 us. Therefore, it s obtained a sample of the distances profile that it is being illuminated by the antenna each 37.5 us. This way, a vehicle driving at 120 Km/h interrogates until 16 times between two consecutive information.

The sequence of two consecutive bits '1' will produce a progressive decrease of the signal level of the peak associated with the bit (does not illuminate properly the dihedral) to appear again with the maximum intensity (which occurs when the radiant system illuminates the dihedral axis of symmetry).

The information from '0' can be generated by the absence of discontinuity at the expected distance in the '1' or by mechanizing a dihedral to a different depth.

To facilitate to the vehicle guidance system the information on the lateral drift thereof, longitudinal bands can be mechanized to lower distances. For example, at 1 cm a longitudinal dihedral can be placed to the left and a 1, 5 to the right 1.5 as shown in FIG. **1**.

This way, when the radiation diagram enlightens the central part of the band will the detections will only be obtained at the distances associated with the region wherein the information has been coded (at a distance of about 15 or 16 cm related to the radar sensor) but if it starts to move laterally towards the left a signal will start to be received at a distance of 12.5 cm which level will be greater as the diagram enlightens to a greater extent the side dihedral. If, in contrast, the vehicle moves towards the right, the peak will appear at a distance of 13 cm.

In the code of '1's and '0's the information about the coordinates by which passes the road can be recorded. Using the 56 bit decoding it is possible to identify uniquely each square decimeter of the ground surface.

That is to say, in less than 0.56 meters of trail decoded, detailed information about the vehicle circulating can be obtained. It should be noted that the guidance system has stored the sequence of positions through which the road passes. This fact offers advantages to the receiver, allowing the reduction of the likelihood of a reading error.

The guidance system of the vehicle may have loaded in its memory the morphology of the road. This way, the guidance system of the vehicle can anticipate changes in the direction, adapt the speed in certain areas o increase the engine power to face a high slope.

In addition to work with very low powers (even of tens of microwatts), the possibility of interference between systems, even of the same model, is not possible. This is due to the high bandwidth transmitted. The interference with systems that operate at different frequencies is discarded.

The radar system can contain 2 antennas (transmitter o receiver) or only one (through the use of circulators or even by taking advantage of the local oscillator signal of the mixer that is transmitted by the receiver horn due to the finite isolation between the door OL and the horn.

Description of the Preferred Embodiment

The proposed invention refers to a system of automatic guidance of vehicles by means of the detection of changes of the dielectric properties in a pre-recorded rail-guide, wherein the dielectric changes are detected by a high resolution radar device and wherein the control system of the vehicle has the ancillary means required to convert it to an auto guidance system.

More particularly, the system is composed of the following elements:

pre-recorded rail-guide (**1**)

information reading device (**11**)

auxiliary means of the control of the vehicle. (**12**)

The pre-recorded rail-guide (**1**) is composed of a piece with a straight rectangular parallelepiped, with various shoulders on their sides (**7**) for correct attachment and its is manufactured in non conductive material, preferably polyethylene.

The rail-guide (**1**) will be installed level with the firm of the road, although it can optionally be hidden under a layer of asphalt treated with a layer of hydrophobic material.

The preferred dimensions of the rail-guide (**1**) are 1.5 cm wide by 5 cm deep.

Inside, the boreholes will be mechanized, being the boreholes preferred form that of dihedrals, since the planes of the dihedrals increase the reflected signal, facilitating therefore its detection.

The situation of the dihedrals that create the borders is the following:

The dihedrals of the centre band (**4** and **5**) are oriented perpendicular to the side strips (**2** and **3**), since in the first case it is pretended obtaining a variable signal level according to the longitudinal advance of the vehicle along the track and in the second case, it is obtained based on the lateral drift thereof by way of border.

The dihedrals of the side strips (**2** and **3**) are located at the same distance from the outer edges but at different heights, so the border established in each end is easily identified.

The dihedrals of the centre band (**4** and **5**) are located in the central area of the lane, located perpendicular to the external dihedrals and at different heights, to determine at least two logical levels, a logical level "1" the upper one and a logical level "0" the lower.

There is also a lower border at the end of track (**6**) in the bottom, as well as a border at the upper part (**8**), being the lower part formed by a borehole and the upper one (**8**) by the dielectric difference between the material of the rail (**1**) and the air or the asphalt (in the case of the rail-guide buried).

The preferred way to code the rail message is based on a binary codification. The logic "1" is associated with the detection of an higher dihedral and the "0" with that of a lower one.

In the code of '1's and '0's the information about the coordinates by which passes the road can be recorded. Using the 56 bit decoding it is possible to identify uniquely each square decimeter of the ground surface.

With the codes of randomization as a help, it is possible to avoid the sequences of '1' or '0' long that may cause ambiguity in the measure.

Once the vehicle has traveled 0.56 m and knows the exact point (with an accuracy of less than 1 cm in the three axes xyz), the number of bits to increase by cm the value of the position can be counted (which will be updated again every 0.56 meters).

That is to say, in less than 0.56 meters of trail decoded (or even at a lower distance), detailed information about the vehicle circulating can be obtained. It should be noted that the guidance system has stored the sequence of positions through which the road passes. This fact offers advantages to the receiver, allowing the reduction of the likelihood of a reading error.

The guidance system of the vehicle may have loaded in its memory the morphology of the road by which it passes. This way, the guidance system of the vehicle can anticipate changes in the direction; adapt the speed in certain areas o increase the engine power to face a high slope.

In addition to working with very low powers (even of tens of microwatios), the possibility of interference between systems, even of the same model, is not possible. This is due to the high bandwidth transmitted. The interference with systems that operate at different frequencies is discarded.

The radar system can contain 2 antennas (transmitter o receiver) or only one (through the use of circulators or even by taking advantage of the local oscillator signal of the mixer that is transmitted by the receiver horn due to the finite isolation between the door OL and the horn.

information reading device.

To read the information of the rail-guide, a a radar sensor installed preferably to the underside of the vehicle is used.

The required antenna is an antenna electrically large to limit the size of the track

To obtain an enlightened area of about 1 square cm (defined area at 3 dB) and to have a resolution related to the distance of 1 cm, it is required to transmit a signal centred on 340 GHz (window of atmospheric attenuation) with a bandwidth of 34 GHz.

With this bandwidth, a resolution at a theory resolution is obtained (capacity to solve two near borders) defined by the equation

$$\Delta R = \frac{C}{2B} = 4.4 \text{ mm}$$

wherein c is the speed of light in the media and B the bandwidth transmitted.

The antenna can be a horn of high gain or its combination a lens or a reflector to concentrate more effectively the energy radiated in the volume of interest.

The antenna is protected by a radome whose material is hydrophobic and water repellent.

The preferred radar sensor is a continuous wave radar and modulated frequency (Linear Frequency Modulated Continuous Wave Radar) that transmits a chirp signal with a period of 37.5 μs. With this ramp period, a vehicle circulating at 120 Km/h will interrogate 16 times between 2 consecutive boreholes separated 1 cm.

The power level transmitted is of the order of a few dozen μW. This power level is easy to obtain using a single horn as element of transmission and reception and a subarmonic mixer.

Applying a local oscillator power of 10 dBm and considering that the product **20**L has a finite isolation towards the horn of 30 dB, it is achieved a transmission power of 10 μW.

The radar signal to transmit is obtained through the generation at a low frequency of a chirp signal through a DDS (Direct Digital Synthesizer) and the use of power multipliers, oscillators and subsequent power amplifiers.

The signal at the mixer output (beat signal) is amplified by an LNA (Low Noise Amplifer), filtered and subsequently digitized by an ADC (Analog to Digital Converter) that samples at a rate of 8 MS/s.

A FPGA (Field Programmable Gate Array) applies a FFT (Fast Fourier Transform) to each period of the received signal to obtain the distances profile of each interrogation.

The rest of the logic of the systems that have to be implemented can be performed using ASICs, FPGAs, PCs etc.

At the work frequency proposed, the water presents a high electromagnetic absorption capacity.

So the radar signal can penetrate the firm of the track and reach the polymer rail-guide, it is necessary the absence of water between the radar and the propagation direction of the waves.

Therefore, the presence of water on the surface of the track where the rail-guide is located has to be avoided or in the same rail-guide when it is positioned at the circulation road level.

In this case, it is proposed that the profile of the rail-guide should have a slight slope towards the sides of the road to facilitate the evacuation of the water which could fall.

Both the rail-guide and the tread of the track that can cover it can be treated with repellent and hydrophobic paints.

The radar sensor may be fitted with a blowing element to point in the area illuminated by the antenna in order to facilitate the evacuation of the water on the surface.

In addition, the blowing jet may be heated to be able to melt snow or ice sheets that can be formed.

Having sufficiently described the nature of the invention, as well as how to be implemented, it must be stated that the provisions referred to above and shown in the accompanying drawings can be modified in detail provided they do not alter the fundamental principles set out in the above paragraphs and summarized in the following claims.

The invention claimed is:

1. A system of automatic guidance of vehicles by means of detection of changes of dielectric properties in a pre-recorded rail-guide, wherein the changes of the dielectric properties are detected by a high resolution radar device and wherein there is a control system of the vehicle that has the ancillary means required to convert it to an auto guidance system wherein the system is composed of the following elements:

a pre-recorded rail-guide

information reading devices

auxiliary means of the control of the vehicle,

wherein the pre-recorded rail-guide is composed of a piece with a straight rectangular parallelepiped with various shoulders located on its side faces, manufactured in non-conductive material, preferably polymeric and with preferred dimensions of 1.5 cm width and 5 cm deep.

2. The system according with claim **1**, wherein, in the pre-recorded rail-guide there are different boreholes mechanized, being the preferred form of the boreholes, in the inner area, that of the dihedral that generate borders of dielectric

change, while in the upper part, the border created by the dielectric differentiation between the lane material and the surrounding air.

3. The system according with claim **2**, wherein the central band dihedrals are oriented in perpendicular form related to that of the side bands, while the side bands dihedrals are located at the same distance from the external edges but a different height.

4. The system according with claim **3**, wherein the dihedrals of the centre band are located in the central area of the rail-guide, located perpendicular to the external dihedrals and at different heights, to determine at least two logical levels, a logical level "1" as the upper one and a logical level "0" as the lower one.

5. The system according with claim **4**, wherein there is a lower border end of trail at the lower part of the rail, as well as a border in the upper part, being constituted said border by the dielectric differentiation between the material of the rail and the surrounding media.

6. The system according with claim **5**, wherein the information reading device in the rail-guide uses a radar sensor installed on the underside of the vehicle with an antenna composed of a dual horn Potter type and a lens or reflector that enlighten a 1 square cm area of the road (area defined by 3 Db) and having a resolution at a distance of 1 centimeter, for what it is required the transmission of a frequency signal and a sufficient bandwidth and being the antenna protected by a radome composed of hydrophobic and water repellent material.

7. The system according with claim **6**, wherein the radar sensor is preferably a continuous wave radar and modulated frequency LFMCW (Linear Frequency Modulated Continuous Wave Radar) that transmits a chirp signal with a period of 37.5 .μ.s.

8. The system according with claim **7**, wherein the power level is obtained using a single horn as element of transmission and reception and a subharmonic mixer.

9. The system according with claim **8**, wherein applying a local oscillator power of 10 dBm and considering that the product 2 OL has a finite isolation towards the horn of 30 dB, it is achieved a transmission power of 10 .μW.

10. The system according with claim **9**, wherein the radar signal to transmit is obtained through the generation at a low frequency of a chirp signal through a DDS (Direct Digital Synthesizer) and the use of power multipliers, oscillators and subsequent power amplifiers.

11. The system according with claim **10**, wherein the signal at the mixer output (beat signal) is amplified by a LNA and subsequently digitized by an ADC (Analog to Digital Converter) that samples at a rate of 8 MS/s. A FPGA applies a FFT (Fast Fourier Transform) to each period of the received signal to obtain the distances profile in each interrogation.

12. The system according with claim **11**, wherein the radar sensor will be provided with a blowing element directed toward the enlightened area by the antenna in order to facilitate the evacuation of the stored water on the thread surface of the road where it is installed or on the same surface of the rail-guide wherein the blowing jet can be heated to be able to melt snow or ice sheets that could be formed.

13. The system according with claim **1**, wherein the means required to control the vehicle would be communication means by systems V2V.

14. The system according with claim **1**, wherein the means required to control the vehicle would be means to detect the rail-guide.

15. The system according with claim **1**, wherein the means required to control the vehicle would be global positioning an navigation means.

16. The system according with claim **1**, wherein the means required to control the vehicle would be vehicle and obstacle detection means.

17. The system according with claim **1**, wherein the means required to control the vehicle would be inertial systems.

18. The system according with claim **1**, wherein the means required to control the vehicle would be incidences and traffic signals communication means.

19. The system according with claim **1**, wherein the rail-guide will be installed at the thread layer level of the road where it is to be installed.

20. The system according with claim **1**, wherein the rail-guide can be hidden under the thread of the road where it is to be installed and said thread is treated with a water repellent paint.

* * * * *

US011814089B2

(12) **United States Patent**
Badolato Martin

(10) **Patent No.: US 11,814,089 B2**
(45) **Date of Patent: Nov. 14, 2023**

(54) **ENCODED INFORMATION MEANS LOCATED ON AN INFRASTRUCTURE TO BE DECODED BY SENSORS LOCATED ON MOBILES**

(71) Applicant: **AUTO DRIVE SOLUTIONS S.L.**, Madrid (ES)

(72) Inventor: **Alejandro Badolato Martin**, Moralzarzal (ES)

(73) Assignee: **AUTO DRIVE SOLUTIONS S.L.**, Madrid (ES)

(*) Notice: Subject to any disclaimer, the term of this patent is extended or adjusted under 35 U.S.C. 154(b) by 1203 days.

(21) Appl. No.: **15/504,329**

(22) PCT Filed: **Mar. 2, 2016**

(86) PCT No.: **PCT/IB2016/051159**
§ 371 (c)(1),
(2) Date: **Feb. 16, 2017**

(87) PCT Pub. No.: **WO2017/149357**
PCT Pub. Date: **Sep. 8, 2017**

(65) **Prior Publication Data**

US 2020/0385037 A1 Dec. 10, 2020

(51) **Int. Cl.**
B61L 25/02 (2006.01)
E01B 1/00 (2006.01)
(Continued)

(52) **U.S. Cl.**
CPC ***B61L 25/025*** (2013.01); ***E01B 1/002*** (2013.01); ***E01B 3/00*** (2013.01); ***G01S 13/751*** (2013.01);
(Continued)

(58) **Field of Classification Search**
CPC B61L 25/025; G01S 13/751; G01S 15/74; G01S 17/74; G01S 7/032; G01S 7/481;
(Continued)

(56) **References Cited**

U.S. PATENT DOCUMENTS

5,318,143 A * 6/1994 Parker E01F 9/30 180/170
2010/0026562 A1 * 2/2010 Hyodo B61L 25/025 342/189
(Continued)

FOREIGN PATENT DOCUMENTS

JP 2008056179 A * 3/2008

Primary Examiner — Bernarr E Gregory
Assistant Examiner — Juliana Cross
(74) *Attorney, Agent, or Firm* — ASLAN LAW, P.C.

(57) **ABSTRACT**

Encoded information means located on an infrastructure to be decoded by sensors located on mobiles, in such a way that these means encode the position they occupy in the infrastructure and allow for a mobile travelling along the same trajectory, provided with the adequate sensor, to read, decode and transform it immediately into information on its exact position in the infrastructure and being characterised by the fact that along the same trajectory described by a mobile it is possible to encode information in the infrastructure by means of different objects presenting dielectric change boundaries or dielectric/metal boundaries at different heights or distances regarding the origin of the onboard sensor, these boundaries being interrogated by a sensor on board the mobile by means of pressure or electromagnetic waves and by measuring the time the waves take to return to the sensor, making it possible to determine the distance at which the reflections occur and in this way to extract the information.

12 Claims, 4 Drawing Sheets

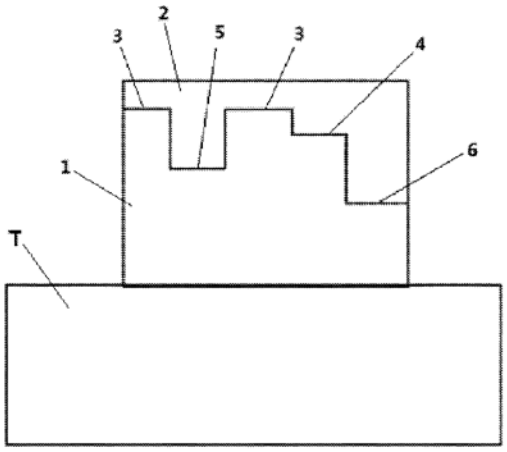

(51) **Int. Cl.**

E01B 3/00	(2006.01)
G01S 13/75	(2006.01)
G01S 15/74	(2006.01)
G01S 17/74	(2006.01)
G06K 19/06	(2006.01)

(52) **U.S. Cl.**
CPC ***G01S 15/74*** (2013.01); ***G01S 17/74*** (2013.01); ***G06K 19/06*** (2013.01)

(58) **Field of Classification Search**
CPC G01S 7/521; G01S 13/04; G01S 13/88; G01S 13/89; G01S 17/66; G01S 17/87; G01S 17/88; G01S 7/41; G01S 7/412; G06K 19/06; G01B 11/14
See application file for complete search history.

(56) **References Cited**

U.S. PATENT DOCUMENTS

2010/0131185	A1*	5/2010	Morris	G01C 15/00 701/19
2014/0368837	A1*	12/2014	Kang	G01B 11/14 356/614
2015/0379314	A1*	12/2015	Schreiber	G01S 13/89 235/494

* cited by examiner

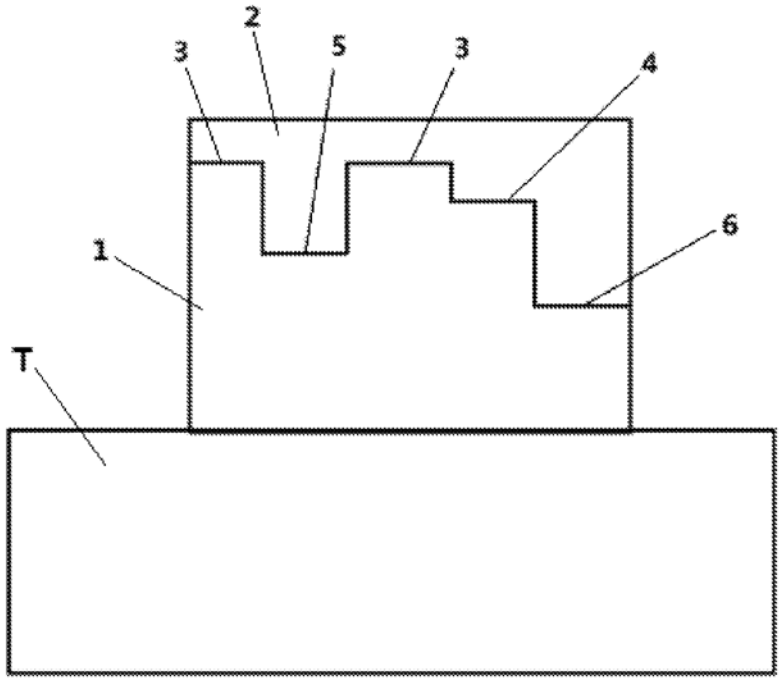

FIG. 1

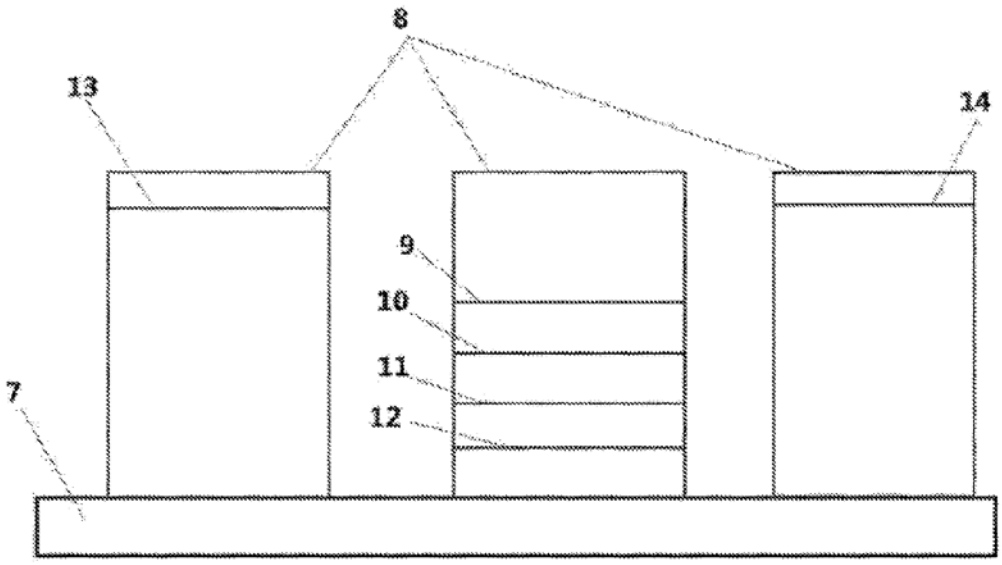

FIG. 2

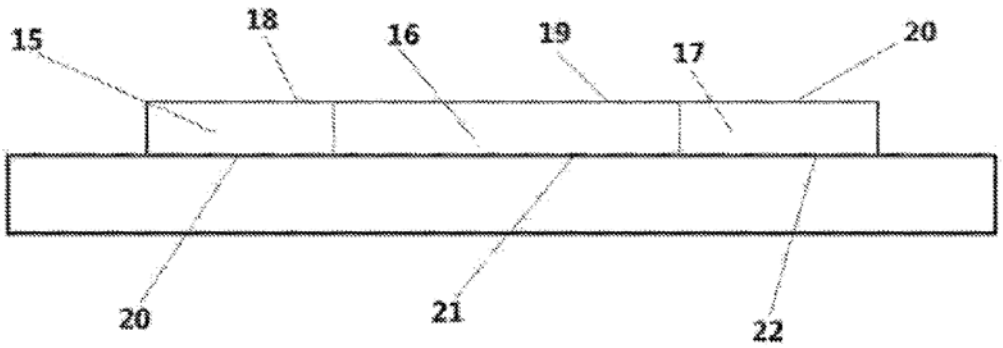

FIG. 3

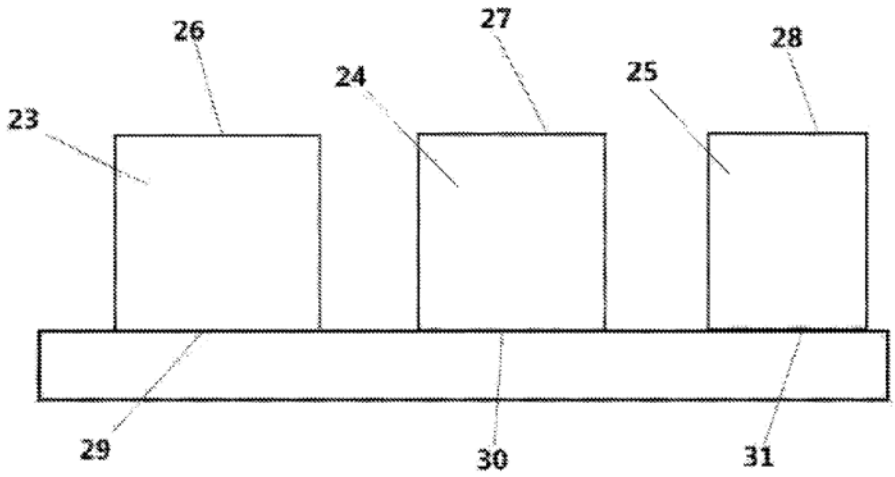

FIG. 4

ENCODED INFORMATION MEANS LOCATED ON AN INFRASTRUCTURE TO BE DECODED BY SENSORS LOCATED ON MOBILES

CROSS-REFERENCE TO RELATED APPLICATIONS

Not Applicable

STATEMENT REGARDING FEDERALLY SPONSORED RESEARCH OR DEVELOPMENT

Not Applicable

STATEMENT REGARDING FEDERALLY SPONSORED RESEARCH OR DEVELOPMENT

Not Applicable

THE NAMES OF THE PARTIES TO A JOINT RESEARCH AGREEMENT INCORPORATION-BY-REFERENCE OF MATERIAL SUBMITTED ON A COMPACT DISC

Not Applicable

BACKGROUND OF THE INVENTION TECHNICAL FIELD

Field of the Invention

The field of the invention is that of the automotive auxiliary industry, the railway industry and the electronic industry.

Description of Related Art

A background does exist regarding devices performing the same function of encoded information which can be located on an infrastructure.

From among these the inventor is similarly the inventor of international patent PCT/ES2015/070378 in which the encoding means is described as a guide rail installed flush with the surface of the road although it can optionally be hidden under a layer of tarmac treated with a layer of hydrophobic material with preferred dimensions of 1.5 cm wide and 5 cm deep and where the internal part has machined cavities, with the preferred shape of the cavities being that of dihedrons as the planes of dihedrons increase the signal reflected therefore enabling their detection.

This device is efficient for some infrastructures, but it does not allow for exploiting all the possibilities offered by the system, for which reason the invention proposed presents other new means adapted very particularly to all types of infrastructures in existence while also offering more simple means, for example discontinuous and economic, for example paint marks, to encode the information.

On the part of the inventor no antecedent is known to include the provisions presented by this invention, or the advantages such provision implies.

BRIEF SUMMARY OF THE INVENTION

The invention proposed refers to encoded information means located on an infrastructure to be decoded by sensors

located on mobiles, in such a way that these means encode the position they occupy in the infrastructure and allow for a mobile travelling along the same trajectory, provided with the adequate sensor, to read, decode and transform it immediately into information on its exact position in the infrastructure.

These encoded information means allow for their use, among others, in automatic guiding systems on all types of mobile travelling along infrastructures, such as automobile vehicles, railway vehicles or even river vehicles.

BRIEF DESCRIPTION OF THE DRAWINGS

For a better understanding of the invention two pages of diagrams are attached showing the following:

FIG. **1**. Representing a side view (view perpendicular to the trajectory of the tracks and parallel to the ground) of a sleeper (T) and the encoding means.

FIG. **2**. Representing a side view of the cross-section perpendicular to the axis of the wearing course of a land infrastructure and with the encoding means in blocks.

FIG. **3**. Representing a side view of the cross-section perpendicular to the axis of the wearing course of a land infrastructure and with the encoding means with a different material thickness.

FIG. **4**. Representing a side view of the cross-section perpendicular to the axis of the wearing course of a land infrastructure and with the encoding means in blocks having different propagation speeds.

DETAILED DESCRIPTION OF THE INVENTION

The invention proposed refers to encoded information means located on an infrastructure to be decoded by sensors located on mobiles, in such a way that these means encode the position they occupy in the infrastructure and allow for a mobile travelling along the same trajectory, provided with the adequate sensor, to read, decode and transform it immediately into information on its exact position in the infrastructure.

Among others, these encoded information means allow for their use in automatic guiding systems on all types of mobile travelling along infrastructures, such as automobile vehicles, railway vehicles or even river vehicles.

The information is given by means of the detection of changes in the dielectric properties of the means located in an infrastructure, in which the dielectric changes are detected by means of sensors such as a high resolution radar device or another similar detector.

Throughout the trajectory described by a mobile it is possible to encode information in the infrastructure by means of different objects presenting dielectric change boundaries or dielectric/metal boundaries at different heights or distances regarding the origin of the onboard sensor.

These boundaries are interrogated by a sensor on board the mobile by means of pressure or electromagnetic waves and by measuring the time the waves take to return to the sensor, it is possible to determine the distance at which the reflections occur and in this way to extract the information.

The following can be distinguished within the different means:

An information means of these characteristics refers to the information given by the railway sleepers as these present several unique characteristics:

a uniform surface with regard to the ballast, or

a different height regarding the track set on a concrete slab

The sleepers are always found at a specific distance from a known point on the locomotive(s) or one of the wagons (coaches).

Moreover, these sleepers can be encoded with a series of bits by means of a series of studs of different heights, with the sleeper being encoded by means of a series of studs which offer a series of levels and these studs being covered with a material permeable to the waves and of a known thickness.

The information on the position is divided into 4-bit groups which are encoded successively at each sleeper by means of the levels.

When 2 consecutive bits of the same level are encoded, a third level of a different height is used to encode this second repeated bit.

This technique allows for the sensor to identify both bits and to determine that the second bit has the same logical level as the previous one.

By alternatively using the repetition level it is possible to identify consecutive 4-bit strings with the same logical level.

A fourth height level is always used as the fifth bit.

In this way the sensor is capable of knowing the reading direction.

If the first detection matches the fourth level the sensor will detect that it is reading the bits in reverse order.

4 bits of information obtain 24=16 different sleepers each encoding 5 bits (4 of information and 1 indicating the reading direction).

A seventeenth sleeper model characteristic for its first bit starting with a repetition bit and its fifth bit indicating the reading direction is used to indicate the start or end of a word made up by 4-bit groups.

In this way, a word start sleeper and 8 more sleepers of information encode 232 possible combinations that can be uniquely assigned to the segment occupied by the 9 sleepers.

The information is encoded redundantly in two different places for two sensors to be able to read the information means simultaneously.

The sensor interrogates the infrastructure with a spot 8 mm in diameter and in order for each stud to be illuminated correctly by the sensor, the surface area of the studs is 1 cm2, with the height separation of each stud associated with a different logical level being 0.5 cm.

These studs are covered with a material (**2**) permeable to waves of a known thickness and has two functions: on the one hand to avoid any material from being deposited between the studs and also to serve as reference to determine the different logical levels.

The locomotive or coach can vary its height due to the action of the suspension but, given that the sensor detects a reflection in the boundary between the permeable material and the air, this can determine the location of the different logical levels independently from the distance of the locomotive to the ground.

Another information means is also a sleeper but one in which the information is encoded by slits instead of studs in such a way the sleeper shows no relief on its upper surface.

The stud or slit techniques described may also be used on tracks set on a concrete slab.

Another information means are encoded blocks but ones that are installed on the sides or the upper part of the trajectory (for example on the catenary, on the arch of a station or tunnel, etc.) turned round appropriately for their encoded part to face the sensor and arranged at a certain height in such a way there is direct view between the sensor and the block even under snow conditions.

The boundary surfaces can form trihedrons to maximise reflection.

If the information is required for land infrastructures and more specifically roads a sequence of specks/lines of paint or another material is foreseen preferably in colour black so as not to confuse drivers.

The specks present different thicknesses with 2 mm separations between boundaries and are stuck longitudinally on the road in the centre/lane.

These specks each have a surface area of 1 cm2 and present an upper coating of another permeable material with hydrophobic properties which serves as a reference point for the sensor.

The information is also encoded by means of different levels with 3 mm separations and in 4-bit groups plus a fifth bit indicating the reading direction.

Between the 5-bit blocks there is a free uncoded space for the water to follow the slope marked by the camber of the road so it does not accumulate next to the information means.

Accompanying the sequence of specks, 2 side bands of different thicknesses serve to encode the lateral drift of the sensor with regard to the information means where the information is encoded.

Another information means is made up by a strip with slits of different depths, preferably out of plastic and with each centimetre encoded.

This strip, among other applications, serves to inform on the advance and the position to a mobile in such a way this can apply controlled accelerations and decelerations thus enabling the mobile to stop precisely.

An example could be the train stopping at a station.

Another way of encoding information consists in using objects (continuous or discontinuous) of the same thickness and permeable to the waves with different transmission properties with regard to propagation speed.

In the case of electromagnetic waves, a different dielectric constant will delay more or less the detection associated with the second dielectric change boundary (back surface of the object).

Another information means is characterised for having the covered surface made up by materials in which the wave propagation speed is different.

This fact causes (when considering a constant propagation speed) the detections of upper boundaries to be distanced in a different manner from the detections of the rear boundaries.

Another information means is characterised for having the coating made up by materials in which wave propagation speed is different and due to which, when considering a constant propagation speed, there is a difference between the detection of the boundaries. such blocks and the corresponding lower ones are different, causing the detection of the upper boundaries to be different from the detection of the lower boundaries according to the material used.

A solution is proposed making it possible to read encoded information on a non-conductive material by means of the existence or not of dielectric constant change boundaries in the middle that can be detected by means of sensors installed on mobiles.

The dielectric change boundaries in a non-conductive material lead to part of the energy irradiated towards the material in question to be reflected.

This reflected energy is detected by the associated sensor making it possible to determine the radial distance at which the discontinuity is found.

The dielectric change boundaries can be obtained by using two materials or substances whose dielectric constants are different or using a single material in which the boundary is established between the material and the vacuum or the material or a gas or substance.

Description of the Preferred Embodiment

The invention proposed refers to encoded information means located on an infrastructure to be decoded by sensors located on mobiles, in such a way that these means encode the position they occupy in the infrastructure and allow for a mobile travelling along the same trajectory, provided with the adequate sensor, to read, decode and transform it immediately into information on its exact position in the infrastructure.

These encoded information means allow for their use, among others, in automatic guiding systems on all types of mobile travelling along infrastructures, such as automobile vehicles, railway vehicles or even river vehicles.

The information is given by means of the detection of changes in the dielectric properties of the means located in an infrastructure, in which the dielectric changes are detected by means of sensors such as a high resolution radar device or another similar detector.

Throughout the trajectory described by a mobile it is possible to encode information in the infrastructure by means of different objects presenting dielectric change boundaries or dielectric/metal boundaries at different heights or distances regarding the origin of the onboard sensor.

These boundaries are interrogated by a sensor on board the mobile by means of pressure or electromagnetic waves and by measuring the time the waves take to return to the sensor, it is possible to determine the distance at which the reflections occur and in this way to extract the information.

The following can be distinguished within the different means:

A) An information means of these characteristics which we will call type a) refers to the information given by the railway sleepers (T) as these present several unique characteristics:

a uniform surface with regard to the ballast, or

a different height regarding the track set on a concrete slab

The sleepers (T) are found at a specific distance from a known point on the locomotive(s) or one of the wagons (coaches).

Moreover, these sleepers can be encoded with a series of bits by means of a series of studs of different heights, as shown in FIG. **1**.

The encoding of the sleeper (T) is performed by means of a series of studs which offer a series of levels (**3**), (**4**), (**5**) and (**6**) and these studs are covered with a material (**2**) permeable to the waves and of a known thickness.

The information on the position is divided into 4-bit groups which are encoded successively at each sleeper by means of the levels (**3** and **4**).

When 2 consecutive bits of the same level are encoded, a third level of a different height (**5**) is used to encode this second repeated bit.

This technique allows for the sensor to identify both bits and to determine that the second bit has the same logical level as the previous one.

By alternatively using the repetition level it is possible to identify consecutive 4-bit strings with the same logical level.

A fourth height level (**6**) is always used as the fifth bit.

In this way the sensor is capable of knowing the reading direction.

If the first detection matches the fourth level the sensor will detect that it is reading the bits in reverse order.

4 bits of information obtain 24=16 different sleepers each encoding 5 bits (4 of information and 1 indicating the reading direction).

A seventeenth sleeper model characteristic for its first bit starting with a repetition bit (**5**) and its fifth bit indicating the reading direction (**6**) is used to indicate the start or end of a word made up by 4-bit groups.

In this way, a word start sleeper and 8 more sleepers of information encode 232 possible combinations that can be uniquely assigned to the segment occupied by the 9 sleepers.

The information is encoded redundantly in two different places for two sensors to be able to read the information means simultaneously.

The sensor interrogates the infrastructure with a spot 8 mm in diameter.

In order for each stud to be illuminated correctly by the sensor, the surface area of the studs is 1 cm2.

The height separation of each stud associated with a different logical level is 0.5 cm.

These studs are covered with a material (**2**) permeable to waves of known thickness.

This coating has two functions:

On the one hand to avoid any material from being deposited between the studs and also to serve as reference to determine the different logical levels.

The locomotive or coach can vary its height due to the action of the suspension but, given that the sensor detects a reflection in the boundary between the permeable material and the air, this can determine the location of the different logical levels independently from the distance of the locomotive to the ground.

B) Another information means we will call type b) is a sleeper in which the information is encoded by slits instead of studs in such a way the sleeper shows no relief on its upper surface.

C) Another information means we will call type c) consists in using the stud or slit techniques on tracks set on a concrete slab.

D) Another information means we will call type d) refers to blocks encoded in an analogous manner to type a) only installed on the sides or the upper part of the trajectory (for example on the catenary, on the arch of a station or tunnel, etc.) turned round appropriately for their encoded part to face the sensor and arranged at a certain height in such a way there is direct view between the sensor and the block even under snow conditions.

The boundary surfaces can form trihedrons to maximise reflection.

E) Another information means we call type e) is an information means similar to type a) only to be used on roads instead of sleepers.

In this case the studs are a sequence of specks/lines of paint or another material is foreseen preferably in colour black so as not to confuse drivers.

The specks present different thicknesses with 2 mm separations between boundaries and are stuck longitudinally on the road in the centre/lane.

FIG. **2** shows a cross section of the wearing course of the road (**7**) and one of the specks.

These specks each have a surface area of 1 cm2 and present an upper coating of another permeable material with hydrophobic properties which serves as a reference point for the sensor.

The information is also encoded by means of 3 different levels (**9-11**) with 3 mm separations and in groups plus a fifth bit (**12**) indicating the reading direction.

Between the 5-bit blocks there is a free uncoded space for the water to follow the slope marked by the camber of the road so it does not accumulate next to the information means.

Accompanying the sequence of specks, 2 side bands (**13**,**14**) of different thicknesses serve to encode the lateral drift of the sensor with regard to the information means where the information is encoded.

F) Another information means called type f) is made up by a strip with slits of different depths (with the levels defined in type a), preferably out of plastic and with each centimetre encoded.

This strip, among other applications, serves to inform on the advance and the position to a mobile in such a way this can apply controlled accelerations and decelerations thus enabling the mobile to stop precisely.

An example could be the train stopping at a station.

G) Another way of encoding information we call type g) consists in using objects (continuous or discontinuous) of the same thickness and permeable to the waves with different transmission properties with regard to propagation speed.

In the case of electromagnetic waves, a different dielectric constant will delay more or less the detection associated with the second dielectric change boundary (back surface of the object).

H) Another way of encoding information we call type h), in accordance with FIG. **3** and consisting in the same means as type a) except for the fact the information is not located in the depth of the material used as coating (T) but because this coating is made up by materials (**15**), (**16**) and (**17**) in which the wave propagation speed is different.

This fact causes (when considering a constant propagation speed) the detections of boundaries (**18**), (**19**) and (**20**) to be distanced in a different manner from the detections of boundaries (**20**), (**21**) and (**22**).

J) Another information means we call type j) is the same as that defined as type e) except for the fact the information is not located in the thickness of the coating (**8**) but because this coating (**24**), and this coating is made up by materials in which the wave propagation speed is different, therefore considering a constant propagation speed there is a difference between the detection of boundaries.

If we consider three blocks that are parallel to each other and perpendicular to the movement axis of the mobile, (**85**), (**86**) and (**87**) then the position difference between the upper boundaries of such blocks, (**26**), (**27**) and (**28**) and the corresponding lower ones (**29**), (**30**) and (**31**) causes the detection of the upper boundaries to be different from the detection of the lower boundaries according to the material used.

A solution is proposed making it possible to read encoded information on a non-conductive material by means of the existence or not of dielectric constant change boundaries in the middle that can be detected by means of sensors installed on mobiles.

The dielectric change boundaries in a non-conductive material lead to part of the energy irradiated towards the material in question to be reflected.

This reflected energy is detected by the associated sensor making it possible to determine the radial distance at which the discontinuity is found.

The dielectric change boundaries can be obtained by using two materials or substances whose dielectric constants are different or using a single material where the boundary is established between the material and the vacuum or the material or a gas or substance.

Having described sufficiently the nature of the invention, together with the way of putting it into practice, it should be stated that the provisions indicated above and represented in the attached drawings are susceptible to detailed modifications as long as they do not alter its basic principles, established in the previous paragraphs and summarised in the following claims.

The invention claimed is:

1. A system comprising:

an encoded information means located along a trajectory on an infrastructure to be decoded by sensors located on mobile vehicles that travel along the trajectory, wherein

said encoded information means encodes the position the encoded information means occupies in the infrastructure;

at least one sensor, to read and decode the encoded information means into information on a position of a mobile vehicle in the infrastructure, wherein

said encoded information means, located along the trajectory of the mobile vehicles, comprising different objects presenting dielectric change boundaries or dielectric/metal boundaries that present different wave propagation times with respect to the at least one sensor on a first mobile vehicle of the mobile vehicles,

said at least one sensor on the first mobile vehicle is configured to interrogate said dielectric change boundaries or dielectric/metal boundaries via pressure or radar waves and to measure propagation times the pressure or radar waves take to return via reflections to the at least one sensor, and to determine the distances at which the reflections occur and to extract encoded information of said different objects that incorporate the encoded information of said encoded information means,

said infrastructure comprises a railway infrastructure including a plurality of railway sleepers, the encoded information means are made up by the railway sleepers themselves, the railway sleepers having a first characteristic, wherein

the first characteristic of the railway sleepers includes a uniform surface with regard to a ballast, or a different height with respect to a track set on a concrete slab, and wherein

the railway sleepers are found at a specific distance from a known point on a railway vehicle, the railway vehicle comprising a locomotive or a wagon or a coach, wherein

the plurality of sleepers are encoded with a series of bits via a plurality of studs, the studs covered with a material permeable to the eaves; wherein

at each stud of the plurality of studs, a respective thickness of the permeable material encodes a logical level of a bit representing or corresponding to the encoded information on the position the encoded information means occupies in the infrastructure, the information on the position being divided into groups of 4 bits according a coding scheme, the coding scheme comprising:

a 4-bit group encoded at each sleeper, wherein the logical level of zero of a bit and ones of bits are representable via first and second levels of thickness of the permeable material;

when the 4-bit group includes 2 consecutive bits of a same logical level of a but, the second consecutive bit is representable via a third level of thickness of the permeable material; and

a fourth level of thickness of the permeable material, which is a fifth bit that indicates a reading direction for the 4-bit group to the at least one sensor, wherein

said coding scheme uses 4 bits of information to indicate 16 different sleepers, each encoding its respective 4-bit group and its respective fifth bit according to the coding scheme.

2. The system according to claim **1**, wherein

distinct from said 16 different sleepers, a seventeenth sleeper encodes its respective 4-bit group via its first bit having the third level of thickness of the permeable material and its fifth bit indicating the reading direction for the seventeenth sleeper, the seventeenth sleeper indicating a start or an end of a word made up by a plurality of 4-bit groups.

3. The system according to claim **1**, wherein

the at least one sensor, on the first mobile vehicle of the mobile vehicles, comprises two sensors,

the encoded information is implanted redundantly in two different places for the two sensors to simultaneously read the encoded information.

4. The system according to claim **1**, wherein

the encoded information means comprises a plurality of studs, each having a surface area, and

the at least one sensor, on the first mobile vehicle of the mobile vehicles, is configured to interrogate the infrastructure with a spot 8 mm in diameter, with the surface area of the studs being 1 cm^2, a height separation of each stud associated with a different logical level of a bit being 0.5 cm, and the studs being covered with a material permeable to the waves.

5. The system according to claim **1**, wherein

the different objects that incorporate the encoded information are located on sides or an upper part along the trajectory, and are configured to face the at least one sensor.

6. The system according to claim **1**, wherein

said at least one sensor is a radar sensor for the radar waves.

7. The system according to claim **1**, wherein

the encoded information means comprises said plurality of studs on tracks set on a concrete slab.

8. A system comprising:

an encoded information means located along a trajectory on an infrastructure to be decoded by sensors located on mobile vehicles that travel along the trajectory, wherein

said encoded information means encodes the position the encoded information means occupies the infrastructure;

at least one sensor, to read and decode the encoded information means into information on a position of a mobile vehicle in the infrastructure, wherein

said encoded information means, located along the trajectory of the mobile vehicles, comprising different objects presenting dielectric change boundaries or dielectric/metal boundaries that present different wave propagation times with respect to the at least one sensor on a first mobile vehicle of the mobile vehicles,

said at least one senor on the first mobile vehicle is configured to interrogate said dielectric change boundaries or dielectric/metal boundaries via pressure or radar waves and to measure propagation times the pressure or radar waves take to return via reflections occur and to extract encoded information of said different objects that incorporate the encoded information of said encoded information means,

the different objects that incorporate the encoded information are made up by a sequence of specks or lines of a paintable material,

the specks or lines have different thicknesses with 2 mm separations between their boundaries and are applied longitudinally on a surface of the infrastructure, each with a surface area of 1 cm^2 and comprising an upper coating of a permeable material with hydrophobic properties, the upper coating providing a reference point for the at least one sensor, for the at least one sensor,

the encoded information is encoded via 3 different levels with 3 mm separations and in 5-bit blocks, each comprising a 4-bit group plus a fifth bit indicating a reading direction for its 4-bit group,

the encoded information is encoded with an uncoded free space between the 5-bit blocks, and

the encoded information is encoded with 2 side bands of different thicknesses to encode a lateral drift of the at least one sensor when the at least one sensor is laterally drifted with respect to the encoded information means.

9. The system according to claim **8**, wherein

the at least one sensor, on the first mobile vehicle of the mobile vehicles, comprises two sensors,

the encoded information is implanted redundantly in two different places for the two sensors to simultaneously read the encoded information.

10. The system according to claim **8**, wherein

the encoded information means comprises a plurality of studs, each having a surface area, and

the at least one sensor, on the first mobile vehicle of the mobile vehicles, is configured to interrogate the infrastructure with a spot 8 mm in diameter, with the surface area of the studs being 1 cm^2, a height separation of each stud associated with a different logical level of a bit being 0.5 cm, and the studs being covered with a material permeable to the waves.

11. The system according to claim **8**, wherein

the different objects that incorporate the encoded information are located on sides or an upper part along the trajectory, and are configured to face the at least one sensor.

12. The system according to claim **8**, wherein

said at least one sensor is a radar sensor for the radar waves.

* * * * *

US011565733B2

(12) **United States Patent**
Badolato Martin et al.

(10) **Patent No.: US 11,565,733 B2**
(45) **Date of Patent: Jan. 31, 2023**

(54) **SPEED CONTROL AND TRACK CHANGE DETECTION DEVICE SUITABLE FOR RAILWAYS**

(71) Applicant: **AUTO DRIVE SOLUTIONS, S.L.**, Madrid (ES)

(72) Inventors: **Alejandro Badolato Martin**, Madrid (ES); **Jesús Antonio Del Castillo Igareda**, Madrid (ES)

(73) Assignee: **AUTO DRIVE SOLUTIONS, S.L.**, Madrid (ES)

(*) Notice: Subject to any disclaimer, the term of this patent is extended or adjusted under 35 U.S.C. 154(b) by 755 days.

(21) Appl. No.: **16/482,311**

(22) PCT Filed: **Feb. 22, 2018**

(86) PCT No.: **PCT/ES2018/070132**
§ 371 (c)(1),
(2) Date: **Jul. 31, 2019**

(87) PCT Pub. No.: **WO2018/154167**
PCT Pub. Date: **Aug. 30, 2018**

(65) **Prior Publication Data**

US 2020/0001905 A1 Jan. 2, 2020

(30) **Foreign Application Priority Data**

Feb. 23, 2017 (ES) ES201730236

(51) **Int. Cl.**
B61L 25/02 (2006.01)
B61L 25/06 (2006.01)
(Continued)

(52) **U.S. Cl.**
CPC ***B61L 25/021*** (2013.01); ***B61L 23/04*** (2013.01); ***B61L 25/02*** (2013.01); ***B61L 25/06*** (2013.01);
(Continued)

(58) **Field of Classification Search**
CPC B61L 25/02; B61L 25/021; B61L 25/06; B61L 23/04; B61L 27/20; B61L 2201/02; B61L 2205/04; B60L 2200/26
See application file for complete search history.

(56) **References Cited**

U.S. PATENT DOCUMENTS

4,027,840 A 6/1977 Blair
6,360,998 B1 3/2002 Halvorson et al.
(Continued)

FOREIGN PATENT DOCUMENTS

WO WO 2004074823 A2 2/2004
WO WO 2016022635 A1 2/2016
(Continued)

Primary Examiner — Zachary L Kuhfuss
(74) *Attorney, Agent, or Firm* — Aslan Law, P.C.

(57) **ABSTRACT**

A speed control and track change detection device for railways is characterised in that it comprises three high-frequency radar sensors located at the vertices of an imaginary triangle and a digital processing device for processing the signals detected by the radars, wherein in the case of the speed control system, both sensors are located at 1 m distance from each other along the axis of the path of the railway and inspect the ground of the infrastructure 2 cm away from the outside of each rail, and according to the temporal offset of the signals obtained the digital processing device estimates the exact speed of the train.

5 Claims, 2 Drawing Sheets

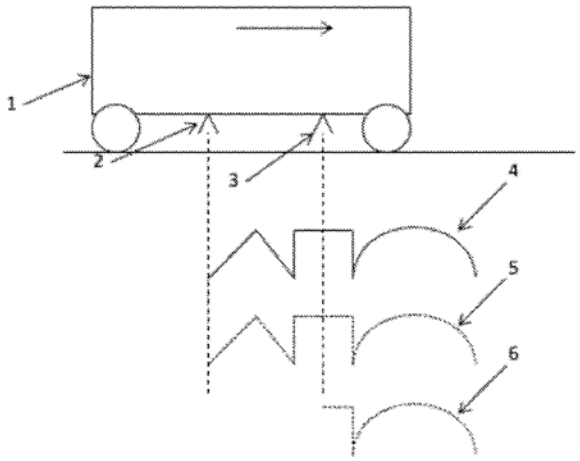

(51) **Int. Cl.**
B61L 23/04 (2006.01)
B61L 27/20 (2022.01)

(52) **U.S. Cl.**
CPC *B60L 2200/26* (2013.01); *B61L 27/20* (2022.01); *B61L 2201/02* (2013.01); *B61L 2205/04* (2013.01)

(56) **References Cited**

U.S. PATENT DOCUMENTS

7,948,613	B2 *	5/2011	Fourcault	B60T 8/172 356/28
9,849,895	B2 *	12/2017	Mesher	B61L 23/04
10,349,491	B2 *	7/2019	Mesher	B61L 23/045
2015/0175178	A1 *	6/2015	Ignatius	B61L 23/041 246/120
2016/0046308	A1 *	2/2016	Chung	B61L 27/70 701/20
2017/0057528	A1 *	3/2017	Green	B61L 25/025
2017/0313332	A1 *	11/2017	Paget	B61L 25/021

FOREIGN PATENT DOCUMENTS

WO	WO 2016180992 A1	11/2016
WO	WO 2017149357 A1	9/2017
WO	WO 2018096388 A1	5/2018
WO	WO 2018115930 A1	6/2018

* cited by examiner

FIGURE 1

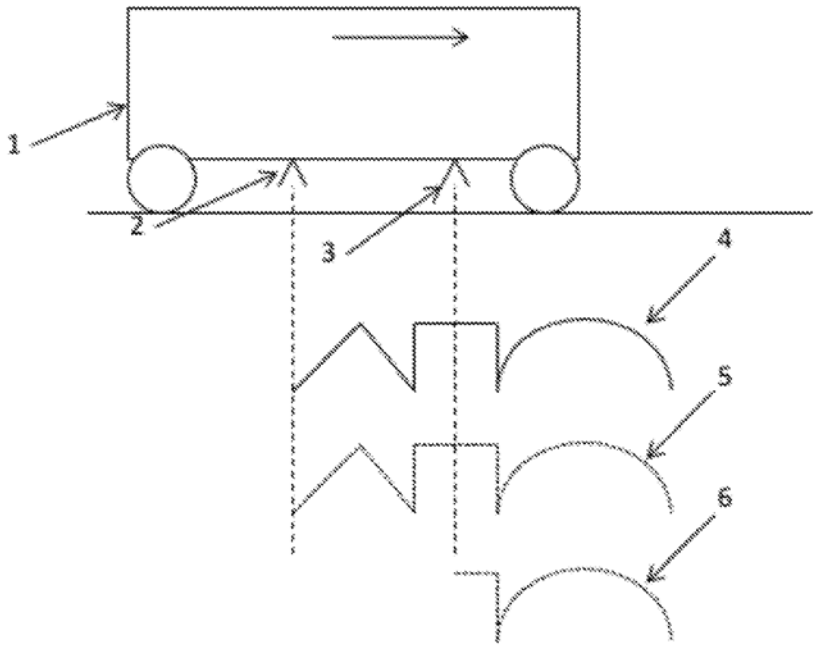

FIGURE 2

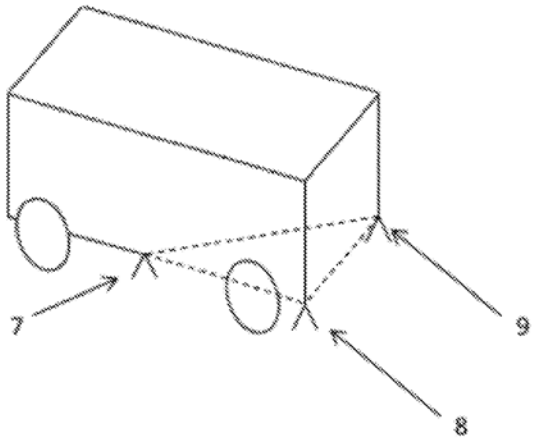

SPEED CONTROL AND TRACK CHANGE DETECTION DEVICE SUITABLE FOR RAILWAYS

CROSS-REFERENCE TO RELATED APPLICATIONS

This application claims priority to ES Patent Application No. P201730236 (ES 201730236) filed on Feb. 23, 2017, and to PCT Application No. PCT/ES2018/070132 filed on Feb. 22, 2018, the entire contents of which are hereby incorporated by reference.

OBJECT OF THE INVENTION

The invention envisaged relates to a speed control and track change detection system.

The inspection of the ground of the infrastructure allows **2** different problems to be solved. The first of them is measuring the speed of the train in unfavourable conditions, such as snowy environments wherein the Doppler radar that is normally used to estimate speed does not function properly, given that the dihedron formed by the railway sleeper and track ballast that serves to reflect the radar signal becomes hidden by the snow. The second solves the identification of the track selected when the point blades are changed without the help of railway signalling equipment.

Each one of the problems is solved with a pair of radar sensors. In the first case, the radar sensors are installed on the longitudinal axis of the train with a known distance between them, and in the second case the two radar modules are on a transverse axis.

FIELD OF THE INVENTION

The field of the invention is the auxiliary railway industry and the supporting electronics industry.

BACKGROUND OF THE INVENTION

There is some prior art relating to devices that carry out a function of reading information of means by similar means.

Among said devices, the inventor is likewise the inventor of international patent PCT/ES2015/070378, which describes as a coding means a guide-rail installed flush with the road surface but which can optionally be concealed under an asphalt layer treated with a layer of hydrophobic material with preferred dimensions of 1.5 cm wide by 5 cm deep, and wherein on the inside thereof cavities are machined, the cavities preferably being dihedral given that dihedral planes increase the reflected signal, thereby facilitating the detection thereof.

Likewise, the same inventor has registered international patent PCT/IB2016/051159, which details other information means with the same purpose. These information-coding and reading systems have more applications wherein it is not necessary for the sensor to be installed on a mobile and the information that is coded does not have the single function of determining the relative position of the sensor with respect to the coded means.

Moreover, the inventor has also filed a similar system to the one proposed, using radar techniques according to PCT/IB2016/057119 or an optical system according to PCT/IB2016/057873.

But the case of using 2 radar sensors to measure the speed of a train or to determine the track selected in a change of the point blades is not contemplated.

The inventor does not know of any prior art that incorporates the arrangements presented by the current invention, or of the advantages said arrangement provides.

BRIEF DESCRIPTION OF DRAWINGS

FIG. **1** illustrates an example of a speed control and track change detection system for railways illustrating at least a train (**1**), a first radar sensor (**2**), a second radar sensor (**3**), a ground profile (**4**), a radar profile of the first ground sensor (**5**) and a radar profile of the second ground sensor (**6**).

FIG. **2** illustrates an example of a speed control and track change detection system for railways illustrating at least three high-frequency radar sensors (**7**, **8**, and **9**).

DESCRIPTION OF THE INVENTION

If both sensors are arranged on a longitudinal axis and separated from one another by a known distance it is possible to determine the speed of a train. Each one of the sensors concentrates its energy on a square centimetre of the surface and precisely measures the distance from the sensor to the ground. This way, each one of the 2 sensors obtains a detailed profile of the ground as the train advances. The processing of the two signals obtained allows the time lag existing between both profiles to be detected, thereby obtaining an estimation of the speed. This system functions in snowy environments since the surface is not entirely uniform.

If both sensors are arranged on an axis perpendicular to the path and inspect the outside of each rail, each sensor is able to detect the presence of the rail when the same crosses it, identifying if the train has changed track.

There is also the possibility of installing sensors on the inside of the rails and detecting which of them has been passed over first and thus detect if the train has changed track.

In both cases, instead of using electromagnetic waves, it is possible to use pressure waves to inspect the infrastructure.

As such, with only three sensors situated in a triangle, two perpendicular to the axis of the path and one on the same axis as any one of the former, it is possible to solve the problem.

PREFERRED EMBODIMENT OF THE INVENTION

The invention envisaged relates to a speed control and track change detection system.

The system is made up of two main elements:

Three high-frequency radar sensors,

A device for digitally processing the radar signals

Thus, the preferred embodiment consists of the installation of three high-frequency radar sensors which, placed underneath the train, concentrate the radiated energy on a square centimetre of the surface with the help of a dielectric lens.

The three sensors are situated at the vertices of an imaginary triangle.

In the case of the speed control system, both sensors are located at 1 m of distance from each other along the axis of the path and inspect the ground 2 cm away from the outside of each rail.

The digital processing device for processing the radar signals detects the temporal offset between both signals, thereby obtaining an estimation of the speed, given that the separation between the sensors is known.

The third sensor is arranged on an axis perpendicular to the path at the height of the first of the former sensors and inspects the outside of each rail, the digital processing device for processing the radar signals being able to detect the presence of the rail when the same crosses it, identifying if the train has changed track.

There is also the possibility of installing sensors on the inside of the rails and detecting which of them has been passed over first and thus detect if the train has changed track.

In both cases, instead of using electromagnetic waves, it is possible to use pressure waves to inspect the infrastructure.

Having sufficiently described the nature of the invention, in addition to the practical embodiment thereof, it is hereby stated that the arrangements indicated above are susceptible to modifications of the details, provided they do not change the fundamental principles thereof established in the foregoing paragraphs and summarised in the following claims.

The invention claimed is:

1. A speed control and track change detection system for railways comprising:

three high-frequency radar sensors situated at vertices of an imaginary triangle, wherein

two longitudinally arranged radar sensors of said three high-frequency radar sensors are arranged on a longitudinal axis, separated from one another by a known distance, each one of said two longitudinally arranged radar sensors concentrates radiated energy thereof on an area of approximately one square centimeter of the surface and measures the distance from a sensor to a ground, such that from each one of the two longitudinally arranged radar sensors a detailed profile of the ground is obtained as a train advances;

a third sensor of said three high-frequency radar sensors is arranged on an axis perpendicular to a path at the height of one of said two longitudinally arranged radar sensors, such that each sensor obtains a detailed profile of the ground on an outside of a rail, so that a digital processing device for processing radar signals is able to detect the presence of the rail when the three high-frequency radar sensors crosses a track, identifying if the train has changed track;

the digital processing device for processing the radar signals that measures a time lag existing between the profiles of the ground obtained by the two longitudinally arranged radar sensors and calculates the speed of the train and identifies, through the profiles of the ground obtained by the transversely arranged radar sensors, the detection of when the rails are passed over and determines when the train changes track;

two radar sensors of said three high-frequency radar sensors are separated by said known distance from each other along the longitudinal axis of the tracks and pointing towards the ground obtain a profile of the infrastructure; and

a digital signal processing is performed with both radar range-profiles to determine a time delay between them and the speed of the train is estimated by dividing a space between said two radar sensors between the time delay.

2. The speed control and track change detection system for railways according to claim **1**, wherein

in the speed control system, said two longitudinally arranged radar sensors, located at 1 m distance from each other along an axis of a path and inspect the ground 2 cm away from the outside of each rail and the digital processing device for processing the radar signals detects a temporal offset between the radar signals, thereby obtaining an estimation of the speed based on the known distance of separation between the two longitudinally arranged radar sensors.

3. The speed control and track change detection system for railways according to claim **1**, wherein

in the track change detection system, said two longitudinally arranged radar sensors are used that are arranged on an axis perpendicular to the path and inspect the outside of each rail, and

the digital processing device for processing the radar signals detects the presence of the rail when the three high-frequency radar sensors crosses the track.

4. The speed control and track change detection system for railways according to claim **1**, wherein

electromagnetic waves are used to inspect an infrastructure of the railway.

5. The speed control and track change detection system for railways according to claim **1**, wherein

pressure waves are used to inspect an infrastructure of the railway.

* * * * *

US 20210232156A1

(19) **United States**

(12) **Patent Application Publication** (10) **Pub. No.: US 2021/0232156 A1**

DEL CASTILLO IGAREDA et al. (43) **Pub. Date: Jul. 29, 2021**

(54) **SEMI-AUTOMATED CONVOY TRANSPORT SYSTEM FOR VEHICLES**

(71) Applicant: **AUTO DRIVE SOLUTIONS S.L.**, Madrid (ES)

(72) Inventors: **Jesús Antonio DEL CASTILLO IGAREDA**, Madrid (ES); **Alejandro BADOLATO MARTIN**, Madrid (ES)

(73) Assignee: **AUTODRIVE SOLUTIONS S.L.**, Madrid (ES)

(21) Appl. No.: **17/050,130**

(22) PCT Filed: **Mar. 21, 2019**

(86) PCT No.: **PCT/ES2019/070190**

§ 371 (c)(1),
(2) Date: **Oct. 23, 2020**

(30) **Foreign Application Priority Data**

Apr. 24, 2018 (ES) ..... U 201830581

Publication Classification

(51) **Int. Cl.**

G05D 1/02	(2006.01)
B60R 16/033	(2006.01)
B60R 16/023	(2006.01)
B60D 1/64	(2006.01)

(52) **U.S. Cl.**

CPC ***G05D 1/0293*** (2013.01); ***G05D 1/0295*** (2013.01); ***B60R 16/033*** (2013.01); ***G05D 1/027*** (2013.01); ***B60D 1/64*** (2013.01); ***G05D 1/0257*** (2013.01); ***G05D 1/0278*** (2013.01); ***B60R 16/0231*** (2013.01)

(57) **ABSTRACT**

A semi-automated convoy transport system for vehicles, wherein a first vehicle referred to as leader includes a system for positioning the vehicle with respect to the infrastructure recording the trajectory over which it drives and transmits said trajectory, together with other information, to the rest of vehicles of the convoy that follow it, via a communication channel. The vehicles that follow the leader include a positioning system and a navigation system which, using the data sent by the leader, follow the trajectory travelled by the leader. In addition, the system includes in the vehicles two front plugs and two rear plugs for receiving respective 8-conductor spiral cables and an extensible rod ending in a V-shaped clamp, which allows the resilient spiral cables to be connected to or disconnected from the vehicle in front or behind.

US 2021/0232156 A1 Jul. 29, 2021

SEMI-AUTOMATED CONVOY TRANSPORT SYSTEM FOR VEHICLES

OBJECT OF THE INVENTION

[0001] The proposed invention relates to a semi-automated convoy transport system for vehicles wherein a first vehicle referred to as leader includes a system for positioning the vehicle with respect to the infrastructure, recording the trajectory over which it drives and transmits said trajectory, together with other information, to the rest of vehicles of the convoy that follow it, via a communication channel.

[0002] The vehicles that follow the leader are referred to as trailers and include a positioning system equal to that of the leader and a navigation system which, using the data sent by the leader, follow the trajectory travelled by the leader.

FIELD OF THE INVENTION

[0003] The field of the invention is the transport industry, and the auxiliary industry of electronic positioning devices, and smart information exchange.

BACKGROUND OF THE INVENTION

[0004] There is a background of similar transport systems referred to as the "platooning" type in which trailers try to follow the trajectory of the leader.

[0005] To do this, a set of sensors capture information from the vehicle that precedes them and the processing of the information enables the relative positioning between both vehicles to be determined in order to, subsequently, try to follow the same trajectory.

[0006] However, these trailing systems suffer from a cumulative error that prevents long vehicle chains.

[0007] Due to technical limitations in determining the position, the separations between vehicles are a few meters long which makes physical connection between vehicles difficult.

[0008] The proposed system does not suffer from cumulative error in determining the position and enables long chains of trailer vehicles. This new guidance system further enables vehicles to drastically reduce the safety distance between each other and thus be able to have a physical connection that enables communication and energy transfer.

[0009] The inventor is not previously aware of any invention that includes the provisions exhibited by the current invention, nor the advantages that said provisions entail.

DESCRIPTION OF THE INVENTION

[0010] The semi-automated convoy transport system for vehicles wherein a first vehicle referred to as leader includes a system for positioning the vehicle with respect to the infrastructure, recording the trajectory over which it drives and transmits said trajectory, together with other information, to the rest of vehicles of the convoy that follow it, via a communication channel.

[0011] This information consists of the main operation and navigation parameters of the vehicle: steering wheel turning position, engine power, acceleration or applied brake force, suspension behaviour, etc.

[0012] All this information is referred to a clock system that is synchronised with the clocks of the rest of the fleet that makes up the convoy.

[0013] The vehicles that follow the leader are referred to as trailers and include a positioning system equal to that of the leader and a navigation system which, using the data sent by the leader, follow the trajectory travelled by the leader.

[0014] The communication channel consists of a physical connection between the convoy vehicles by way of a chain by means of resilient spiral cables that are connected at both ends. The leader and the trailers exchange information and electrical energy via this communication channel.

[0015] The trailers have at least one radar sensor capable of measuring the distance from the vehicle that precedes them. In the event that a trailer experiences disconnection from the channel via which it receives the information from the leader, the trailer initiates a controlled braking process which, imitating the leader's trajectory to the point wherein communication was lost, guarantees a safe distance with the vehicle that precedes it that prevents rear-end collisions.

[0016] The leader knows the maximum acceleration and braking capacity of each one of the trailers according to the load and the slope. The trailers have sensors for measuring the load they transport and gyroscopes for determining the slope to which they are subjected. The leader receives this information and limits the accelerations or decelerations thereof to prevent rear-end collisions or those due to elongation of the convoy.

[0017] The leader determines what is the maximum error of supported lateral displacement with respect to the marked trajectory. If a trailer exceeds the authorised limit, a warning takes place that alerts the leader vehicle's driver or navigation system of following issues.

[0018] The proposed transport system enables it to be propelled by means of electrical energy that is stored in batteries fitted in, at least, one of the trailers.

[0019] To increase convoy autonomy, the replacement of battery trailers when necessary is contemplated. These trailers transfer power to the engines of the other vehicles or recharge the batteries of other trailers.

[0020] Moreover, the coupling of new convoys for the same purpose is further contemplated. This coupling can take place at the head or the tail of the convoy with the help of a semi-rigid pole.

[0021] For this, the involved convoys establish a prior wireless communication by means of which they share position and trajectory information to facilitate the approach.

[0022] Thus, the leader of the convoy preceding the other one assumes the provisional leadership of the entire convoy.

[0023] In the event that the wireless link does not have the required quality or the link is lost, the leader who has delegated responsibilities to the provisional leader takes the leadership of its convoy back. As long as the wireless connection has sufficient quality, the provisional leader communicates the trajectory thereof and the position of the last trailer thereof and the leader of the other convoy tries to follow the same trajectory, progressively reducing the distance to the last trailer of the convoy that it follows. When both convoys are close together, an articulated system deployed from one of the vehicles involved in the attachment of the convoys extends a robotic pole at the end of which the connector of the interconnection hose that will connect both convoys is attached. The pole facilitates the coupling of the connector and retracts once the connection takes place.

[0024] In this way, the new convoy is coupled and the provisional leader becomes the definitive leader of the convoy.

[0025] Similarly, it is envisaged that a convoy can be divided in two during the drive so that, once the necessary load has been transferred, the convoy that has supplied the load can uncouple. In this case, the pole is used to collect the connector of the hose that is to be released.

DESCRIPTION OF THE DRAWINGS

[0026] The contribution of drawings is not considered necessary, since the specification offers all the information with clarity.

PREFERRED EMBODIMENT OF THE INVENTION

[0027] The semi-automated convoy transport system for vehicles wherein a first vehicle referred to as leader includes a system for positioning the vehicle with respect to the infrastructure, recording the trajectory over which it drives and transmits said trajectory, together with all the remaining necessary information, to the rest of vehicles of the convoy that follow it, via a communication channel.

[0028] The following elements are distinguished in the system:

[0029] (1).—infrastructure over which the convoy drives

[0030] (2).—positioning device in the infrastructure.

[0031] (3).—several vehicles and the following elements are located in said vehicles:

[0032] (4).—high definition radar sensor for exact positioning of the vehicle.

[0033] (5).—it can further include a positioning system not necessarily by means of the infrastructure.

[0034] (6).—a distance sensor, both in front of and behind the vehicle.

[0035] (7).—a high precision quartz clock.

[0036] (8).—a GNSS receiver for synchronising the clocks (7)

[0037] (9).—an independent navigation system.

[0038] (10).—a load sensor.

[0039] (11).—a precision gyroscope for measuring the inclination of the vehicle at any of the coordinates thereof at all times.

[0040] (12).—a CPU for managing all the parameters according to the inserted program.

[0041] (13).—two front plugs and two rear plugs for receiving respective 8-conductor spiral cables (21).

[0042] (14).—a transmitter/receiver antenna for radio, coded information and Wi-Fi.

[0043] (15).—an extensible rod ending in a V-shaped clamp (16) that allows the resilient spiral cables (21) to be connected to or disconnected from the vehicle in front or behind.

[0044] (16).—Wi-Fi interface for communication between vehicles.

[0045] All vehicles are attached by means of two sets of resilient spiral cables (21) with 8 conductors each.

[0046] Said set of two cables (21) are redundant, that is, they carry the same information but it is doubled up for safety, and wherein the conductors carry the following information:

[0047] (21.1).—transfers electrical energy (+) and has a larger cross section

[0048] (21.2).—transmits electrical energy (−). And it has a smaller cross section

[0049] (21.3).—ground conductor bus.

[0050] (21.4).—data conductor bus

[0051] (21.5).—conductor bus of the information of the clock (7).

[0052] These three buses operate in both directions and are also of the contention type, that is, at the moment that one vehicle wants to transmit it takes control of the bus and once it is done, it transmits information indicating who is the recipient or recipients by means of a routing recorded in the message itself.

[0053] The buses (21.6), (21.7) and (21.8) only operate as the leader vehicle, as single transmitter. In addition to all the elements already mentioned, the load of one of the convoy vehicles consists of a significant amount of batteries for supplying electrical energy to the group and which can be recharged by the group of vehicles during the drive.

[0054] Having sufficiently described the nature of the invention, as well as how to put into practice, it should be noted that the provisions indicated above and represented in the attached drawings are susceptible to modifications in details as long as they do not alter the fundamental principles thereof, established in the preceding paragraphs and summarised in the following claims.

1. A semi-automated convoy transport system for vehicles, wherein a first vehicle referred to as leader includes a system for positioning the vehicle with respect to the infrastructure, recording the trajectory over which it drives and transmits said trajectory, together with other information to the rest of vehicles of the convoy that follow it, via a communication channel, in the system comprising:

an infrastructure over which the convoy drives,

positioning device of the infrastructure,

several vehicles in each of which the following positioning, control and safety elements are located:

a high definition radar sensor for exact positioning of the vehicle,

distance sensor, both at the front and at the rear portion of the vehicle,

a high precision quartz clock,

GNSS receiver for synchronising the clocks (7),

an independent navigation system,

a load sensor,

a precision gyroscope for measuring the inclination of the vehicle at any of the coordinates thereof at all times,

a CPU for managing all the parameters according to the inserted program,

two 8-conductor spiral cables connected to two front plugs and two rear plugs,

a transmitter/receiver antenna for radio, coded information and Wi-Fi,

an extensible rod ending in a V-shaped clamp that allows the resilient spiral cables to be connected to or disconnected from the vehicle in front or behind,

a Wi-Fi interface for communication between vehicles.

2. The semi-automated convoy transport system for vehicles, according to claim **1**, wherein the communication channel is made up of the two sets of resilient spiral cables, which are redundant and have 8 conductors each; and in that conductors carry the following information:

transfers electrical energy (+) and has a larger cross section,

transmits electrical energy (−) and has a smaller cross section,

ground conductor bus,
data conductor bus, and
conductor bus of the information of the clock.

3. The semi-automated convoy transport system for vehicles, according to claim **1**, wherein the conductor buses located in each one of the vehicles, operate in both directions and are also of the contention type, while the conductors are buses that only operate as single transmitter.

4. The semi-automated convoy transport system for vehicles, according to claim **1**, wherein at least one of the convoy vehicles, in addition to all the elements already mentioned, includes batteries which supply electrical energy to the group and which can be recharged by the group of vehicles during the drive by means of the cables.

5. The semi-automated convoy transport system for vehicles, according to claim **2**, wherein the conductor buses located in each one of the vehicles, operate in both directions and are also of the contention type, while the conductors are buses that only operate as single transmitter.

6. The semi-automated convoy transport system for vehicles, according to claim **5**, wherein at least one of the convoy vehicles, in addition to all the elements already mentioned, includes batteries which supply electrical energy to the group and which can be recharged by the group of vehicles during the drive by means of the cables.

7. A semi-automated convoy transport system comprising:
a positioning device;
a high definition radar sensor configured to and/or programmed to exact positioning of a vehicle,
a distance sensor;
a high precision quartz clock;
a GNSS receiver configured to and/or programmed to synchronize the high precision quartz clock;
an independent navigation system;
a load sensor;
a precision gyroscope configured to and/or programmed to measure inclination of the vehicle;
a CPU configured to and/or programmed to manage all parameters according to an inserted program;
two 8-conductor spiral cables connected to two front plugs and two rear plugs;
a transmitter/receiver antenna configured for and/or programmed for communications;
an extensible rod ending in a V-shaped clamp configurable to allow the resilient spiral cables to be connected to and/or disconnected from the vehicle; and
an interface configured for and/or programmed for communication between vehicles.

* * * * *

Annex C: METRO DE MADRID TEST REPORT

INFORME DE LAS PRUEBAS DEL SISTEMA RPS EN METRO DE MADRID

En Madrid, a 4 de abril de 2017

Ver. 1.02

INTRODUCCIÓN

El pasado jueves 30 de marzo se efectuaron las primeras pruebas embarcadas del sistema RPS.

Previamente (con fecha 28 de marzo) se realizaron las gestiones necesarias en materia de prevención de riesgos laborales. Se hizo entrega por parte de Metro de Madrid la siguiente documentación:

- Información para empresas externas sobre riesgos y medidas preventivas a aplicar en lugares de trabajo de Metro de Madrid (rev. Febrero-2017).
- Medidas de emergencia a aplicar en Metro de Madrid (rev. Junio-2014).
- Normas internas de seguridad de Agentes en relación con la circulación (2013).
- Política de Seguridad y salud (2012).

Dichas pruebas pudieron realizarse gracias a la colaboración de Metro de Madrid. El objetivo de las pruebas era el de comprobar la capacidad de lectura del sistema RPS. Para ello se instaló el equipo RPS en un tren, se equipó una vía de pruebas con 2 balizas y se realizaron varias pasadas a distintas velocidades sobre las mismas.

La supervisión de las pruebas corrió a cargo de Carlos Rodríguez Sánchez y Juan José de Juan Gómez (Área de Ingeniería), quienes estuvieron presentes durante todo el proceso de preparación y de ejecución de las mismas, así como en el posterior desmontaje. Además, capturaron la información registrada por un radar doppler existente en el tren, y que se encuentra instalado junto al sensor RPS durante las pruebas con 2 objetivos: Comprobar que el sistema RPS no interfiere en la lectura del radar doppler y contrastar los datos registrados por el sistema RPS con los datos de velocidad registrados por el radar doppler.

Las medidas obtenidas por el sensor RPS fueron almacenadas y procesadas posteriormente en las oficinas de ADS. Las medidas obtenidas por el radar doppler fueron procesadas por personal de Metro de Madrid y facilitadas a ADS para su posterior comparación.

Estas primeras pruebas han permitido validar la viabilidad del sistema. Está previsto que, en las próximas semanas, se realicen nuevas medidas en vía de pruebas empleando un nuevo sistema que contemple:

- Un sistema de fijación del equipo al bastidor de la caja del tren más robusto.
- Un equipo RPS en caja metálica con disipador de calor acoplado y con una protección IP67, según norma UNE 20324:2000.
- Conector militar con la protección anteriormente citada y disipador de calor acoplado.
- Una lente que permita mayor rango de enfoque.
- Unas balizas de mayor tamaño similares a las RFID balizas que se emplean actualmente, fabricadas con plástico reciclado

Una vez validado el nuevo diseño en las instalaciones de Metro de Madrid, se procederá con las pruebas en vía principal.

SETUP

Los equipos fueron montados en la unidad 9805/9809/9810 en una vía de foso (vía 24 de zona 7 de la nave de mantenimiento de ciclo corto del recinto de Canillejas), con la unidad fuera de servicio. Una vez verificado el correcto montaje y la comunicación con los equipos registradores, se solicitó la salida a vía de pruebas.

Instalaciones Metro de Madrid

Las pruebas se llevaron a cabo durante tres horas aproximadamente, en la vía de pruebas 1 de zona 7 de depósito 4 (Canillejas), con un tren de la serie 9000 MRM (M9805/R9809/M9810) monotensión. En la siguiente figura se muestra una fotografía aérea de las instalaciones donde se ha marcado en color rojo la ubicación de la vía de pruebas cuya longitud es aproximadamente de 400 m.

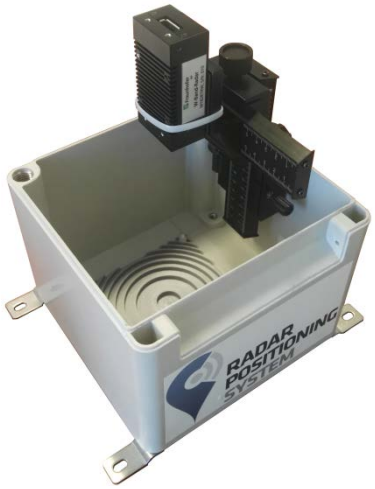

El equipo RPS empleado utiliza un modulo radar cuyas características técnicas están disponibles en este enlace. En el fondo de la caja, una lente fresnel de 12 cm de diámetro fabricada con una impresora 3D enfoca el haz del radar a 28 cm de distancia en un spot de 1 cm^2. El radar transmite 15 GHz de ancho de banda (desde 85 hasta 100 GHz) con una forma de onda de diente de sierra y un periodo de señal chirp de 300 µs. La señal reflejada se mezcla con una copia de la señal transmitida (principio de funcionamiento de un radar de onda

continua) y de tal proceso se obtiene una señal denominada señal de batido. Esta señal es digitalizada por un conversor ADC y un microprocesador interno envía las muestras de cada rampa chirp cada 600 μs mediante protocolo UDP hasta el ordenador donde son almacenadas para su posterior procesado.

Las balizas empleadas en las pruebas tienen unas dimensiones de 12cm de longitud, 5 de ancho y 4 de alto que codifican cada una de ellas 6 bits de los cuales 4 son de información. Cada una de ellas está constituida por 2 piezas de plástico PEHD separadas 0.5 mm por aire. Esta separación es necesaria para obtener una reflexión en el interior de la baliza. En futuros ensayos estas piezas se fijarán entre sí con un adhesivo que presente una constante dieléctrica diferente a la del PEHD (K=2.4). Ambas balizas presentan la misma codificación:

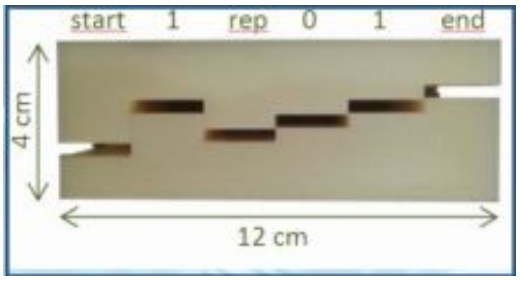

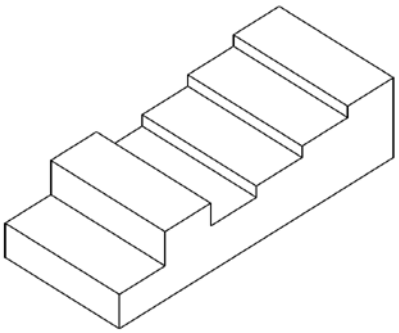

S 1 R 0 1 E donde S equivale a un bit de Start, R a un bit lógico repetido y E a un bit de stop y donde la información codificada se corresponde con la secuencia lógica 1101.

El equipo RPS se acopló bajo el bastidor de la caja R1 que también integra el ATP. La instalación del equipo se realizó en los talleres y se aprovechó el carril disponible en la caja para su fijación según se muestra en las siguientes figuras:




El sensor RPS se ubicó a una distancia de 28 cm respecto del nivel medio de las traviesas. Esta distancia está determinada por el diseño de la lente actual y podrá modificarse en el futuro según las necesidades. Sendos ordenadores portátiles registraron los datos enviados tanto por el radar doppler como por el sensor RPS. La comunicación entre el sensor RPS y el PC se realizó mediante conexión Ethernet 100 BaseT.

DESCRIPCIÓN DE LAS PRUEBAS

Las pruebas consistieron en un conjunto de pasadas a diferentes velocidades y en ambos sentidos sobre 2 balizas de plástico ubicadas junto a una baliza RFID que se muestra en la siguiente figura. Durante las pruebas, la baliza RFID se retiró dejándose únicamente el taco de madera. Tras el taco de madera, se deja una traviesa libre, a continuación, en la siguiente traviesa se coloca una baliza y nuevamente se deja otra traviesa libre y en la siguiente traviesa se instala una segunda baliza.

Se realizaron 4 pasadas a distintas velocidades. La siguiente figura muestra una gráfica donde se representa la velocidad del tren a lo largo de una de las pruebas. Esta velocidad se obtuvo a partir de los datos facilitados por el radar doppler.

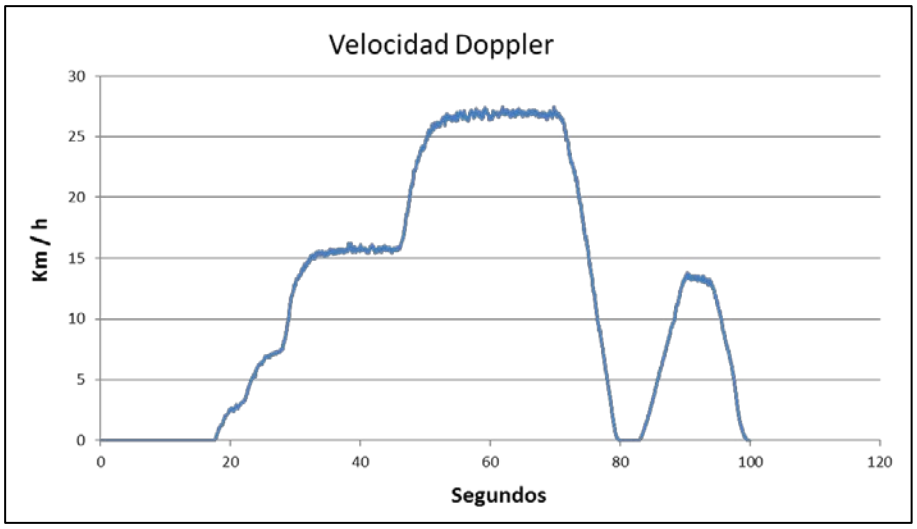

RESULTADO DE LAS PRUEBAS

En la siguiente figura se muestra las detecciones del radar a lo largo de 35 metros a su paso por las balizas de la primera pasada. El color de los puntos representa el nivel de potencia de las detecciones. Las detecciones más potentes se corresponden con cada una de las traviesas.

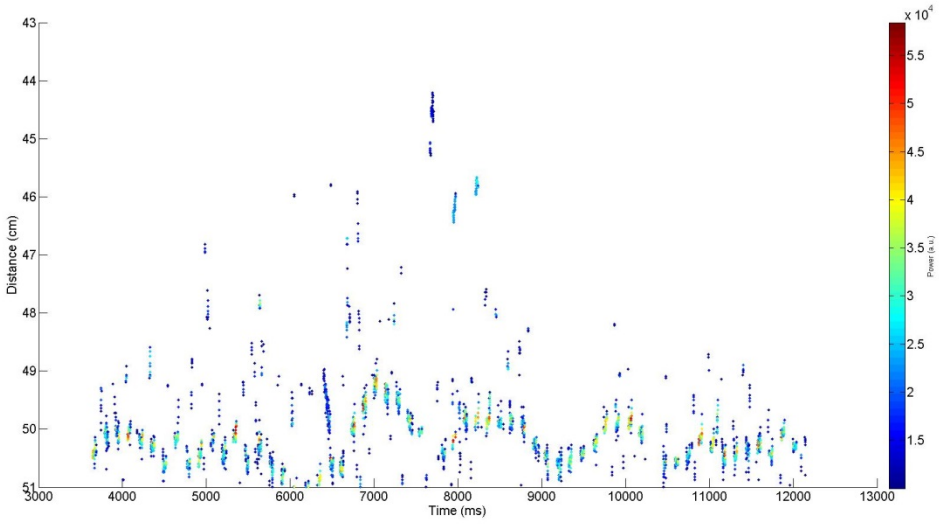

La siguiente figura muestra un zoom de la gráfica anterior donde se aprecia con mayor detalle cada una de las traviesas. A pesar de ser una superficie uniforme,

se aprecia un rizado de 5 mm. Este rizado está provocado por las vibraciones que el tren ha inducido en el soporte del radar (véase el brazo de color negro que sustenta el módulo radar). Las detecciones menos potentes que están a distancias menores de 50 cm se corresponden con hierba presente en la infraestructura.

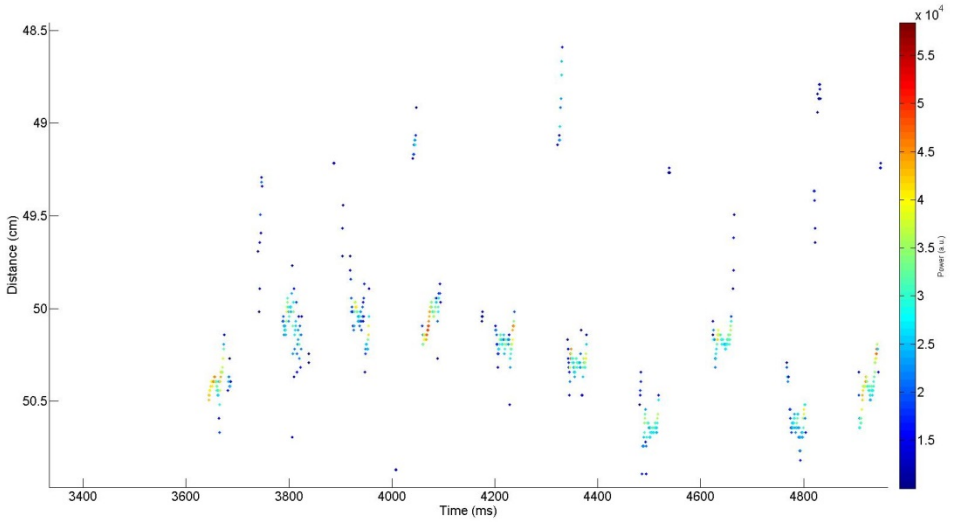

El procesado de estas detecciones mediante un filtro adaptativo permite la identificación perfecta de cada una de las traviesas según se muestra en la siguiente figura:

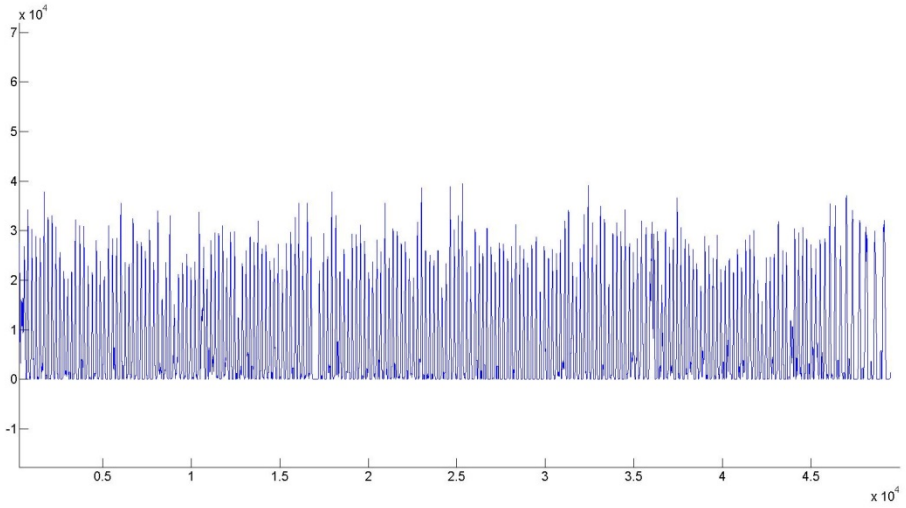

En la siguiente gráfica, se muestra un zoom de la figura anterior donde se puede apreciar la presencia de cada traviesa que se asocia a existencia de un pico. Se ha calculado la velocidad del tren contabilizando el tiempo transcurrido en la detección de 10 traviesas que están separadas 60 cm entre sí. El valor obtenido es 16 km/h.

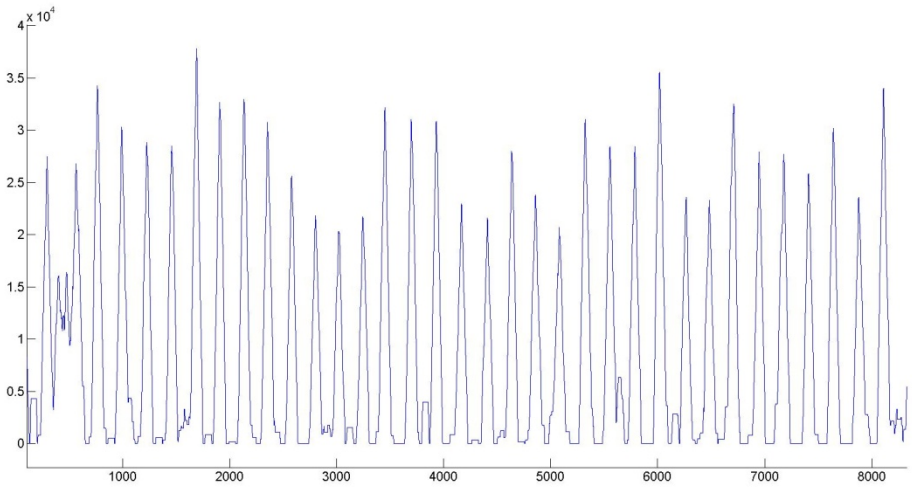

Realizando un nuevo zoom sobre la figura de las detecciones de la primera pasada, identificamos la presencia del taco de madera y de las dos balizas de plástico. La traviesa sobre la que apoya el taco de madera queda completamente oculta debido a que el tamaño del taco es mayor. Sin embargo, en las traviesas donde hay ubicadas balizas, se detecta su presencia a ambos lados de la baliza.

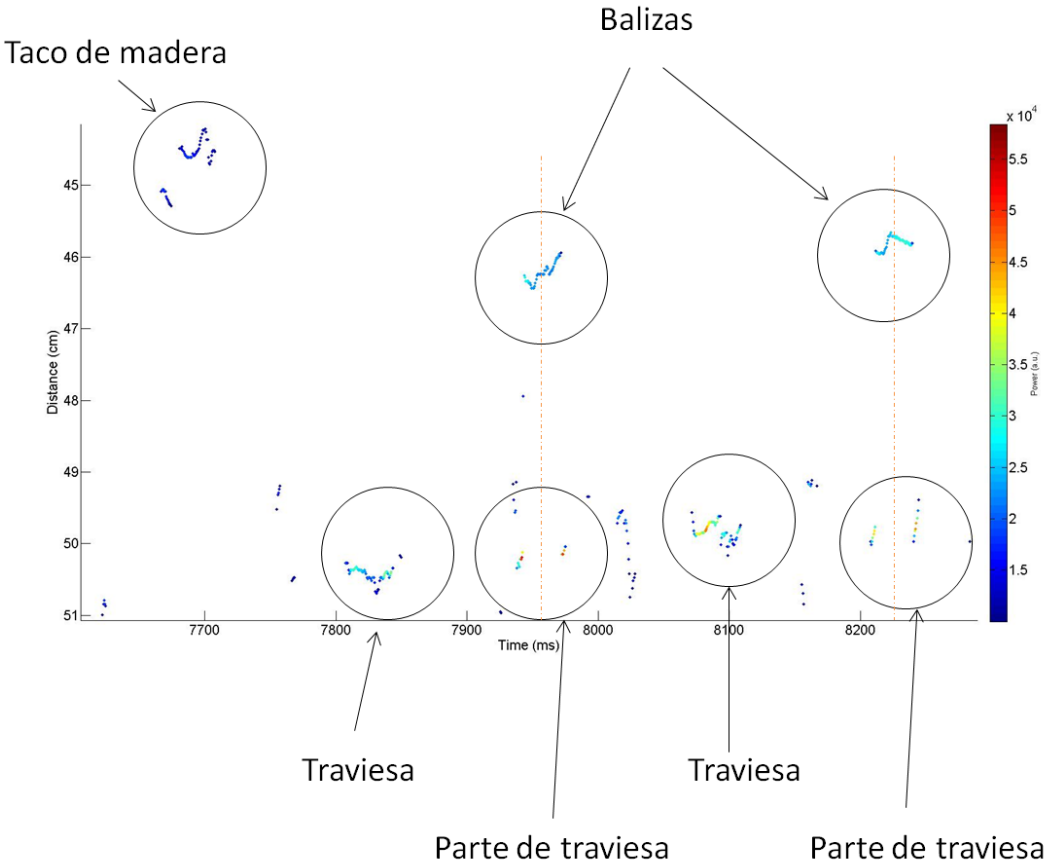

Realizando un zoom mayor sobre la figura y representando 2 detecciones por interrogación, obtenemos la siguiente figura, donde la detección superior se corresponde con la tapa superior de la baliza y la inferior con la reflexión que se produce en la separación existente entre las piezas de cada baliza

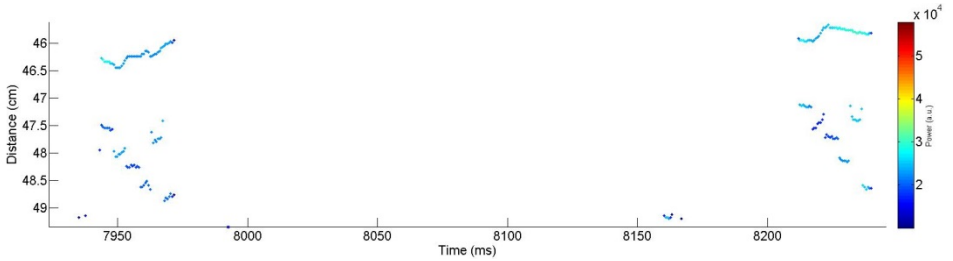

Las vibraciones no permiten a simple vista identificar la codificación de la baliza. Sin embargo, las vibraciones afectan igual a la primera y segunda detección. Sabiendo que la tapa superior de la baliza es una superficie uniforme es posible aplicar un simple procesado de la señal que iguala todas las detecciones a la misma distancia moviendo solidariamente las segundas detecciones. La nueva figura obtenida permite identificar perfectamente cada uno de los niveles lógicos de la baliza.

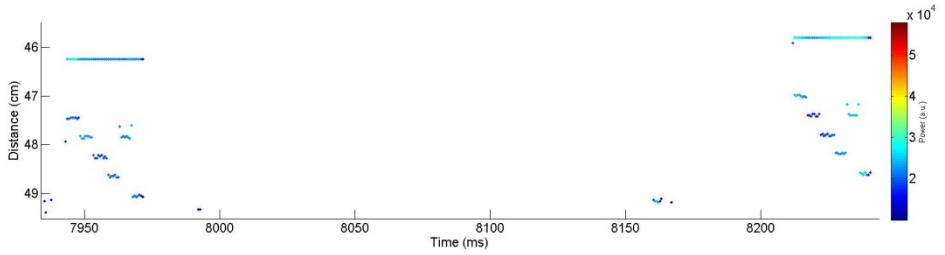

En la siguiente figura se muestran las detecciones de las dos balizas tras aplicar el mismo procesado en una captura realizada en sentido inverso.

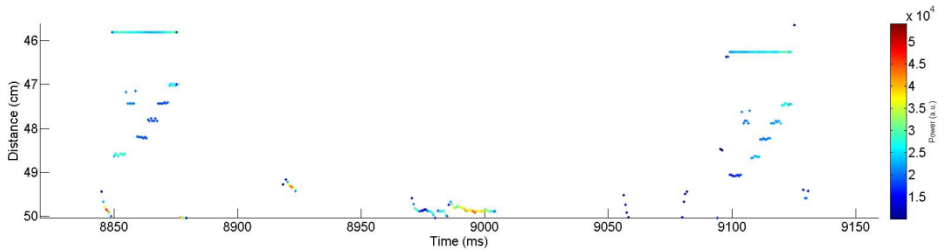

En un primer instante, se pensó que la forma ondulada del perfil generado por las traviesas se debía a la amortiguación de la caja. Sin embargo, al procesar el resto de pasadas se pudo comprobar que, en realidad, esta ondulación es el perfil que presenta la propia infraestructura ya que siempre presenta la misma forma.

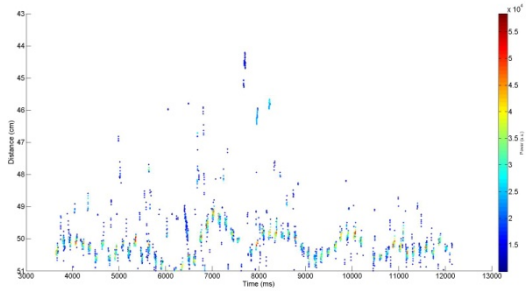

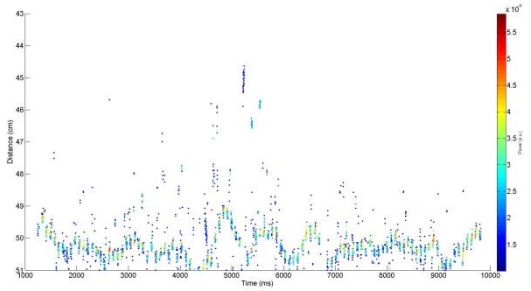

Las 2 primeras figuras muestran 2 capturas en el mismo sentido. La velocidad del tren en las respectivas capturas es de 16 y 26.5 km/h.

Las siguientes 2 figuras muestran las mismas balizas capturadas en sentido contrario a velocidades de 17.3 y 16.5 km/h. En la última figura, se aprecia cómo las últimas traviesas se van espaciando cada vez más por efecto de la frenada del tren.

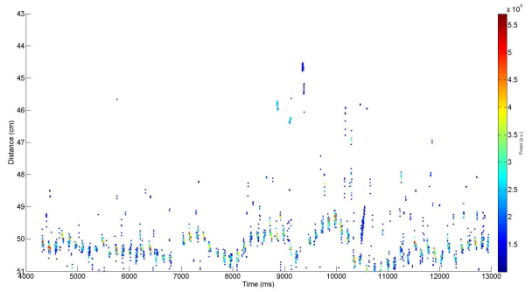

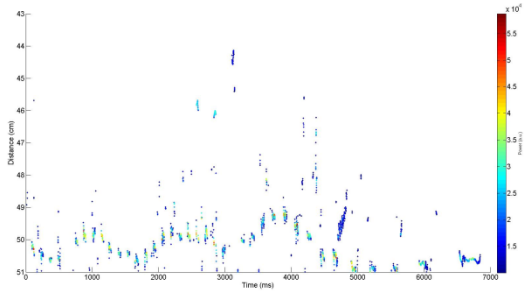

CONCLUSIONES

El equipo RPS ha demostrado la capacidad de lectura de las balizas de plástico según lo esperado. Se ha detectado que el sistema de fijación del módulo radar no es el idóneo, ya que las vibraciones del tren distorsionan la medida de la distancia en unos 5 mm. Dado que la información codificada en las balizas es independiente de la distancia hasta el radar (la información se codifica en la distancia entre dos detecciones equivalentes al espesor del plástico), la lectura de las balizas es posible incluso en estas condiciones. Sin embargo, una disminución de las vibraciones permitiría una mejor identificación de las traviesas.

El radar doppler existente en el tren, no se ha visto afectado en absoluto por el equipo RPS conforme a lo esperado ya que el radar doppler trabaja a 24 GHz y el equipo RPS entre 75 y 100 GHz. Las estimaciones de velocidad obtenidas a partir de las capturas RPS han coincidido con la lectura del radar doppler.

MEJORAS A TENER EN CUENTA EN EL FUTURO

Además de las mejoras que ya están previstas para la segunda prueba (Armario, lente y sistema de fijación nuevos), es necesario disminuir el tiempo de interrogación para poder soportar velocidades mayores. Para ello, se deberá sustituir el sistema de generación de señal actual -basado en una síntesis de señal a partir de un PLL (Phase Lock Loop)- por un sistema de generación que emplea un DDS (Direct Digital Synthesis). Este nuevo sistema de generación permitirá reducir el tiempo de interrogación de 300 a 6 μs.

AGRADECIMIENTOS

Agradecemos enormemente la colaboración de Metro de Madrid durante las etapas de asesoramiento inicial y durante la ejecución de las pruebas con la especial implicación personal de Antonio de Santiago Laporte, Laura Carmen Simón Vena, Santiago Rincón Arévalo, Carlos Rodríguez Sánchez y Juan José de Juan Gómez. Sin su colaboración, estas pruebas no habrían podido llevarse a cabo.

Annex D: REPORT OF PRECISE STOP TESTS AT FGC

INFORME PRUEBAS PARADA PRECISA

COR Rubí FGC 17-18 de octubre de 2022

Alejandro Badolato Martín
(alejandro@autodrive.solutions)

Javier Agustín Sáenz
(javier.agustin@autodrive.solutions)

Versión 1.0 (4 de diciembre de 2022)

AUTO DRIVE SOLUTIONS

Tabla de contenido

AUTODRIVE SOLUTIONS

1. Objetivo

El objetivo principal de las pruebas realizadas por Masats y Autodrive Solutions en las instalaciones de Ferrocarrils de la Generalitat de Catalunya situadas en el Centro Operativo de Rubí es el de validar el sistema de parada precisa desarrollado por Autodrive Solutions.

Este sistema de parada precisa tiene una precisión teórica de 2,5 cm que permite la determinación del punto de parada de forma absoluta y única en cualquier punto de la infraestructura que haya sido digitalizado previamente mediante el despliegue de una serie de balizas.

El sistema de parada precisa proporciona una interfaz de ayuda al maquinista que facilita la maniobra de aproximación y frenado para que el tren se detenga en las proximidades de un punto de parada previamente definido. De tal manera, se facilita el despliegue de sistemas de seguridad tales como las puertas de andén o los gap fillers.

Esta primera fase de pruebas comprende la puesta en marcha del sistema el COR de Rubí así como la calibración del equipo para esta instalación particular y la toma de datos necesaria para la implementación del sistema completo de parada precisa en la siguiente fase de pruebas.

AUTO DRIVE SOLUTIONS

2. Descripción de las pruebas

Tal como se definió en el documento de planificación de las pruebas, el plan de actuación se resume en las siguientes dos tablas:

JORNADA 1:

Nº	DESCRIPCION	TIEMPO ESTIMADO	COMENTARIOS
1	Instalación de la tubería codificada de 30 metros en la vía de pruebas. Se fijará cada metro aproximadamente mediante tornillos roscados en las traviesas de madera	2 h	
2	Instalación del equipo embarcado en el tren. Esta tarea se realiza con la UT estacionada dentro del taller.	1 h	Utilizaremos el enchufe con alimentación de 220Vac en la cabina
3	Una vez completadas las tareas 1 y 2, se procederá a realizar el primer recorrido de prueba sobre la pista codificada a la velocidad máxima permitida. NOTA: Es posible que después del primer recorrido, sea necesario algún reajuste de la tubería codificada. En tal caso, sería necesario descender del tren y trabajar en el equipamiento instalado durante unos 10-15 minutos.	1-1.5 h	
4	Segundo recorrido de prueba en sentido contrario.		
5	Repetición del recorrido de prueba a velocidad máxima permitida		
6	Recorrido de prueba en sentido contrario.		
7	Desmontaje del equipo embarcado. Esta tarea se realiza con la UT estacionada dentro del taller.	45 minutos	

JORNADA 2:

Nº	DESCRIPCION	TIEMPO ESTIMADO	COMENTARIOS
1	Instalación del equipo embarcado en el tren. Esta tarea se realiza con la UT estacionada dentro del taller.	1 h	Utilizaremos el enchufe con alimentación de 220Vac en la cabina
2	Primer recorrido de prueba sobre la pista codificada a la velocidad máxima permitida. NOTA: Es posible que después del primer recorrido, sea necesario algún reajuste de la tubería codificada. En tal caso, sería necesario descender del tren y trabajar en el equipamiento instalado durante unos 10-15 minutos.	2 h	
3	Se realizarán unos recorridos sobre los 30 metros de la tubería donde se pedirá al maquinista que circule a la máxima velocidad autorizada y, una vez sobre la pista, aplique el freno de servicio con distinta intensidad en cada prueba: (a) 25%, (b) 50% (c) 75% (d) 100%		
4	Repetición del recorrido en sentido contrario.		
5	Desmontaje del equipo embarcado. Esta tarea se realiza con la UT estacionada dentro del taller.	45 minutos	
6	Desmontaje de la tubería en la vía.	2 h	

AUTO DRIVE SOLUTIONS

2.1. Jornada 1

2.1.1. Instalación de la tubería codificada de 30 metros en la vía de pruebas

Las siguientes imágenes muestran la instalación que ser realizó en el COR. El primer proceso consistió en la selección del tramo de vía de prueba en el que se iban a instalar las balizas y realizar las pruebas.

Tras realizar una inspección visual del tramo de vía dinámica, se seleccionó el tramo que aparece en la primera imagen. Esto fue así por dos características principales, la primera es que era un tramo de 30 metros en los cuales no había instalada ninguna baliza ni otro elemento en vía que obligara a discontinuar la instalación de los elementos en vía, y el segundo factor fue el consistir en el tramo de curva con menor radio. De esta forma, el sistema se expone a las condiciones más desfavorables posibles.

El siguiente paso fue el despliegue y fijación de las balizas como queda presente en las siguientes figuras. Las balizas fueron instaladas en el eje central de la vía.

Cada segmento de 3 metros de baliza codifica un patrón de bits que se repite con la siguiente secuencia: Bit Start – Bit Datos – Bit Stop. Mediante repeticiones de este patrón se consigue codificar diferentes códigos. De tal manera, la codificación en la posición es única en cada punto de la vía. A continuación, se representa en formato hexadecimal la secuencia de datos desplegada en los 30 metros de vía adaptada:

0x25EC2, 0x30517, 0x08939, 0x04A04, 0x331E7, 0x0x0378C, 0x38254, 0x1087E, 0x3598E, 0x290AB

2.1.2. Instalación del equipo embarcado en el tren

Las pruebas se realizaron con la unidad 112.58. Tal como se muestra en las dos primeras imágenes, el equipo se instaló en la cabina del convoy utilizando el bastidor que había sido diseñado para ese punto concreto de la máquina. En la segunda imagen puede apreciarse cómo quedó la instalación definitiva del equipo embarcado.

Para realizar la comunicación con el equipo y la recogida de datos, se utilizó un PC en la cabina junto con una fuente de alimentación de 12 V y un inyector PoE. Todo ello alimentado mediante una toma de 230 V procedente de un enchufe de servicios auxiliares ubicado en la cabina. En las siguientes imágenes puede apreciarse cómo fue la instalación interior de los equipos de conexión y registro.

AUTO DRIVE SOLUTIONS

2.1.3. Primer recorrido de prueba sobre la pista codificada

Después de realizar la configuración y puesta en marcha del equipo, se pasó a movilizar el tren para realizar una primera medida de las balizas instaladas en la vía.

Tras analizar los resultados del sensor y determinar que los mismos no eran satisfactorios, se comprobó que el radio de la curva y el hecho de que el sensor no estuviera sobre uno de los ejes de rodadura provocavan que el sensor se desalineara respecto del centro de la vía tal y como se puede apreciar en la siguiente imagen.

La solución a este problema consiste en desplazar las balizas para lograr un correcto alineamiento entre sensor y baliza. La medida del desplazamiento depende de la distancia del sensor al eje del bogie y del radio de la curva. En el caso específico de las pruebas, este desplazamiento fue de 10cm con respecto al eje central de la vía. En las siguientes dos imágenes, puede apreciarse la instalación antes y después de la realización de este desplazamiento.

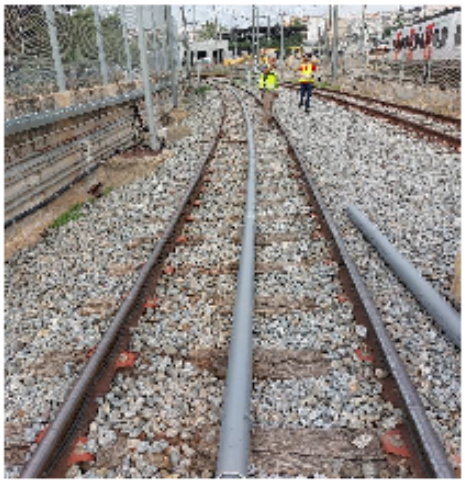

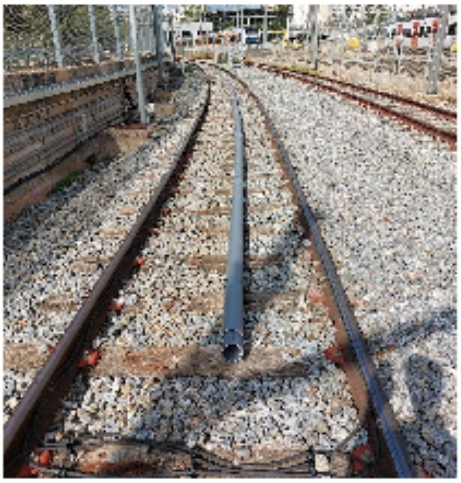

Una vez solucionado el problema de alineamiento del sensor, se procedió a realizar diversos recorridos a lo largo del tramo balizado en ambos sentidos y a comprobar la correcta instalación de las balizas mediante el análisis de datos. El trazo superior de la siguiente imagen muestra el perfil radar registrado durante un proceso de parada. Se puede observar como los pulsos de dicho trazo van ensanchándose progresivamente de izquierda a derecha por efecto de la reducción de velocidad del tren.

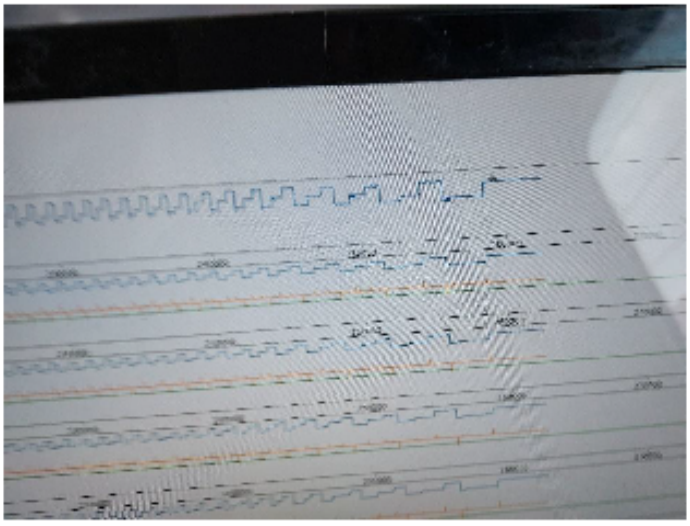

Comprobado que todas las balizas estaban correctamente instaladas, se dio por finalizada la jornada 1 de pruebas y se procedió a desmontar el equipo embarcado dejando la máquina en su estado original como puede apreciarse en la siguiente imagen.

AUTO DRIVE SOLUTIONS

2.2. Jornada 2

2.2.1. Instalación y puesta en marcha del equipo embarcado

Utilizando los resultados de la jornada 1 presentados anteriormente, la instalación y puesta en marcha del equipo embarcado consistió en la repetición de la instalación del día anterior y la movilización del tren sobre las balizas visualizando que los datos obtenidos en la lectura de los mismos eran exactamente los datos obtenidos el día anterior.

2.2.2. Realización de recorridos en diferentes condiciones y determinación de la distancia a un punto de parada determinado

Una vez realizada la comprobación inicial, se realizó una primera frenada sobre la serie de balizas. Con el tren detenido, se marcó una referencia en la vía en la proyección vertical del primer eje de rodadura sobre la misma. Además de esta marca de referencia se dispuso un cono naranja en las proximidades de esta referencia para que sirviese de referencia al maquinista. Se solicitó al maquinista que realizara una serie de aproximaciones al cono con distintas intensidades de frenada con dos objetivos. El primero era ver la capacidad del maquinista para detener el tren en un punto concreto. El segundo objetivo era comprobar que el sensor medía correctamente la distancia entre la referencia marcada en la vía y la posición del primer eje de rodadura. Es decir, la distancia entre el punto real de parada y la referencia marcada en la vía. La comprobación consistía en comparar el dato suministrado por el sensor respecto de la medida real realizada con una cinta métrica por operarios desplegados en la vía.

En el siguiente enlace, puede verse una de las aproximaciones realizadas:

https://photos.app.goo.gl/8N14cqHbe4bxRAvF6

Se realizaron varias aproximaciones modificando la posición del cono en cada prueba para dificultar, en la medida de lo posible, un posible entrenamiento por repetición por parte del maquinista. Se observó que, si el maquinista se aproxima de manera conservadora reduciendo drásticamente la velocidad antes del punto de parada y, posteriormente, con el tren circulando a muy baja velocidad en las proximidades del punto de parada actúa de nuevo el freno con mayor intensidad, el error en el punto de parada suele ser inferior a 50 cm. Cabe destacar que, a pesar de esta elevada precisión en la parada sin ningún tipo de ayuda, cuando se le preguntaba al maquinista por su estimación respecto del punto de parada no sabía indicar si se había quedado antes o después de la referencia ni a qué distancia aproximada se había detenido. Por otro lado, cuando el maquinista se aproximaba a la referencia a mayor velocidad y aplicaba una curva de frenado más agresiva, el error cometido aumentaba hasta los 2 metros.

Como resumen de estas pruebas se van a presentar varias figuras que muestran las medidas realizadas con su correspondiente explicación.

En la siguiente figura y se muestra el perfil registrado a lo largo de una serie de bits donde se puede apreciar las diferentes alturas que se asocian con los diferentes niveles lógicos.

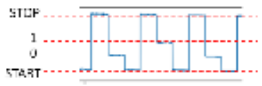

En el siguiente perfil, se muestra la lectura radar de una baliza en sentido inverso. Leyendo el perfil de izquierda a derecha se observa que, después de un bit de stop, sucede un bit de datos y otro de start. Si el recorrido fuese el contrario, después de un bit start le sucedería un bit de datos en lugar de un bit de stop.

Cabe destacar que, en el primer bit de datos comenzando por la izquierda, se puede apreciar un bit con una altura superior a la de los bits 1 y 0. Esta altura de bit se corresponde con el bit de inicio de palabra y sirve para identificar el inicio de una nueva baliza. De tal manera, la baliza mostrada tiene la siguiente codificación en binario: 011111100001000010.

A continuación se muestra el perfil registrado de tres balizas en sentido inverso cuando el tren circula con una velocidad constante.

El radar realiza 10,000 medidas por segundo. De tal manera es capaz de determinar con precisión las transiciones de cada uno de los bits de 5 cm de longitud. En este caso, la velocidad del tren es constante a 10km/h durante el paso por los 33 metros de balizas.

Segundo recorrido sentido marcha adelante con frenada en punto de referencia

En la siguiente figura, se muestra el perfil registrado marcha adelante. A diferencia del perfil anterior, se observa que, después de un bit de start, sucede un bit de datos.

En la siguiente figura, se muestra el perfil registrado a lo largo de la frenada. Se puede apreciar ondulaciones en el perfil provocadas por la acción de la suspensión debido a la frenada. Esta capacidad de detección podría servir para estimar el comportamiento de la suspensión en pruebas dinámicas.

Se observa cómo, a medida que el tren va frenando, los bits se hacen más largos puesto que la velocidad es menor y el eje de abscisas representa el orden de la captura de la muestra. El bit sobre el que el tren para es el el bit de datos final de la baliza 0x1087E. Se puede apreciar al final del perfil cómo, en el instante final de la parda, el tren logró rebasar el bit de datos y se detectó el

AUTO DRIVE SOLUTIONS

siguiente bit de stop. No obstante, el tren retrocedió y volvió a posicionarse sobre el último bit de datos.

Este bit de datos se tomará en adelante como referencia para el resto de medidas como punto de parada de referencia y se marcó en las pruebas con un cono de color naranja de forma visual para marcar al maquinista el punto de parada objetivo.

Si, sobre el mismo perfil obtenido, representamos la velocidad estimada del tren a partir del número de medidas registradas sobre cada bit (velocidad instantánea de bit), obtenemos la siguiente figura. En la mism se puede apreciar que el tren circulaba a 15km/h cuando se comenzó a leer la serie de balizas y comenzó a frenar después de recorrer 3 metros. En la figura, se observa en la curva de descenso ligeros saltos en determinados puntos. Estos saltos se deben a las imperfecciones que tiene la pista codificada en la transición entre balizas consecutivas. Es decir, las balizas no están perfectamente solapadas y existe un ligero espacio entre ellas que provoca una medida incorrecta de la velocidad de bit. Este error quedará subsanado en las siguientes pruebas ya que se modificará el modo en el que se acoplan las balizas entre sí.

Tercer recorrido sentido marcha atrás reanudando desde la parada

Estas medidas corresponden al movimiento del tren desde el punto de parada hacia atrás para poder realizar una nueva frenada junto con la velocidad derivada

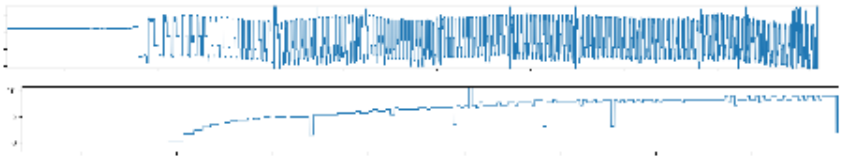

Cuarto recorrido sentido marcha adelante con intento de frenada en punto de referencia

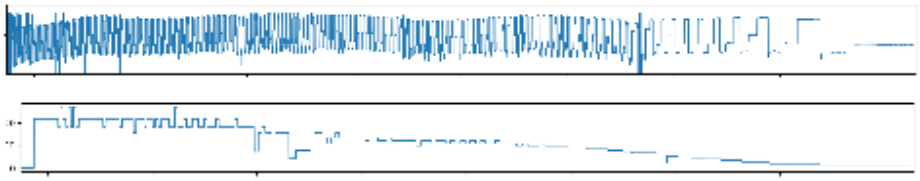

En este caso, el tren entro en la zona digitalizada a 20 km/h y el punto de parada fuen en el bit 9 de la baliza 0x1087E, por lo tanto, el maquinista fue capaz de para el tren a 150 cm del punto de parada de referencia.

Resumen de todas las paradas realizadas

La siguiente tabla muestra un resumen de los resultados obtenidos en todas las pruebas de paradas realizadas puesto que la muestra del resto de perfiles de medida no tiene mayor valor adicional que el ya presentado.

Orden de parada	Velocidad inicial (km/h)	Punto de parada	Precisión de la parada
1	15	Bit final baliza 0x1087E	Parada de referencia
2	20	Bit 9 de 0x1087e	-150 cm
3	18	Bit final baliza 0x1087E	0 cm
4	18	Bit 14 de 0x3598E	215 cm
5	17	Bit 16 de 0x38254	310 cm
6	18	Bit 5 de 0x38254	505 cm

Annex E: RADAR GROUND-PROFILE CORRELATION FOR ACCURATE SPEED MEASURING

Radar Ground-Profile Correlation for Accurate Speed Measuring

Alejandro BADOLATO[1], Jesus Antonio del CASTILLO[2], Juan de Dios SANZ BOBI[1], Cesar OTERO[2]
[1] Departamento de Ingenieria Mecanica Universidad Politecnica de Madrid, Madrid, Spain
[2] Departamento de Ingenieria Geografica y Tecnicas de Expresion Grafica Universidad de Cantabria, Cantabria, Spain
Corresponding Author: Alejandro BADOLATO(alejandro@autodrive.solutions)

Abstract

The recent development of sub-terahertz Si-Ge devices enables new sensing capabilities at low cost. mm-Wave radar devices can focus their energy over the ground into a circular spot with 1cm diameter and measure the distance with an accuracy better than 1mm. In this way, a radar sensor installed in the underbody of a train can obtain a high-detailed profile of the ground while the train is moving. Two radar devices pointing to the ground that are deployed along the longitudinal axis of the tracks with a known gap between them can be used for measuring the delay between profiles and estimate the speed of the train precisely. An accuracy better than ±0.5% accuracy can be achieved with 60 cm gap between sensors at 360 km/h. Accuracy can be improved up to more than 600 times by installing one sensor at the head of the train and the other one at the tail. Train speed estimation based on the time-correlation of ground profiles works fine in snowed environments without losing accuracy. A prototype successfully tested in laboratory is presented. Radar ground profilers can also be used for reading information encoded in the infrastructure through passive tags made of plastic or concrete with a specific shape.

1. Introduction

Precise odometry estimation is crucial in modern signaling systems but also a requirement for implementing efficient speed driving algorithms that takes into account the track profile. In most trains, odometry systems use tachometer data and speed sensors based on Doppler effect[1-2]. Both sensors are not accurate enough for these scenarios. Tachometer accuracy is affected by wheel slipping and blockage and requires continuous diameter calibration while speed sensors are typically +-1% error due to a variable angle of incidence of the radar beam over the ground surface. Other methods based on GNSS and IMUs have been explored in the past with limited commercial success[3].

We present a novelty method for estimating the speed of the train based on time-correlation of the ground profile obtained by two mm-wave radar sensors. The main benefit of the method is that the accuracy of the estimation can be delimited by increasing the gap between both sensors.

2. Time-Correlation for train speed estimation

2.1 Working principle

Train speed estimation based on time-correlation consists of two sensors on-board deployed along the longitudinal axis of the tracks. When the train is running, the two sensors scan the same infrastructure and produce a similar response which is dependent on the infrastructure characteristics providing a specific signature. The cross correlation of both sensor responses determines the delay between them and due to sensors are separated by a well known distance speed can be estimated. The main advantage of this technique is that accuracy can be improved by increasing the gap between both sensors. This method has already been explored in the past by optical, electromagnetic and Doppler radar sensors[4-6]. However, results were not good enough for precise and reliable speed estimation.

2.2 Time-Correlation based on the shape of the ground profile

2.2.1 Introduction to mm-wave radars

Due to a high cost of components, the use of mm-Wave sensors has been typically limited to space exploration and security applications[7-10]. In recent years, technological advances in radio frequency have given rise to new Silicon-Germanium components in the millimeter band [30-300GHz]. An example of this is the low-cost frequency modulation continuous-wave (FMCW) radar shown in Fig. 1. The radar[11] works in the 120-125 GHz band and most of its components, including also transmitter and receiver antennas, are embedded in a single chip.

Fig. 1: Silicon-Germanium 120 GHz SoC radar

The working principle of a FMCW radar consists in transmitting a chirp signal (a signal that changes its frequency along the time) and measuring the time of flight that this signal takes to bounce on the target and returns to the sensor. The Fig. 2 shows the architecture of a FMCW radar and a saw tooth radar waveform with linear frequency modulation.

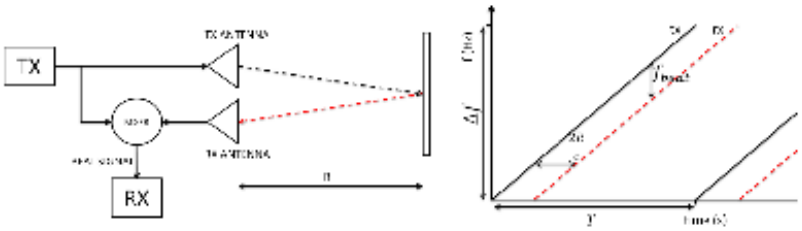

Fig. 2: Architecture of a FMCW radar and a saw-tooth radar waveform

The returned signal (dotted red trace) is mixed with a copy of the transmitted signal (continuous black trace). As a result of mixing both signals, we obtain a signal, called beat signal, whose frequency is proportional to the distance to the target. The frequency of the beat signal is determined by equation 1 where R is the distance to the target, c is the speed of light in the medium, Δf is the total transmitted bandwidth and T is the period of the chirp signal.

$$f_{beat} = \frac{2R}{c}\frac{\Delta f}{T}(Hz) \qquad \text{(Equation 1)}$$

mm-Wave radar sensors have many advantages in comparison with optical sensors since the radar signal is reflected over any type of surface even on those that present a low retro-reflectivity or are covered by sand or dust. Furthermore, radar reliability does not depend on light conditions and works well under heavy rain or fog conditions. These properties make mm-wave radars ideal for non-clean outdoor environments.

2.2.2 Proposed Sensor

The proposed sensor shown in Fig. 3 uses two mm-Wave radars with 60 cm gap between them that is installed in the underbody of the train pointing to the ground. At mm-wave frequencies, plastics are permeable and it is possible to use them for designing lenses [12]. Taking advantage of these properties, the radiation team of the Portuguese Institute of Telecommunications has designed two Bessel PEHD lenses for focusing the radiated energy on the ground. The radiated energy by the radar SoC is focused by the lens into a 1 cm diameter circular spot. This spot is formed 20 cm far from the lens and is still focused with the same spot size for another 50 cm. At higher ranges than 70 cm, the spot becomes bigger.

Inside the enclosure, two radar SoC like the one shown in Fig. 1 transmit a 4 GHz saw tooth waveform with 32 µs period. This means that the radar is able to measure the distance to the ground every 3.2 mm of train advance while running at 360 km/h. Radar signal is reflected on any type of material due to a different dielectric constant of the air. The accuracy of the measurement depends on the wavelength of the transmitted signal and is better than 1mm.

Fig. 3: Two radar sensors for scanning the ground shape

The beat signal of each radar is digitized and the radar signal processing required to calculate the distance to the target is performed into a FPGA. Then, the two range measurements are stored into 2 memory arrays. The cross correlation of both memories will find a maximum

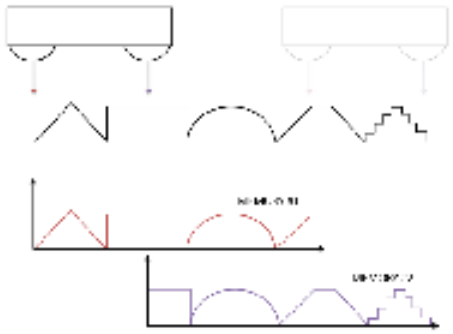

Fig. 4: Cross correlation of ground profiles

The theoretical cross-correlation error should be ±1 sample while the number of samples where the correlation will find the maximum will be the time that radar A takes to reach the initial position of the radar B divided by the period T and will depend on the gap between radars and the speed of the train. Equation 2 shows the theoretical error where $t_{measured}$ is the delayed obtained in the cross-correlation, T_{chirp} is the scanning time of 1 measurement of range, Gap is the distance between sensors and V_{train} is the real speed of the train.

$$\varepsilon_{speed} = \frac{t_{measured}}{\frac{Gap}{V_{train}}} = \frac{\frac{Gap}{V_{train}} \pm T_{chirp}}{\frac{Gap}{V_{train}}} = 1 \pm \frac{V_{train} * T_{chirp}}{Gap} \ (adim) \qquad \text{(Equation 2)}$$

Figure 5 shows the function of the theoretical speed estimation relative error versus train speed for a 60 cm gap. This error can be reduced up to 600 times by placing the first sensor at the head of a 400 hundred meters train and the second sensor in the tail.

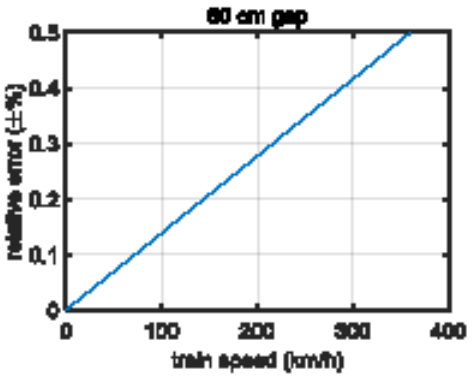

Fig. 5: Theoretical relative speed error for a 60 cm gap between sensors

If we consider that sleepers are deployed every D distance, a rough estimation of the speed can be obtained using only a single radar by performing a Fast Fourier Transform (FFT) of the ground profile obtained which should include multiple sleepers. The presence of the sleepers in the profile will generate a periodic signal due to the flat surface of the sleeper in comparison with the irregular ballast surface. In infrastructures where ballast is not present the periodic signal is obtained by scanning the supports of the tracks that are concrete blocks protruding from the grade. This periodic signal will generate a recognizable relative maximum in the power spectrum density when FFT is calculated.

The accuracy of the speed estimation is not degraded by snowed surfaces. The effect of the wind while the train passes through could change slightly the shape of the snowed surface and this fact would impact the correlation with a lower height of the relative maximum. However, the position of the peak which is associated with the speed of the train will not change, especially if the correlation is made with the last scanned 100 meters of infrastructure.

2.2.3 Preliminary results

A brief description of the internal architecture of the SoC is given below in order to explain the measurements shown in Fig. 6. The radar SoC includes an embedded 60 GHz Voltage Controlled Oscillator (VCO). Then, the output of the VCO is coupled to a frequency doubler for achieving 120 GHz. The output of the VCO is also internally divided by a 32X prescaler and connected to two output pins of the SoC. An external Phase Lock Loop (PLL) receives this feedback signal and manages appropriately the charge pump of the VCO for performing the required chirp signal. All the signals outside the SoC are below 1.9 GHz allowing the use of standard FR-4 substrates for the printed circuit board (PCB) instead of using high frequency substrates.

Fig. 6a shows the charge pump signal that manages the VCO while figure 6b shows the FFT of the beat signal for a wood target placed 28 cm far from the lens. The relative maximums placed at 12 and 28 cm corresponds to the lens and to the target respectively.

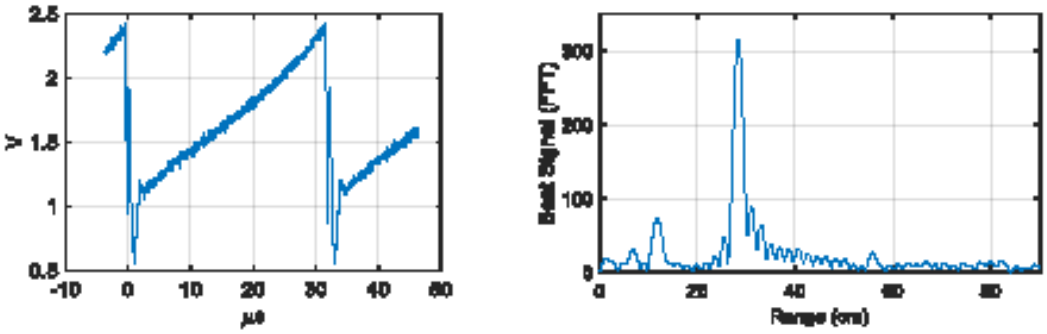

Fig. 6: a) charge pump of the VCO for a 32us chirp swapping 5 GHz b) FFT of the beat signal for a 28 cm wood target

A test model has been constructed for simulating the railway environment. Fig.7a shows the test model and the measurement setup. The sensor has been installed in a fixed position and the test model has been shifted appropriately for being scanned. Fig 7b shows the radar profile obtained.

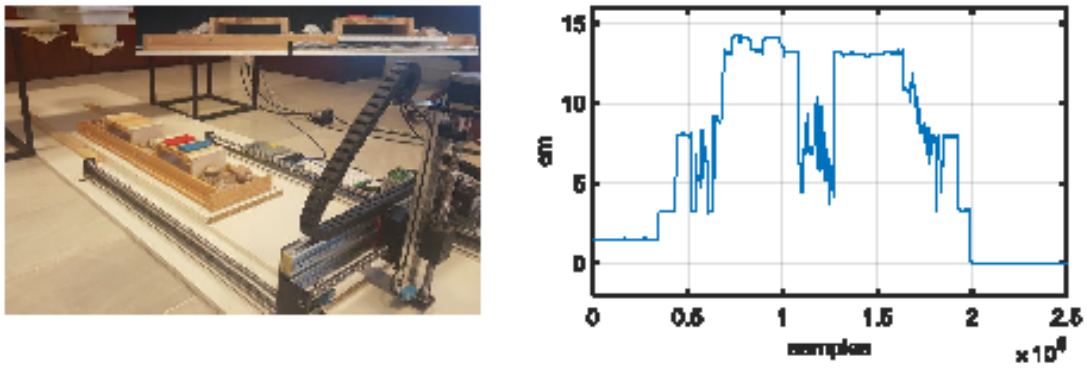

Fig. 7: a) Test setup for range measurement **b) Ground profile measured**

3. Other potential applications of mm-wave radars in the railway industry

There are multiple applications based on a precise ground profile measurement. Precise train location can be achieved without odometry data by storing in memory the ground profile of the infrastructure from station A to station B and comparing it with the last 100 meters scanned by the train. Centimeter positioning accuracy can be achieved by deploying passive elements such as plastic or concrete balises over the tracks that encodes information into its shape. By deploying encoded passive elements along the station, adaptive braking can be achieved for a reliable precise stop at stations with platform screen doors. Following this approach, intelligent sleepers that consist in a slight modification of its shape can be deployed. Encoding 4 data bits in each sleeper creates a set of 16 types of sleepers. Combining them randomly will create a pseudo random code that will increase the signature of the ground profile.

4. Conclusions

A novelty method for determining the speed of a train have been detailed. The method consists in the time correlation of two mm-wave radar ground profiles. The main advantage of this new technique is that accuracy can be controlled by setting the distance between both radar sensors. A 120 GHz prototype has been constructed with a 60cm gap between sensors. Each radar focuses the radiated energy into a 1cm diameter circular spot and measures the distance to the ground with 0.1 mm accuracy every 30 µs. The time correlation of both radar profiles enables speed estimation accuracies better than ±0.5% at speeds up to 360km/h.

Acknowledgment

We would like to thank the Spanish Economic Ministry through the CDTI for funding the project NEOTEC for the development of the speed sensor based in radar ground profile time-correlation. We would like also to thank Carlos A. Fernandes, Jorge Rodrigues da Costa and Antonio Miguel de Almeida from the Portuguese Instituto de Telecomunicações for the lens design. Finally, we would like to thank the Spanish team at Keysight Technologies for their kind and professional support.

References

[1] M. Malvezzi, P. Toni, B. Allotta and V. Colla, "Train speed and position evaluation using wheel velocity measurements," 2001 IEEE/ASME International Conference on Advanced Intelligent Mechatronics. Proceedings (Cat. No.01TH8556), Como, Italy, 2001, pp. 220-224 vol.1.

[2] A. J. Beesley, "Distance/velocity measurement by Doppler [rail traffic control]," IEE Colloquium on Where Are We Going? (And How Fast!) Seminar Exploring Speed And Positioning Systems For The Transport Sector, London, UK, 1997, pp. 5/1-512.

[3] B. Stadlmann and S. Mandl, "GNSS based train localization for automatic train operation," 2017 15th International Conference on ITS Telecommunications (ITST), Warsaw, 2017, pp. 1-7.

[4] M. Spindler, D. Stein and M. Lauer, "Low power and low cost sensor for train velocity estimation," 2016 IEEE International Conference on Intelligent Rail Transportation (ICIRT), Birmingham, 2016, pp. 259-264.

[5] D. H. Murillas and L. Poncet, "Safe odometry for high-speed trains," 2016 IEEE International Conference on Intelligent Rail Transportation (ICIRT), Birmingham, 2016, pp. 244-248.

[6] E. A. Mortlock and G. Hubbs, "Implementing optical speed measurement (OSMES) for communications based train control," ASME/IEEE Joint Rail Conference, 2004. Proceedings of the 2004, Baltimore, MD, USA, 2004, pp. 205-211.

[7] A. Badolato et al., "A 300 GHz imaging radar for standoff anomaly detection," 2015 9th European Conference on Antennas and Propagation (EuCAP), Lisbon, 2015, pp. 1-5.

[8] J. Grajal et al., "3-D High-Resolution Imaging Radar at 300 GHz With Enhanced FoV," in IEEE Transactions on Microwave Theory and Techniques, vol. 63, no. 3, pp. 1097-1107, March 2015.

[9] K. B. Cooper et al., "A High-Resolution Imaging Radar at 580 GHz," in IEEE Microwave and Wireless Components Letters, vol. 18, no. 1, pp. 64-66, Jan. 2008.

[10] A. Tang and T. Reck, "Hybrid CMOS System-on-Chip/InP MMIC systems for deep-space planetary exploration at mm-Wave and THz," 2017 IEEE Compound Semiconductor Integrated Circuit Symposium (CSICS), Miami, FL, 2017, pp. 1-4.

[11] W. Debski, W. Winkler, Y. Sun, M. Marinkovic, J. Borngräber and J. C. Scheytt, "120 GHz radar mixed-signal transceiver," 2012 7th European Microwave Integrated Circuit Conference, Amsterdam, 2012, pp. 191-194.

[12] Álvaro F. Vaquero, Manuel Arrebola, Marcos R. Pino, S.A. Matos, J.R. Costa, C. A. Fernandes, Low-cost Dielectric Flat Lens for Near-Field Focusing, IEEE International Symp. on Antennas and Propagation - IEEE AP-S/USNC-URSI, Boston, United States, Vol. -, pp. - - -, July, 2018

Annex F: RADAR POSITIONING SYSTEM FOR SURFACE TRANSPORT

IRF GLOBAL R2T Conference
November 19-22, 2019 – Las Vegas, NV USA

PAPER TITLE	Radar Positioning System for surface transport		
TRACK			
AUTHOR (Capitalize Family Name)	POSITION	ORGANIZATION	COUNTRY
Alejandro BADOLATO	CO-CEO	AUTO DRIVE SOLUTIONS	SPAIN
CO-AUTHOR(S) (Capitalize Family Name	POSITION	ORGANIZATION	COUNTRY
Jesus Antonio CASTILLO	CO-CEO	AUTO DRIVE SOLUTIONS	SPAIN
Juan José ARRIOLA	Head of Autonomous & Connected Mobility	Spanish Traffic Administration	SPAIN
Juan de Dios SANZ	Professor	Universidad de Politecnica de Madrid	SPAIN
Cesar OTERO	Professor	Universidad de Cantabria	SPAIN
E-MAIL (for correspondence)	alejandro@autodrive.solutions		

KEYWORDS: (include up to 5 keywords)

radar; guidance; positioning; handover; infrastructure; vehicle orientation

ABSTRACT:

The abstract should be written in English, readily understandable to most readers and may contain up to maximum of 250 words. Authors are invited to use Times New Roman Size 10 and the full type width of the page (single column).

Precise location and orientation of vehicles is a must for reliable Advanced Driver Assistance Systems. In this paper we present a novelty method of vehicle positioning and orientation based on infrastructure adaptation called Radar Positioning System. RPS consists in 3D land markings that encode information in a similar way of the Braille system (the reading system for blind). As a result, a vehicle that reads this encoded line thanks to mm-wave radar sensors installed in the underbody is able to obtain its position with 1cm accuracy in a reliable, low cost and safe manner. Furthermore, vehicle orientation against the longitudinal axis of the lane is achieved with less than 1 degree error.
The main advantage of such precise vehicle orientation and location besides on the ability for solving the problems related with the handover at level 3 SAE systems. When perception fails, dead-reckoning can keep the vehicle in its lane along 200 extra meters due to a precise starting point. This extra distance can be used for reducing the speed and provide more response time to the driver for an appropriate handover.

Furthermore, thanks to RPS, vehicle perception can be improved exponentially by enabling target-data sharing between vehicles. RPS can also be suitable for supporting Intelligent Speed Assistance and un-manned Platooning.

Radar Positioning System for surface transport
IRF Global R2T Conference

Alejandro Badolato[1]
Jesus Antonio Castillo[1]
Juan Jose Arriola[2]
Juan de Dios Sanz[3]
Cesar Otero[4]

[1]Auto Drive Solutions S.L. , SPAIN
[2]Spanish Traffic Administration, SPAIN
[3]Universidad Politecnica de Madrid, SPAIN
[4]Universidad de Cantabria, SPAIN

Email for correspondence, alejandro@autodrive.solutions

1 INTRODUCTION

Precise location and orientation of vehicles is a must for reliable Advanced Driver Assistance Systems (ADAS) and Autonomous Vehicles (AVs). Current ADAS and AVs typically rely on stereo optical cameras, GNSS, IMUs and LIDAR sensors for these purposes. Optical cameras can estimate the lateral displacement and the orientation of the vehicle into the lane by detecting the land markings. Unfortunately, the reliability of optical cameras for detecting land markings depends on a good retro-reflectivity of land markings and favorable sunlight conditions. Wet surfaces, bad maintenance of land markings, snow, fog or heavy rain can reduce significantly the reliability of camera detection. GNSS provides a global positioning but the lack of accuracy and the low availability due to the absence of a clear line of sight with the satellite constellation under certain situations make them unsuitable for vehicle guidance. IMUs can improve GNSS positioning but this enhancement is not enough for guiding a vehicle safely. Most AVs developers are also relying on LIDAR and 3D maps for location purposes especially at urban environments. In these areas, GNSS accuracy is typically poor but surroundings have a lot of recognizable objects like buildings or traffic signals that create a signature which is easy to identify. Once the vehicle has scanned the environment, the computer tries to match the 3D cloud detection with the 3D map stored in memory. When the match is achieved, the vehicle performs triangulations with known objects on the map and can determine its position and orientation precisely.

However, generating 3D maps is very costly. The tasks of object identification and the pinpoint of these known objects that will be used for triangulation have to be done by operators. Furthermore, maps must be updated continuously due to a time-changing environment. As a result, these maps can only be available for a limited set of constrained areas. Under favorable weather conditions, LIDAR positioning is a reliable technique with few centimeters accuracy. Nevertheless, big size objects such as buses or trucks placed near the sensor can block LIDAR rays avoiding an appropriate environment scan. Ray blocking, snow, fog or heavy rain reduce significantly LIDAR positioning reliability.

Infrastructure adaptation by deploying magnets on the road has been explored in the past for supporting AVs localization. This adaptation allows to measure the lateral shift from the center of the lane [1]. However, the proposed solution has been commercially discarded due to a high cost of implementation.

In this paper we present a novelty method of vehicle positioning and orientation based on infrastructure adaptation called Radar Positioning System. RPS consists in 3D land markings that encode information in a similar way of the Braille system (the reading system for blind). As a result, a vehicle that reads this encoded line thanks to radar sensors installed in the underbody is able to obtain its position with 1cm accuracy in a reliable, low cost and safe manner. Furthermore, vehicle orientation against the longitudinal axis of the lane is achieved with less than 1 degree error.

2 3D LAND MARKINGS FOR ENCODING THE ROADS

Nowadays, there are multiple 3D land markings deployed in many roads worldwide for improving visibility in rainy conditions. 3D land markings have attached glass beads on their surface as shown in Fig. 1 which reflect lights in all directions improving retro-reflectivity. They are typically 25mm in diameter and 6mm high and are made of thermoplastic or cold plastic. Thermoplastic is a soft material and has the advantage that, when glass beads are removed and the retro-reflectivity is degraded, new glass beads can emerge from inside when the material is getting worn out. Cold plastic 3D paint drops are 90% plastic and 10% catalyst. When both are mixed, a chemical reaction is performed and in less than 5 minutes the paint drop gets extremely hard and is fixed to the asphalt. They can be applied at lower temperatures than thermoplastic ones, however, they are very hard and when glass beads are gone the cold plastic still remains without wearing down and the glass beads from inside cannot emerge to the surface. This kind of 3D land markings are currently printed by trucks at speeds up to 16 km/h.

Fig. 1 Cold Plastic 3D paint drops

We propose to encode the infrastructure by deploying cold-plastic 3D land markings along the center axis of the lane. Data is encoded in a row by associating different combinations of 3D paint drops to different logical levels as shown in Fig 2.

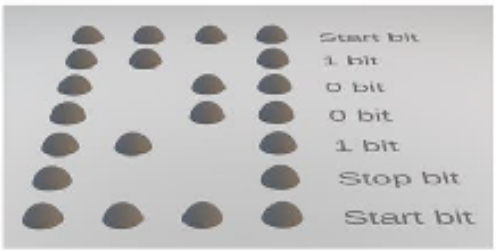

Fig. 2 Encoding pattern

3D paint drops will be black color remaining invisible to regular drivers. They will only perceive a slight noise when changing the lane. Radar sensors can obtain a detailed 3D image of the surface, detect the presence of the 3D paint drops and read the encoded track.

Earth surface, including mountains, oceans and poles, is 510.1 million of square kilometers. According to Equation 1, every square cm of the Earth surface can be univocally encoded by using 62 bits.

$$Log_2(510{,}1\ km^2) = Log_2(5{,}101 \cdot 10^{18}\ cm^2) = 62.1 \qquad (1)$$

Taking into account that roads are only a small portion of the Earth surface and a complete code can require hundreds of square cm for being deployed, 64 bits word length can address the complete lane network worldwide. There will be also enough spare codes available for re-asphalt tasks and future infrastructures. Considering a 5 cm gap between two consecutive rows, a complete word code can be deployed along 3.3 meters of lane segment (including also the start and stop bits).

In order to simplify the deployment, a pseudo random code will be printed. Every truck will be provided with a unique pool of codes and will print those avoiding repeated codes. Once the lane is adapted, a vehicle with calibrated odometry will run over the track and will generate a road map storing the code sequence, the misalignment of the track respect the central axis of the lane and the shape of the road thanks to data from the encoders of the wheel and the steering wheel, optical cameras and a GNSS receiver. This road map information is low-weight data and the global lane network will fit in a single flash memory. The road map will remain stable and will not change in time. If the infrastructure is modified, new free codes will be used.

The length of European lane network, including highways, main and secondary roads, is about 5,265,000 Km [2]. Considering a printing speed of 16 km/h, 50 trucks working 24 hours/day and 365 days/year can encode the complete lane network in less than 1 year. However, this is not a realistic number. Infrastructure adaptation will take more time but a progressive approach can be tackled starting at principal highways and main roads.

The costs of painting the encoded track are negligible compared with the costs afforded by infrastructure operators in maintenance tasks. Due to the encoded track is deployed along the center axis of the lane and to the extreme wear resistance of cold plastic 3D paint drops, they will last at least more than 15 years. In this sense, no maintenance is expected since re-asphalt tasks should be required first. Small errors on the track are not an issue due to the radar has the advantage that is reading a known message. Furthermore, Forward Error Correction (FEC) techniques can also be implemented.

3 mm-WAVE RADARS FOR READING THE ENCODED TRACK

mm-Wave sensors have been typically used for space exploration and security applications [3-7] due to a high cost of components. Thanks to the technological advances in Silicon-Germanium, low cost components are available in the millimeter band [30-300GHz]. An example of this is the low-cost frequency modulation continuous-wave (FMCW) radar shown in Fig. 1. The radar [8] works in the 120-135 GHz band and most of its components, including also transmitter and receiver antennas, are embedded in a single chip.

Fig. 3 Silicon-Germanium 120 GHz SoC radar

The working principle of a FMCW radar consists in transmitting a signal that changes its frequency along the time and measuring the time of flight that this signal takes to bounce on the target and returns to the sensor. The Fig. 2 shows the architecture of a FMCW radar and a saw tooth radar waveform with linear frequency modulation.

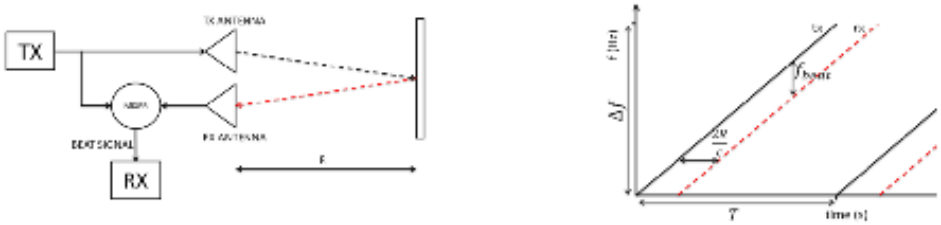

Fig. 4 Architecture of a FMCW radar and a saw-tooth radar waveform

The returned signal (dotted red trace) is mixed with a copy of the transmitted signal (continuous black trace). As a result of mixing both signals, we obtain a signal, called beat signal, whose frequency is proportional to the distance to the target. The frequency of the beat signal is determined by equation 1 where R is the distance to the target, c is the speed of light in the medium, Δf is the total transmitted bandwidth and T is the period of the chirp signal.

$$f_{beat} = \frac{2R\,\Delta f}{c\ \ T}(Hz) \quad (2)$$

mm-Wave radar sensors have many advantages in comparison with optical sensors since the radar signal is reflected over any type of surface even on those that present a low retro-reflectivity or are covered by sand or dust. Furthermore, radar reliability does not depend on light conditions and works well under heavy rain or fog conditions. These properties make mm-wave radars ideal for non-clean outdoor environments.

At mm-wave frequencies, plastics are permeable and, it is possible to use them for constructing lenses [9]. Fig. 5 shows a 15 mm diameter lens attached to the SoC radar that has an aperture of 6 degrees. The typical distance from the underbody of a vehicle to the ground is about 15 cm. At this distance, the 6 degree aperture angle results in a 1cm diameter circular spot over the asphalt where the radar concentrates its radiated energy

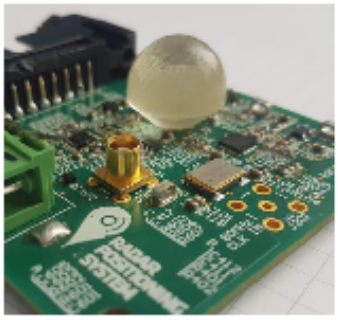

Fig. 5 Plastic lens attached to the radar SoC

Radar signal is reflected on any type of material due to a different dielectric constant of the air. The accuracy of the measurement depends on the wavelength of the transmitted signal and is better than 1mm. The radar measures every 30 µs the distance to the asphalt. This means that the radar is able to measure the distance to the ground every mm of vehicle advance while running at 120 km/h. In this way, the radar is able to obtain a high detailed profile of the asphalt when the vehicle runs and can detect the presence of a 3D paint drop. In order to read appropriately the encoded track, multiple radar sensors are installed in the underbody forming a linear array along the transversal axis of the vehicle. Hence, every time the encoded track is located between the 2 front wheels of the vehicle, the track can be read.

Radar sensors are hack free due to the following characteristics: a) there are no powerful sources at these frequencies b) the radiation pattern of the radar is high directive and pointing to the ground. c) due to a high bandwidth transmitted, hacking signals cannot be properly integrated in the receiver when they are mixed with a copy of the transmitted signal.

4 READING THE 3D LANDMARKINGS

A vehicle equipped with the RPS sensor that starts to run over an encoded infrastructure, reads a complete word code after 3.3 m. Then, the onboard computer searches in its database the read code and obtains the position coordinates. When the sensor is still pointing to the stop bit of the code, a radar SoC of the linear array is scanning with 1cm diameter spot over a 25mm diameter 3D paint drop (meaning, the paint drop of the left that encodes the stop bit). In this way, a precise location with 1cm accuracy in the three axis is achieved (height is measured by the SoC radar). The database also provides the following sequence of codes and the shape of the road. It will not be necessary to run another 3.3 m to update the position since, if the following bits are in accordance with the expected ones, position can be updated bit by bit (row by row) instead of reading a complete new code. Precise vehicle orientation is also obtained with an accuracy better than 1 degree.

The main advantage of such precise vehicle orientation and location is based on the ability for solving the problems related with the handover at level 3 SAE systems. When a Level 3 vehicle is running at high speed and the perception of the land markings fails, the driver has to take the handover immediately. However, a driver that is not paying attention requires more than 5 seconds to identify the situation and react properly [10]. Thanks to a precise starting point and thanks to a recorded shape of the road stored in memory, when perception fails, the encoders of the wheels and the steering wheel in combination with IMU and GNSS data can be used for maintaining the vehicle into its lane along 200 meters [11]. This safety distance can be used for recovering perception while reducing the speed. Furthermore, it will provide enough response time to the driver for an appropriate handover. In worst case, it can be used for stopping the vehicle in a safe stop area.

Odometry accuracy depends on a good estimation of the wheel effective radius. This effective radius depends on, among others, the ware down of the tire, the temperature, the air pressure and the vehicle load. The encoded track is a well-known reference that can act as a ruler for calibrating odometry. This calibration will impact on a longer safety distance when perception fails beyond the 200m.

In case of land marking manipulation, a mismatch will be produced between the gathered odometry data and the recorded roadmap. This mismatch will turn the vehicle into safe mode and odometry will be used at the last trusted position. In the same way, the vehicle will activate the safe mode if new codes that are not stored in the database are read. In the meantime, the computer of the vehicle will ask for new roadmap updates to the infrastructure administrator.

Snowed environments are the worst possible conditions for ADAS and AVs. When road markings are covered by snow, optical cameras cannot detect it. Lidar rays are bounced on snowflakes generating false alarms on obstacle detection and reference objects for triangulation in 3D maps change its shape. GNSS signals are reflected on snowed surfaces causing loss of accuracy. Snow is also challenging for mm-wave radars for reading information encoded on the road with 3D paint- drops. RPS sensors cannot penetrate snow and this means that they cannot read 3D paint drops covered by snow. Although snow is challenging for ADAS and AVs and requires extra measures to deal with, fortunately, most of the accidents that happen under these conditions are not critical since vehicle speeds are typically low. This means that snowed environments should not be a priority when facing traffic accidents reduction at short or medium term. However, ADAS and AVs must tackle snow issues. For dealing with RPS into snowed roads, a snow-plow robot equipped with a circular sweeper has to be used first for removing the snow over the track. The robot will act as a platoon leader adapting the speed of the convoy for ensuring an appropriate cleaned track and informing the rest of the vehicles that they can follow it. In worst case, the guidance system will work safely by reading only 3 meters of the encoded track every 200 meters which means less than 2% of the code.

RPS for railways has been successfully tested in real scenarios thanks to the collaboration of Metro de Madrid and a RPS sensor for road transport is currently under development.

5 OTHER APPLICATIONS

In addition to solving the problem of handover, encoding the roads with 3D paint drops has numerous benefits. Nowadays, a vehicle is able to detect a target, to measure the range and the angle of arrival and even to classify it. However, this data cannot be shared between vehicles due to uncertainty in the position and orientation of both vehicles, transmitter and receiver. 3D paint drops provide an absolute reference system and, when both vehicles are properly pinpointed and oriented, the target vector can be transferred from one vehicle to another. Extending this idea, vehicle perception can be improved exponentially by using data gathered from multiple vehicles running into its neighborhood.

Intelligent Speed Assistant (ISA) uses GNSS and stored roadmaps as well as optical cameras for detecting speed-limit traffic signs. In case of over speed, ISA will warn the driver. However, ISA is not reliable due to the lack of accuracy or availability of GNSS under certain conditions or due to unread traffic signs that are blocked by other big vehicles near the cameras. RPS can be an extra source of data for locating the vehicle enhancing ISA reliability.

RPS can be also helpful for providing synchronized traffic flows at cities. ADAS and AVs would work in a standalone manner for warranting a fast response but, most of the time, its movements would be controlled by a central host for

improving mobility and prioritizing public transport and emergencies. In this case, a precise positioning system will be required for scheduling vehicle movements appropriately.

Finally, RPS can provide support to unmanned platooning. Current unmanned platooning are limited to 2 or 3 vehicles due to the difficulties for keeping long convoys into the lane. The virtual engagement is coupled between two consecutive vehicles and suffer of a cumulative error that can make that a vehicle placed at the end of the tail will get out of the lane into a curve. For preventing this situation, the leader vehicle which is the first truck of the platoon, will provide its trajectory to the other vehicles thanks to RPS reading capabilities. Then, the other vehicles of the platoon will repeat precisely the trajectory of the leader.

6 CONCLUSIONS

Precise location and orientation of vehicles is a must for reliable Advanced Driver Assistance Systems and Autonomous Vehicles. Current solutions based on GNSS, IMUs, stereo optical cameras or LIDAR are not reliable enough under certain conditions. At high speed, safety may be compromised if land marking detection is not achieved. Dead-reckoning techniques can guide a vehicle safely along 200 meters by using the encoders of the wheels and the steering wheel and a pre-recorded roadmap. However, a precise starting point and vehicle orientation is required. A slight modification of the infrastructure will enable precise vehicle positioning with 1 cm accuracy and vehicle orientation with few degrees error in a reliable, secure and low-cost manner. It consists in deploying black color 3D paint drops along the center of the lane for encoding information in a similar way of the Braille code (the reading system for blind) and use mm-wave radars installed in the underbody of the vehicles for reading them. 3D road markings will remain invisible to regular drivers. After running 3m over the encoded track, the vehicle can determine its position and orientation precisely. Then, position can be updated every 10 cm. In case of loss of perception, dead-reckoning will guide the vehicle along 200 meters while reducing the speed and providing enough response time to the driver for an appropriate handover.

A low cost, single chip radar is able to concentrate all the radiated power into a 1cm diameter circular spot over the asphalt. The radar can read the distance to the asphalt with accuracy better than 1mm at 33 kHz rate. Measurement reliability is not affected by sunlight conditions.

Infrastructure adaptation is feasible and affordable thanks to machines able to print at 16 km/h cold plastic 3D paint drops. Due to high durability of cold plastic, no maintenance tasks are expected since re-asphalt should be performed first. Small errors in the encoded track are not an issue and infrastructure manipulation is easily detectable thanks to a mismatch against the recorded roadmap. In this case, vehicle can enable safe mode and use dead-reckoning till finding an appropriate encoded track or stop the vehicle in a safe stop area.

Precise location is also suitable for sharing target data between vehicles for improving vehicle perception, support unmanned platooning or Intelligent Speed Assistant or provide synchronized traffic flows at cities.

7 ACKNOWLEDGEMENTS

We would like to thank to the Subdirección de Movilidad from the Spanish Traffic Administration (DGT) for its support to RPS project. We would like also to thank Spanish Economic Ministry (CDTI) for funding a railway project related with RPS technology. Finally, we would like to thank to Metro de Madrid, Faplisa S.A. (Spanish road marking manufacturer), Silicon Radar GmbH and the Spanish delegation of Keyshight Technologies for its kind collaboration.

REFERENCES

[1] W.-B. Zhang and R. E. Parsons, "An intelligent roadway reference system for vehicle lateral guidance/control," in Proc. American Control Conf., San Diego, CA, 1990, pp. 281–286.
[2] YEARBOOK 2017 ROAD STATISTICS - European Union Road Federation http://www.erf.be/wp-content/uploads/2018/01/Road_statistics_2017.pdf
[3] Badolato, A., Castillo, J., Dios, J., Otero, C., "Radar Ground-Profile Correlation for Accurate Speed Measuring" World Congress Rail Research, Tokyo 2019
[4] Badolato, A. et al., "A 300 GHz imaging radar for standoff anomaly detection," 2015 9th European Conference on Antennas and Propagation (EuCAP), Lisbon, 2015, pp. 1-5.
[5] Grajal, J., Badolato, A. et al., "3-D High-Resolution Imaging Radar at 300 GHz With Enhanced FoV," in IEEE Transactions on Microwave Theory and Techniques, vol. 63, no. 3, pp. 1097-1107, March 2015.
[6] Cooper, K. B. et al., "A High-Resolution Imaging Radar at 580 GHz," in IEEE Microwave and Wireless Components Letters, vol. 18, no. 1, pp. 64-66, Jan. 2008.
[7] Tang, A. and Reck, T., "Hybrid CMOS System-on-Chip/InP MMIC systems for deep-space planetary exploration at mm-Wave and THz," 2017 IEEE Compound Semiconductor Integrated Circuit Symposium (CSICS), Miami, FL, 2017, pp. 1-4.
[8] Debski, W., Winkler et al., "120 GHz radar mixed-signal transceiver," 2012 7th European Microwave Integrated Circuit Conference, Amsterdam, 2012, pp. 191-194.
[9] J.R. Costa, C. A. Fernandes et al., "Low-cost Dielectric Flat Lens for Near-Field Focusing", IEEE International Symp. on Antennas and Propagation - IEEE AP-S/USNC-URSI, Boston, United States, Vol. -, pp. - - -, July, 2018
[10] C. Gold, D. Dambck, L. Lorenz, and K. Bengler, "Take over! How long does it take to get the driver back into the loop?" Proceedings of the Human Factors and Ergonomics Society Annual Meeting, vol. 57, no. 1, pp. 1938–1942, Sep. 2013.
[11] D. Gruyer, R. Belaroussi and M. Revilloud, "Map-aided localization with lateral perception," 2014 IEEE Intelligent Vehicles Symposium Proceedings, Dearborn, MI, 2014, pp. 674-680.

Annex G: NEW METHODS AND FUNCTIONALITIES FOR RAILWAY MAINTENANCE THROUGH A DRAISINE PROTOTYPE BASED ON RADAR SENSORS

Received: 10 December 2021 | Revised: 14 February 2023 | Accepted: 3 March 2023

DOI: 10.1049/itr2.12353

IET Intelligent Transport Systems

The Institution of Engineering and Technology WILEY

ORIGINAL RESEARCH

New methods and functionalities for railway maintenance through a draisine prototype based on RADAR sensors

Valentin Gomez-Jauregui[1] | Javier Agustín[2] | Alejandro Badolato[1,2] | Jesús del-Castillo-Igareda[2] | Juan de Dios Sanz Bobi[3] | Ana Carrera-Monterde[4] | Cristina Manchado[1] | César Otero[1]

[1]Research Group EgiCAD, Universidad de Cantabria, Santander, Spain

[2]Auto Drive Solutions S.L., Madrid, Spain

[3]Department of Mechanical Engineering of the Universidad Politécnica de Madrid (UPM), Madrid, Spain

[4]ETSIIT, Universidad de Cantabria, Santander, Spain

Correspondence
Valentin Gomez-Jauregui, Research Group EgiCAD, Universidad de Cantabria, Avda. de los Castros 44, Santander 39005, Spain.
Email: valen.gomez.jauregui@unican.es

Abstract

Inspection of the railway tracks requires relying on a precise positioning system that accurately determines the location of potential failures and deficiencies. Therefore, measuring the speed and precise location of rail vehicles is essential. Many methods and approaches have been proposed, but most of them lack several conditions that do not allow them to be optimal for this task. In this paper, the authors present a novel method for measuring the speed of a train by means of the time correlation approach, by using 2-mm wave radar sensors. Additionally, it is also an accurate positioning system because the authors prove that the track has a unique profile, sufficiently characteristic and stable over time, that serves as a distinctive signature, which can be used to locate the vehicle at any point on that track. As a result, this new methodology, combined with a laser profilometer device, can be used as an effective inspection system for cracks or deficiencies in the rails, sleepers, fastenings, bolts etc., locating them precisely on the railway track.

1 | INTRODUCTION

Train operation control systems, including precise localization of rail vehicles, are a key element for many reasons related to security and efficiency, among others. For instance, to carry out the inspection of the railway track as effectively as possible, the maintenance service needs to rely on a precise positioning system that accurately determines the location of potential failures deficiencies.

1.1 | Positioning in inspection systems

Precise odometry is crucial for reducing the wayside equipment, which is expensive and requires maintenance. When train positioning is based on odometry, which suffers from cumulative errors, high precision is required. The simplest approach is the use of a tachometer. However, the slipping, the blockage and the variable radius of the wheel due to its conicity limit its precision [1].

Odometry can be also estimated based on instantaneous speed measurements. The typical approach for measuring the speed is the use of a radio Doppler sensor. Doppler effect measures the relative radial speed between two objects by detecting the change of the frequency of the signal that is transmitted by the first object (the train) and the second one (the sleeper) where the signal is reflected to the first object. To increase the reflected power, the Doppler sensor is tilted down with a known angle for pointing to the corner between the sleepers and the ballast. Unfortunately, this angle is variable due to an irregular surface and, typically, its accuracy is $\pm$ 1% error [2].

A different manner for measuring the speed is to use time correlation between sensors that are aligned according to the longitudinal axis of the tracks with a known gap between them. The main advantage of this technique is that speed error can be reduced to a certain value by increasing the gap between both sensors. Several methods have been explored with this approach. One of them is to induce currents in the track and measure the magnetic field that typically changes due to the presence of the rail clamps, the turnouts and the cables [3],

TABLE 1 Positioning systems and their disadvantages.

Positioning system	Disadvantages
GPS Odometry	Lack of coverage in underground stretches and low accuracy.
Taco-generators	Failure in case of traction skating or braking locking.
RADAR Doppler	Flat surface failure.
Monoaxial accelerometer	Need for continuous monitoring to determine speed and position.

but this method is not accurate enough at low speeds. Another method is to use optical sensors for measuring the irregularities of the surface of the tracks [4]. However, optical devices are not optimal for dirty environments and maintenance is required for cleaning. Finally, time correlation of two Doppler sensors has been proposed with limited results [5]. None of these solutions have been commercially exploited due to their lack of reliability and repeatability.

The implementation of MEMS (Micro Electro Mechanical Systems) technology in the sensors of the Inertial Motion Units (IMUs) has increased its sensibility. However, the calculation of distance and speed cannot rely on a single sensor because they depend on operating conditions (rain, snow, fog, hills, slipping etc.) and, thus, must be combined, for instance by means of fusion algorithms [6]. For instance, speed measurement is the result of the combination of wheel sensor, radar and Global Navigation Satellite System (GNSS). However, the GNSS receiver should be able to autonomously perform integrity monitoring, including detection of faulty observations [7].

Therefore, the IMUS have been used for supporting GNSS receivers in the areas where they do not have availability. An example is based on onboard sensors such as a velocity sensor and a GNSS sensor [8]. The other examples are based on particle filters that fuse the position and direction observations to estimate the vehicle position [9]. However, this approach has had a limited commercial success [10], mainly because of the absence of satellite signals in places that are important for railroad applications (railway stations, tunnels etc.) [11]. Additionally, increasing the number of onboard sensors is cost intensive and only gradually improves reliability and availability of localization information [11].

Table 1 summarizes the positioning systems currently used in the railway environment, along with their main drawbacks.

Within this context, the authors of this work, who belong to Auto Drive Solutions (ADS), have developed a new positioning system based on millimeter-wave (mm-wave) RADAR sensors that tries to solve all the disadvantages that current systems have. Its function is based on previous works already registered by ADS [12]. In this paper, we present a novel method for measuring the speed of the train by means of the time correlation approach, by using 2-mm wave radar sensors. We have based our methodology on the precise and continuous extent of the profile of the railway track, acquired by means of radar sensors. The purpose of using mm-wave radars is to obtain an infrastructure signature that is sufficiently characteristic and stable over time to allow the speed and position of the train to be determined with a precision never seen before

In this way, each one of the disadvantages shown in Table 1 is solved as follows:

- Lack of coverage in underground sections and low accuracy: There is no lack of coverage because the positioning system is embarked on the vehicle itself that is performing the inspection of the railway track.
- Failure in case of traction skating or braking locking: Since, in these cases, the vehicle continues to move, the on-board measuring equipment continues to move equally and is not influenced by this fact.
- Flat surface failure. Flat surfaces are not a problem for this system. The result will be a measurement of a 'flat' profile. The precision of the developed system is able to measure distances of less than 1 mm, so a flat surface for the human eye is not really flat for this positioning system.
- Need for continuous monitoring to determine speed. Our positioning system continuously calculates the absolute position of the vehicle within the entire railway track. Therefore, continuous monitoring is not necessary.

1.2 | Aims and structure of the paper

The main objective of this project is to verify, by means of a set of tests designed and customized to such an effect, that the use of mm-wave RADAR sensors (which had never been used previously for this purpose) is suitable for their application to railway operation and maintenance. In particular, the specific objective of this work is to verify the adequacy of the performances of a new prototype:

- mm-wave RADAR sensors can be used as an accurate positioning system because the track has a unique profile that serves as a distinctive signature, which can be used to locate the vehicle at any point of that track.
- RADAR systems can be used as a precise speedometer, by comparison of the profile of the track recorded by two consecutive sensors.
- They can be used as an effective inspection system of cracks or deficiencies in the railway track and to locate them precisely on the track.

The structure of this paper is as follows: previous work in the field is briefly reported in the following paragraphs of this section. Then, Section 2 introduces the operative of the new system, including the methodology for the positioning, speed measuring and inspection of the railway track with the different sensors. The described methodology is applied for performing the four experimental tests presented on Section 4. The paper closes in Section 5 with the main conclusions and some indications for plans about future work in the field.

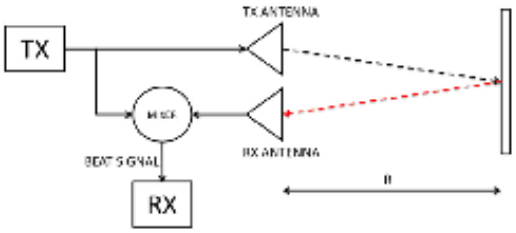

FIGURE 1 Architecture of a FMCW radar. FMCW, frequency modulation continuous-wave.

2 | OPERATIVE OF THE NEW SYSTEM

2.1 | Functioning of mm-wave radars and ground-profile correlation

A radar is a system that uses electromagnetic radiation reflected by an object to determine the location or speed of the object. In practice, a radar system may be able to measure direction, height, distance, heading or speed from the echo reflected by both static and mobile objects.

Due to a high cost of components, the use of mm-wave sensors has been typically limited to space exploration and security applications [13–16]. In recent years, technological advances in radio frequency have given rise to new Silicon-Germanium components in the millimetre band [30–300 GHz]. An example of this is the low-cost frequency modulation continuous-wave (FMCW) radar [17], which works in the 120- to 125-GHz band and most of its components, including also a transmitter and receiver antennas, are embedded in a single chip.

It is worth noting that mm-wave radar sensors have many advantages in comparison with optical sensors, since the radar signal is reflected over any type of surface even on those that present a low retro-reflectivity or are covered by sand or dust. Furthermore, radar reliability does not depend on light conditions and works well under heavy rain or fog conditions. These properties make mm-wave radars ideal for non-clean outdoor environments.

The working principle of a FMCW radar consists in transmitting a chirp signal (a signal that changes its frequency along the time) and measuring the time of flight that this signal takes to bounce on the target and returns to the sensor. Figure 1 shows the architecture of a FMCW radar.

Figure 2 shows a saw tooth radar waveform with linear frequency modulation. The returned signal (dotted red trace) is mixed with a copy of the transmitted signal (continuous black trace). As a result of mixing both signals, we obtain another signal, called beat signal, whose frequency is proportional to the distance to the target. The frequency of the beat signal is determined by Equation (1) where R is the distance to the target, c is the speed of light in the medium, Δf is the total transmitted bandwidth and T is the period of the chirp signal.

$$f_{beat} = \frac{2R}{c}\frac{\Delta f}{T}\,(Hz) \tag{1}$$

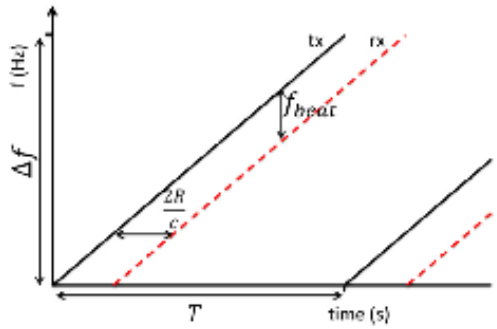

FIGURE 2 Graph of the saw-tooth radar waveform.

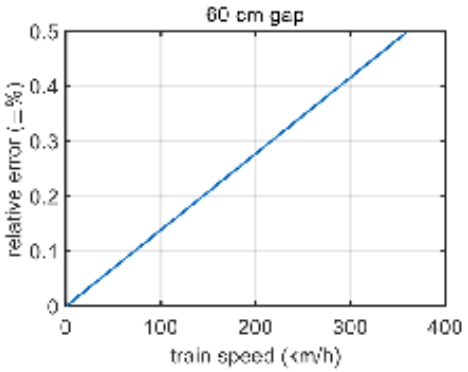

FIGURE 3 Theoretical relative speed error for a 60-cm gap between sensors.

The theoretical cross-correlation error should be ± 1 sample; the number of samples where the correlation will find the maximum will be the time that second radar (A) takes to reach the initial position of the first radar (B) divided by the period T. This value will depend on the gap between radars and the speed of the train. Equation (2) shows the theoretical error where $t_{measured}$ is the delayed obtained in the cross-correlation, T_{chirp} is the scanning time of one measurement of range, Gap is the distance between sensors and V_{train} is the real speed of the train.

$$\varepsilon_{speed} = \frac{t_{measured}}{\frac{Gap}{V_{train}}} = \frac{\frac{Gap}{V_{train}} \pm T_{chirp}}{\frac{Gap}{V_{train}}} = 1 \pm \frac{V_{train} * T_{chirp}}{Gap}\ (adim) \tag{2}$$

Figure 3 shows the function of the theoretical speed estimation relative error versus train speed for a 60-cm gap. This error is typically about 10 times better than the error of current systems for determining train speed. However, it can be reduced up to 600 times by placing the first sensor at the head of a 400-m train and the second sensor in the tail.

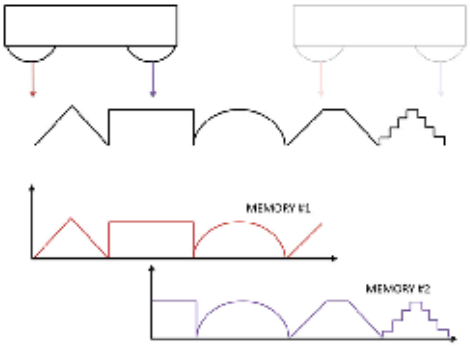

FIGURE 4 Example of a schematic profile of the railway track.

2.2 | Operative of the positioning system

Once the need for an accurate positioning system to increase the efficiency of rail maintenance systems has been defined, this section will describe the operative of the positioning system used in this work.

In short, the system is based on the following assumption: the railway track has a unique signature at every point, a surface identity, determined by surface characteristics like irregularities or inaccuracies depending on construction systems or maintenance. Based on this premise, the reading of the railway track in a given section results in a surface identity profile that allows defining precisely the positioning of the vehicle that carries the measurement system. It is important to distinguish this surface track profile that we will take into consideration to the infrastructure profile defined by the elevation of the different mileage point along the alignment.

Let us suppose that, schematically, the entire railway track had a profile like Figure 4, where the triangle rectangle and the circle represent different patterns found on the railway track (e.g. sleepers, bolts, ballast, clips etc.).

Moreover, let us suppose that the profile of the last leg measured by the positioning system has had a rectangular shape. Conceptually, it would have been easily determined that the vehicle was in the middle of the railway track.

However, although the operation of the developed positioning system may seem simple, it must meet two requirements to make it effective. The first one is that the profile measurement is extremely accurate, and the second one is that it is extremely fast.

On the one hand, it has to be extremely precise because the characteristics that will determine the uniqueness of the railway track signature are small, for example, the centimetre difference in separation between several consecutive sleepers, the uniqueness of the ballast shape, or the average distance between the vehicle and the sleeper in a given section.

On the other hand, it has to be extremely fast because the inspection of the railway track could be done at any speed.

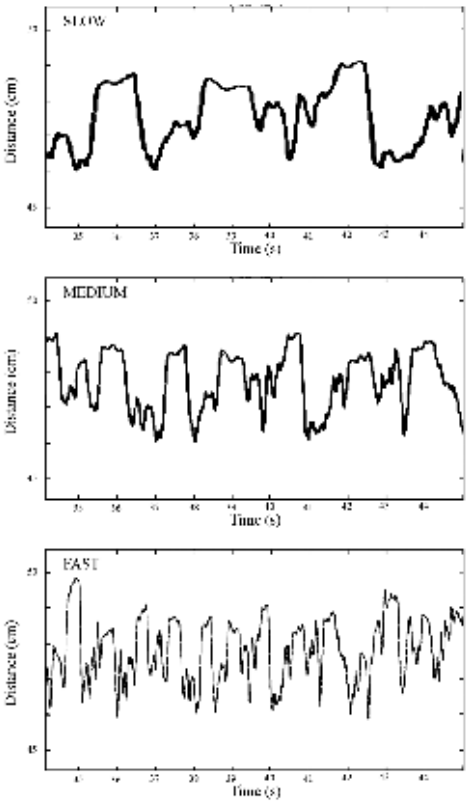

FIGURE 5 Readings of three equal track profiles at different speeds: Slow (above), Medium (middle) and Fast (below).

This, coupled with the first requirement, obliges that the profile measurement has to be 'almost' continuous.

In addition, the fact that the speed of inspection of the railway track is variable requires that the profile reading system must know constantly the speed of the vehicle to be able to perform an accurate positioning. For example, Figure 5 shows the schematic readings of three equal profiles, but at different speeds.

Therefore, it is necessary to correct the measured profile with speed information to determine with accuracy the exact position of a vehicle within the entire railway track. Thus, the procedure that summarizes the operation of the complete positioning system would be as the following steps:

1) Measurement and storage of the full profile of the railway track and the speed at which it was made.
2) Normalization and storage of the normalized full profile at a certain rate (normalization rate) of the measured profile.

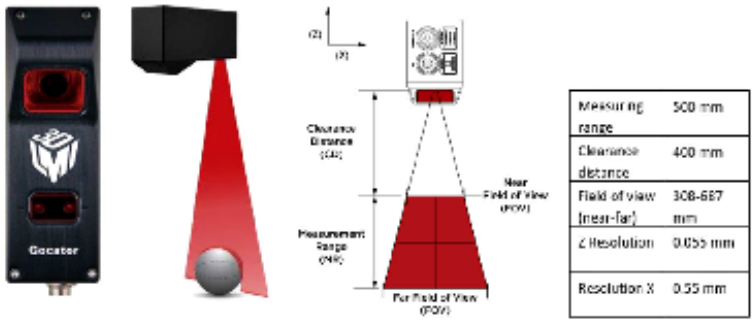

FIGURE 8 Photo, functioning scheme and features of profile sensor Gocator 2170.

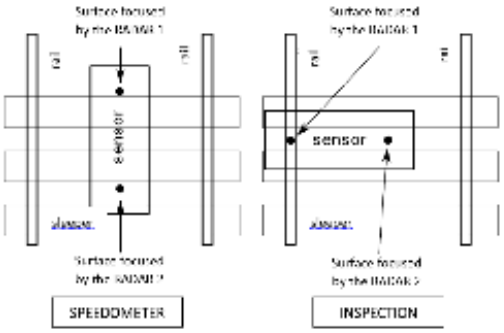

FIGURE 9 Disposition of sensors 1 and 2 for the speedometer (left) and for the inspection (right).

- PC for communication with the measurement system. Toshiba Satellite Pro P500-11Z.
- Wireshark software for storing all measurement data.
- Helmets, vests and safety boots.

Figure 10 shows the graphical interface developed to read the data generated by the measurement equipment. This software allows it to read the data, start testing or annotate it in real time in order to process it as shown in the Results section of this document.

3.2 | Characteristics of the railway tracks for the tests

Table 2 presents and compares the characteristics of the two different railway tracks used for performing the tests of the present study.

3.3 | Matrix of test design

Table 3 represents a matrix for understanding the different tests carried out in this study. As can be seen, it classifies the experiments depending on the railway track on which they have been performed, the equipment used and the validation of results that have been sought for each one. Related to the radar sensors, it establishes if both of them were aligned parallel (=) or perpendicular (+) to the railway track.

3.4 | Test 1 on railway track 1

3.4.1 | Assembling of the equipment

This section explains how was the assembly of both equipment in the vehicle modified as a draisine during the tests for positioning and speed measurement: the radar sensors and the laser device.

On the one hand, Figure 13 shows the prototype of radar sensors, which is located in a frame anchored at the back of the draisine, parallel to the rails of the railway track at approximately 40 cm above the floor. This distance is within the focus (20–70 cm) for which the sensor lens has been designed. In this way, the two sensors of the equipment will read exactly the same points of the railway track and, as explained previously, will determine both the positioning and the speed of the vehicle.

On the other hand, Figure 14 shows the location of the laser profilometer for the inspection of the track elements. As can be seen, the placement of this additional equipment did not cause any problems or interference for the measurements of the speedometer developed by ADS.

3.4.2 | Tests design

The tests that have been carried out are mainly divided into two different blocks, according to the two configurations that have been proposed

- Positioning system and speed measurement by means of the radar sensors and inspection of the track by means of the laser profilometer.

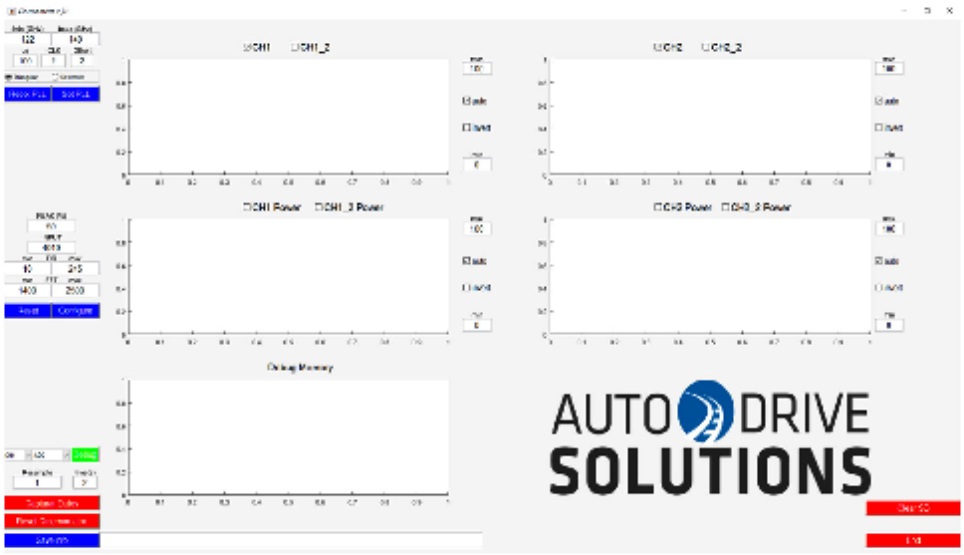

FIGURE 10 Graphical interface of the software developed to read the data from the measurement equipment.

TABLE 2 Characteristics of the two railway tracks for the tests.

	Railway track 1	Railway track 2
Type of track	On ballast	On ballast
Width	Iberian width (1668 mm)	Iberian width (1668 mm)
Approx. length	1 km	10 km
Placement	Outdoors	Outdoors
Sleeper material	Wooden	Concrete
Track clamping	Directly on the sleepers	With clips
Approx. sleeper separation	40 cm	40 cm
Approx. sleeper width	20 cm	20 cm
State of conservation	Poor	Good
Maintenance	Poor	Low (some areas full of ballast)
Appearance	Figure 11	Figure 12

- Tests carried out:
  - Fifteen repetitions in a single direction of the track with the two sensors positioned parallel to the rails.
- Objectives:
  - Corroborate that the railway track has a unique signature
  - Complete characterization of the track
  - Test and calibrate of the speedometer prototype

FIGURE 11 (Left) Image of the railway of railway track 1.

  - Test and calibrate of the positioning system
  - Detect damages on the sleepers.
  - Detect abnormal elements on the track
- Acquired data:
  - Profile of the track recorded by the two radar sensors reading the same points
  - Vehicle speed with OBD-II to calibrate speedometer prototype.
- Expected results:
  - Storage of the standardized stretch of track profile
  - Comparison of the 15 repetitions of the entire stretch
  - Individual characterization of each sleeper.

TABLE 3 Matrix presenting the different tests carried out in this study.

		Equipment			Results and validation		
No. test	Railway track	Radar sensors	Laser device	OBD-II	Positioning	Speedometer	Inspection
1	1	−		x	x	x	x
2	1	+			x		x
3	2	−	x	x	x		x
4	1	−	x	x			x

OBD-II, on board diagnostics-II.

FIGURE 12 (Right) Image of the railway of railway track 2.

FIGURE 13 (Left) Assembling of the equipment for developing tests 1 on railway track 1.

- Speed accuracy of the prototype with respect to OBD-II

3.4.3 | Test results

According to the two types of tests defined, the presentation of the result will follow the same structure (first position system and then speedometer); in this way, the results of the tests performed are as follows:

FIGURE 14 (Right) Location of the laser profilometer at the draisine.

- Characterization of the positioning system:

Figure 15 is just an example of the 15 couples of track profiles (see all of them in Appendix 3) that summarize the measurement of the profiles of the reading tests performed in the railway track 1. Each couple consists of the profiles recorded by the two radar sensors. The average duration of each recording is 1 min and each sensor performs one measurement every 100 μs. Therefore, the total amount of data acquired is 18 million measurements.

Even though the amount of data can seem overwhelming, two quick conclusions can be drawn at first sight

- The profiles of the two channels are very similar in each of the individual recordings.
- All profiles are very similar and it is possible to determine matches with the naked eye.

These two statements allow us to validate the initial hypothesis on which the positioning system is based: the railway track has a unique profile that gives it a unique signature, which allows it to position an element in the railway track with just a measure of the track profile.

To define it more precisely, let us zoom to a random area of the track profile. Let us take, for example, the profile segment from the second 34 of test No. 15 and profile of radar sensor 1 (Figure 16). At first glance, it is possible to determine at the profile where there is a sleeper and where there is ballast, as is pointed out in the graph.

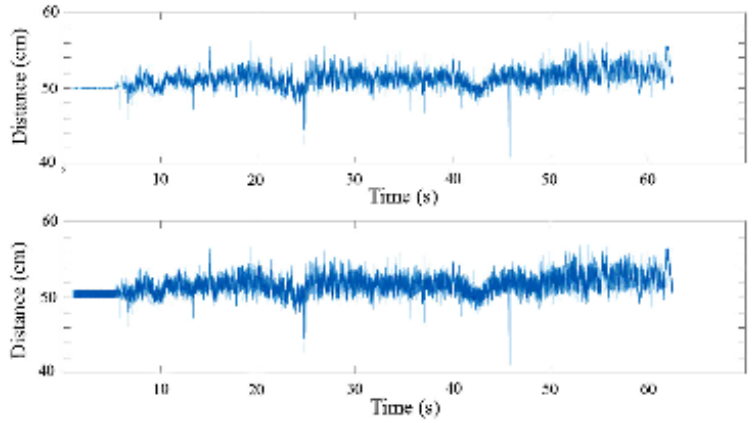

FIGURE 15 Track profiles recorded by each one the two radar sensors in each one of the 15 readings (see all of them in Appendix 3).

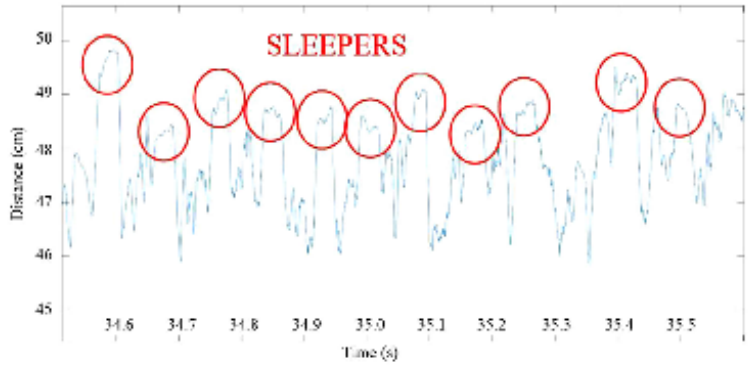

FIGURE 16 Zoom to segment of second 34 of test 15 and radar sensor 1.

As can be appreciated, each sleeper is totally different and independent of the adjoining sleeper, just as the ballast is at different heights and has a layout that may seem random. However, the graphic is clear enough to provide very useful information.

To characterize the railway track exhaustively, we have carried out a data processing of all the tests to characterize each sleeper individually and we have tabulated it. All this information is attached in Appendix 1 in a table with the following format or fields (first row in English, second row in Spanish):

- Index. It is the index of each sleeper within the stretch of railway track under study.
- Approximate PK. It is the approximate kilometre point of each sleeper. It is calculated taking on average the distance of two sleepers on the 0.6-m track.
- OBD-II speed. It is the average speed at which the vehicle was moving when it passed over that sleeper, determined by the OBD-II device.
- RPS speed. It is the average speed at which the vehicle moved when it passed over that sleeper, determined by our prototype of speedometer.
- Norm. profile. It is the average normalized profile of the sleeper with respect to the speed difference between the normalization speed (20 km/h) and the speed at which the draisine circulated at the time of each measurement.
- Height. It is the average height of the sleeper measure.
- Std. height. It is the typical deviation of the measurement of the height of the sleeper taking as data the values of the 15 tests and the two channels (one per radar sensor).
- Width. It is the average width of the sleeper measure.

TABLE 4 Statistical results on the sleepers of railway track 1.

No. of sleepers	Average height	Standard deviation in height	Average width	Standard deviation in width	Track condition (0–3)
1432	41.22 cm	5.24 cm	24.12 cm	2.38 cm	1.2

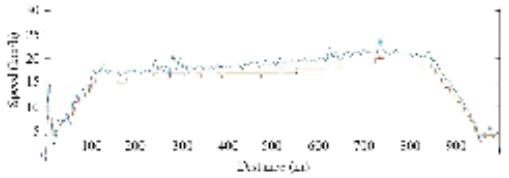

FIGURE 17 Graph comparing speeds taken with the OBD-II (red line) and the speedometer prototype (blue line) (see the 15 recordings in Appendix 4). OBD-II, on board diagnosties-II.

- Std. width. It is the typical deviation of the measurement of the width of the sleeper taking as data the values of the 15 tests and the two channels (one per radar sensor).
- State. Depending on the measured profile of each sleeper, we determine that the sleeper in in good, average, bad or very bad condition. These thresholds are based on the statistical data of mean and variance of measurements on the profile of the sleepers. When the variance is above 10%, 15% or 20% of the width of the sleeper, the state is defined respectively as average, bad or very bad. The results are weighted with the difference to the averages of the five previous and subsequent sleepers. Thus, this classification can be considered a first approach to a system for the inspection and maintenance of any railway track.

Taking into account all the information in the table of Appendix 1, Table 4 shows the most relevant statistical results.

As indicated in the section related to the characteristics of the railway track, the maintenance conditions of this railway are quite poor, having sleepers with important damages. Table 4 can prove this fact by means of the standard deviations, which will be confirmed in the images included in the following sections.

- Characterization of the speedometer accuracy

Figure 17 exposes just one of the 15 graphs showing the results of the speed measurements (see all of them in Appendix 4). These graphs compare the measurements obtained by our prototype of speedometer (blue line) with the diagnostic tool that uses the OBD-II standard of the draisine (red line).

In short, all speed curves in all 15 tests exhibit similar behaviour. The initial acceleration is quite smooth until the maximum speed (between 30–40 km/h) is reached. The only exception is the first test, in which the maximum speed was around 20 km/h to inspect the track for safety reasons.

The first conclusion that can be drawn is that our prototype of speedometer, which uses the railway track profile, is able to achieve an accuracy of 0.01 km/h, while the OBD-II system has an accuracy of only 1 km/h. In addition, the OBD-II system offers a lower measurement of speed than our speedometer. This may be due to two reasons:

I. the frequency of the OBD-II system (1 measure every 0.5 s) is much lower than the system under study (1 measured every 0.01 s), so the measurement in the first case is filtered and compensated, which does not happen in the second case;
II. the international regulations require vehicle speedometers to reduce the actual speed values for safety reasons; therefore, it is an induced error, mandatory and legal, established by the international legal institutions.

According to the results, our prototype of speedometer has presented low resolution at low speeds (under 5 km/h). This is because the profile size that is used for speed calculation is not sufficient at these speeds. It is an amendable error that will be corrected in subsequent field tests.

Finally, we detected that some of the errors in the measurement of the vehicle's speed are the result of the loose anchorage system that was used, which generates undesirable vibrations. Being the measurement of speed a system based on the comparison of profiles with some delay, the elimination of any type of vibration is fundamental and affects the measurement and the resulting values of speed. For correcting this problem, the following tests were developed after the construction of a new damped system that would promote the increased accuracy of the speedometer and positioning system as a whole.

3.5 | Test 2 on railway track 1

This time, the aim of the test was focused on the inspection system, using both the radar sensors and the laser device. The assembling of the equipment was similar to test 1, but the radar sensors were placed perpendicular to the railway track: one of the sensors was placed over the sleepers and the other one placed over the rail.

3.5.1 | Tests design

The tests that have been carried out are the following:

- Positioning system and inspection of the rail only by means of the radar sensors.
  - Tests carried out:

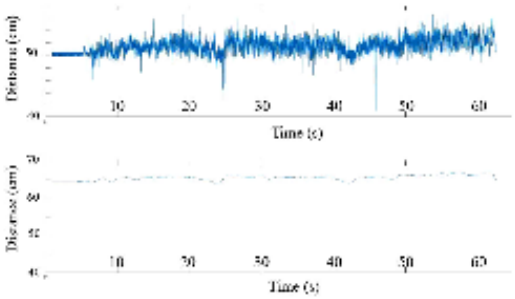

FIGURE 18 Reading for the inspection of the railway track 1 (track above, rail below) with the radar sensors (see all of them in Appendix 5).

- Five repetitions in each direction of the track (10 in total), with one of the sensors placed over the sleepers and the other one placed over the rail.

- Objectives:
  - Detect rail damage.
  - Use the positioning system in conjunction with the inspection system.
- Acquired data:
  - Profile of the track by one radar sensor (for positioning system).
  - Profile of the rail by the other radar sensor (for rail inspection).
  - Profile of the track recorded by the laser device (failed)
  - Vehicle speed with OBD-II to normalize measurements of the profiles.
- Expected results:
  - Detection of possible damages in the rail and their exact position.
  - Determination of the severity of each damage by assessing the measurements.

3.5.2 | Test results

The results of the tests performed are as follows:

- Railway track inspection with the laser device

Related to the laser device, unfortunately, it did not deliver satisfactory results due to the light conditions of the tests. The results thereof will not be set out in the Results section of this work.

- Railway track inspection with the radar sensors

Figure 18 shows one of the 10 couples of graphs obtained in this test. All of them are exposed in Appendix 5, where the first five tests correspond to the inspection of the left rail and the last five to right rail. In Figure 18, the upper image shows the track profile (over the sleepers, at the centre of the railway) and the lower image shows the rail profile. They can be used to

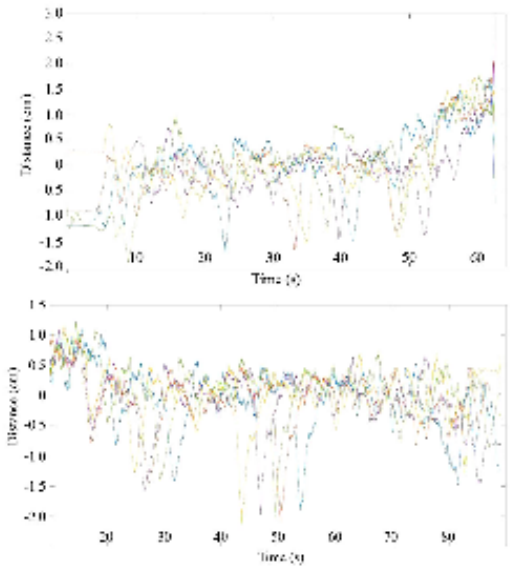

FIGURE 19 Rail profiles overlapped (left rail above and right rail below).

summarize the results of the tests performed to characterize the rail inspection system along with its use as a positioning system.

The main conclusions that can be drawn based on the results of the graphs above are

- As expected, the measurements of radar sensor 2, which performs the rail profile, are much more stable than the measurement of radar sensor 1 over the track, with sleeper and ballast. There is hardly a variation of 2 cm in the measurements of sensor 2 and they are largely due to the vibrations of the fixing structure.
- It can be seen that the duration of the first five repetitions is shorter (around 60 s) than those of the last five tests. This is because the last five tests to measure the right rail had to be performed driving reverse the draisine due to safety reasons.
- It can be determined at first sight that there appear to be several areas with out-of-average measurements; this study will try to demonstrate whether they can be characterized as problems in the rail.

Figure 19 is used to appreciate all the rail profiles overlapped (left rail and right rail) to determine if the imperfections that are going to be analyzed are repeated coherently and, therefore, are not false positives.

Table 5 shows the problems encountered throughout railway track 1.

After performing a visual examination on positions that the inspection system had considered to be problematic, it is determined that the problem at the three points detected is the discontinuity of the rail because their junctions are not welded (Figure 20). Therefore, this is not a railway track failure.

FIGURE 20 Rail with flange joint without welding, confirmed during visual inspection.

FIGURE 21 Assembling of the equipment for developing the test 3 on railway track 2.

TABLE 5 Problems found in railway track 1 during test 2.

No.	Repetitions	Approx. location (m)	Severity	Visual inspection
1	5	212	Medium	Flange joint without welding
2	4	521	High	Flange joint without welding
3	5	951	Medium	Flange joint without welding

3.6 | Test 3 on railway track 2

3.6.1 | Assembling of the equipment

As explained in the previous section, we had found that the measurements on the tests on railway track 1 had a low-frequency error component due to vibrations produced by the anchorage system. To avoid these vibrations, we designed and manufactured a new anchorage system for the tests on railway track 2, which allows it positioning the sensor supported on the track over a trolley with two nylon wheels (Figure 21). This system offers greater stability against vibrations than the previous anchoring device, in which the vibrations were fought by cable tensioners.

As for the laser-based inspection system, since light conditions are extremely important for its proper operation, we also design a new covering structure that allows it to generate a shadow zone over the area of interest. Being this the case, it is possible to perform a correct inspection of the railway track, in this case over the rail. Figure 22 shows the placement of the laser device under the covering structure and the laser beam it emits to perform the corresponding measurement of the profile.

3.6.2 | Tests design

In this case, as railway track 2 is longer than railway track 1 (10 km vs. 1 km), the number of repetitions has been reduced to two. Since the radar sensor is less versatile than the laser profilometer when performing track inspection (it is only useful for inspecting sleeper or rail discontinuities), it was decided to use only the laser device as the inspection sensor, using the radar-based prototype as a positioning system and speedometer. Therefore, the two devices performed measurements simultaneously.

In this way, tests such as positioning system, speedometer and railway track inspection method consisted of:

- Tests carried out:

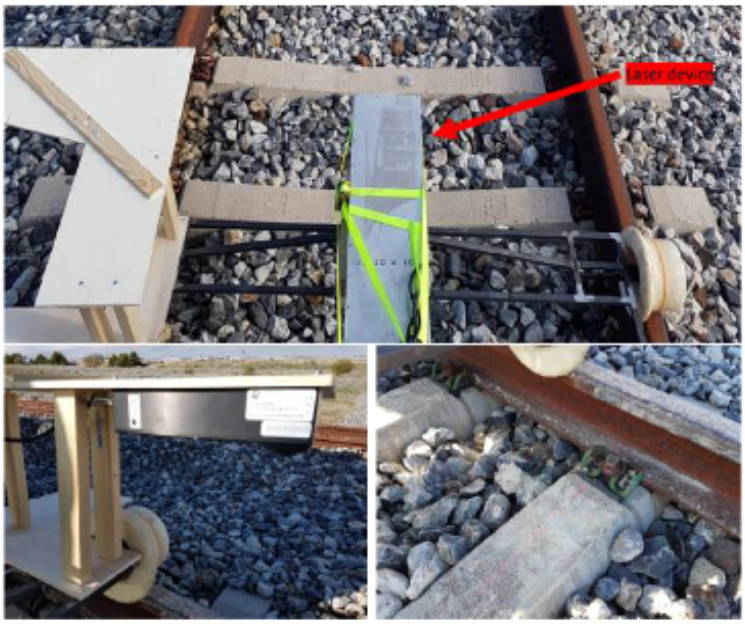

FIGURE 22 Assembling placement of the laser device and laser beam is emits (tight down image).

- Two repetitions in a single direction on the track with the two sensors positioned parallel to the rails.

- Objectives
  - Corroborate that the railway track has a unique signature.
  - Complete characterization of the track.
  - Test and calibrate of the speedometer prototype.
  - Test and calibrate of the positioning system.
  - Detect damages on the sleepers.
  - Detect damages on the elements of the railway track (rail, clips, bolts etc.).
  - Detect abnormal elements on the track.
  - Take an inventory of railway track elements.
  - Use the positioning system in conjunction with the inspection system.
- Acquired data:
  - Profile of the track recorded by the two sensors reading the same points.
  - Vehicle speed with OBD-II to calibrate speedometer prototype.
  - Profile of the elements of the railway track inspected by the laser device.
  - Accurate positioning at every point of the test.
- Expected results:
  - Storage of the standardized stretch of track profile.
  - Comparison of the two repetitions of the entire stretch.
  - Individual characterization of each sleeper.
  - Speed accuracy of the prototype with respect to OBD-II.
  - Detection of possible damages in the railway track along with their position.
  - Determination of the severity of each damage using the readings taken by the laser device.
  - Inventory of the most important elements of the railway track and their condition.

3.6.3 | Test results

Although the tests were performed simultaneously, the results of the tests will be presented differentiating the two different systems that have been tested.

- Characterization of the positioning system

As in the test on the railway track 1 test, the first conclusion at a glance is that, qualitatively, the profiles of both the two radar sensors for each reading are very similar (Figure 23). Therefore, it can be uniquely determined that the railway track has a signature that is unique and corroborates the hypothesis on which the authors have developed this new positioning system.

As for the differences that can be seen within each graph, the analysis of the track has been split into two types of zones: (1) areas where the sleepers are exposed and (2) areas where the ballast completely covers the sleepers and where it would be necessary cleaning the railway track. Graphically, Figure 23

TABLE 6 Statistical results on the sleepers of railway track 2.

No. of sleepers	Average height	Standard deviation in height	Average width	Standard deviation in width	Track condition (0–3)
16,584	58.84 cm	2.15 cm	14.57 cm	1.22 cm	2.5

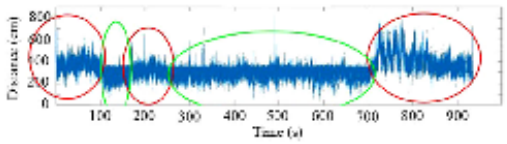

FIGURE 23 Track profile recorded by one of the two radar sensors, distinguishing 'clean' areas (circled in green) and 'dirty' areas (circled in red).

distinguishes these two zones, where 'clean' areas are circled in green and 'dirty' areas are circled in red.

Figure 24 is a close-up of a clean sleeper area, while Figure 25 shows a dirty area where ballast is placed over the sleepers.

Clearly, these graphs have pointed out the sleepers that are detected in each of the areas. As expected, the dirty areas that are covered by ballast hide much of the sleepers; those detected areas have a shape that determines the existence of a sleeper underneath, which is very useful for maintenance purposes. Therefore, the radar sensor is able to determine the dirtiness of the railway track 2 and also the condition, characterization and inventory of each one of the railway track's sleeper.

Again, like the results of the previous paragraph, a table is attached in Appendix 2 with the characterization of each of the sleepers that have been scanned along the route, with the same format and fields as for railway track 1 of Appendix 1. Taking into account these data, Table 6 shows the most relevant statistical results.

- Railway track inspection with the laser device.

The readings with the laser profilometer have two main objectives: The first one is to perform the rail inspection and the second is to perform the inspection of the railway fastenings of the rail to the sleepers (clips, bolts, washers, nuts, plates etc.). According to these objectives, the results that have been obtained in the tests carried out are as follows:

A. Inspection of the rail:

The structure of a rail is usually divided into three different zones: foot, web and head. When performing an inspection of the railway rail, it is important to determine not only the possible cracks and wear of its elements but also its position. The left of Figure 26 shows a 2D reading of the railway track 2, while the right represents a 3D scanning of a short segment of the same railway.

The technology proposed in this work is able to determine areas that can compromise safety, such as wear and tear. This is achieved by comparing the shape of the rail profile along the railway track, as registered by the laser profile, with the theoretical cross section of the rail, and then measuring the drift that exists between both shapes.

In the rail inspection measurements of railway track 2, we have detected a fissure that we determine as severe and several imperfections due to the accumulation of ballast in the web of the rail. Table 7 lists the most relevant imperfections detected during the railway track inspection and the confirmation after a visual inspection.

A. Inspection of railway fastenings:

The purpose of this type of inspection is to perform a scan of the status of the railway fasteners, including clips and bolts, as well as their preserved condition.

Figure 27 (left) shows the laser beam that scans the profile and registers the shape of a clip along with the bolt, while the right-hand side of the same figure displays the three-dimensional reconstruction of the same fastening as recorded by the laser device. As can be seen, the latter is able to accurately determine the damage or loss of a clip, as well as the situation of the bolt with respect to it.

In this way, Table 8 summarizes the results of the measures of all fasteners that have been analyzed in railway track 2.

3.7 | Test 4 on railway track 1

Once the previous set of tests on railway track 2 were performed satisfactorily, new tests on railway track 1 were carried out in order to acquire the readings of the profilometer (laser device). This is possible after having improved the stability of the measurements thanks to the use of the new anchoring method (Figure 21), as well as the creation of a shadow zone that allows the laser profilometer to be used in more tolerant light conditions (Figure 22).

3.7.1 | Tests design

The tests that have been carried out are only to perform the inspection of the railway track with the laser device:

- Visual inspection of the track and its shortcomings
  - Tests carried out:
    - Two repetitions in a single direction on the track with the laser profilometer.
  - Objectives

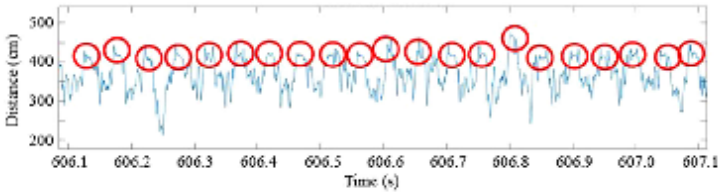

FIGURE 24 Close-up of a 'clean' sleeper area.

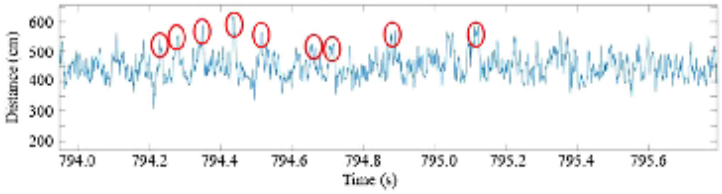

FIGURE 25 Close-up of a 'dirty' sleeper area.

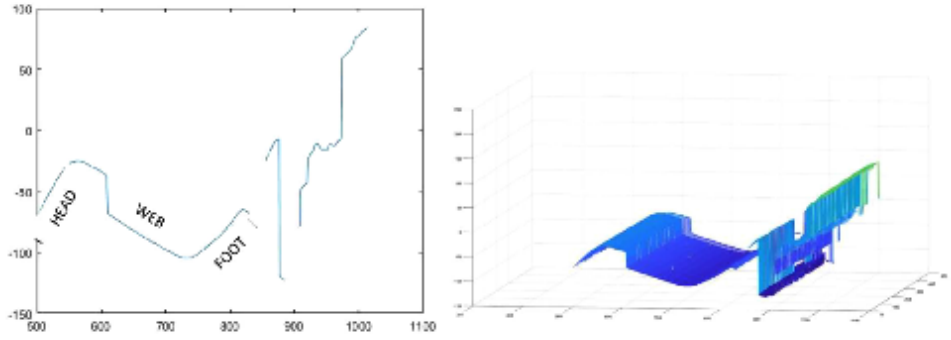

FIGURE 26 Examples of readings of the railway track 2 with the laser device, in 2D (left) and 3D (right).

TABLE 7 Imperfections after inspection of railway track 2.

No.	Approx. location (m)	Severity	Possible failure	Visual inspection	Severity after inspection
1	1200	Low	Fissure	Mild rail deformation	Low
2	4500	Medium	Ballast	Ballast accumulation	Medium
3	4700	Medium	Ballast	Ballast accumulation	Medium
4	4800	Medium	Ballast	Ballast accumulation	Medium
5	6400	Low	Fissure	Deformation	Low
6	7200	Low	Ballast	Ballast accumulation	Low
7	8100	Medium	Ballast	Ballast accumulation	Low
8	9300	High	Fissure	Opening in railway switch	None

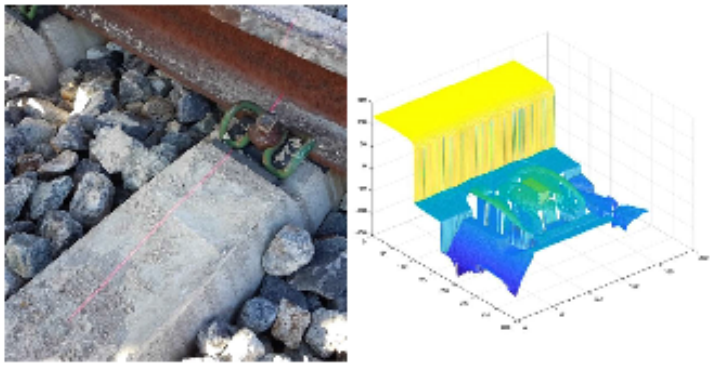

FIGURE 27 Laser beam scanning the fastening system (left) and its three-dimensional representation (right).

TABLE 8 Statistical results on the sleepers of railway track 2.

	Number	Good condition	Medium wear and tear	Severe wear and tear	Absence
Clips	32,843	90.2%	4.8%	0.2%	4.8%
Bolts	32,843	90.2%	4.7%	0.2%	4.9%

TABLE 9 Inventory of fasteners depending on their preserved condition.

	Number	Good condition	Medium wear and tear	Severe wear and tear	Absence
Bolts	4254	40.4%	27.2%	32.4%	18.7%
Junction flanges	72	31%	43%	26%	0%

- Detect damages on the elements of the railway track (rail, clips, bolts etc.).
- Take an inventory of railway track elements.
- Use the positioning system in conjunction with the inspection system.
- Acquired data:
- Profile of the track recorded by the radar sensor to position the vehicle.
- Vehicle speed with OBD-II to normalize profiles.
- Profile of the elements of the railway track inspected by the laser device.
- Accurate positioning at every point of the test.

• Expected results:
- Detection of possible damages in the railway track along with their position.
- Determination of the severity of each damage using the readings taken by the laser device.
- Inventory of the most important elements of the railway track and their condition.

3.7.2 | Test results

The first part of the test consisted of a visual inspection of the damages existing on the railway track 1 and several problems were observed. After visual inspection, the railway track was inspected with the laser device, obtaining their three-dimensional representations of the detected imperfections. Real and represented images are presented in the following images, as follows:

- Poor condition of junctions with flange joint (Figure 28).
- Surface defects on railway rails (Figure 29).
- Lack of bolts (Figure 30).
- Bolts out of place (Figure 31).
- Damages on fixation plaques (Figure 32).
- Very bad condition of sleepers (Figure 33).
- Fixations covered by ballast (Figure 34).

Figure 34 shows, for instance, a three-dimensional representation of a clip with ballast inserted between its wings, which can generate a situation of danger and breakage in case of crushing or hitting. Therefore, this would be one of the situations that should be avoided and that need special maintenance of the railway track.

The next two tables try to summarize the preserved condition of this particular railway track: Table 9 recaps the inventory of fasteners classifying them upon their preserved condition, and Table 10 lists the 20 most severe potential pathologies that have been detected on the railway track route 1.

4 | CONCLUSIONS

In this study, we have monitored two railway tracks in very different states of maintenance, using different tools and devices, with the objective of testing a new system developed entirely by ADS. The main conclusions that have been obtained after performing the four sets of tests are the following:

4.1 | As for the positioning system

- It has been verified that the railway track has a unique signature (a surface identity) that allows the inspector vehicle to be positioned unequivocally

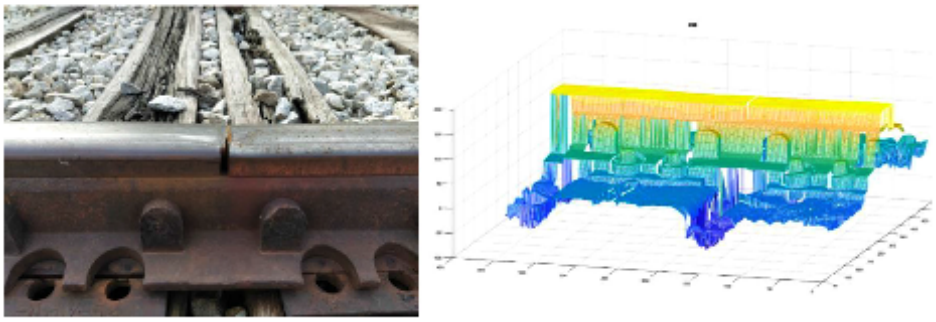

FIGURE 28 Poor condition of junctions with flange joint.

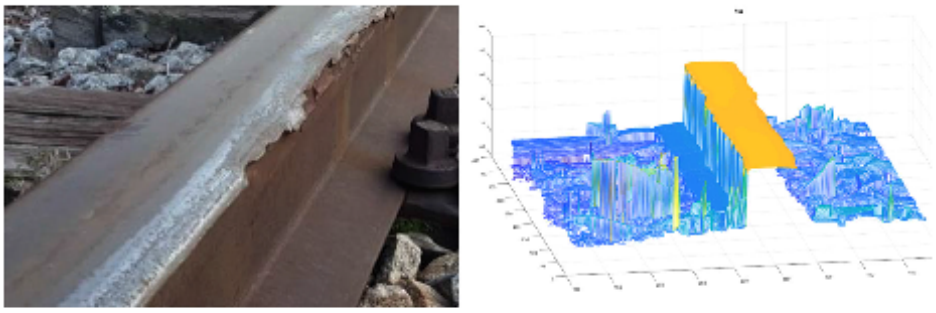

FIGURE 29 Surface defects on railway rails.

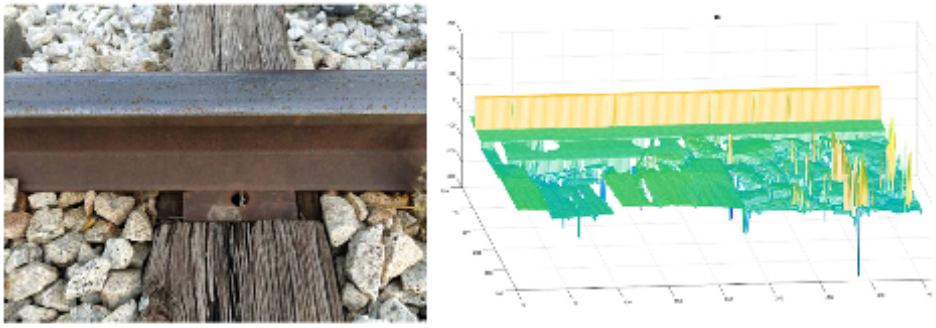

FIGURE 30 Lack of bolts.

- The radar system (which had never been used previously for this purpose) is capable of precisely positioning the vehicle on the railway track.
- The radar system is also capable of determining the exact speed of the vehicle at all times.
- The accuracy of the developed speedometer improves the accuracy of odometer-based speed measurement systems (OBD-II) by 5.8%.

4.2 | As for the inspection system

- The use of the radar sensor to inspect the railway track has been discarded because its current design is developed to focus its power on only 1 square centimetre, and therefore it is not wide enough to read the whole rail or fasteners.
- The inspection system based on a laser profilometer is very dependent on environmental light conditions; therefore, it

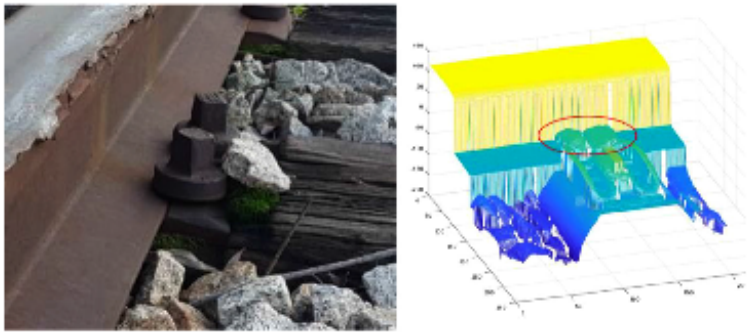

FIGURE 34 Fixations covered by ballast.

TABLE 10 Most severe pathologies detected on railway track 1.

No	Location (m)	Severity	Possible failure	Real failure [a]	Severity [a]
1	154	Very high	Rail breakage	Joint without welding	Medium
2	285				
3	21				
4	758	Very high	Poor condition of flange joint	Junctions with flange joint	Very high
5	63				
6	176	Very high	Missing bolt	Missing bolt	High
7	853				
8	241				
9	386				
10	147	High	Rail surface defect	Rail surface defect	Medium
11	586				
12	493	High	Bolt out of place	Bolt out of place	High
13	120				
14	51				
15	574				
16	698				
17	180	High	Poor condition of fixation	Fixation covered by ballast	Low
18	234				
19	482				
20	778				

[a]After visual inspection.

inspection system as damaged areas or with potential problems. Those images can be post-processed automatically or can be used as a visual support system.

- Improvement of the assembling of the equipment to fix the measurement systems to the draisine, which will make it steadier and will reduce possible errors due to vibration.
- Design of an array of radar sensors, or adding new optics allows their inspection zone to be expanded, so that they can be used as an inspection system.
- Detection of other problems such as cracks in the foot or web of the rail, requiring a new lens design for the radar sensor capable of focusing on these points, in addition to the railhead.

AUTHOR CONTRIBUTIONS

Valentin Gomez-Jauregui: Conceptualization; Investigation; Supervision; Writing—original draft; Writing—review & editing. Alejandro Badolato: Conceptualization; Formal analy-

sis. Juan de Dios Sanz Bobi: Conceptualization; Resources; Writing—review & editing. Ana Carrera-Monterde: Data curation; Investigation; Supervision; Writing—review & editing. Cristina Manchado: Investigation; Validation. César Otero: Project administration, Supervision, Writing – review & editing

ACKNOWLEDGEMENTS

The authors would like to thank and acknowledge Julie McNamara for proof-reading the manuscript and improve the writing quality of the text.

CONFLICT OF INTEREST STATEMENT

None of the co-authors have a conflict of interest to disclose

FUNDING INFORMATION

This research did not receive any specific grant from funding agencies in the public, commercial, or not-for-profit sectors.

DATA AVAILABILITY STATEMENT

Data available in article supplementary material. The data that supports the findings of this study are available in the supplementary material of this article in the form of 5 Appendices.

ORCID

Valentin Gomez-Jauregui https://orcid.org/0000-0002-7810-9589

REFERENCES

1. Malvezzi M., Toni P., Allotta B., Colla V.: Train speed and position evaluation using wheel velocity measurements. In: 2001 IEEE/ASME International Conference on Advanced Intelligent Mechatronics. Proceedings (Cat. No.01TH8556) Como, Italy, vol. 1, pp. 220–224 (2001)
2. Beesley A.J.: Distance/velocity measurement by Doppler [rail traffic control]. IEEE Colloquium on Where Are We Going? (And How Fast) Seminar Exploring Speed And Positioning Systems For The Transport Sector, pp. 5/1–5/2. London, UK (1997)
3. Spindler M., Stein D., Lauer M.: Low power and low cost sensor for train velocity estimation. In: 2016 IEEE International Conference on Intelligent Rail Transportation (ICIRT), Birmingham, pp. 259–264 (2016)
4. Murdock E.A., Hubbs G.: Implementing optical speed measurement (OSMES) for communications based train control. In: ASME/IEEE Joint Rail Conference, 2004. Proceedings of the 2004, Baltimore, MD, USA., pp. 205–211 (2004)
5. Murillas D.H., Poncet L.: Safe odometry for high-speed trains. In: 2016 IEEE International Conference on Intelligent Rail Transportation (ICIRT), Birmingham, pp. 244–248 (2016)
6. Muniandi G., Deenadayalan, E.: Train distance and speed estimation using multi sensor data fusion. IET Radar Sonar Navig. 13, 664–671 (2019). https://doi.org/10.1049/iet-rsn.2018.5359
7. El-Mowafy: A fault detection and integrity monitoring of GNSS positioning in intelligent transport systems. IET Intell. Transp. Syst. 14(3), 164–171 (2020). https://doi.org/10.1049/iet-its.2019.0248
8. Lauer M., Stein D.: A train localization algorithm for train protection systems of the future. IEEE Trans. Intell. Transp. Syst. 16(2), 970–979 (2015). https://doi.org/10.1109/TITS.2014.2345498
9. El Mokhari K., Reboul S., Choquel J.-B., Sotiene G., Amami B., Benjelloun M.: Circular particle fusion filter applied to map matching. IET Intell. Transp. Syst. 11(8), 491–500 (2017). https://doi.org/10.1049/iet-its.2016.0231
10. Stadlmann B., Mandl S.: GNSS based train localization for automatic train operation. In: 15th International Conference on ITS Telecommunications (ITST), Warsaw, pp. 1–7 (2017)
11. Hensel S., Hasberg C., Stiller C.: Probabilistic rail vehicle localization with eddy current sensors in topological maps. IEEE Trans. Intell. Transp. Syst. 12(4), 1525–1536 (2011). https://doi.org/10.1109/TITS.2011.2161291
12. Auto Drive Solutions S.L: Coded-information means located on an infrastructure in order to be decoded by sensors located on mobiles. Patent WO/2017/149357 (2017)
13. Badolato A., et al.: A 300 GHz imaging radar for standoff anomaly detection. In: 9th European Conference on Antennas and Propagation (EuCAP), Lisbon, vol. 2015, pp. 1–5 (2015)
14. Grajal J., et al.: 3-D high-resolution imaging radar at 300 GHz with enhanced FoV. IEEE Trans. Microw. Theory Techniq. 63(3), 1097–1107 (2015)
15. Cooper K.B., et al.: A high-resolution imaging radar at 580 GHz. IEEE Microw. Wirel. Compon. Lett. 18(1), 64–66 (2018)
16. Yang A., Reck T.: Hybrid CMOS system-on-chip/InP MMIC systems for deep-space planetary exploration at mm-wave and THz. In: IEEE Compound Semiconductor Integrated Circuit Symposium (CSICS), Miami, FL, vol. 2017, pp. 1–4 (2017)
17. Debski W., Winkler W., Sun Y., Marinkovic M., Borngräber J., Scheytt J.C.: 120 GHz radar mixed-signal transceiver. In: 7th European Microwave Integrated Circuit Conference, Amsterdam, pp. 191–194 (2012)

SUPPORTING INFORMATION

Additional supporting information can be found online in the Supporting Information section at the end of this article.

How to cite this article: Gomez-Jauregui, V., Agustin, J., Badolato, A., del-Castillo-Igareda, J., Bobi, J.D.S., Carrera-Monterde, A., Manchado, C., Otero, C.: New methods and functionalities for railway maintenance through a draisine prototype based on RADAR sensors. IET Intell. Transp. Syst. 17, 1608–1628 (2023). https://doi.org/10.1049/itr2.12353

Affiliation change request

1 mensaje

Alejandro Badolato <********@alumnos.upm.es> 25 de septiembre de 2024, 19:03
Para: theiet_its.office@wiley.com

Dear IET ITS team,

I am a PhD student finishing my PhD that has published the manuscript ITS-2021-12-0487 (**https://doi.org/10.1049/itr2.12353**)

In this manuscript, my affiliation appears as: Auto Drive Solutions which is my Company. However, I would like to change or add a second affiliation to Universidad Politécnica de Madrid.

Please, would you be so kind to indicate me how to proceed?

Thanks in advance.

Best regards,

Alejandro Badolato